Microscale Methods To Establish Scalable Operations For Protein Impurity Removal Prior To Packed Bed Steps

By

Razwan Hanif

A thesis submitted for the degree of Doctor of Philosophy in

The Department of Biochemical Engineering

UCL

December 2013

I, Razwan Hanif, confirm that the work presented in this thesis is my own. Where information has been derived from other sources, I confirm that this has been indicated in the thesis.

_____ Date _____

ABSTRACT

The purification of monoclonal antibodies and Fab' antibody fragments are of central importance to the pharmaceutical industry. In 2008, 29 new therapies based on such molecules were approved for the US market. Traditionally, a multistep process achieves purification with the majority of steps being packed bed chromatography. Chromatography is the major contributor to the unit operation costs in terms of initial capital expenditure for packing and recurrent replacement costs.

When considering the demand for biopharmaceuticals, it becomes necessary to consider alternative process strategies to improve the economics of purification of such proteins. To address this issue, this thesis investigates precipitation to selectively isolate Fab' or remove protein impurities to assist the initial purification process. The hypothesis tested was that the combination of two or more precipitating agents will alter the solubility profile of Fab' or protein impurities through synergistic multimodal effects. This principle was investigated through combinations of polyethylene glycol (PEG) with ammonium sulphate, sodium citrate and sodium chloride at different ratios in a novel multimodal approach.

A high throughput system utilising automated robotic handling was developed in microwells at 1 mL scale per well to enable the rapid screening of a large number of variables in parallel using a Design of Experiments (DoE) approach to statistically design studies in a two stage process, based on Quality by Design principles.

In the first stage, Fab' precipitation using PEG was investigated using a screening study in the form of a full two level factorial DoE to investigate a large design space. This was followed by a second more focused central composite face centred DoE to find optimal experimental conditions to deliver a high Fab' yield and purification factor in the range investigated. A design space comprised of the responses percentage Fab' yield and purification factor was created to give a robust region where Fab' yield was ≥ 90% with a maximum purification factor of 1.7. A normal operating range (NOR) was defined within this design space for operational simplicity when working at process scale. A confirmatory run was performed within the NOR with PEG 12000 15% w/v pH 7.4, which delivered a Fab' yield and purification factor of 93% and 1.5 respectively.

In the second stage, optimum conditions from the first study were used in a central composite face centred DoE incorporating multimodal conditions combining PEG with three salts from the Hofmeister series namely, ammonium sulphate, sodium citrate and sodium chloride. It was found that 90% Fab' yield with a purification factor of 1.9 was achievable with PEG 12000 15% w/v/0.30 M sodium citrate/0.15 M ammonium sulphate pH 7.4. This was an improvement of 26% relative to the use of 15% w/v PEG 12000 pH 7.4 in single mode. However an alternative precipitation strategy to precipitate ~20% of protein impurities whilst Fab' remained soluble using PEG 12000 6.25% w/v/0.4 M sodium citrate pH 7.4 was proposed instead. The advantage of this approach at process scale is the potential ease of processing due to removal of a solubilisation step and the significantly reduced viscosity of the precipitating agent relative to that of high concentrations of PEG. It was shown that this system could mimic process scale, which was verified at laboratory scale (50 mL stirred tank reactor (STR)) and pilot process scale (5 L STR).

A process run through was performed using a 1 mL SP Sepharose Hi Trap pre packed bed column (GE Healthcare, Uppsala, Sweden) to capture Fab' from homogenate (control), multimodal (PEG 12000 6.25% w/v/0.4 M sodium citrate pH 7.4) and single mode (PEG 12000 15% w/v pH 7.4) feedstreams. The final process purification factor for the three feedstreams were 2.5, 4.4 and 3.5 respectively. The use of multimodal precipitated impurities prior to a packed bed step had improved process performance by a purification factor of 1.9. This underlines the importance of assessing the interaction of individual processing steps, and the implementation of appropriate scale down models as a means of achieving process parameter ranging understanding. The impact of which has the further potential to improve the longevity of chromatography resins and reducing overall downstream purification cost.

ACKNOWLEDGEMENTS

The last prophet (may peace be upon him) said "A servant of God will remain standing on the Day of Judgement until he is questioned about his time on Earth and how he used it; about his knowledge and how he utilised it; about his wealth and where he acquired it and in what activities he spent it; about his body and how he used it" [Tirmidhi]

CONTENTS

LIST OF FIGURES

17

LIST OF TABLES

LIST OF EQUATIONS

LIST OF SYMBOLS AND ABBREVIATIONS

ANOVA	Analysis of variance ………………………………………	(-)
BCA	Bicinchoninic acid ………………………………………	(-)
BSA	Bovine serum albumin ……………………………………	(-)
C	Solute concentration ………………………………………	$(g\ L^{-1})$
C$_o$	Initial solute concentration ……………………………..	$(g\ L^{-1})$
Ca	Camp Number (= $\bar{G}t$) ……………………………………	(-)
CCF	Central composite face centred ………………………….	(-)
d_i	Impeller diameter	(mm) (m)
d_v	Vessel diameter …………………………………………...	(mm) (m)
DBC	Dynamic Binding Capacity ……………………………….	$(g\ L^{-1})$
DF	Dilution factor ……………………………………………	(-)
DoE	Design of Experiments ……………………………………	(-)
DOT	Dissolved Oxygen Tension ………………………………	(%)
d_{50}	Average particle size …….………………………………..	(μm) (m)
E.coli	_Escherichia coli_ ……………………………………….…	$(-)$
Fab'	Fragment antibody ………....……………………………...	$(-)$
$\bar{G}$	Mean velocity gradient ………….…………………………	(s^{-1})
$g\ L^{-1}$	Grams per Litre …………………………………………...	(-)
HETP	Height Equivalent of a Theoretical Plate …………………	(-)
HPH	High pressure homogenisation ……………………………	(-)
HPLC	High Performance Liquid Chromatography ……………….	(-)
_I_	Ionic strength ……………………………………………...	[M]
ICH	The International Conference on Harmonisation of Technical Requirements for Registration of Pharmaceuticals for Human Use ………………………….	(-)
IgG	Immunoglobulin ………………………………………….	(-)
IPTG	Isopropyl-β-D-thiogalactopyranoside ……………………...	(-)
L	Litre …………………………………………………….….	(-)
mAb	Monoclonal antibody ……………………………………...	(-)
mL	Millilitre ……………………………………………….….	(-)
mM	Millimolar ……………………………………………..…..	(-)
MW	Molecular weight …………………………………………..	(-)
N	Stirrer speed	$(revs\ s^{-1})$

NOR	Normal Operating Range …………………………………	(-)
OD	Optical density …………………………………………..	(Au)
P	Power …………………………………………………….	(W)
P$_0$	Power number ($P/\rho N^3 d_i^5$)	(-)
PEG	Polyethylene glycol ……………………………………..	(-)
PF	Purification factor ………………………………………	(-)
PLS	Partial Least Square …………………………………..	(-)
Q	Filtrate flowrate …………………………………………	(m^3 s^{-1})
QbD	Quality by Design ………………………………………	(-)
Re	Reynolds Number ………………………………………	(-)
STR	Stirred Tank Reactor ………..……………….............	(-)
t	Time ……………………………………………………...	(s) (min) (hour)
TMP	Transmembrane pressure ……………………………...	(bar)
USD	Ultra scale down ………………………………………..	(-)
w/v	Weight/Volume …………………………………………	(-)
w/w	Weight/Weight ………………………………………….	(-)
μL	Microlitre ……………………………………………….	(-)
V	Volume …………………………………………………	(m^3)
V$_{max}$	Maximum capacity (normalised) that can be filtered at time infinity ……………………………………………….	(L m^{-2})
VVM	Volume per volume per minute ………………………..	(-)
μ	Liquid viscosity ………………………………………..	(N s m^{-2}) (Pa s)
ρ	Density	(kg m^{-3})
σ	Liquid surface tension …………………………………	(N m^{-1})
∑	Sigma factor for centrifuge …………………………..	(m^2)

1. INTRODUCTION

1.1 Relevance of the Project

In today's pharmaceutical industry, pipelines bursting with drug candidates have pushed companies to invest in novel technologies to find quicker, cheaper and more robust routes through process development. Biotech drugs or biologics that include therapeutic proteins present new challenges, opportunities and options for optimising process development. Over the past decade, monoclonal antibodies (mAbs) synthesised by an animal in response to a foreign species, an antigen, have been responsible for several advances in the treatment of infectious diseases, cancer and autoimmune diseases (Farid 2006). They are increasingly accounting for a larger share of the pharmaceutical market. Monoclonal antibodies currently represent the second largest single category of biopharmaceutical substances under investigation as therapeutic drugs (Farid 2006). Forecasting firm EvaluatePharma predict that six of the top ten drugs in 2014 will be biologics. In contrast in 2008 only three biologics were in the list of top ten drugs, and not only will biotech drugs make up the majority of the bestsellers, EvaluatePharma predict that half of the top 100 drugs in 2014 will be biologics (Wenger 2010). The therapeutic protein sector has observed exponential growth in recent years due to the success of mAbs (Hood *et al.,* 2002, Low *et al.,* 2007), (figure 1.1). In 2008, there were 29 mAbs approved in the US market (Aggarwal 2009) with a projected growth of 14% per year through to 2012 (Reichert 2008). Developing and validating a process requires time and money, which is often restricted to unproven candidates in early clinical trials. Any delay to market of a potential blockbuster (defined as ≥ $1 billion in sales) risks losing over $3 million per day of potential revenue (Aggarwal 2009). The large (multi-hundred kilograms to tonne) quantities of monoclonal antibody production puts considerable economic pressure on both the current processes and the facilities required for purification (Low *et al.,* 2007).
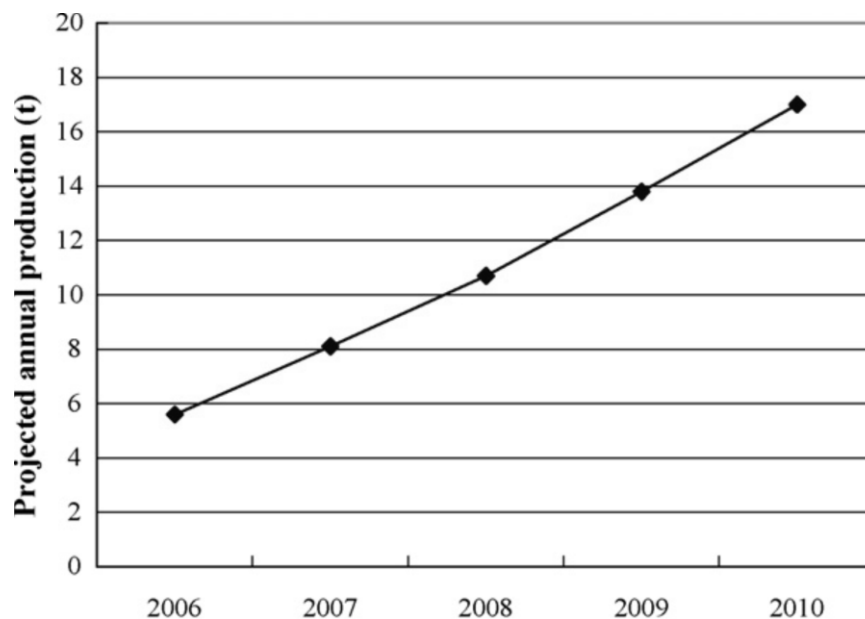
Figure 1.1: *Projected annual production of monoclonal antibodies. Numbers are in metric tonnes (Low et al., 2007)*

1.2   Aims of Project

This thesis seeks to create a novel, robust and cost effective multimodal precipitation process prior to packed bed steps. The primary focus will evaluate the precipitation of Fab' antibody fragments from partially clarified homogenised material using precipitating agents that are readily acceptable by regulatory bodies. The optimisation of these precipitation procedures involve a large number of experiments due to the large number of variables involved in the process. In this thesis, polyethylene glycol (PEG) and salt combinations as a route to improve the performance of the precipitation step was investigated using a Design of Experiments (DoE) approach based on Quality by Design (QbD) principles outlined in ICH (The International Conference on Harmonisation of Technical Requirements for Registration of Pharmaceuticals for Human Use) guidelines. ICH guidelines help to ensure that safe and effective medicines are developed and registered in the most resource efficient manner. This approach was used to select process parameters and unit operations that impact critical quality attributes to define design spaces and create a robust scalable process.

The number of variables and hence experimental space to be studied increases considerably when considering multimodal precipitation relative to single mode precipitation. This led to the development of a high throughput system utilising automated robotic handling at 1 mL microscale to enable rapid screening of a large number of variables quickly.

Volume reduction and product concentration have become major issues in early downstream processing steps and conventional processes based on adsorption or filtration will soon reach their limits in terms of economics, processing speed and scale in part due to high cell density (Bensch *et al.,* 2007). The next generation of bioprocess development will integrate microscale bioprocessing techniques into bioprocess development to alleviate the challenges facing it. Microscale techniques accelerate process development by enabling parallel experimentation and automation while requiring microscale quantities of material (Galaev *et al.,* 2005, Titchener-Hooker *et al.,* 2008). Critical bioprocess information can be obtained earlier in the development timeline providing better opportunities to understand more process parameters. These microscale systems should be developed to mimic key engineering characteristics for scale up (Titchener-Hooker *et al.,* 2008).

Specific milestones of this project include:

1. Development of a high throughput system utilising automated robotic handling in 96 deepwells at 1 mL scale per well to enable rapid screening of large design spaces in a Quality by Design (QbD) approach to integrate microscale bioprocessing techniques into conventional bioprocess development.

2. Developing a novel multimodal precipitation process combining polyethylene glycol (PEG) with ammonium sulphate, sodium citrate and sodium chloride for the precipitation of Fab' and or protein impurities from partially clarified homogenised *E.coli* feedstocks.

3. Scale up validation of the microscale approach to 50 mL laboratory scale and 5 L pilot scale for process interaction studies

1.3 Production of Fab' Antibody Fragments

Every immunoglobulin (IgG) antibody consists of four polypeptide chains (2 identical light chains and two identical heavy chains joined by disulphide bonds) and has two antigen binding sites (i.e. is bivalent). Each light chain and heavy chain consists of a variable region and a constant region (Hames and Hooper 2000). It is this variable region, which gives antibodies the ability to bind to a number of different antigens. The removal of the fragment crystallisable region (Fc) in antibody fragment molecules reduces the potential for an adverse immune response in recipients (Neal *et al.,* 2003). Monoclonal antibodies currently represent the second largest single category of biopharmaceutical substances under investigation as therapeutic drugs (Farid 2006). However, whole antibodies are large (~150 kDa) and require mammalian host organisms for expression, which require long culture times (~14 days). An IgG molecule with the Fc region removed produces two Fab' or fragment antibodies, which retain the antigen binding properties of the original IgG. The production of Fab' fragments are beneficial as they are stable, retain antigen binding properties, are smaller (~54 kDa) and are less immunogenic molecules than the whole antibody (Berg *et al.,* 2002). A benefit of Fab's, due to their smaller size, is that Fab's can be expressed in microbial cells, which results in significantly shorter culture times (~7 days) than mammalian based systems.

Truncated forms of antibodies such as Fab's and single chain Fv forms have many clinical applications. They are often used where Fc-mediated effector functions are not beneficial (Ljunglöf *et al.*, 2007). Exhibiting a shorter circulating half-life than full length antibodies and due to their smaller size, they are often used in applications such as tumour penetration and for medical imaging (Anderssen and Reilly 2004). ReoPro, a product that blocks the final common pathway to platelet aggregation manufactured by Lilly and Centocor is an example of a Fab' fragment used as a therapeutic (Farid 2006). For many applications, the effector functions of the antibody Fc region are not required for therapeutic activity (Chapman 2002). Furthermore, when trying to suppress an immune response, the presence of the Fc region is undesirable (Bowering 2004). In such cases, a Fab' fragment containing a single antigen binding domain can be formatted to provide the required binding activity, optimal pharmacokinetic properties and an alternative structure to the full length IgG. For instance, it has been demonstrated that Fab' can neutralise cytokines with equivalent potency to whole IgG antibodies (Weir *et al.,* 2002).

Schematic representations of IgG and Fab' are shown in figure 1.2.
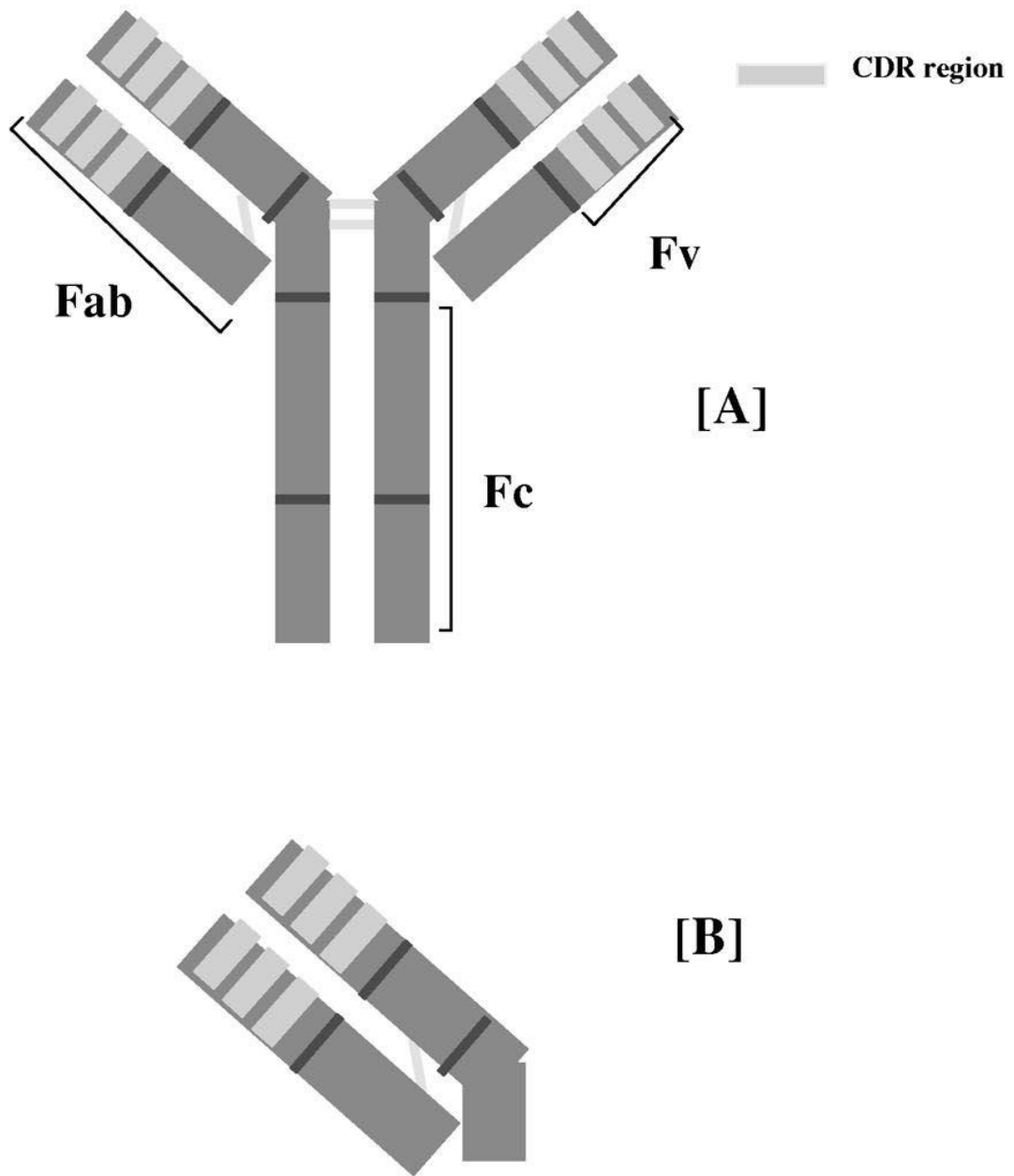
Figure 1.2: *Schematic representations of IgG (A) and Fab' (B) antibody molecules. Complementarity determining regions (CDRs) are regions within antibodies that complement an antigen's shape. CDRs determine the protein's specificity for specific antigens (Chapman 2002)*

The increasing commercial demand for antibody based molecules, such as Fab' fragments, and the large requirement for the treatment of chronic illnesses

necessitate the development of processes, which allow efficient, high volume, impurity free production at low cost, whilst maintaining high quality of the product.

There are a number of methods in the biotechnology industry for the production of protein products (Dainiak *et al.,* 2000). The type of protein produced whether extracellular or intracellular will determine the route chosen for the purification of the product. Extracellular proteins are separated from the whole cell allowing easier purification relative to intracellular proteins. Intracellular proteins require the cells to be disrupted to release the product complicating purification due to the release of impurities. Microbial expression systems provide a more economical means of production than traditional mammalian expression systems for fragment production (Chapman 2002). Microbial platforms are currently the system of choice for producing Fab' based antibody therapeutics, intercellularly, and the preferred expression host for Fab's is *E.coli.* The advantages of shorter processing time and increased scale of operation associated with *E.coli* production counter some supply and cost-of-goods constraints inherent in mammalian cell expression. Furthermore, its faster growth rate provides shorter culture times, and fermentation processes can be operated at up to five times the scale of mammalian cell cultures (Bowering 2004). It is possible that high production levels of antibody fragments are attainable when *E.coli* is used as the production organism (Anderssen and Reilly 2004). In addition, this process is virus free relative to mammalian systems and as there are no virus removal steps, which can reduce the downstream purification costs.

In the manufacture of Fab's, the costs of upstream processing are related to the production of the crude product, the fermentation media and fermentation plant. The costs that are associated with downstream processing are also substantial (Humphreys *et al.,* 2004). The downstream purification process can be divided into three categories, primary recovery, capture of the product and purification/polishing. Primary recovery involves the initial removal of cell debris by filtration or centrifugation. In the case of Fab' produced as an intracellular product, a cell disruption stage is required to release the product prior to primary recovery. Disruption of cells at industrial scale can be performed by mechanical means by using a homogeniser (Middelberg 1995).

A homogeniser consists of a positive displacement pump and a homogenising valve. Effluent from the homogeniser is chilled to minimise thermal damage to the

product caused by frictional heat generated due to the high fluid velocity that elevates the feed temperature. The pump is used to force the fluid under pressure into the homogenising valve (Middelberg 1995). Effluent is forced through a small orifice between the valve and the valve seat shown in figure 1.3. The fluid leaves the gap in the form of a radial jet that stagnates on an impact ring before leaving the homogeniser (Diels and Michiels 2006).
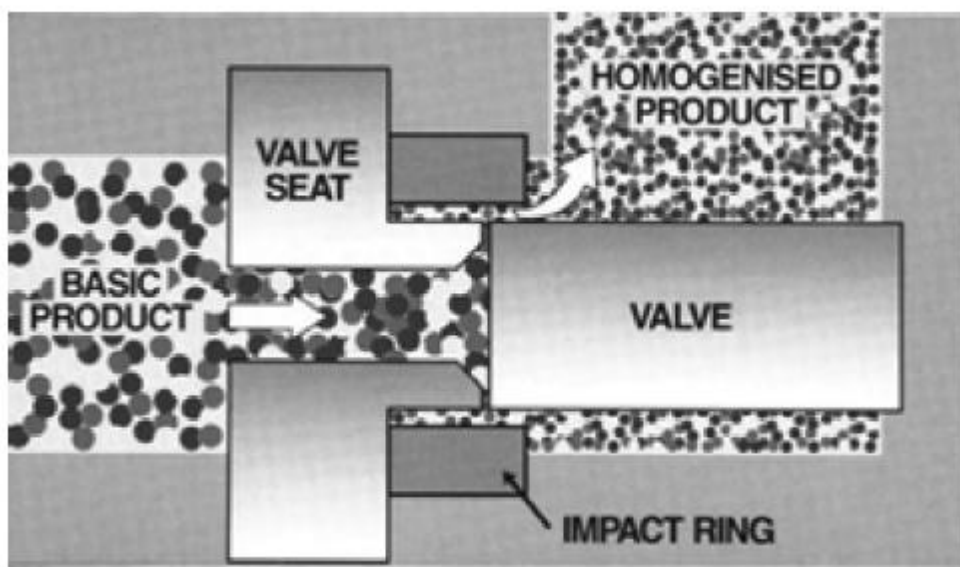
Figure 1.3: *Flow path of fluid through a homogenising valve (Diels and Michiels 2006)*

Following primary recovery, the product is isolated and purified from impurities by steps such as chromatography and ultrafiltration. Finally prior to drug formulation the product is further purified by filtration, chromatography and other affinity methods. The goal in this process is to maximise yield and purity while maintaining product stability and functionality. The current purification strategy is defined by cost and productivity of which half is associated with packed bed steps (Farid 2006). An example purification of a Fab' process by Celltech UK (figure 1.4) illustrates the significant number of steps required for purification and thus cost (Chapman *et al.,* 1999).
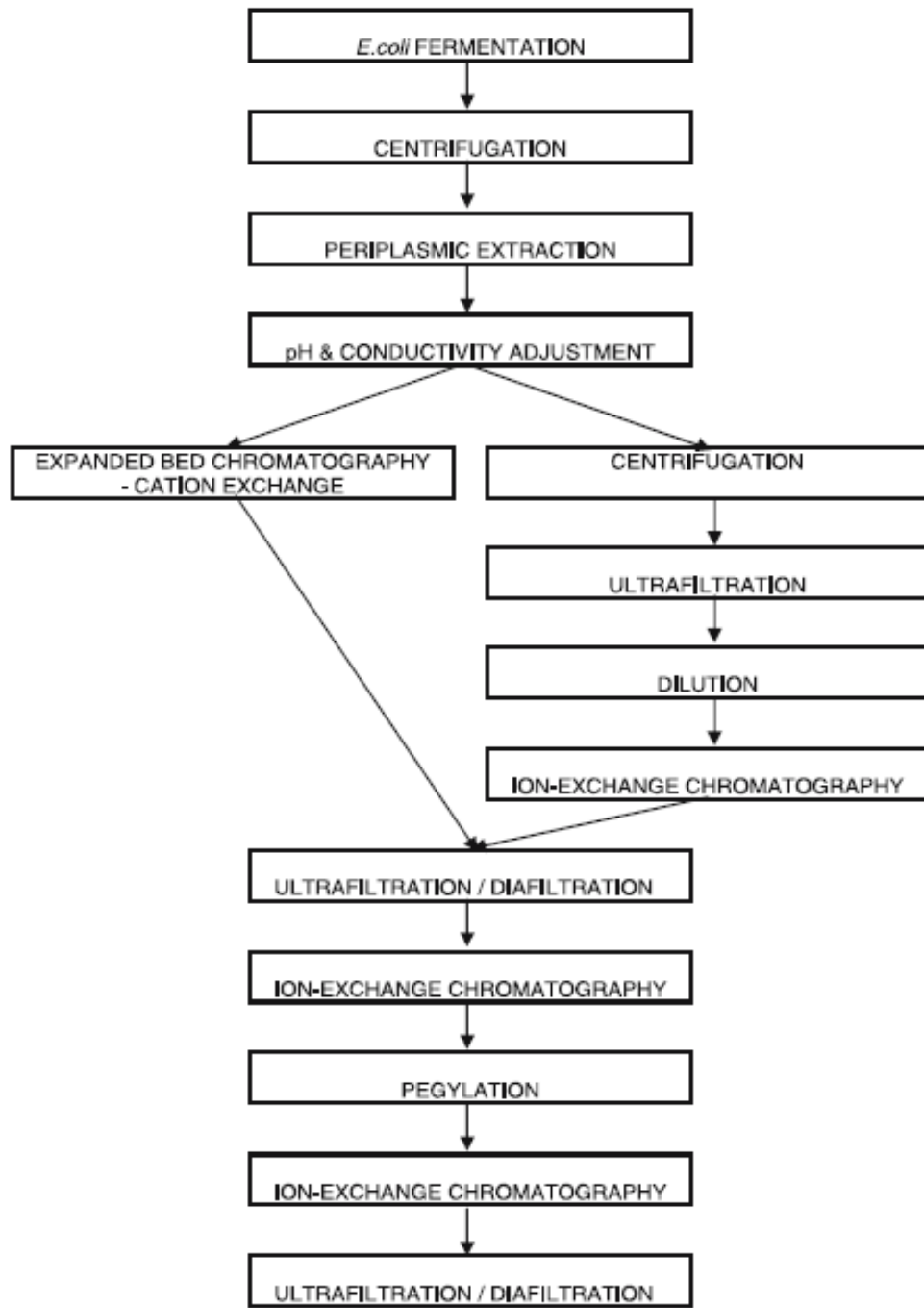
Figure 1.4: *Production of antibody fragments based on Celltech's E.coli process (Chapman et al., 1999)*

1.4 Mechanisms of Protein Precipitation

The efficient purification of recombinant proteins for therapeutic applications from cell culture fluid is a major bottleneck of the industry (Taipa *et al.,* 2001). Traditional purification techniques are based upon a number of separation steps. Each step contributes to a loss of product, yield and an increase in overall production time (Taipa *et al.,* 2001). The major process limitations are currently dominated by chromatography, specifically Protein A based resins (Hahn *et al.,* 2003). Protein A is a popular generic ligand for purification of monoclonal and antibody fragments (Hahn *et al.,* 2003). Protein A binds immunoglobulin's primarily through the Fc-region, although the low affinity binding sites in the Fab' region can also be used for purification of Fab' fragments (Hansen *et al.,* 1999). Chromatography can account for more than 70% of downstream costs, mainly from media cost and long cycle times (Przybycien *et al.,* 2004). In a typical, bind-elute chromatography step, the product of interest is captured, whilst the unbound material flows through the column. The product is then eluted by a change of mobile phase composition (Jungbauer 2005). Recent progress has enabled the use of these affinity interactions in alternative applications to overcome issues with packed bed chromatography such as column fouling and high pressures (Chen 1990).

A means of purification prior to a costly chromatography process is precipitation. Precipitation can be used to remove impurities in upstream feeds that may interfere with further downstream purification methods, and is therefore more effective early in the downstream purification process. A typical protein will have a surface that consists of regions with positive and negative charges along with hydrophilic and hydrophobic regions (Hilbrig and Freitag 2003). The complex interaction of these charged surfaces with its surrounding liquid environment will determine solubility. Precipitation achieves separation by causing the previously soluble protein to become insoluble or by adjusting the characteristics of the solvent resulting in precipitation of the product of interest (Stavrinides *et al.,* 1993, Rothstein 1994). It has been observed that protein solubility is a property of its molecular surface groups and a surrounding hydration layer (colloid model). Electrostatic groups keep the protein soluble whereas hydrophobic patches are induced in precipitation to form weak bonds between molecules resulting in aggregation (Stavrinides *et al.,* 1993). This change in state is explained by Gibb's free energy as the system strives to maintain high entropy so rather than opening a cavity around hydrophobic solute

particles it groups them together minimising entropic losses (Horváth *et al.,* 1976). The precipitated solids may be removed from the bulk fluid by a solid-liquid separation step such as filtration or centrifugation (Hilbrig and Freitag 2003).

Precipitation is a key process in the manufacture of chemicals and especially pharmaceuticals (Englard and Seifter 1990). Precipitation is most effective after having removed large solids (i.e. cell debris) from the processing stream. Precipitation allows low cost and high yield operation on much cruder feeds. Its early incorporation into the purification chain allows removal of major impurities and a reduction in processing volume whilst retaining a high product yield (Stavrinides *et al.*, 1993, Bonnerjea *et al.,* 1986). Thus, a "cleaner" process stream can be sent for column processing for which a reduced protein load can greatly reduce inventory costs and extend resin lifetime (Bonnerjea *et al.,* 1986). However, precipitation of proteins is not new, although its application is not widely used for monoclonal antibodies.

Fractional precipitation is the most common form of this operation due to its selective ability to precipitate impurities and proteins according to their solubilites such as the "double cut" fractionation method (Richardson *et al.,* 1990). Precipitant is first added to sufficient concentration to precipitate less soluble impurities ("1st cut") after which the concentration is further increased to recover the desired protein in a fresh precipitated phase ("2nd cut") leaving the more soluble impurities in solution. Temperature and pH can also be adjusted to enhance yield and purification factor.

There are seven techniques most commonly used to cause proteins precipitation of which four are described:
1. Salting out by the addition of high concentrations of neutral salts
2. Addition of non ionic polymers such as polyethylene glycol (PEG) to protein solutions
3. pH adjustment to utilise the fact that solubility is a function of net charge and is at a minimum at the isoelectric point – zero net charge
4. Addition of acids
5. Reduction in the solvent dielectric constant by addition of miscible organic solvents
6. Addition of charged polyelectrolytes which act as flocculating agents
7. Interaction of polyvalent metal ions

1.4.1 Hofmeister Series

The minimum solubility is considered the point at which the pH of the solution corresponds to the isoelectric point of the protein (Harden and Harris 1952). The isoelectric point being the point at which there is no net charge on the surface of the protein. The presence of hydrophobic residues and hydrogen bonds in the protein structure make the prediction of solubility properties difficult. A barrier to aggregation of protein may be considered to come from a number of sources. Surface associated water can interfere with the aggregation process by means of a small layer several tenths of a nanometre deep (Stavrinides *et al.*, 1993). This induces a barrier to aggregation and it is only if this barrier is overcome that the effectiveness of collisions is improved. Adding a precipitation agent changes the surface characteristics so that the energy barrier is greatly reduced and aggregation can take place (Stavrinides *et al.*, 1993). There are a number of factors, which effect protein solubility including availability of solvent, pH, ionic strength, dielectric constant, temperature and specific ion or solute effects (Janson and Rydén 1998).

However, the protein solubility depends on the salt content of solvent and their location in the Hofmeister series (Zhang and Cremer 2006). The Hofmeister series is useful in considering the reagent for use in precipitation processes using salt. It was originally thought the Hofmeister series classifies ions based on their ability to change water structure. The mechanism is unclear, and it has recently been suggested that the interactions between protein ions and water ions are important in the mechanism (Zhang and Cremer 2006). The series ranks anions based on their effect on solubility of proteins in solution. The highest members such as sulphate increase the solvent surface tension and decrease the solubility of non polar molecules (the process of salting out). The lower ranked salts in the series weaken the hydrophobic effect thereby increasing solubility, known as the salting in effect (Richardson *et al.,* 1990). The highest members of the series, such as sulphate, strengthen the hydrophobic effect by shielding dissociated ions, effectively salting out the protein.

The choice of salt is mainly determined by its solubility and valency by its potential for denaturation (Melander and Horváth 1977). The anions of both acids and salts have been ranked in the Hofmeister series by their ability to reduce protein

solubility; additionally, this property is also inversely related to denaturation (figure 1.5).

Citrate → Phosphate → Sulphate → Acetate → Chloride → Nitrate →Thiocyanate

Kinder to protein   Protein denaturation
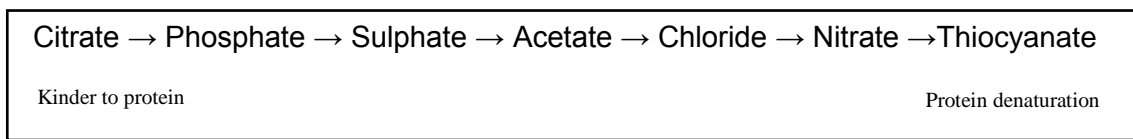
Figure 1.5: *Hofmeister series in order of decreasing ability to cause salting out and increasing ability to cause denaturation*

The higher members of the series such as citrate work by increasing solvent surface tension, consequently affecting the solubility of non polar molecules (Melander and Horváth 1977). Ammonium sulphate is the industry's most common reagent, owing its popularity to its high solubility, low cost operation and stabilising effect on proteins (King 1972, Walsh and Headon 1994). The density of the protein-ammonium sulphate precipitate is sufficiently low that it does not interfere with sedimentation significantly. However, precipitate sizes are small and large amounts of ammonium sulphate must be used, which can be potentially corrosive to downstream chromatography resins. Dialysis or diafiltration would be required to remove it, and there are environmental issues with disposal of large volumes of ammonium sulphate at scale (Hahn *et al.,* 2003).

Melander and Horváth (1977) proposed that the observed change in protein solubility was directly linked to the electrostatic free energy available for solvation (the protein forming a hydrophobic cavity). The presence of electrolytes raises the surface tension of the solvent (Przybycien and Bailey 1989). They found that the increase in the solution's molar surface tension from adding salt ions was directly proportional to the hydrophobic interaction potential between protein particles and this forms the basis of the Hofmeister series.

Sodium citrate is also a very capable precipitating agent as shown by the high position in the Hofmeister series but falls foul of limited solubility at room temperature (Kim and Bae 2003). Sodium sulphate has been used for IgG precipitation, as the precipitated IgG is usually very stable. Sodium sulphate is especially suited to heat stable proteins due to its high solubility at temperatures over 40°C (Kim and Bae 2003).

1.4.2 Salting Out

Melander and Horváth (1977) proposed a mechanism of salt precipitation (figure 1.6). The addition of neutral salts results in their ions bonding with water molecules, which would otherwise be hydrating proteins. Proteins will be forced by reduced hydration to aggregate in these conditions (utilising hydrophobic surface patches). The entropy cost of forming a cavity around non polar molecules is lower (the amphiphilic protein as opposed to polar salt ions) and thus the effect is driven by the loss of hydrogen bonding and the higher entropic. These losses can be minimised by forcing non polar molecules together. The loss in the water monolayer surrounding the protein reduces the barrier to aggregation as high concentrations of salt ions are introduced to the system allowing aggregation from solute collisions (formation of hydrophobic bonds), which is intensified by mixing. An increase in free energy is required to accommodate the protein in its dissolved state, i.e. opening a cavity in the solvent becomes unfavourably high in a high salt environment. However, at low ionic strengths, protein solubility is raised above that of its pure aqueous solution (termed salting in) because of solvating electrostatic interactions between salt ions and charged groups on the protein surface (Stavrinides *et al*., 1993).

The cavity theory proposed by Melander and Horváth (1977) was an extension of a theory by Sinanoglu and Abdulnar (1965). Sinanoglu and Abdulnar (1965) have suggested that the free energy of cavity formation reflected in the surface tension of solvent has a key role in the stability of proteins. The consequence of the proposed theory states that protein solubility is derived from a composite salting out constant, which incorporates an electrostatic salting in term and an opposing hydrophobic salting out term. Therefore, at low salt concentrations there is a salting in effect, however, by increasing the salt concentration the hydrophobic cavity increases resulting in precipitation due to a reduction in solubility (Richardson *et al.,* 1990).
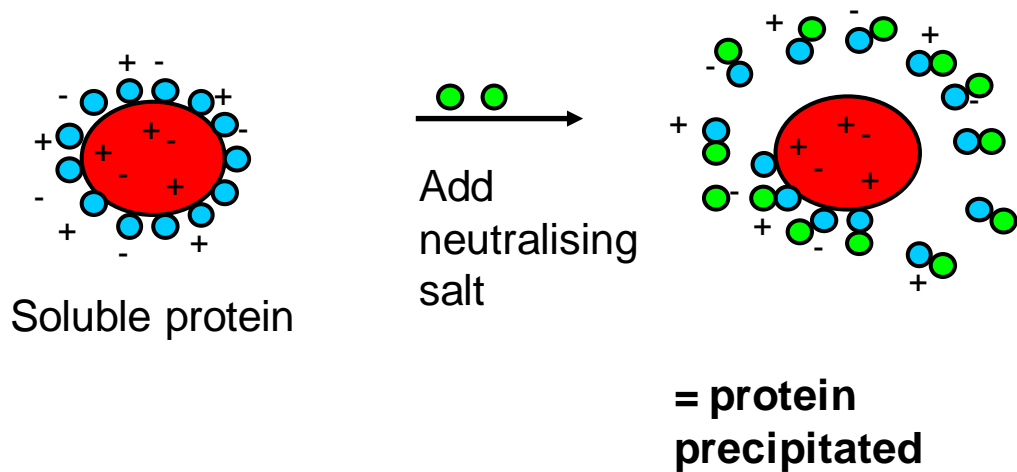
Figure 1.6: *A potential mechanism of protein precipitation using neutralising salts (Melander and Horváth 1977)*

Salting out is generally used to for the purposes of protein purification by fractional precipitation (Richardson *et al.,* 1990). Fractional precipitation is performed adding the first precipitant to precipitate less soluble impurities. After recovery, the concentration of the precipitant is increased to precipitate the desired protein, leaving impurities that are more soluble in solution (Richardson *et al.,* 1990, Cheng *et al.,* 2005). The decrease in solubility of a protein with the addition of increasing concentration of salt can be represented by the equation developed by Cohn (Foster *et al.,* 1971, Atha and Ingham 1981).

$$\text{Log } S = \beta - Kc \qquad \text{(1.1)}$$

Equation 1.1: *Cohn equation, where S is protein solubility (grams per litre) and c is precipitant ionic strength (moles per litre). β is protein solubility constant extrapolated to zero ionic strength. K is a salting out constant, which is a function of protein type and is independent of pH and temperature (Richardson et al., 1990). This equation is represented in figure 1.7 (Foster et al., 1971)*
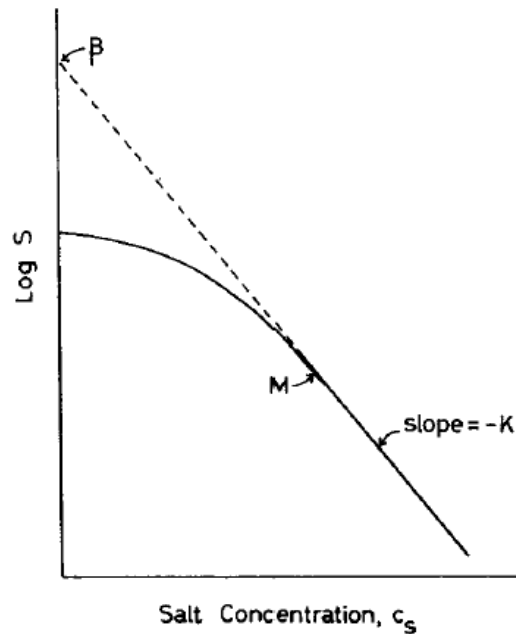
Figure 1.7: *Salting out curve (Foster et al., 1971)*

The range of ionic strength is only valid until the point at which the protein solubility curve meets the straight line, which is represented by M in figure 1.7 (Foster *et al.,* 1971). This position has variability caused by the nature of the system and the initial concentration of the protein in solution (Foster *et al.,* 1971).

Salting out can be described as a phenomenon by which water is removed from the protein bringing opposing charges on the proteins surface together (Scopes 1987 and figure 1.6). Water can also be removed by the addition of an organic solvent or by the addition of a non ionic polymer such as polyethylene glycol (PEG) (Scopes 1987). The addition of an organic solvent will increase the hydrophobic regions of the protein, thus decreasing solubility. However, this property can also destabilise the hydrophobic protein core potentially denaturing the protein (Scopes 1987).

1.4.3 Non Ionic Polymers

It is known that the addition of non ionic polymers to a protein solution decreases protein solubility (Thrash *et al.,* 1991). The use of non ionic polymers such as PEG has recently become a popular choice due to its cost, availability and stable use in affinity columns (salts can denature the affinity ligands so must be removed prior to

material being loaded onto a column) (Chapman 2002). Its precipitating action is similar to salts in that it works by volume exclusion, effectively minimising the water monolayer for protein solvation (Stavrinides *et al.,* 1993).

PEG is a non toxic, water soluble polymer available in many degrees of polymerisation commonly ranging from 4000 to 20000 (Atha and Ingham 1981, Scopes 1987, Lewis and Metcalf 1988). PEG is soluble in water due to the ether oxygen's spread along the length of the polymer, which form hydrogen bonds with the surrounding water molecules. PEG has interesting biological properties, which have been exploited for use as a precipitating agent for proteins (Atha and Ingham 1981). It has the advantage over salts of reducing the time required for precipitated material to equilibrate and achieve a physical state suitable for centrifugation (Ingham 1990). PEG has been used to concentrate a product of interest. Lewis and Metcalf (1988) successfully demonstrated PEG 6000 as an effective concentrating agent for the detection of human virus pathogens such as Hepatitis A.

It has been suggested that the Cohn equation (equation 1.1) can be applied to PEG precipitation (equation 1.2). A theoretical expression has been developed based on the excluded volume effect (Foster *et al.,* 1973). The equation has a similar form to that of the Cohn equation and is represented in equation 1.2.

$$\ln S = \ln S^o - aC \qquad \textbf{(1.2)}$$

Equation 1.2: *Solubility of proteins in polymer solutions, where S is the solubility of the protein, C is the concentration of the polymer, and S^o and a are constants. S^o is the solubility of the protein in the polymer free solution, a is the coefficient indicating the interaction between PEG and the protein (Atha and Ingham 1981)*

This equation is valid for dilute protein solutions. Higher concentrations of protein in solution require an additional *bS* term to be added to the left hand side of the above equation. This incorporates protein-protein interactions present at high protein concentrations in solution (Atha and Ingham 1981).

Middaugh *et al.,* (1979) found that at low concentrations, a linear relationship between log solubility and PEG was discovered based upon experimental data

using various haemoglobin proteins. Subsequently, an extrapolation of the protein solubility to zero PEG could be made to determine the thermodynamic activities of that protein in its saturated state. However, under conditions of high solubility the extrapolated intercept exceeds the actual solubility of the protein. The difference can be mathematically calculated and is a function of the protein-protein interactions and activity coefficient (Atha and Ingham 1981). The nature of the protein PEG complex at the extrapolated regions are poorly understood (Middaugh *et al.,* 1979). However, to understand the thermodynamic solution process of proteins, two mechanisms have been suggested to account for the use of PEG as a precipitating agent (Lewis and Metcalf 1988).
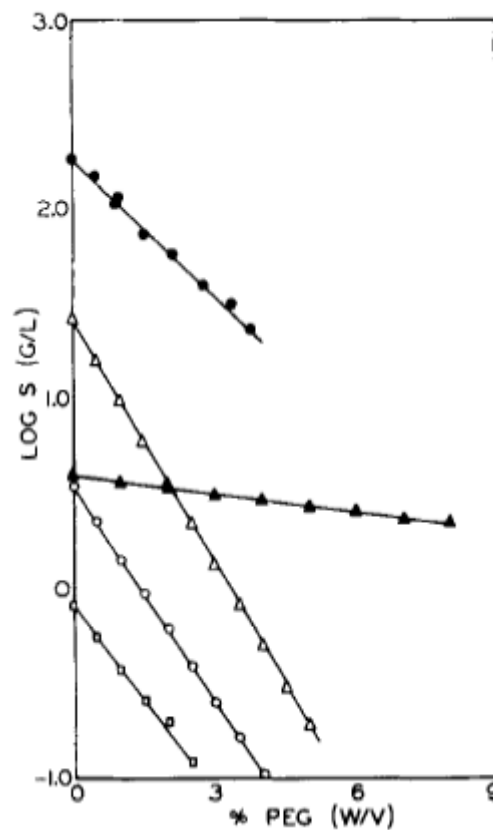
Figure 1.8: *Effect of PEG (% w/v) on the solubility of various haemoglobin proteins at various concentrations on a semi log plot (Middaugh et al., 1979)*

The first mechanism was discussed by Atha and Ingham (1981). Their experimental work was designed to evaluate the excluded volume concept and how the theory applies to the precipitation of proteins with the addition of PEG. They evaluated a range of molecular weight PEG's with a range of protein sizes. They suggested that

the effectiveness of PEG to precipitate proteins increases with the size of the polymer (figures 1.8 and 1.9).
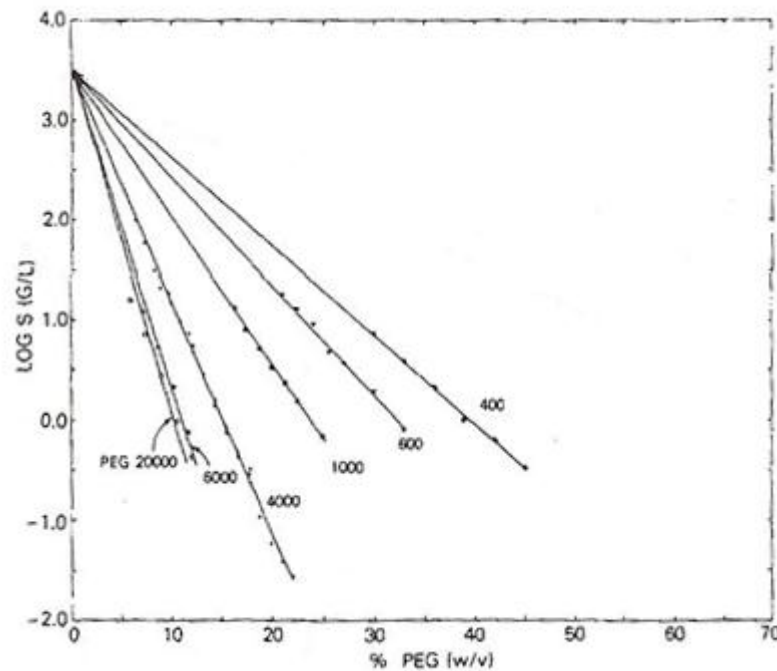
Figure 1.9: *Effect of various polymers of PEG (% w/v) on the solubility of human serum albumin 14k-670k proteins on a semi log plot (Atha and Ingham 1981)*

However, their results based upon protein polymer interactions suggest that PEG has little interaction with proteins and precipitation is caused by excluded volume effects (Middaugh *et al.,* 1979, Atha and Ingham 1981). Excluded volume refers to that part of the PEG molecule that cannot occupy space that is already occupied by another part of the same PEG molecule (Atha and Ingham 1981). They suggested that PEG acts as an "inert solvent sponge" that prevents interaction of all proteins present with the solvent, effectively increasing their concentration until solubility is exceeded and precipitation occurs (Lewis and Metcalf 1988). The approach is similar to salting out, and precipitation will be affected by factors including protein size, concentration, charge, and initial ionic strength (Lewis and Metcalf 1988).

Lee and Lee (1981) have suggested the second mechanism, which emphasises the importance of protein charge. To understand the mechanism of PEG and protein interactions, the solvent interactions between PEG and lysozyme were studied by varying polymer size and concentration of PEG. They suggested that PEG does not

induce any structural changes to the protein, although PEG maintains the native confirmation of the protein. However, the addition of PEG to the system destabilises the solvent system to an unfavourable thermodynamic state. Therefore, the addition of PEG in the protein solution would provide the driving force for precipitation so that the system would return to a thermodynamically favourable state. The driving force effect is proportional to the size of the polymer, and it is assumed that the protein surface is fully charged. The addition of PEG results in an unfavourable thermodynamic effect on the solubilised PEG causing it to be excluded from the protein domains, resulting in precipitation of the protein (Lewis and Metcalf 1988). Therefore, highly charged and hydrophobic proteins will be more easily precipitated (Lee and Lee 1981).

Furthermore, Lee and Lee (1981) suggested based on their work with tubulin and PEG of varying molecular weights that PEG does not induce any structural changes in proteins. It was found that PEG helps to maintain the native conformation of proteins under conditions in which the protein might otherwise assume structures other than its native form (Lee and Lee, 1981). It has also been found that in all cases the addition of protein to all PEG-water systems induces destabilisation allowing for phase separation (Perumalsamy and Murugesan 2006, Rosa *et al.,* 2007, Azevedo *et al.,* 2009 (b)). The system always provides a driving force to a thermodynamically more favourable state, which generates phase separation. The magnitude of this driving force was found to increase with increasing concentration of the polymer. They also discovered a relationship between the driving force and molecular weight of the polymer used in which the concentration of PEG required decreased with increasing molecular weight (Lee and Lee 1981).

Mahadevan and Hall (1990) have suggested that stearic constraints where polymers are excluded from the space separating two protein molecules are significant. The distribution of the polymer causes a "pressure imbalance" that pushes the proteins against each other. However, this fails to explain the effect of protein charge on protein precipitation by non ionic polymers, though it incorporates the effect of pH on protein precipitation by non ionic polymers. The positive chemical potentials of the proteins on the addition of PEG indicate that the predominant interactions between PEG and proteins in an aqueous medium are repulsive in nature and that this repulsion becomes stronger with an increase in PEG size (Mahadevan and Hall 1990). These models are approximate as they

assume that the solvent is a continuous fluid, ignoring the contribution of hydration forces to protein stability.

When considering the choice of reagent, the entire process must also be considered. The precipitant must meet processing limitations, for example, hydrochloric acid (HCl) is highly corrosive and its use in high pressure devices such as homogenisers is ill advised. Salt precipitation can be integrated with a hydrophobic interaction chromatography column (HIC) to minimise the process steps prior to purification. A HIC column consists of a chromatographic matrix containing hydrophobic groups, and can bind proteins in the presence of high salt concentrations. It binds proteins from aqueous solutions to different extents depending on protein structures and a range of controllable factors including concentrations of salts, pH and organic solvents.

PEG is a useful precipitant to combine with affinity purification techniques, as it does not denature the ligands, as some salts are known to. Protein integrity, ease of operation, the fractionation ability and the final use of the product are other factors to be considered. Some precipitants such as metal ions are associated with denaturation and safety concerns; ammonium sulphate is toxic with respect to clinical use (Dainiak *et al.,* 2000). Medicinal products are subject to strict purity requirements so any reagent residues in the final product need to be safety tested or removed.

1.4.4 Isoelectric Precipitation

Isoelectric precipitation works at the isoelectric point (pI) of the protein so that a zero net surface charge is exhibited and thus diminishing hydrophilic interactions (figure 1.10). This technique works best for proteins with hydrophobic surfaces and low hydration constants (Radola 1973). Caution should be exercised with proteins with an acidic pI to avoid denaturation (pH < 4); otherwise, acids are mostly inexpensive and well tolerated by proteins (Bramaud *et al.*, 1997).
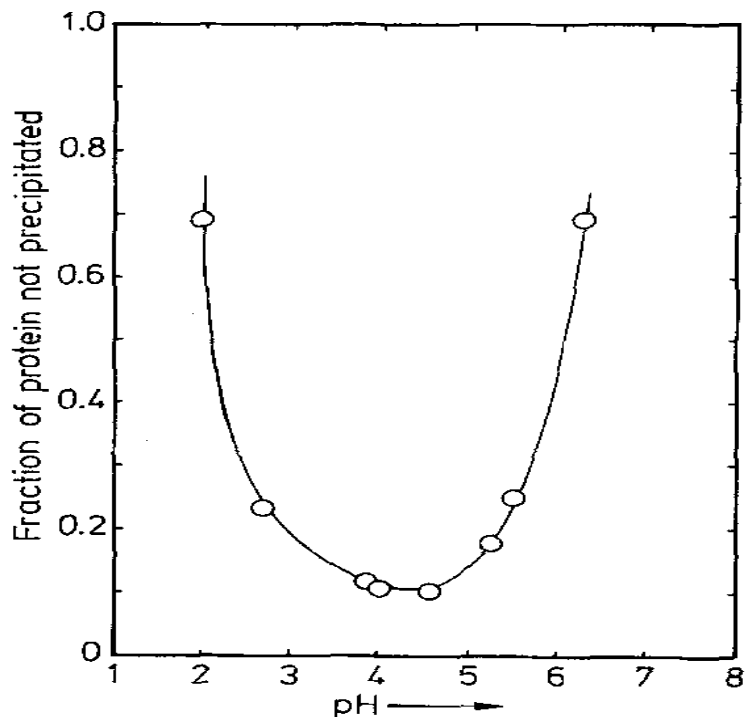
Figure 1.10: *The effect of pH on soya protein concentration remaining in solution, expressed as a fraction of initial concentration of total water extract (Virkar et al., 1982)*

Other methods used to precipitate proteins utilise ionic polyelectrolytes such as in flocculation and polyvalent metal ions, which are known for a strong precipitating action. They can subsequently be removed by chelating (formation or presence of two or more bonds between a ligand and central ion) or ion exchange chromatography.

1.4.5 Acids

Acids are usually inexpensive, require lower concentrations with respect to salts and are accepted in many protein food products. In fractional precipitation, it is sometimes possible to directly move to the next cut without removing the acid (contrary to many salts). However, acid use runs the risk of protein denaturation.

Figure 1.11 shows the effect of pH on precipitation of lysozyme with sodium chloride (Shih *et al.,* 1992). Lysozyme's pI is at pH 10.5 where, as expected, its concentration is lowest but precipitation is also seen in the acidic data range.
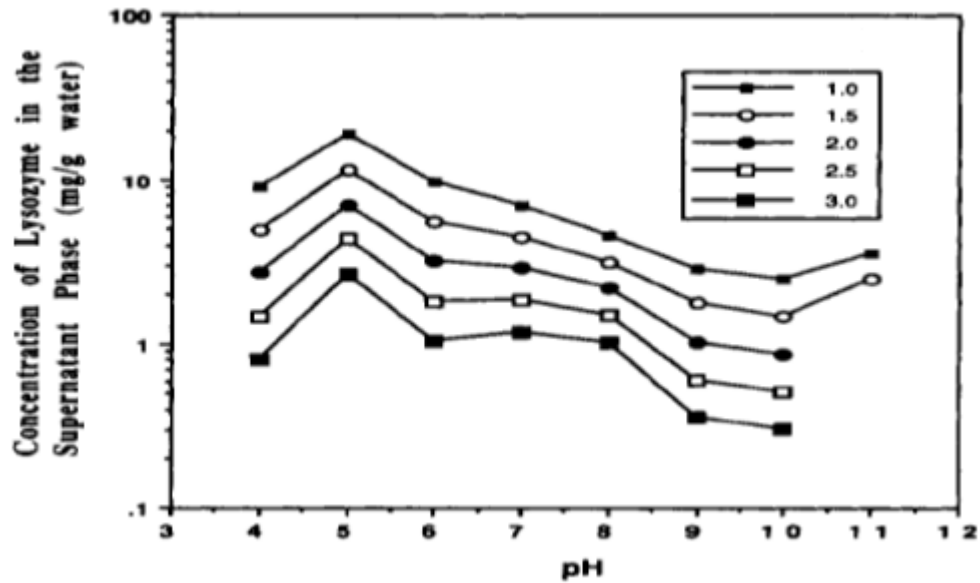
Figure 1.11: *Effect of pH on lysozyme solubility with sodium chloride (▪ 1 M, ○ 1.5 M, ● 2 M, □ 2.5 M and ■ 3 M) (Shih et al., 1992)*

1.5 Precipitate Formation

Precipitation is generally described to take place over five distinct stages:

Mixing→ Nucleation→ Growth by diffusion→ Growth by fluid motion→ Ageing (Bell and Dunnill 1982).

The precipitant is responsible for creating a favourable environment for hydrophobic interactions between proteins resulting in aggregation upon molecular collisions during mixing.

1.5.1 Nucleation

Nucleation is the formation of miniature "crystals" that will eventually grow to sedimentation size. Following the onset of aggregate formation, both the number and size of aggregates increase while the native protein population is depleted (Chi *et al.,* 2003). If the concentration of nuclei is too high, the precipitate will be too fine, as the growth of the precipitate will be spread over too many sites. This kind of precipitate will be difficult to sediment. Therefore, the control of nucleation will

determine the quality of the precipitate. The optimal strategy for precipitation is to keep the degree of super saturation low.

Nucleation and growth is determined by diffusion controlled (Brownian motion), perikinetic growth resulting in a "primary particle" of roughly 0.2 µm (Virkar *et al.*, 1982, Bell *et al.,* 1983). Therefore, at a greater rate of collisions a faster growth and higher particle concentration is observed. There is also a linear rate of increase of particle volume with time (figure 1.12). When surface properties of protein molecules have been changed, collisions between molecules will result in aggregate formation. Growth rate then becomes orthokinetic (convective collisions of primary particles) as large particles (> 1 µm) need additional energy provided by macro mixing to overcome the energy barrier for aggregation (Bell *et al.,* 1983). This means that the growth rate of particles will increase with a greater mean velocity gradient ($\bar{G}$) and greater particle concentration (equation 1.3). The size of the particle will increase exponentially with time. However, Smoluchowski's collision frequency theory, states that the probability of collision between small and large particles is greater than the probability of collision between small particles, and that large particles behave as nuclei around which small particles collect. Therefore, the effectiveness of a collision in forming an aggregate will decrease with greater size of the colliding particles (Bell and Dunnill 1982). Upon arrival at a critical size, growth stops and the ageing stage commences. Ageing is optimal in a low shear environment where erosion and rearrangement enhance particle strength.
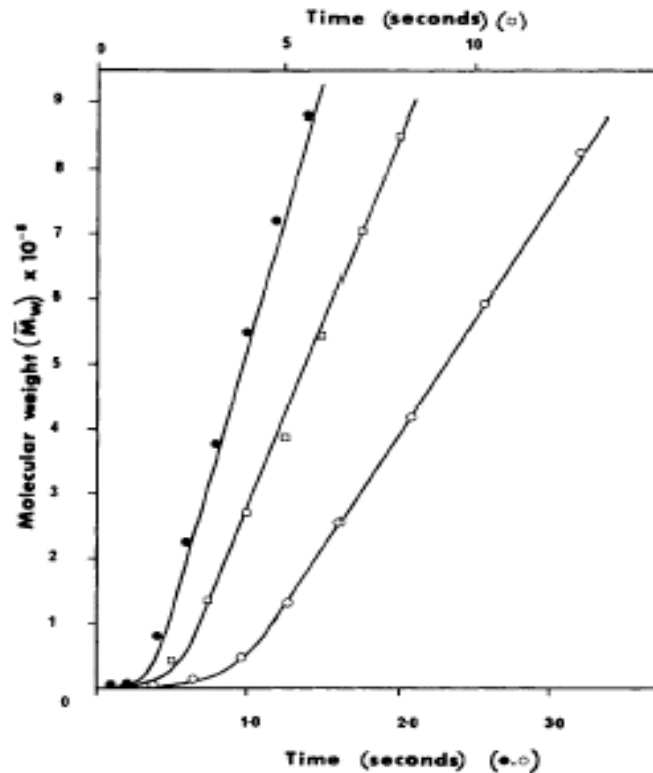
Figure 1.12: *Molecular weight-time plots for three concentrations of casein. Initial non linear phase of growth is due to modification of protein surface with calcium ions (Parker and Dalgleish 1977)*

1.5.2 Growth by Diffusion

There are other factors affecting the rate of particle collisions and growth, such as protein concentration and temperature (Parker and Dalgleish 1977). Temperature also determines the strength of the hydrophobic bond between proteins (Gibb's free energy). Overall, the final particle size is mainly determined by the mean velocity gradient ($\bar{G}$) and particle strength.

The mean velocity gradient ($\bar{G}$) is a common engineering parameter for describing the shear rate within a stirred vessel (Camp and Stein 1943).

$$\bar{G} = [P / V\mu]^{0.5} \qquad\qquad (1.3)$$

Equation 1.3: *Mean velocity gradient (s^{-1}), where μ is the dynamic viscosity ($N\ s\ m^{-2}$), V is the volume (m^3) and P is the Power input (W) (Rushton et al., 1950)*

$\bar{G}$ has long been used to characterise turbulent velocity gradients in a variety of stirred vessels (figure 1.13). It is based on Power dissipation (P) per unit volume (V) for turbulent flow (Re > 10^5) where the Power number (P_o) is 4-6 for a four baffled stirred tank with a 6 blade Rushton impeller (Rushton *et al.*, 1950). In studies with soya protein it was seen that low $\bar{G}$ values (< 200 s^{-1}) produced large precipitates while higher $\bar{G}$ values (> 400 s^{-1}) gave rise to smaller aggregates (Bell and Dunnill 1982). It has been suggested that there is a direct correlation between the final particle size and $\bar{G}$ (Tambo and Hozumi 1979).
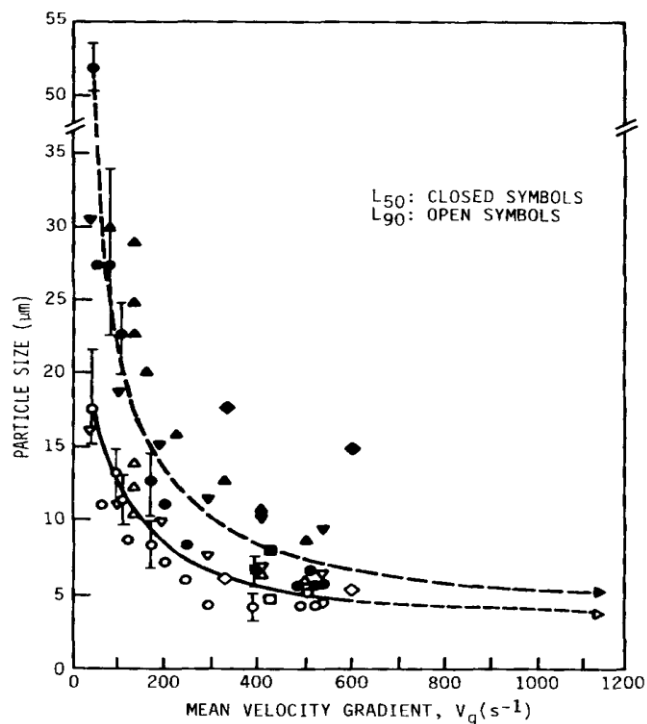
Figure 1.13: *The effect of the mean velocity gradient ($\bar{G}$) on particle size for soya protein precipitates (Glatz et al., 1986)*

1.5.3 Ageing

The dimensionless, Camp number (Ca) can be used to describe overall mixing conditions in a stirred vessel.

$$Ca = \bar{G}t \qquad\qquad (1.4)$$

Equation 1.4: *Camp number to indicate mixing conditions. Where t is the time of mixing (s) and $\bar{G}$ is the mean velocity gradient (s^{-1}) (Camp and Stein 1943)*

Ca gives an indication of mixing conditions and the role of agitation in stabilising precipitates (Bell and Dunnill 1982). The approach has long been used in the water treatment industry for flocculation processing (Bell and Dunnill 1982). The strength and density of particles have been shown to be directly related and both are critical variables in centrifugal separation (Tambo and Hozumi 1979). Trouble arises when precipitates break up by experiencing shear stresses inherent to the recovery process (i.e. harsh pumping, centrifuge feed zones, etc.) and clarification becomes compromised. In such situations, the revised challenge is to create strong precipitates, which are smaller. To maximise particle strength it is recommended that a Ca value greater than 10^5 is used (Bell and Dunnill 1982). In the water treatment industry values of 10^4-10^5 (with $\bar{G}$ ranging from 10-100 s^{-1}) are used (Camp and Stein 1943).

Figure 1.14 illustrates the response of precipitates formed under a range of Ca to equivalent shear treatment. Soya protein precipitates were strongest when the Ca value were > 10^5 as were seen in the small change of final to initial mean diameter (Bell and Dunnill 1982). The shear treatment for these may have utilised similar shear conditions as during precipitate formation.
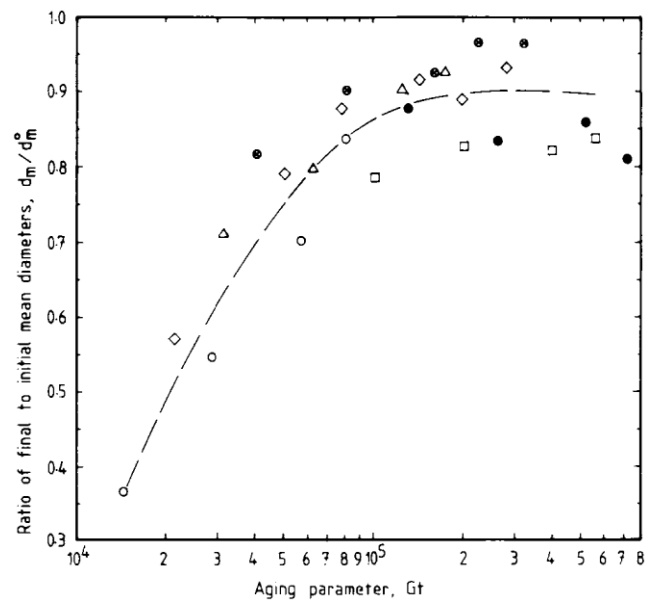
Figure 1.14: *Camp number (Ca) versus precipitate susceptibility to capillary shear (Bell and Dunnill 1982)*

The precipitate will develop a tight and compact structure when it is sufficiently deformed under shear (Bell and Dunnill 1982). Extensive ageing has been shown to increase particle strength and consequently improve recovery (Bell and Dunnill 1982). Fines are "mopped up" by larger particles, "filling in" gaps and increasing density. Figure 1.15, shows the reduction in the number of aggregates disrupted with increased ageing and by the increasing uniformity of the particle fragments that are broken off (Bell and Dunnill 1982).
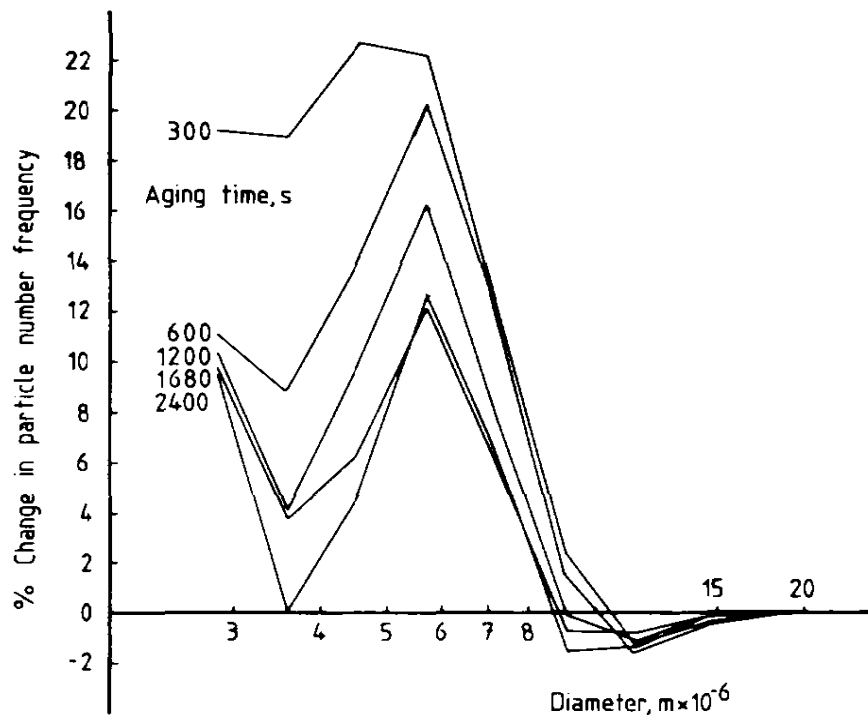
Figure 1.15: *The effect of ageing on the frequency of "broken particles" after capillary shear (Bell and Dunnill 1982)*

During ageing the final mean particle size is determined by a dynamic equilibrium between the rates of aggregate growth and impeller induced breakage (Shamlou *et al.,* 1996).

1.5.4 The Effect of Mixing, Turbulence and Time on Precipitate Particle Size Distribution (PSD)

It is important to achieve good mixing between the feed and the precipitant solution particularly during nucleation. Otherwise, super saturation and under saturation regions will be present in the solution.

Mixing, turbulence and time have a direct effect on precipitate PSD. Research has shown that precipitates which undergo turbulent flow result in particle breakage (Byrne and Fitzpatrick 2002). This is especially true for precipitates formed and aged under mild agitation conditions. Particles formed and aged under low shear conditions, though initially larger, are in fact weaker and fragment largely in turbulent flow. The strength of precipitate particles are important to withstand the fluid shear forces encountered in pumps and centrifuge feed zones without reducing the particle size. The particle size must meet the particle size criteria in the subsequent centrifugation stage for successful separation (Byrne and Fitzpatrick 2002).

For microscale data to be useful for designing large scale processes, the engineering environment within microwells needs to be understood and characterised. Rapid and efficient mixing is a key bioprocessing feature and underpins the quantification of precipitation reactions. There has been work on different forms of macro mixing within microwells including jet mixing, magnetic impellers and shaken microplates (Nealon *et al.,* 2006, Titchener-Hooker *et al.,* 2008). The versatility of liquid handling robots has been studied in producing "micro-substitutes" for large scale engineering parameters (Nealon *et al.,* 2006).

For many bioprocess applications, particularly biocatalysts and stability assays, shaken systems are not appropriate and mixing should be performed in static microplates (Aucamp *et al.*, 2005). Rapid and efficient mixing can be provided from the liquid addition by the pipette tip of a liquid handling robot followed by repeated reaspirations and dispenses. However, this method does not suit the high throughput nature of the tests (Nealon *et al.*, 2006).

In precipitation reactors the mechanical impellers are an important source of shear, which helps, define precipitate size and structure (Shamlou *et al.*, 1996). The longer a particle resides in the high shear impeller region, the stronger it is thought to be,

as shown in studies comparing continuous and batch prepared precipitates (Bell and Dunnill 1982). Jet mixing by entrainment can provide the appropriate homogenous distribution, but the shear element to cap particle growth and induce strengthening by rearrangement requires a high energy dissipation zone (Tambo and Hozumi 1979, Shamlou *et al.*, 1996). This can be provided by repeatedly aspirating and dispensing the forming precipitate at speed through a pipette tip. Shearing of this nature has previously been accomplished with homogenisers and may provide insight into this substitute to the ageing phase (Aucamp *et al.,* 2005).

1.6 Precipitation Reactors

The size, strength and rheological characteristics of aggregates have all been linked to precipitation reactor design and configuration. Vessel geometries, baffles, impellers and whether the operation is continuous or batch all contribute to the precipitate's characteristics.

Larger and faster impellers have greater tip speeds and hence higher maximum energy dissipation at the tip to shear the aggregates. The precipitates circulation time and the proportion spent near the impeller (turbulent viscous dissipation sub-range) define precipitate strength and ageing (Shamlou *et al.*, 1996).

Bell and Dunnill (1982) demonstrated that continuous tubular reactors produced large, irregular, low density particles as compared with the stronger, smaller particles of the batch stirred tank (figure 1.16). They attributed the differences to the magnitude and distribution of mean velocity gradients ($\bar{G}$), and residence times within the reactors. They observed that batch aggregates had been exposed to high flow stress zones (impeller region) for longer periods than their continuous counterparts had. The larger continuous precipitates had a more open structure and a wider distribution of sizes. Particles had infrequently been exposed to impeller action in the continuous system (a lower residence time in a high velocity gradient zone). Their centrifugal recovery predictably resulted in reduced clarification (shear in the feed zone had broken these large, hollow particles into fine fragments found in the supernatant). There was also a larger volume of fine particles (< 5 µm) in the continuous precipitate (figure 1.16).
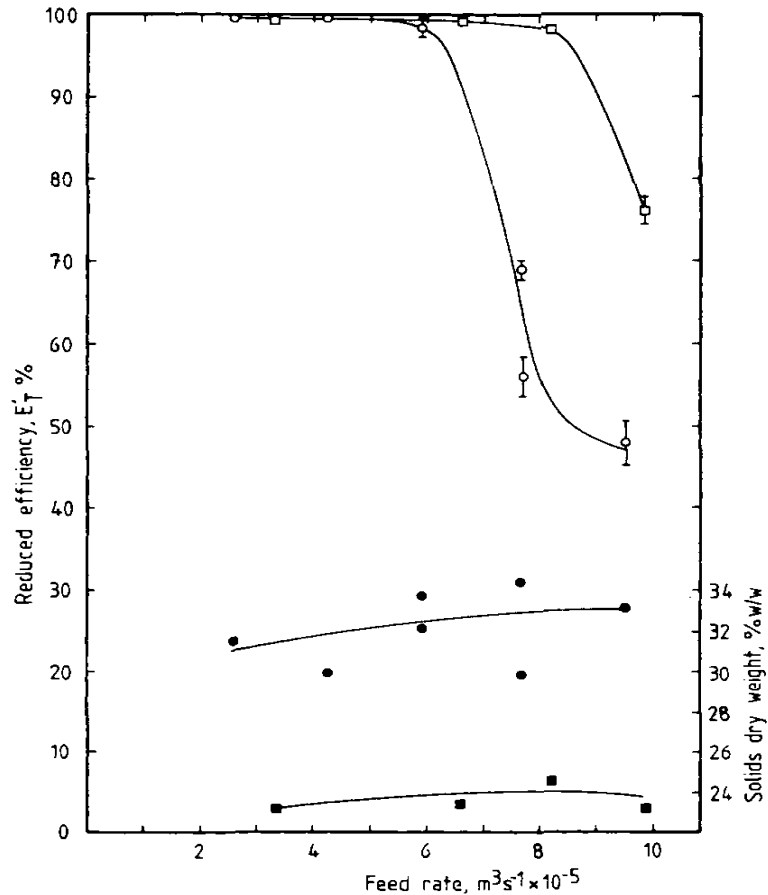
Figure 1.16: *Effect of preparation conditions on the separation efficiency and sludge dry solids content using a scroll discharge centrifuge (●○) and batch stirred tank (■□) (Bell and Dunnill 1982)*

1.7 Filtration

Protein precipitates are mostly colloidal and compressible in nature, which would lead to fouling issues with filter meshes unless filter aids are used. Cartridge or guard filters have been used to protect more expensive unit operations such as ultrafiltration and chromatography, by removing fine solids, which may foul them. This use of guard filtration often results in lower pressure drops and higher fluxes for downstream membranes (Bracewell *et al.,* 2008). Filter aids are not always suited to protein precipitates as they can decrease recovery efficiency or contaminate the product (Cui 2005). Filtration equipment is usually large and long start up times are required, creating containment concerns.

Filtration-centrifugation methods have been used where the centrifugal force provides the filter transmembrane pressure across a perforated bowl, although the compressible precipitate can cause severe blinding (Boulding *et al.,* 2002). The substantial costs per filter and high driving forces used restrict the use of filtering centrifuges to high value products.

1.8 Centrifugation

Centrifugation coupled with depth filtration has become the main set of unit operations employed for the primary recovery of therapeutic proteins in recent years (Roush and Lu 2008). Centrifugal sedimentation clarifies the precipitate according to density differences between it and the solution. The precipitation and centrifugal recovery sequence is a mainstay of many industrial processes and is dependent on good separation for high yields (Hutchinson *et al.,* 2006). However, the step can be made difficult by small aggregates and a low density difference between the precipitate and solution, requiring high centrifugal forces (Hutchinson *et al.,* 2006). Nonetheless, centrifugation is the principal recovery method for protein precipitates, offering low cost continuous operation, lower contamination risks, brief preparation times and a smaller footprint than filtration.

An efficient clarification and high level of dewatering ensures high product yields and a reduced drying load for subsequent protein purification. Due to the high capital and operating costs involved in solid-liquid separation, it is imperative that a high degree of clarification and solids dryness/dewatering is achieved.

1.9 Scale Down of Development Processes

Rapid volume reduction and product concentration have become major issues in early downstream processing steps. To date, conventional processes based on adsorption or filtration are about to reach their limits in terms of economics, processing speed and scale (Bensch *et al.,* 2007). Microscale bioprocessing techniques offer a change in bioprocess development by accelerating process development by enabling parallel experimentation and automation while requiring microscale quantities of material (Galaev 2005, Titchener-Hooker *et al.*, 2008). Critical bioprocess information can be obtained earlier in the development process, and it provides a better opportunity to understand more process parameters. These

microscale systems should be developed to mimic key engineering characteristics for scale up (Biddlecombe and Pleasance 1999).

Microscale processing is an extension of ultra scale down (USD) by the use of microlitre quantities of material. It can be divided into two main branches, microwell systems and microfluidics (manipulation of fluids). Both techniques offer to significant benefits for the translation of new drugs to market by reducing development time and costs. Furthermore, USD combined with automation can increase experimental throughput in the early stages of process development (Micheletti and Lye 2006).

This approach can be invaluable at the process definition stage of drug development when pilot scale trials are unfeasible or material is scarce i.e. for high value products. Large volumes of process data can be provided from low resource usage during route scouting enabling strong drug candidates to be spotted earlier and increasing process robustness. Rapid and accurate process development also holds the key in weeding out weaker candidates and saving company resources.

Current research on microwell unit operations has mostly focused on fermentation with little to show for downstream unit operations (Kostov *et al.,* 2000, Duetz *et al.*, 2001, Jackson *et al.,* 2006, Micheletti and Lye 2006). Microwells are small plates of identical wells capable of holding microlitre volumes and are available in various geometries. Their origins are in analytical and high throughput screening applications and are now finding their way into process design (Ferreira-Torres *et al.,* 2005). "Microwell bioprocessing" offers an automated platform to translate unit operations and even whole bioprocesses to microscale for generating process information (Ferreira-Torres *et al.,* 2005). They are suited to automated batch and fed batch experimentation to be carried out with microlitre quantities (20-2000 µL) of representative samples. Mainstream acceptance is dependent upon defining the engineering fundamentals of microscale techniques and range of bioprocess unit operations that can be performed at this scale (Micheletti and Lye 2006).

USD devices can be used to mimic critical process parameters at industrial scale, which may be missed in ideal laboratory equipment. The difficulties in replicating complex fluid flow patterns at bench scale can be alleviated with the USD device.

As stated by Pollard (2001), the bottleneck of process development is its initial stage of "route-scouting" that involves evaluating alternative process options, often with limited data. The stage usually consists of laboratory scale (10-100 mL) experiments using limited material, analysing changes to different conditions, reagents and operations. The experiments can be time consuming due to the sparing use of automation, slowing down data generation. Single step success not only requires the optimisation of its own performance (e.g. yield, purification factor, product quality) but also depends critically on subsequent processing (e.g. column chromatography) as well as the consequence of feed composition.

1.9.1 Scale Down of Protein Precipitation Using Quality by Design (QbD) Principles

At pilot or larger scale, it is not economically feasible to investigate a large number of operating conditions due to the number of resources that would need to be employed. To date, conventional processes based on adsorption or filtration are about to reach their limits in terms of economics, processing speed and scale (Bensch *et al.,* 2007). Techniques, which can generate data with minimal resource expenditure by mimicking large scale processes, are in high demand. Microscale bioprocessing techniques offer an improvement in bioprocess development by accelerating timelines and enabling parallel experimentation using automation while requiring microscale quantities of material (Galaev 2005, Titchener-Hooker *et al.*, 2008). Critical bioprocess information can be obtained earlier in development providing better opportunity to understand a wide range of process parameters.

In this thesis, microwell unit operations were used to scale down downstream unit operations. Microwells are small plates of identical wells capable of holding microlitre volumes and are available in various geometries. The scale down of protein precipitation should be generally simple and geometric; many of the parameters found in larger vessel including the Power per unit volume, Camp number, tip speed, rate of precipitant addition and diameter ratios ($d_{impeller}$:d_{tank} and d_{baffle}:d_{tank}) are kept constant. The scale down model should be able to create a comparable range of particle sizes and strengths. Scale down studies of subsequent recovery and high resolution chromatography steps depends on having precipitate available that qualitatively represents production material.

When scaling down precipitation it is vital that the ability to generate comparable results is maintained across an agreed predetermined set of operating conditions. Geometric similarities (e.g. aspect ratio, impeller, tip speed, etc.) and operational conditions (e.g. mean velocity gradient, residence time, tip speed, etc.) are usually kept constant although it should be stressed that it is material quality that is to be replicated and not the unit. Successful scale down of precipitation reactors has previously been accomplished by keeping Power dissipation per unit volume constant over the range 0.27 to 200 L (Bell *et al.,* 1983). Many authors suggest a direct relationship between the mean velocity gradient and precipitate size, and the Camp number and particle strength (Tambo and Hozumi 1979, Bell *et al.,* 1983, Shamlou *et al.*, 1996).

Sometimes the scale down to laboratory scale fails to reproduce the operational complexities of larger scales. Fluid flow patterns in stirred tanks are likely to change during scale down as it is difficult to replicate them exactly. The mean velocity gradient encompasses a wide range of velocity gradients in the vessel and scale up may change the distribution of the velocity profiles. Distinguishing the mixing between the high shear impeller region and the low shear bulk fluid may allow for further insight. The maximum spatial shear rate is thought to be at the impeller tip and this along with Reynolds Number (equation 5.1) and particle circulation time are known to change relative to a constant Power input per unit volume (Byrne and Fitzpatrick 2002).

For more complex operations, where the engineering fundamentals are not fully characterised, pilot trials are more appropriate. Innovative devices such as the rotating disc shear device are sometimes available to fill in for the inadequacies of laboratory equipment (centrifuges) in mimicking larger scale equipment (section 5.4.1). The effect of clarification by centrifugation can be seen from Stoke's law, which describes the inverse relationship between viscosity and the particle settling velocity (u) of cell debris during solid–liquid separation (equation 1.5). Thus, particle settling can be increased by reducing the viscosity of the feedstream (Balasundaram *et al.,* 2009).

$$u = \frac{(\rho_p - \rho_l)d_p^2 g}{18\mu}$$

<div align="right">**(1.5)**</div>

Equation 1.5: *Particle settling velocity (m s^{-1}) where ρ_p is the density of the particle (kg m^{-3}), ρ_1 is the density of the suspension (kg m^{-3}), d_p is the diameter of the particle, (m), g is the acceleration due to gravity, (m s^{-2}), and µ is the viscosity of the process suspension in Pa s (Balasundarum et al., 2009)*

However, in terms of bioprocess development in the current biotech industry, product quality and robustness is tested at numerous stages in the manufacturing process against a number of FDA approved parameters. If a batch does not meet the required specification then it is discarded resulting in a waste of resources and money. Any changes to the manufacturing process require FDA approval and there is little scope on how the design of process scale up and subsequent manufacturing process can ensure product quality and robustness.

An alternative to this approach is the Quality by Design (QbD) approach. The concept promotes greater understanding of all the critical parameters in the manufacturing process starting with product development, essentially building quality into the process, not testing it in the product. This is highlighted in figure 1.17.

The diagram shows a pyramid with the following labels:

- Left vertical arrow: **Process builds from bottom up**
- Top section (dark green): Process monitoring — pointing arrow from right: **Continuous improvement ICH Q10**
- "Launch" label with dashed line across
- Middle section: **Regulatory approval Process control implementation** — pointing arrow from right: **Process control ICH Q9**
- Bottom section: **Design space Experimentation Process development** — pointing arrow from right: **Process understanding ICH Q8 (R2)**

Figure 1.17: *Quality by Design: The International Conference on Harmonisation of Technical Requirements for Registration of Pharmaceuticals for Human Use (ICH) guidelines Q8 (R2), Q9 and Q10. Processes are designed to be robust and to deliver consistent quality*

QbD is part of a regulatory driven initiative in how process development and manufacturing is conducted. As part of this process PAT (Process Analytical Technology) defined as a system for designing, analysing, and controlling manufacturing during processing of critical quality and performance attributes of processes, can be used to ensure the final product quality (Rathore and Winkle 2009).

ICH (The International Conference on Harmonisation of Technical Requirements for Registration of Pharmaceuticals for Human Use) is a collaborative body in the pharmaceutical industry combining the regulatory authorities of Europe, Japan and the USA to discuss scientific and technical aspects of drug registration. Its aim is to ensure that safe and effective medicines are developed and registered in the most resource efficient manner. A number of guidelines denoted ICH Q8 (R2), Q9, Q10 and Q11, concern methods and principles to achieve this in a complex production process or analytical system. ICH guidance Q8 (R2) is intended to provide understanding of the product using the concept of "design space" (ICH Q8 (R2) 2009). ICH guidance Q8 (R2) defines design space as "the multidimensional combination and interaction of input variables and process parameters that have been demonstrated to provide assurance of quality" (ICH Q8 (R2) 2009). Moving the

process parameters within the design space is not considered as a process change. Movement out of the design space is considered a change and would normally initiate a regulatory post-approval-change process. In this thesis, the effect of PEG and salts on the precipitation of Fab' and or protein impurities are described to generate a process design space to characterise a suitable operating range. This type of experimental design will define whether operating conditions are safe, consistent and robust.

As part of this process critical quality attributes and critical performance attributes are identified so that those process characteristics having an impact on product quality can be studied and controlled. Critical quality attributes are biological or chemical properties, which should be within range, and the critical process parameters whose variability has an impact on critical quality attributes should be controlled to ensure process robustness. Examples of these attributes for precipitation as described in this thesis are shown in table 1.1.

Critical Quality Attributes	
Aggregation	Charge variants
Concentration	Salts
pH	PEG

Table 1.1: *Examples of critical quality attributes for Fab' and or protein impurity precipitation with PEG and salts*

ICH Q9 is trying to better define the principles by which risk management will be integrated into decisions by the industry, regarding quality and GMP compliance. Risk is defined as the combination of the "probability of harm and severity of that harm" (ICH Q9 2005). The importance of systems to maintain product quality throughout the lifecycle of the product is becoming increasingly important to ensure the high quality of the drug. The outcome should be a risk management framework intended to lead to a more consistent science based decision making across the lifecycle of a product (Rathore and Winkle 2009). Failure Mode Effects Analysis (FMEA) is a risk assessment tool for identifying and summarising factors that are likely to cause failures in the process. FMEA provides for an evaluation of potential risks in processes and their effect on product performance and quality. Once these

modes have been established appropriate risk reduction can be used to control these factors.

ICH Q10 incorporates the concepts behind ICH Q8 (R2) (development/understanding) and Q9 (risk management) by providing a model for quality that can implemented throughout product life cycle. In essence, the overall goal is to complement the manufacturing processes for continual improvement and strengthen the link between the other guidelines (Rathore and Winkle 2009).

ICH Q11 provides further clarification on the principles described in ICH guidelines Q8 (R2), Q9 and Q10. This guideline provides further clarification on the enhanced approach to process development. In an enhanced approach, risk management and scientific knowledge are used to select parameters that impact critical quality attributes to establish a design space and control strategies to be implemented throughout the lifecycle of the product. Therefore, as mentioned in ICH Q8 (R2), a greater understanding of operational design spaces can allow for flexibility and robustness at manufacturing scale, which gives a degree of flexibility with regulatory approaches.

In the QbD approach, the product and processes are understood prior to commercialisation so that when adjustments or issues occur, they are quickly dealt with without requiring further investigation. For example, the adoption of QbD in this case will include the design of the manufacturing process from basic principles with a good understanding of the operating space by a Design of Experiments (DoE) approach. The identification of critical process parameters such as the concentration of PEG, salts, pH, feed concentration and potential sources of variability will achieve the most consistent quality and robustness.

The complexity of biotech products and processes makes complete characterisation a challenge. Biologics present unique issues such as the differences in the manufacturing process for different molecules, which will need to be addressed in order for QbD to be implemented (Rathore and Winkle 2009).

1.10 Methods of Presenting Data

1.10.1 Fractionation Diagram

A fractionation diagram can provide a clear way to represent the purification of a product protein relative to total contaminating protein. The use of tie lines in this approach makes the determination and optimisation of purification factor versus yield more straight forward (Dixon and Webb 1961, Juckles 1971, Richardson *et al.,* 1990). Previous graphical methods included the specific property solubility test (Richardson *et al.,* 1990), and while successful at predictions for final stages of purification of liver esterase for example, it may not be suitable for crude cell extract fractionation (Richardson *et al.,* 1990). Figure 1.18 shows an example of this where total protein concentration on the y-axis is related to a property specific to desired product on the x-axis. The most favourable conditions for the purification of the active component will occur when the curve BCD approaches its tangent ECD as closely as possible. Precipitation conditions should therefore be adjusted to reduce the area BCE (Richardson *et al.,* 1990).
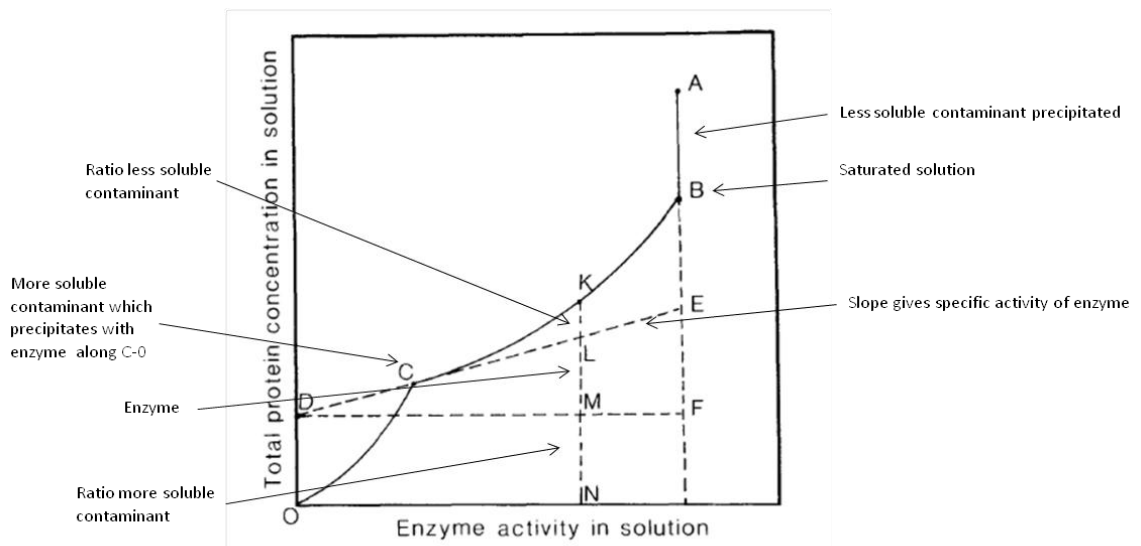
Figure 1.18: *Example of specific property solubility test (Richardson et al., 1990)*

A second graphical method in existence was the derivative solubility curve method (Richardson *et al.,* 1990). These plots essentially show the solubility curve gradient versus precipitant concentration, with the area bounded by the resultant peak and the ordinates of the two precipitant cuts is proportional to the amount of protein

precipitated (Richardson *et al.,* 1990). This method is not ideal as while it shows the fractionation of proteins, solubility curve gradients must be obtained and reintegrated to determine the area of overlap. This makes the quantification and subsequent application cumbersome. For total protein no theoretical model exists to describe solubility unless the sum of all Cohn lines are combined, which can become complicated (Richardson *et al.,* 1990).

To overcome these previous problems, the fractionation diagram approach can be used. Firstly, enzyme and protein concentrations are plotted versus precipitant concentrations; this fractionation diagram eliminates precipitant concentration between the enzyme and protein solubilities by plotting one against the other. Figure 1.19 shows this representation as a process equilibrium curve.
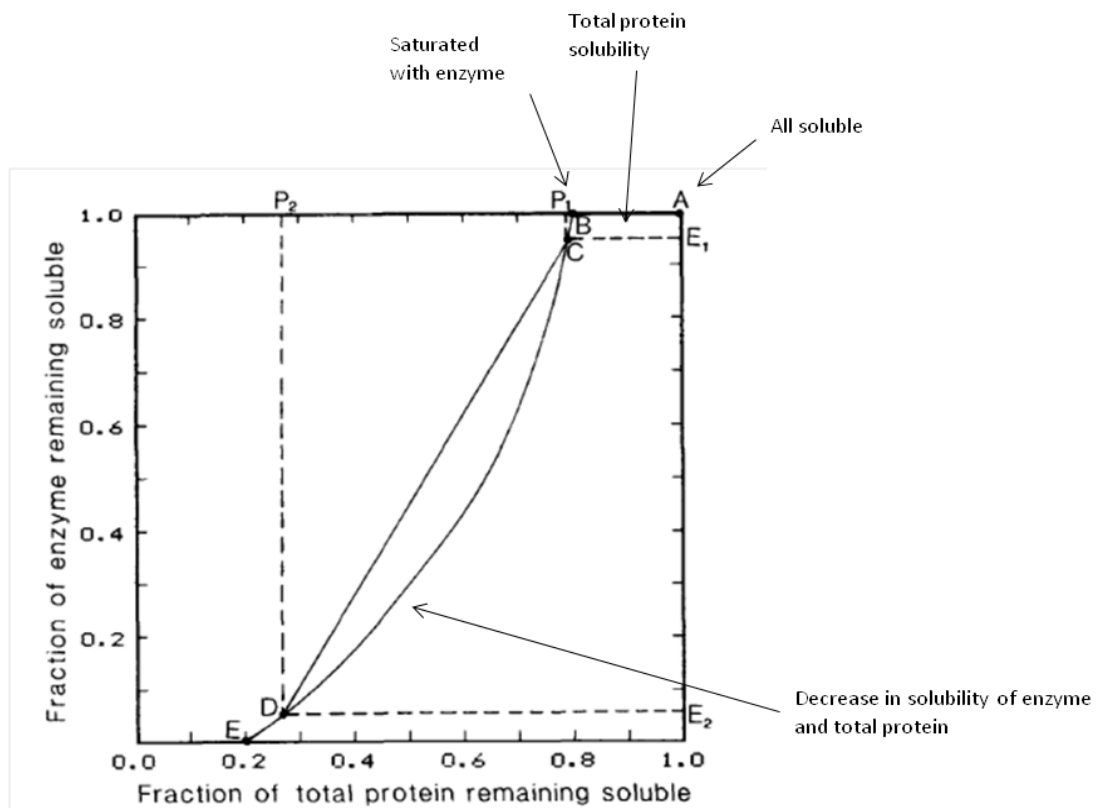
Figure 1.19: *Enzyme-total protein fractionation diagram derived from the solubility profiles (Richardson et al., 1990)*

1.10.2 Statistical Design of Experiments (DoE)

The experimental approach based on statistical experimental design or Design of Experiments has been used extensively in research (Lundstedt *et al.,* 1998). The purpose is to systematically analyse how the response of a system changes when parameters of that system are changed. DoE accommodates the variation of experimental conditions in a planned fashion. Doing this gives detailed information about how different experimental parameters influence the system response through the completion of only a limited number of experiments (dependent on the experimental design selected). Speed of research is essential and the structured carrying out of experiments with DoE has the ability to gain a maximum level of information from a minimum number of trials (Olsson *et al.*, 2006). DoE is used for three main experimental objectives, regardless of scale. The first of these is screening, which is used to identify the most influential factors, and to determine the ranges across which they should be investigated. The second experimental objective is optimisation, which builds on the influential factors identified in screening to find optimal operating conditions. Optimisation requires a greater number of experiments per factor due to its complexity. The third experimental objective is robustness testing to determine how robust the process is with small changes in factor levels. For example, small changes can occur during production of therapeutic proteins, which can lead to batch failure. Therefore, understanding how design parameters affect process behaviour can provide an informed way to decide how to operate at large scale.

The theoretical basis of experimental design can be found in a number of texts (Hicks 1974, Box *et al.,* 1978) and more appropriate examples for biotechnology systems can be found in Haaland (1989). Statistical modelling using DoE can be used for the identification of the optimal process conditions. It allows the relationship between the variable factors and their response to be shown graphically in a response surface. DoE can identify interaction effects between variables, which are difficult to be realised in a traditional experimental approach. These complex interactions are often found in biological systems. Without the use of statistical design and analysis, these effects may never be realised. Statistical modelling software can analyse the response data and create a model. This model, no matter how simple, is powerful as it then enables predictions of any variety of conditions possible (Lutz *et al.*, 1996).

DoE models created are only powerful if the most significant variables are chosen and their appropriate ranges are investigated. Having prepared a list of possible variables for the system, an initial screening study is performed in order to estimate the influence of these variables on the result. This can be achieved by using a full factorial or fractional factorial design. In either design, each of the factors or variables are varied in a systematic way. A possible way of doing this is measuring the response at extremes of the operating range of each factor. A linear or polynomial function can then be used to model the region between these points (Lundstedt *et al.*, 1998).

A linear model describes the linear relationship between the experimental variables and the response, and takes the form:

$$y = b_o + b_1x_1 + b_2x_2 + residual$$ (Lundstedt *et al.*, 1998)

Where b_o, b_1, b_2 are unknown constants determined by the software. x_1 and x_2 are the variables in the system and y is the response.

The next level of polynomial models contains extra terms, which represent the interaction between different experimental variables. Thus, a second order interaction model takes the form:

$$y = b_o + b_1x_1 + b_2x_2 + b_{12}x_1x_2 + residual$$ (Lundstedt *et al.*, 1998)

These models are usually sufficient for purposes of screening to determine the greatest variables and identify interaction effects. To locate an optimum on the response surface, quadratic terms are required. A quadratic model is obtained by using a different type of experimental design, such as central composite design. A quadratic model therefore has the form:

$$y = b_o + b_1x_1 + b_2x_2 + b_{11}x_1^2 + b_{22}x_2^2 + b_{12}x_1x_2 + residual$$ (Lundstedt *et al.*, 1998)

The combination of factors leads to the effect of each factor and the interaction between each factor to be found. Two levels are usually chosen which represent the upper and lower expected limits of the variables. For a total of k factors investigated at two levels, the design will require 2^k experiments. The design can be shown graphically for 3 factors as a cube (figure 1.20).
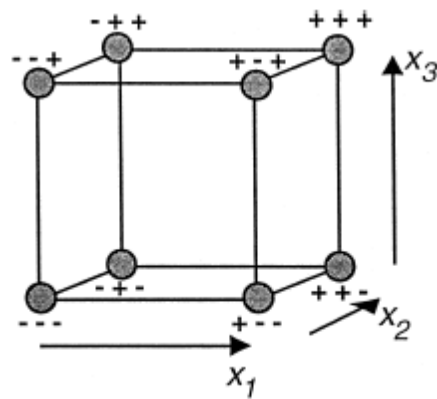
Three variables			
Exp. no.	Variables		
	x_1	x_2	x_3
1	−	−	−
2	+	−	−
3	−	+	−
4	+	+	−
5	−	−	+
6	+	−	+
7	−	+	+
8	+	+	+

Figure 1.20: *Experiments in a full factorial design of three variables (Lundstedt et al., 1998)*

Centre points should always be included in factorial designs, as they will show non linear relationships in the middle of intervals and by repeating the centre point a number of times will determine the confidence intervals in the data (Lundstedt, *et al.,* 1998).

A fractional factorial design offers a compromise between the information obtained and the total number of individual experiments required to model the system. With fewer experiments, less detail about the interactions is known, and depending on the resolution of fractional factorial design undertaken a certain amount of confounding is present. Confounding is a term used to refer to effects, that are either factors or interactions, which cannot be estimated independently. Instead, the constants are grouped together (Lutz, *et al.,* 1996). A number of software packages such as MODDE by Umetrics will design the list of experiments required to be performed once a type of design is selected, and the list of factors and levels chosen. With the experimental data, a response surface can be modelled. Response surface modelling describes the use of the mathematics to determine a relationship between the factors and responses of the system. The models are usually presented in terms of contour or surface plots. Initial data is sufficient to provide an overall response surface; however, for added definition around the optimum, further experiments will be required (Lutz, *et al.,* 1996).

Using this approach, a large number of potentially expensive, and time consuming experiments are not needed, and it can provide a better understanding of the

investigated system or process. Several studies have successfully employed the use of robotic liquid handling and DoE in a number of biological systems. A similar approach will be used throughout this thesis for precipitation studies.

1.11 Organisation of the Thesis

This thesis seeks to characterise the microwell platform and demonstrate its use as an approach to accelerate process development. The material generated used throughout the thesis is described in chapter 2. In chapter 3, DoE studies using PEG are described. In chapter 4, DoE experimental studies on multimodal PEG-salt precipitation are investigated. Chapter 5 describes a clarification strategy based on conditions investigated in chapters 3 and 4. An overview is detailed in figure 1.21.

Chapter 2   **Materials and Methods**

75 L fermentation
Homogenisation
Primary recovery

↓

Chapter 3   **Development and Automation of a Microscale Down Platform for Fab' Precipitation using PEG**

Timescale experiments
6 mL baseline data
Development of 1 mL automated platform
Full factorial DoE using PEG
Central composite face centered DoE using PEG

↓

Chapter 4   **Microscale Multimodal Precipitation to Establish Polyethylene Glycol and Salt Interaction Effects**

Use of a alternative mixing system
Full factorial DoE using PEG and salts
Central composite face centered DoE using PEG and salts

↓

Chapter 5   **Integration of Precipitation into a Downstream Process**

Investigation of particle size
Precipitation scale up to laboratory scale
Defining the centrifugation stage of the precipitation process
Pilot scale precipitation and centrifugation

Process Run Through

Automated depth filter investigation using eight well custom filter block design
Tangential flow diafiltration prior to packed bed studies
The purification of antibody fragments using packed bed chromatography

Figure 1.21: *Organisation of thesis*

2. MATERIALS AND METHODS

This chapter describes common materials and analytical procedures used throughout this thesis. Method details to certain experiments are described in the subsequent chapters.

All the chemicals used in the current study were purchased from Sigma (Sigma Chemical Co., Dorset, UK) and were of analytical grade. All buffers were prepared using ultra pure water 0.22 µm filtered (Millipore, Hertfordshire, UK). 1.3 mL 96 deepwell plates were sourced from Nunc (Nunc GmbH & Co., KG, Denmark) and 96 well flat bottom Costar UV microwell plates from Corning (Corning, Leicestershire, UK). All buffers and reagents used for precipitation studies described in chapters 3-5 had a pH range of ± 0.2 pH units.

2.1 Quantification of Antibody Fab' Fragments

Fab' concentration was determined by using a 1 mL GE Healthcare Protein G affinity column (GE Healthcare, Uppsala, Sweden) and a Agilent 1200 HPLC system (Agilent Instruments, Edinburgh, UK), consisting of a pump, an autosampler and an UV detector. Effluent was monitored at 220 nm. Solvents used were 20 mM sodium phosphate pH 7.4 for equilibration and 20 mM sodium phosphate pH 2.5 for elution at a pH range of ± 0.05 pH units. The column was equilibrated using 100% 20 mM sodium phosphate pH 7.4 at a flowrate of 2 mL min^{-1} for 15 column volumes. 100 µL of sample was injected, a one minute linear gradient to 100% 20 mM sodium phosphate pH 2.5 was run, and held at that point for a further 15 minutes before returning to the equilibration conditions. The HPLC was configured to accept 96 well plates and allowed a maximum of 2x 96 plates to be assayed in one run. Rubber plate covers by Nunc (Nunc GmbH & Co., KG, Denmark) were used to seal the plates to limit evaporation over long runs. Triplicate set of Fab' standards were run on the column as a calibration curve and replicates of standards samples were within 5% of their mean. Unknown sample concentrations were then determined by interpolation from the curve by linear regression. A typical calibration curve is shown in figure 2.1.
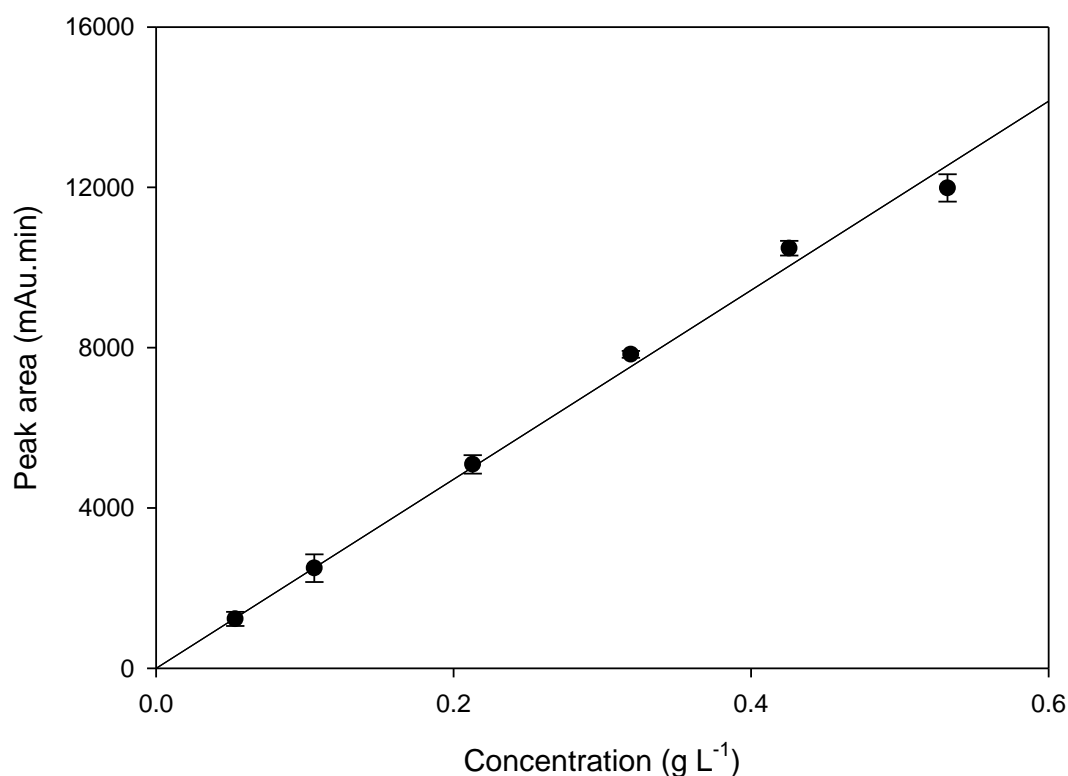
Figure 2.1: *A typical calibration curve of Fab' standards (●). The solid line extended to axes represents linear fit of data (r^2 = 0.99). Error bars are shown for one standard deviation for triplicate experiment repeats*

2.2 Total Protein Concentration by the Bicinchoninic Acid (BCA) Assay

Total protein concentration was determined by using the Pierce BCA kit (Pierce, Rockford, USA) in a 96 well format with liquid transfer performed using either a Multiprobe II EX (Packard Instrument Co., Meriden, USA) or a Tecan Freedom EVO 200 (Tecan, Reading, UK) liquid handling robots. The assay was calibrated with bovine serum albumin (BSA) standards. Samples were prepared and analysed as per manufacturer's instructions. Unknown concentrations were then determined by interpolation from the curve by linear regression. A typical calibration curve is shown in figure 2.2.
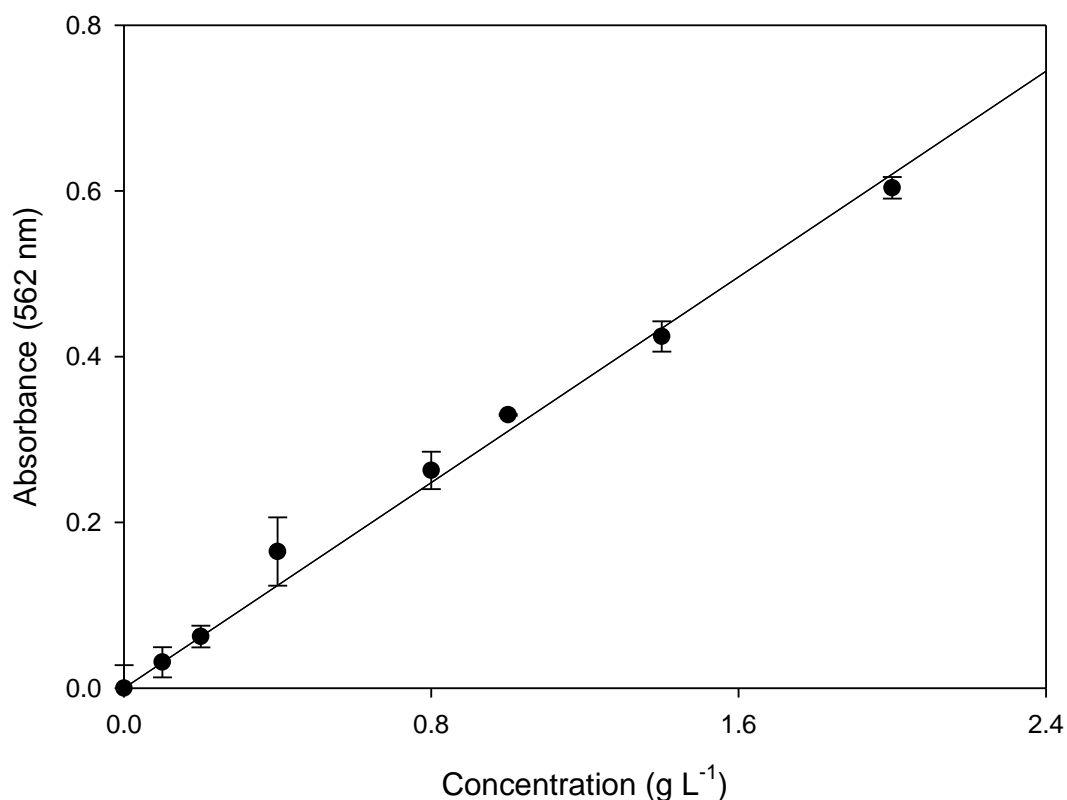
Figure 2.2: *A typical BCA total protein calibration curve (●). The solid line extended to axes represents linear fit of data (r^2 = 0.98). Error bars are shown are for one standard deviation for triplicate experiment repeats*

2.3 Quantification of Optical Density

The optical density of samples were measured at 600 nm (OD_{600}) with a Beckman DU 650 Spectrophotometer (Beckman Coulter Ltd., High Wycombe, UK). The OD was measured in triplicate with a standard deviation of ≤ 3%.

2.4 Particle Size Analysis

Protein precipitate suspensions were characterised by a Malvin Mastersizer (Malvern Instruments, Southborough, UK) to determine the particle size distribution of the precipitated material from a 2 mL sample. The detecting range of the instrument was 0.02-2000 μm. Particle size measurements were calculated based on particle volume percentage, which was then calculated and represented graphically as normalised volume frequency. Burgess *et al.,* (2004) have reported

that the biopharmaceutical industry prefers particle size distributions to be reported on a volume basis. In all cases, the d_{50} values quoted were given by the instrument. The d_{50} is a value of particle size indicating that 50% of the total volume of analysed particles has a diameter equal to or less than this reference value. Measurements were made in triplicate and the standard deviation was ≤ 5%. Each precipitated suspension to be analysed was well mixed before being added dropwise to the small volume dispersion unit until an obscurance of 11% to 13% was reached. The samples were mixed adequately during measurement (1400 rpm).

2.5 Viscosity Measurements

The viscosity of the samples were measured using a plate and cone viscometer (Bohlin Instruments, MA, USA). The temperature was maintained at room temperature using a cooling water bath. Approximately 1 mL of the sample was placed in the chamber and the shear rate (s^{-1}) and the apparent viscosity data (in Pa s) was recorded on a PC using Wingather software (Bohlin Instruments, MA, USA). Measurements were made in triplicate and typical standard deviation was 0.64%.

2.6 Light Microscope Images

Particle size was assessed qualitatively by light microscopy. Microscopic images were taken on an Axioscope 2 plus microscope at 100x magnification (Carl Zeiss Micro Imaging Inc., Thornword, USA).

2.7 Statistical Software

The full factorial and central composite face centred DoE designs that were used to optimise precipitation operations were designed and analysed using MODDE 9.1 statistical software (Umetrics, Malmö, Sweden). In all cases, the data was not transformed for analysis and the appropriate DoE design (for example, quadratic models) were selected using ANOVA assessments. Further details of these designs are discussed in chapters 3, 4 and 5. The overlay plots for yield and purification factor were performed in MODDE 9.1 (Umetrics, Malmö, Sweden). All other graphs and fitting of data was performed in SigmaPlot 11.0 (Systat Software, CA, USA).

2.8 Production and Primary Recovery of Fab' to Generate Material for Study

This section describes the production and primary recovery of Fab' fragments from *E.coli* cells for the use throughout this thesis. A number of research fellows from the Department of Biochemical Engineering, UCL performed this work.

2.8.1 Introduction

E.coli bacteria have been used as the host cell of choice for the production of many antibody fragments (Ali *et al.,* 2012). The process materials used in this study is based on an *E.coli* host expressing a Fab' antibody fragment. The fermentation protocol for the cultivation of *E.coli* strain W3110 with plasmid pTTOD A33 has been reported previously (Tustian *et al.,* 2007). The increasing commercial demand for antibody based molecules, such as Fab' fragments and the large requirement for the treatment of chronic illnesses necessitate the development of processes, which allow efficient, high volume production at low cost.

2.8.2 75 L Fab' Fermentation Process Overview

2.8.3 Complex Shake Flasks

For cultivation in shake flasks, a 1 mL vial of *E.coli* stock working cell bank (stored at -80°C in glycerol) was used for growth in 200 mL of complex media. Cells were incubated at 37°C in an orbital shaker (250 rpm) for approximately 4 hours to an OD_{600} 1-2 with 10 μg mL^{-1} tetracycline. The complex media is defined in table 2.1.

Compound	Concentration (g L^{-1})	Volume (L)	Mass (g)
Phytone	16.0	0.4	6.4
Yeast Extract	10.0	0.4	4.0
NaCl	5.0	0.4	2.0

Table 2.1: *Complex media for 2x 2 L baffled shake flasks containing 200 mL PY media plus 10 μg mL^{-1} tetracycline*

2.8.4 Defined Shake Flasks (New Brunswick)

400 mL portion of the culture from the complex shake flasks was used to inoculate each defined medium shake flask (9x 2 L baffled shake flasks) defined in table 2.2. pH was maintained at 6.95 using 15% v/v ammonia solution and 20% v/v ammonium hydroxide. 400 mL portion of culture from the defined media shakes were used to inoculate a 4 L v/v New Brunswick fermenter (Eppendorf UK Ltd., Cambridge, UK). The fermenter was operated at 30°C until OD_{600} reached 5 at approximately 18 hours.

Compound	Concentration (g L^{-1})	Mass (g)
$(NH_4)SO_4$	5.20	18.72
$NaH_2PO_4.H_2O$	4.40	15.84
$MgSO_4.7H_2O$	1.04	3.74
KCl	4.03	14.51
SM6 elements	10 mL L^{-1}	36 mL
Citric Acid.H_2O	4.16	14.98
Glycerol	112.00	403.20
$CaCl_2.2H_2O$	0.25	0.90

Table 2.2: *Defined media for 9x 2 L baffled shake flasks containing 400 mL defined media plus 10 μg mL^{-1} tetracycline and 112 g L^{-1} glycerol as a carbon source*

2.8.5 75 L Fermenter

Table 2.3 lists the media preparation for the 75 L fermenter (Infors, AG, Switzerland), which contained 40 L defined minimal media including 112 g L^{-1} of glycerol as a carbon source. Foaming was manually controlled by addition of sterile solution of 0.28 mL L^{-1} of 25% v/v polypropylene glycol (PPG) as antifoam.

Dissolved oxygen tension (DOT) was maintained above 30% where possible by computer controlled increases in stirrer speed to a maximum of 1000 rpm, and by manual control of airflow. Temperature was initially set at 30°C and was reduced to 25°C when an OD_{600} of 38 was reached. Additions were made when OD_{600} = 38 (360 mL 1 M $MgSO_4$), OD_{600} = 54 (240 mL 1 M NaH_2PO_4), OD_{600} = 78 (360 mL 1 M

NaH$_2$PO$_4$ and glycerol feed induced) and when OD$_{600}$ = 88 was reached for the start of induction (100 mL of 15.3 g L^{-1} IPTG on DOT spike). Online monitoring and control was performed using the Infors HT X-Controller software package. Growth was monitored by measuring OD$_{600}$ with a spectrophotometer (Beckman Coulter Ltd., High Wycombe, UK) at hourly intervals. Samples were suitably diluted with pH 7.4 phosphate buffered saline (PBS) solution and absorbance was measured in triplicate.

Compound	Concentration (g L^{-1})	Mass (g)
(NH$_4$)SO$_4$	5.20	208.00
NaH$_2$PO$_4$.H$_2$O	4.40	176.00
MgSO$_4$.7H$_2$O	1.04	41.60
KCl	4.03	161.20
SM6 elements	10 mL L^{-1}	400 mL
Citric Acid.H$_2$O	4.16	166.40
Glycerol	112.00	4480.00
CaCl$_2$.2H$_2$O	0.25	10.00

Table 2.3: *Defined media for 75 L fermenter (Infors, AG, Switzerland)*

2.8.6 Fab' Fermentation Results

Cell growth in the shake flask and the 75 L fermenter (Infors, AG, Switzerland) was assessed through OD$_{600}$ (Beckman Coulter Ltd., High Wycombe, UK) by taking samples over regular intervals, diluting as required. Figure 2.3 shows the cell growth (OD$_{600}$) over the whole fermentation cycle at 75 L. In the second growth phase, the maximum agitation and air flow rate (1 VVM) were not sufficient to maintain dissolved oxygen above 30% and air supply was switched to 40% oxygen. Cell density at stationary phase for Fab' (OD$_{600}$ = 102) fell within the 20% variation between fermentations typically observed in 75 L scale fermenters (Nesbeth *et al.,* 2012). Furthermore, decrease in cell densities was observed after 50 hours (figure 2.3).
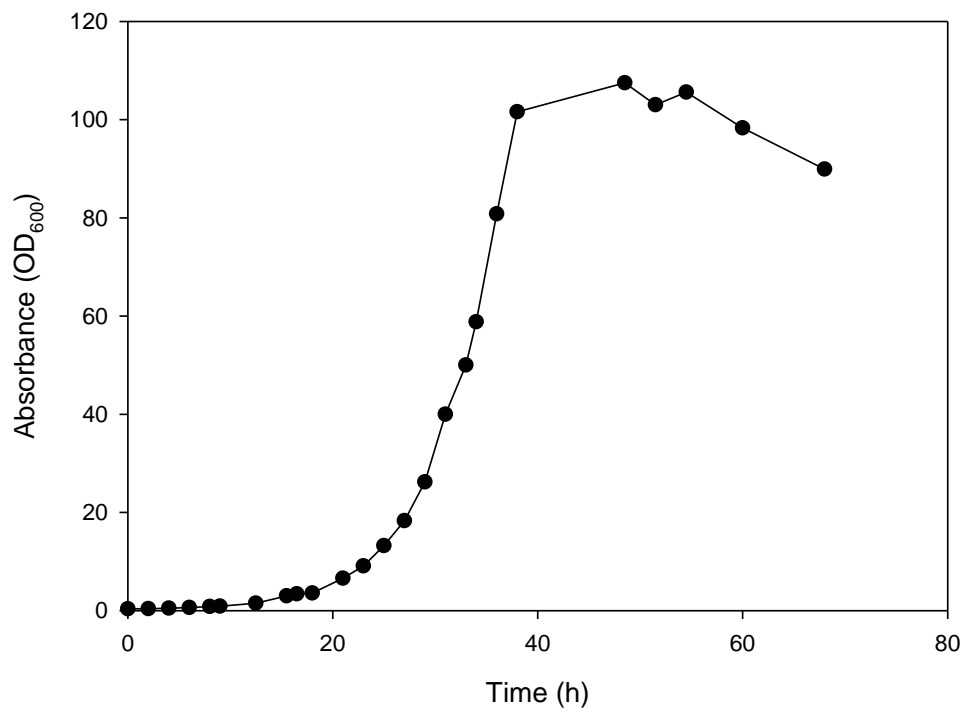
Figure 2.3: *E.coli cell biomass profile for the 75 L fermentation (●) determined by absorbance measurements in triplicate at OD_{600}. The standard deviation of the sample readings were ≤ 3%*
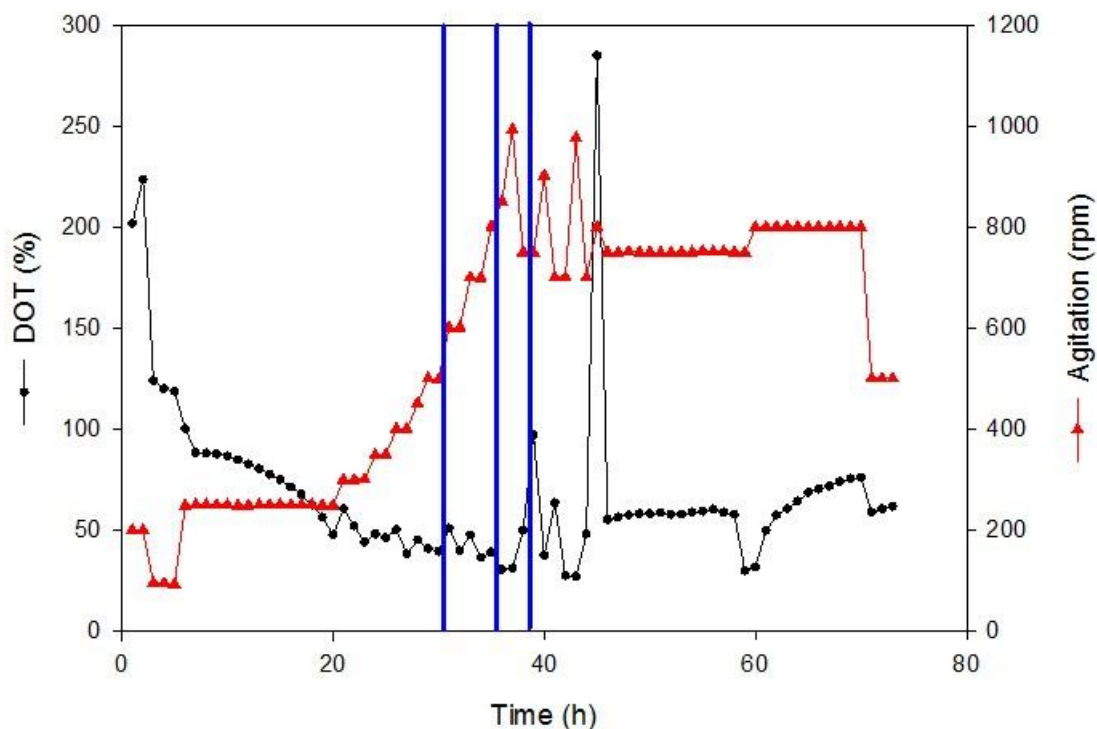
Figure 2.4: *DOT (●) and agitation profiles (▲) for the 75 L fermentation. At 30 hours oxygen cylinder changed to 40% enriched cylinder. At 36 hours oxygen cylinder changed to 75% enriched oxygen cylinder and at 38 hours DOT spike was observed at which point glycerol feed was started and ITPG added. This is represented by the three lines respectively at 30, 36 and 38 hours*

Figure 2.4 shows the dissolved oxygen tension (DOT) and agitation profiles for the 75 L fermenter (Infors, AG, Switzerland). The pH and temperature profiles are not shown as the pH values were controlled at 6.67 ± 0.83 and temperature was controlled at 30°C ± 5°C. At 30 hours, the oxygen cylinder was changed to the 40% oxygen enriched cylinder. At 36 hours, the oxygen cylinder was changed to the 75% enriched oxygen cylinder and the depletion of the carbon source was noted in at approximately 38 hours upon which the glycerol carbon source was added at a limiting rate that was sufficient to maintain cell survival. At this point isopropyl-β-D-thiogalactopyranoside (IPTG) was added to induce the production of Fab'. These changes are represented by the three lines on figure 2.4 at 30, 36 and 38 hours respectively. The cell culture was harvested 36 hours after addition of the IPTG. The change in agitation profile can be explained by the changes in oxygen and glycerol content at these points. Typically, glycerol limitation is indicated by rise in DOT and

constant glycerol feed in batch culture leads to decreasing growth due to volume increases. The addition of glycerol at 1.6 mL L^{-1} h^{-1} was found by Tustian *et al.,* (2007) to be optimal for productivity. Final harvest produced 5 kg of cell paste and ~0.9 g L^{-1} of Fab'.

2.9 Homogenisation and Primary Clarification

Cells were harvested 36 hours post induction and centrifuged using a Carr Powerfuge P6 centrifuge (Pneumatic Scale Corporation, FL, USA) at a flowrate of 60 L h^{-1} at 15000 rpm (20000 g). Cells were stored at -80°C and homogenised prior to clarification studies.

The release of intracellular Fab' from *E.coli* was achieved by a high pressure homogenisation (HPH) unit, which was optimised for maximal cell disruption (Nesbeth *et al.,* 2012). This typically results in significant levels of homogenate viscosity and contamination due to release of chromosomal DNA from disrupted cells, which can reduce performance of subsequent downstream purification steps (Nesbeth *et al.,* 2012). However, additional rounds of HPH can reduce viscosity by breaking chromosomal DNA strands by mechanical shear stress (Balasundaram *et al.,* 2009). However, this can result in increased micronisation of debris particles, which can compromise performance of key downstream purification steps such as centrifugation (Balasundaram *et al.,* 2009). Centrifugation is one of the key unit operations in downstream processing, employed for solid–liquid separations following fermentation, cell disruption or precipitation. Particle settling in a centrifuge is a function of many variables such as the size of the particles and the viscosity of the feedstream, as shown in equation 1.5.

The homogenisation step was investigated for the optimum release of Fab'. Frozen cells were resuspended in 100 mM Tris HCl pH 7.4 to give 15% w/v solids content and homogenised with an APV Manton-Gaulin Lab40 homogeniser (APV International, West Sussex, UK). The initial d_{50} value for the resuspended cell paste was 0.82 μm measured using a Malvin Mastersizer (Malvern Instruments, Southborough, UK). After one pass at 500 and 750 bar pressure, d_{50} value had decreased to 0.30 μm and 0.23 μm respectively. However, after five passes at 500 bar, the initial particle size had decreased to d_{50} 0.12 μm (figure 2.6). It was observed that an increase of micronisation of cell debris occurred with increasing

number of passes, increasing the difficulty in solid liquid separation (figure 2.6). This is in agreement with findings by Balasundaram *et al.,* (2009), although they worked with fresh cell paste. Siddiqi *et al.*, (1996) reported that the relationship between micronisation and disruption conditions, and thus product release profile, at discharge pressures greater than 115 bar was found to be non linear. The results from the current study are in agreement with the results of Siddiqi *et al.*, (1996). Thus, maximal product release with the least number of passes to reduce the micronisation of cell debris was chosen as the criteria to determine the number of cycles required for homogenisation to maximise clarification by centrifugation. The release profile of Fab' is presented in figure 2.5. It was observed that homogeniser pressure of 500 bar and 750 bar at one pass was sufficient to release the product. The equivalent d_{50} for the cell debris resulting from homogenisation using the APV Manton-Gaulin Lab60 homogeniser (APV International, West Sussex, UK) was 0.25 μm at 500 bar for one pass, which is comparable to the APV Manton-Gaulin Lab40 homogeniser (APV International, West Sussex, UK).

The initial measured viscosity of the fresh harvest was 0.002 Pa s at a shear rate of 38 s^{-1} measured using a cone and plate viscometer (Bohlin Instruments, MA, USA). The measured viscosity of the freeze-thawed cells homogenised at 500 bar for 1 pass was 0.003 Pa s at a shear rate of 38 s^{-1}. The increase in viscosity was in part caused by the release of chromosomal DNA, which was further investigated by Balasundarum *et al.,* (2009).
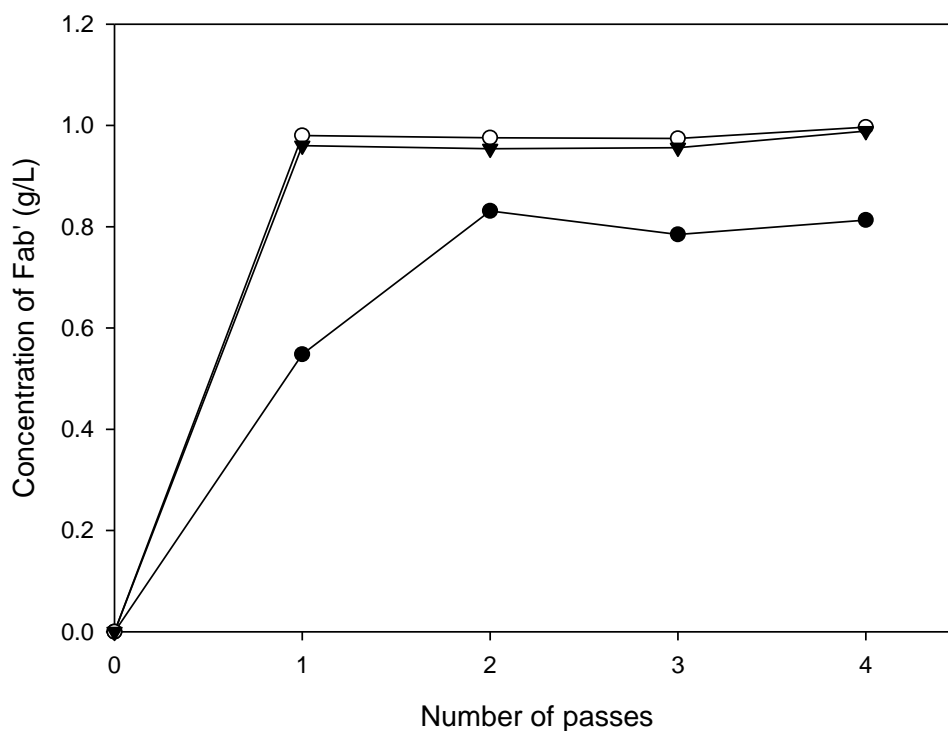
Figure 2.5: *The release of Fab' from the periplasm of E.coli cells as a function of the number of homogenisation passes at 250 (●), 500 (○) and 750 bar (▼) discharge pressures. A 40 mL suspension of E.coli cells (which were resuspended in 100 mM Tris HCl pH 7.4 to give a 15% w/v solids content) were homogenised using an APV Manton-Gaulin Lab40 homogeniser (APV International, West Sussex, UK) at these discharge pressures. The Fab' concentration was determined by the Protein G assay as described in section 2.1*
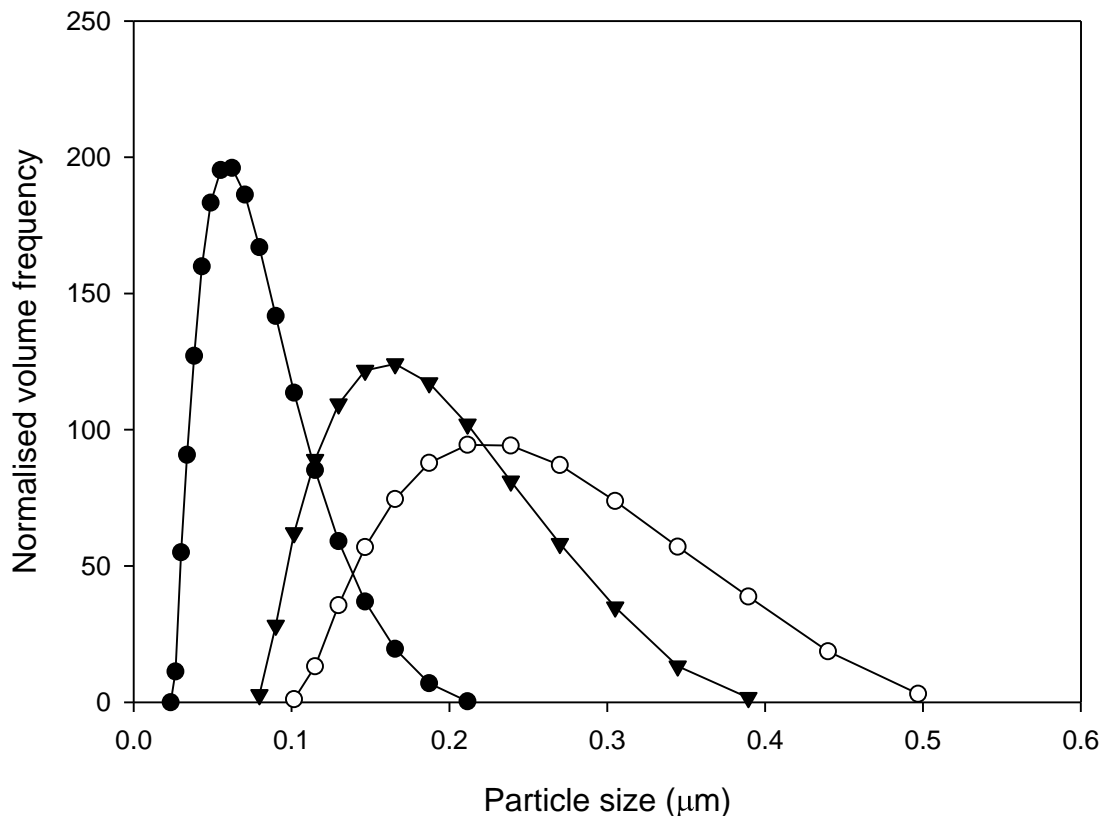
Figure 2.6: *The particle size distribution of E.coli cell debris at 500 bar for 5 passes (control) (●), 500 bar for 1 pass (○) and 750 bar for 1 pass (▼). The starting suspension of E.coli was 15% w/v in 100 mM Tris HCl pH 7.4. Measurements were made using a Malvin Mastersizer (Malvern Instruments, Southborough, UK) in triplicate as described in section 2.4. The standard deviation for measurements were ≤ 5%*

2.9.1 Material Preparation for Subsequent Studies

For subsequent studies homogenisation conditions of 500 bar for one pass was used unless stated. 2 L homogenised material using a APV Manton-Gaulin Lab60 (APV International, West Sussex, UK) homogeniser and was primarily clarified for 30 minutes at 15000 rpm using a CARR Powerfuge P6 centrifuge (Pneumatic Scale Corporation, FL, USA) at a flowrate of 25 L hr^{-1}. Clarification achieved at these conditions was 85% calculated from OD$_{600}$ readings. This material was stored in forty 50 mL falcon tubes at -20°C until needed. Material from a different falcon tube

was used for each experiment to prevent possible aggregation effects caused by multiple freeze thaw processes.

3. DEVELOPMENT AND AUTOMATION OF A MICROSCALE DOWN PLATFORM FOR FAB' PRECIPITATION WITH POLYETHYLENE GLYCOL

3.1 Abstract

A high throughput system utilising robotic handling has been successfully developed in microwells for the precipitation of Fab' antibody fragments. This process was designed to accurately mimic that of an identical process at 6 mL scale, and to evaluate several process parameters quickly.

A Fab' precipitation screening study in the form of a full factorial design was performed to investigate a large design space based on Quality by Design principles stated in the ICH guideline Q8 (R2). Parameters of investigation were PEG concentration (% w/v), PEG molecular weight (MW), pH and dilution of the homogenate. This was followed by a central composite face centred DoE to find an optimal range of experimental conditions to deliver a high Fab' yield and purification factor within the ranges investigated. A design space comprised of the responses percentage Fab' yield and purification factor was created to give a robust region where Fab' yield was ≥ 90% with a maximum purification factor of 1.7. A normal operating range (NOR) was defined within this design space and a confirmatory run was completed with PEG 12000 15% w/v at pH 7.4 and undiluted homogenate, which resulted in a Fab' yield and purification factor of 93% and 1.5 respectively. In essence, the knowledge of the factors affecting Fab' yield and purification factor can assist in the development of a manufacturing design space which lies at the heart of a practical realisation of Quality by Design.

3.2 Introduction

This chapter seeks to create a set of baseline data at 6 mL scale, which would be used as part of a strategy to apply one or a combination of pre column steps to target the removal of protein impurities. This chapter has been split into two sections, the first, investigated the precipitation of Fab' with varying molecular weights of PEG at 6 mL total volume, and the second focusses on the development of a high throughput system designed to mimic this scale. The high throughput system was developed to enable screening of a large number of process variables using a DoE approach. The ability to understand how design parameters affect

processes can provide information on how to operate at full scale. This capability is the practical basis on which Quality by Design is realised. This allowed key factors in Fab' precipitation from *E.coli* homogenates to be investigated including possible interaction effects between variables.

Figure 3.1 highlights the structure of the chapter. At stage 1, a set of baseline data at 6 mL was created for development of an automated microscale platform. At stage 2, a full two level factorial design was undertaken to investigate Fab' precipitation using PEG with yield and purification factor as key responses using the automated microscale platform. A more detailed central composite face centred DoE was then performed, which examined potential operating regions identified in stage 2 in more depth.

Stage 1

Create a set of baseline data at 6 mL scale for the development of a high throughput system to mimic this scale.

Stage 2

Full two level factorial DoE to investigate Fab' precipitation using PEG by varying PEG molecular weight (4000 to 20000), pH (5 to 9), homogenate dilution factor (1 to 5) and PEG concentration w/v (5% to 20%) with yield and purification factor as key responses. Blue dots represent experiments conducted in the DoE design space.
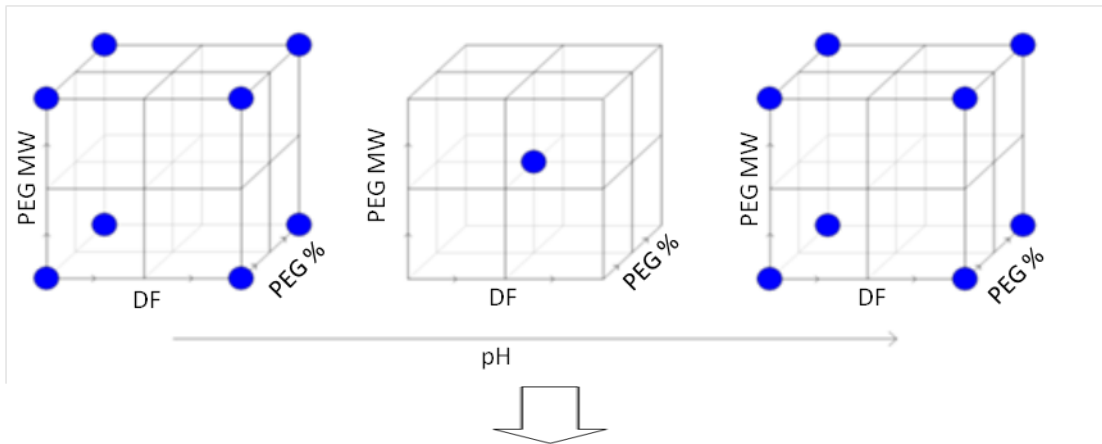
Stage 3

Central composite face centred DoE (response surface methodology) was completed to find an optimal range of conditions to deliver high Fab' yield and purification factor within the ranges investigated. Red dots represent the additional experiments in a CCF DoE compared to the full factorial DoE shown above. The midpoint of the original factorial design was repeated for data robustness.
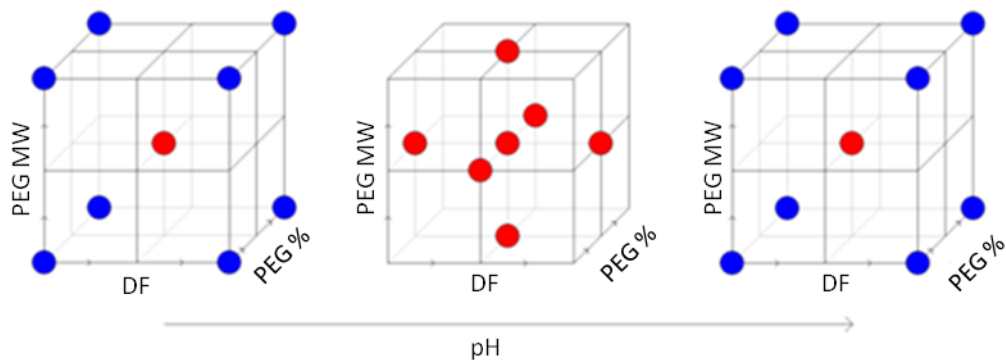
Figure 3.1: *Flowchart of the approach used in this chapter to explore conditions for the initial Fab' precipitation steps. Since the primary aim of such steps was to recover and purify the product, yield and purification factor was used as the key responses to judge performance*

STAGE 1

3.3 Results and Discussion

3.3.1 Timescale Precipitation Experiments

The time taken for the precipitation of Fab' was investigated using PEG 4000 and 20000. For each condition, a range of PEG concentrations (% w/v) was investigated shown in table 3.1.

Stock solutions of PEG 4000 and 20000 were made at 50% w/v in 100 mM Tris HCl pH 7.4. The experiments were performed in 15 mL bijoux tubes using 10 mm stirrer bars for mixing controlled by a VWR magnetic stirrer plate (VWR International Ltd., Leighton, UK). This mixing plate did not have the speed of mixing as a quantitative output (a dial is numbered 1 to 10, with 10 being the fastest mixing speed) and therefore a mixing speed was used that was sufficient to enable turbulent conditions (number 8 on dial). The total experimental volume was 10 mL of which 3.3 mL consisted of homogenate, and the remainder 6.7 mL was a combination of 100 mM Tris HCl pH 7.4 and PEG. In all cases, feed was added to the precipitant. 2 mL samples of each condition as highlighted in table 3.1 were taken at 0, 30, 60, 90, 120, 240 and 1000 minutes, and centrifuged in an Eppendorf 5415D centrifuge (Eppendorf UK Ltd., Cambridge, UK) for 10 minutes at 10000 rpm.

The supernatant post centrifugation was analysed for Fab' and total protein concentration using a 1 mL Protein G column (GE Healthcare, Uppsala, Sweden) on a Agilent 1200 HPLC system (Agilent, Edinburgh, UK) and the Pierce BCA total protein assay (Pierce, Rockford, USA) as described in sections 2.1 and 2.2 respectively. The precipitated pellets readily dissolved in 2 mL of 100 mM Tris HCl pH 7.4 and the total protein mass balance was between 95% to 105%.

Final PEG 4000 concentration (% w/v)	Volume of PEG (mL)	Volume of 100 mM Tris HCl pH 7.4 (mL)	Homogenate volume (mL)
2.5	0.5	6.2	3.3
10.0	2.0	4.7	3.3
20.0	4.0	2.7	3.3
Final PEG 20000 concentration (% w/v)	Volume of PEG (mL)	Volume of 100 mM Tris HCl pH 7.4 (mL)	Homogenate volume (mL)
2.5	0.5	6.2	3.3
20.0	4.0	2.7	3.3

Table 3.1: *Table lists the volumes of homogenate pH 7.4, PEG (from a stock concentration of 50% w/v pH 7.4) and 100 mM Tris HCl pH 7.4 that were used in this experiment. C_0 for Fab' and total protein was 0.7 g L^{-1} and 4.6 g L^{-1} respectively. Experiments were performed in 15 mm bijoux tubes at 10 mL scale. Samples were mixed using 10 mm stirrer bars for a total of 1000 minutes at turbulent mixing conditions on a VWR magnetic stirrer plate (VWR International Ltd., Leighton, UK). 2 mL samples were taken periodically, centrifuged and then the supernatant was analysed for Fab' and total protein concentration as described in sections 2.1 and 2.2 respectively. The experiments were repeated in triplicate for robustness*

The Fab' and total protein solubility profiles are shown in figures 3.2 and 3.3. There was an insignificant difference in the solubility of Fab' with PEG 4000 and 20000 at 2.5% w/v after 1000 minutes (65% and 66% Fab' remaining soluble respectively). In both cases, total soluble protein remaining was 70% and 63% respectively as determined by the BCA assay (Pierce, Rockford, USA). However, with PEG 20000 the plateau for maximum Fab' precipitation was observed at 2.5% at 30 minutes relative to 60 minutes by PEG 4000.

There was an insignificant change in the solubility of Fab' by PEG 4000 and 20000 at 20% w/v after 60 and 30 minutes respectively (0.4% and 0.3% Fab' remaining soluble respectively). However, 27% total protein was remaining in solution with PEG 4000 compared to 18% with PEG 20000, which continued to decrease till 1000 minutes. These results correlate with previous work performed by Atha and Ingham (1981) and Lewis and Metcalf (1988), where they reported that protein precipitation increased with increasing size of PEG polymer.

The initial drop in solubility can be explained by aggregation of fine particulates formed during nucleation resulting in a reduction of the concentration of solids and

hence turbidity. This is in part due to the initiation of precipitation (the nucleation stage), which is characterised by the appearance of very fine particulates. This is in agreement with previous work by Knevelman *et al.,* (2010). It was observed that the addition of PEG 4000 at 20% w/v resulted in 0.4% soluble Fab' and 35% soluble protein remaining in solution after 60 minutes. Similarly, PEG 20000 at 20% w/v caused 0.3% soluble Fab' and 29% soluble protein remaining in solution after 30 minutes. The use of PEG 20000 20% w/v resulted in 50% reduction in the time taken for Fab' precipitation to complete relative to PEG 4000 at 20% w/v. The difference in the time taken to precipitate Fab' by PEG can be explained via the excluded volume effect further described in section 1.4.3. Excluded volume refers to that part of the PEG molecule that cannot occupy space that is already occupied by another part of the same PEG molecule (Atha and Ingham 1981). Lewis and Metcalf (1988) suggested that PEG acts as an "inert solvent sponge" that prevents interaction of all proteins present with the solvent, effectively increasing their concentration until solubility is exceeded and precipitation occurs.
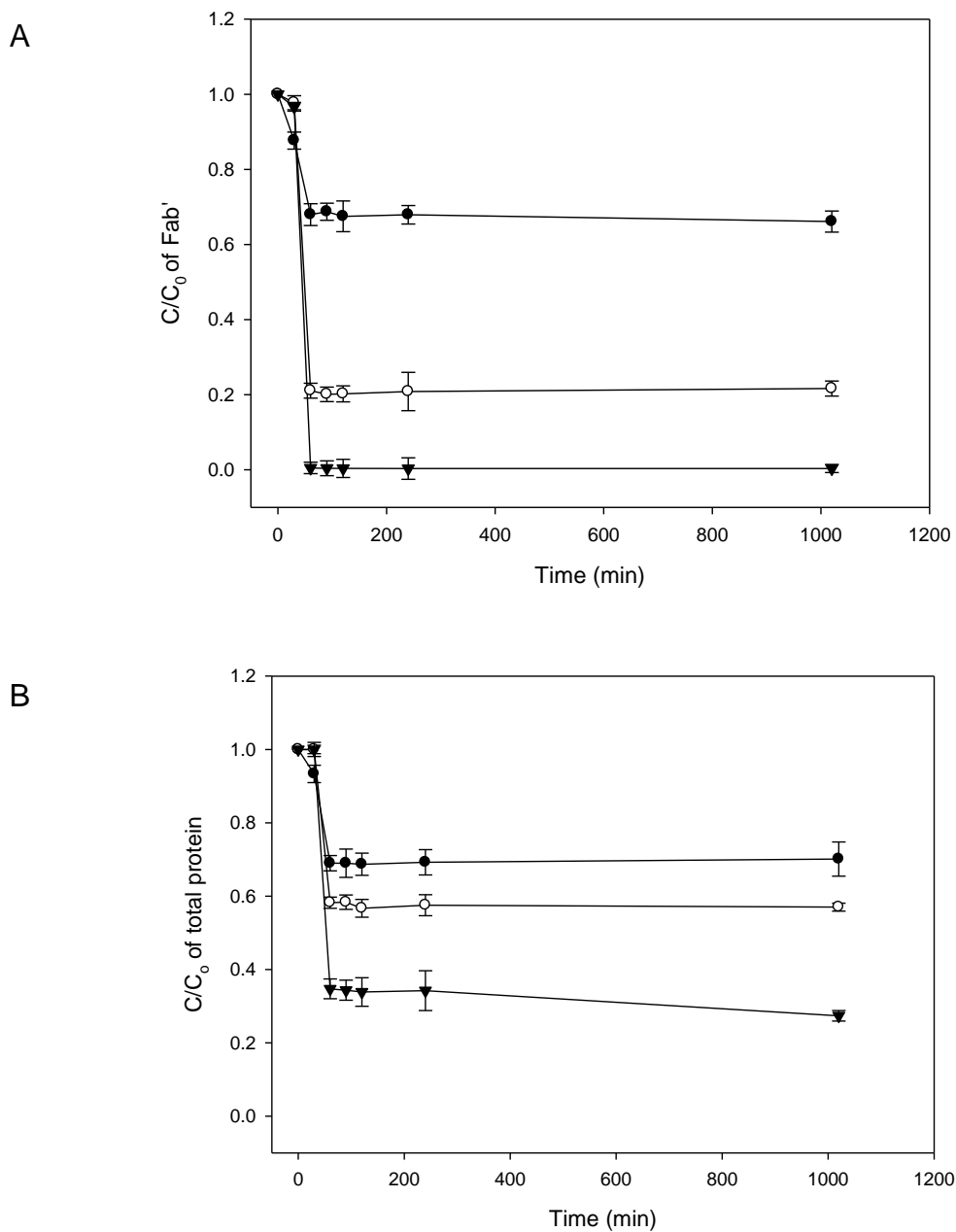
Figure 3.2: *Effect of PEG 4000 on the solubility of Fab' (A) and total protein (B) over time at 2.5% (●), 10% (○) and 20% (▼) w/v at pH 7.4. C_0 for Fab' and total protein was 0.7 g L^{-1} and 4.6 g L^{-1} respectively. Total experimental volume in each reactor was 10 mL. Samples were mixed for a total of 1000 minutes at turbulent mixing conditions. 2 mL samples were taken periodically, centrifuged and then the supernatant was analysed for Fab' and total protein concentration as described in sections 2.1 and 2.2 respectively. Error bars are shown for one standard deviation for triplicate experiment repeats*
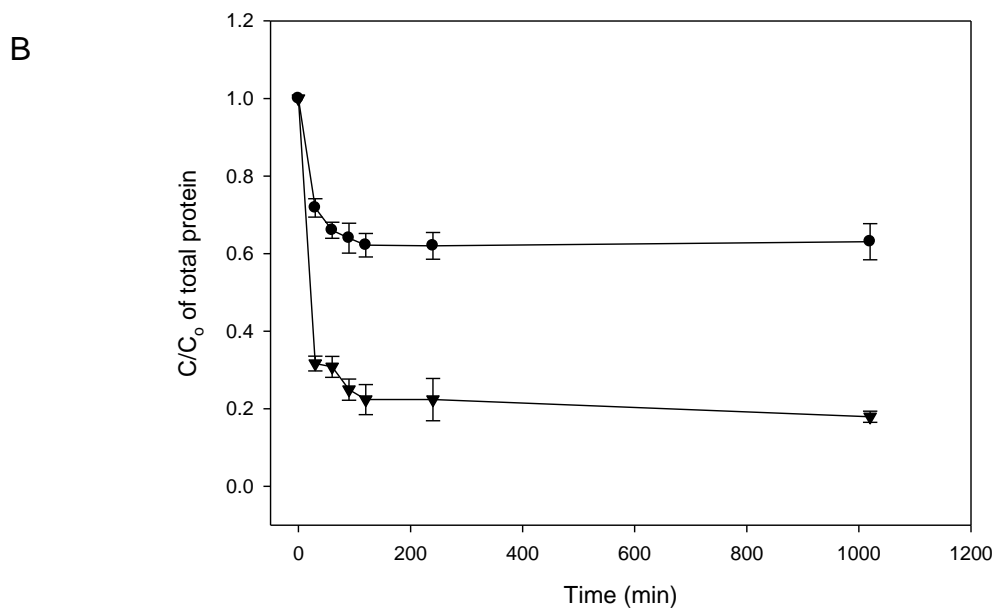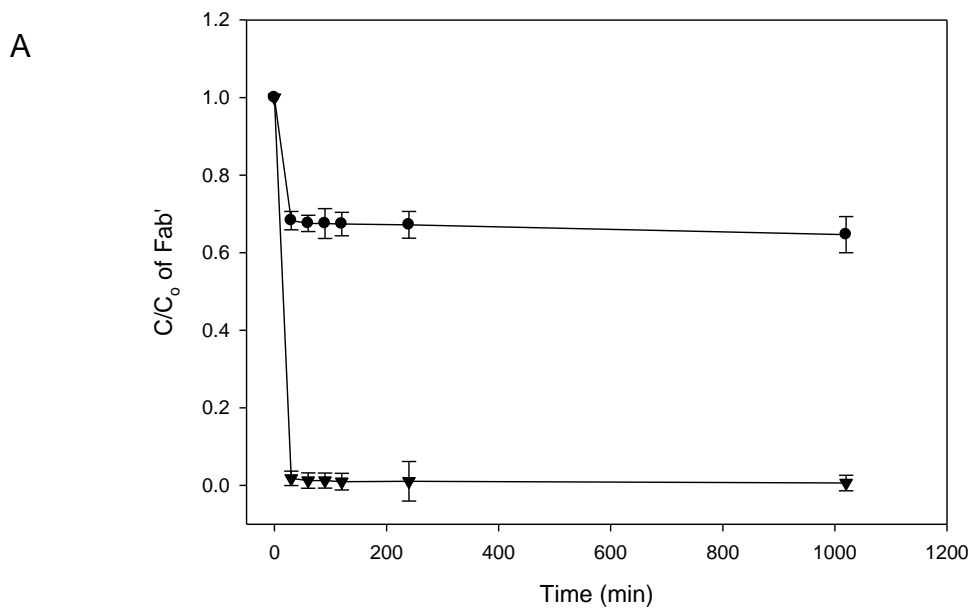
Figure 3.3: *Effect of PEG 20000 on the solubility of Fab' (A) and total protein (B) over time at 2.5% (●), and 20% (▼) w/v at pH 7.4. C_0 for Fab' and total protein was 0.7 g L^{-1} and 4.6 g L^{-1} respectively. Total experimental volume in each reactor was 10 mL. Samples were mixed for a total of 1000 minutes at turbulent mixing conditions. 2 mL samples were taken periodically, centrifuged and then the supernatant was analysed for Fab' and total protein concentration as described in sections 2.1 and 2.2 respectively. Error bars are shown for one standard deviation for triplicate experiment repeats*

3.3.2 Precipitation of Fab' by the Addition of PEG at 6 mL Scale

Stock solutions of PEG 4000, 6000, 8000, 10000, 12000 and 20000 were made at 50% w/v in 100 mM Tris HCl pH 7.4. Experiments were performed in 15 mL bijoux tubes with a total working volume of 6 mL. 10 mm stirrer bars were used for mixing, controlled by a VWR magnetic stirrer plate (VWR International Ltd., Leighton, UK). This mixing plate did not have the speed of mixing as a quantitative output (a dial is numbered 1 to 10, with 10 being the fastest mixing speed) and therefore a mixing speed was used that was sufficient to enable turbulent conditions (number 8 on dial). 2 mL of reaction mixture consisted of homogenate, and the remainder 4 mL was a combination of 100 mM Tris pH 7.4 and PEG. In all cases, feed was added to the precipitant. 2 mL samples were taken after 60 minutes and centrifuged in an Eppendorf 5415D centrifuge (Eppendorf UK Ltd., Cambridge, UK) for 10 minutes at 10000 rpm. Table 3.2 lists the conditions used for all PEG molecular weights. The precipitated pellet dissolved readily in 2 mL of 100 mM Tris HCl pH 7.4 and total protein mass balance was between 95% to 105%. These experiments were repeated at 3 mL total volume for comparative purposes.

Final PEG concentration (% w/v)	Volume of PEG (mL)	Volume of 100 mM Tris HCl pH 7.4 (mL)	Homogenate volume (mL)
0.0	0.0	4.0	2.0
2.5	0.3	3.7	2.0
5.0	0.6	3.4	2.0
7.5	0.9	3.1	2.0
10.0	1.2	2.8	2.0
12.5	1.5	2.5	2.0
15.0	1.8	2.2	2.0
17.5	2.1	1.9	2.0
20.0	2.4	1.6	2.0

Table 3.2: *Table lists the volumes of homogenate pH 7.4, PEG 4000, 6000, 8000, 10000, 12000 and 20000 (from a stock concentration of 50% w/v pH 7.4) and 100 mM Tris HCl pH 7.4 that were used in this experiment. C_o for Fab' and total protein was 0.7 g L^{-1} and 4.6 g L^{-1} respectively. This experiment was performed in 15 mL bijoux tubes at 6 mL scale. Samples were mixed using 10 mm stirrer bars for a total of 1000 minutes at turbulent mixing conditions on a VWR magnetic stirrer plate (VWR International Ltd., Leighton, UK). 2 mL samples were taken and centrifuged, and then the supernatant was analysed for Fab' and total protein concentration as described in sections 2.1 and 2.2 respectively. Experiments were repeated in triplicate for robustness*

Figures 3.4 and 3.7 show the effect of PEG 4000 to 20000 on the solubility of Fab' and total protein. It was found that greater than 15% w/v PEG concentration had minimal effect on the precipitation of Fab' at all PEG molecular weights tested. At this point on average there was 0.04% and 82% soluble Fab' and total protein remaining in solution. At 10% w/v, PEG 20000, 81% of total protein was soluble, which decreased to 50% at 20% w/v, comparatively to PEG 4000 which at 10% and 20% w/v had 97% and 88% total protein remaining in solution (figures 3.6 and 3.7). This is agreement with Polson *et al.,* (1964) who showed that as the size of PEG increases, its effectiveness for precipitating out proteins increased. The experiments repeated at 3 mL suggest there is an insignificant difference between Fab' and total protein solubility profiles at 3 mL and 6 mL, suggesting a robust precipitation process.

PEG is a viscous polymer at 50% w/v for polymer size 20000. The viscosity of PEG 4000, 6000, 8000, 10000, 12000 and 20000 was measured using a cone and plate viscometer (Bohlin Instruments, MA, USA) and was determined to be 0.1, 0.1, 0.1, 0.2, 0.3 and 1.8 Pa s at 50% w/v at shear rate of 38 s^{-1} respectively. The viscosity of PEG did not change with increasing shear rates to a maximum shear rate tested of 152 s^{-1}. This suggested a Newtonian fluid system (Gonzalez-Tello *et al.,* 1994).

An increase in Fab' solubility with PEG 12000 and 20000 in the region between 2.5% w/v was observed. It is possible that at 0% w/v PEG, Fab' was aggregated, which gave a measured concentration that is lower than its actual concentration, with the addition of low PEG concentrations, a salting in effect may have been induced. The mechanism could be similar to that of salts in the Hofmeister series, which weaken the hydrophobic effect by increasing solubility, resulting in the salting in effect (Richardson *et al.,* 1990). This effect with PEG could be termed "PEGing in".

Polson *et al.,* (1964) observed that the ability to precipitate a protein is an inverse function of the molecular weight of PEG used. Therefore, relatively low concentrations of high molecular weight polymers are required to precipitate Fab', and thus high concentrations of low molecular weight varieties are required to effect the same degree of precipitation of Fab'. This study to precipitate Fab' is not in agreement with work performed by Polson *et al.,* (1964) as little difference in Fab' solubility was observed with the PEG molecular weights in the range investigated, with this feedstream. They concluded that the precipitation by PEG cannot be explained by a possible dehydrating effect, which the polymer may have on the protein molecules. If this were the case, it might be expected that the low molecular weight varieties would dehydrate the protein molecules more rapidly largely because of their higher osmotic pressures than the higher molecular PEG weight varieties.
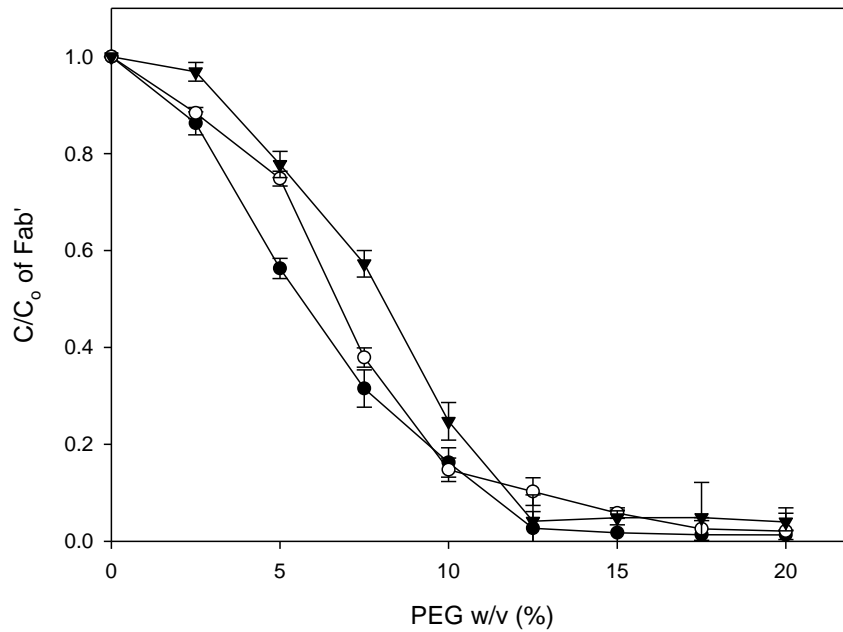
Figure 3.4: *Effect of PEG 4000 (▼), 6000 (○) and 8000 (●) on the solubility of Fab' at 6 mL scale at pH 7.4. C_o for Fab' was 0.7 g L^{-1}. The samples were mixed for a total of 60 minutes at turbulent mixing conditions. 2 mL samples were taken and centrifuged, and then the supernatant was analysed for Fab' concentration as described in section 2.1. Error bars are shown for one standard deviation for triplicate experiment repeats*
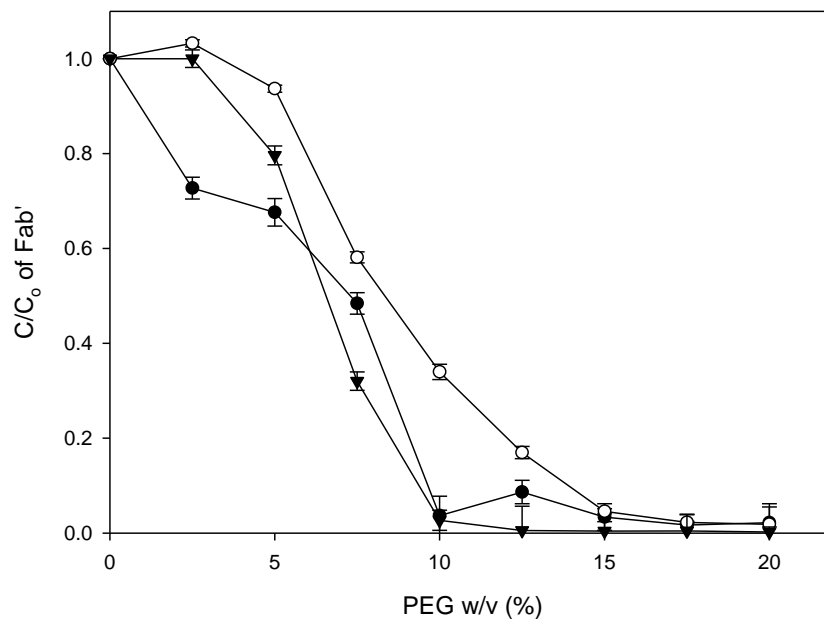
Figure 3.5: *Effect of PEG 10000 (○), 12000 (●) and 20000 (▼) on the solubility of Fab' at 6 mL scale at pH 7.4. C_o for Fab' was 0.7 g L^{-1}. The samples were mixed for a total of 60 minutes at turbulent mixing conditions. 2 mL samples were taken and centrifuged, and then the supernatant was analysed for Fab' concentration as described in section 2.1. Error bars are shown for one standard deviation for triplicate experiment repeats*
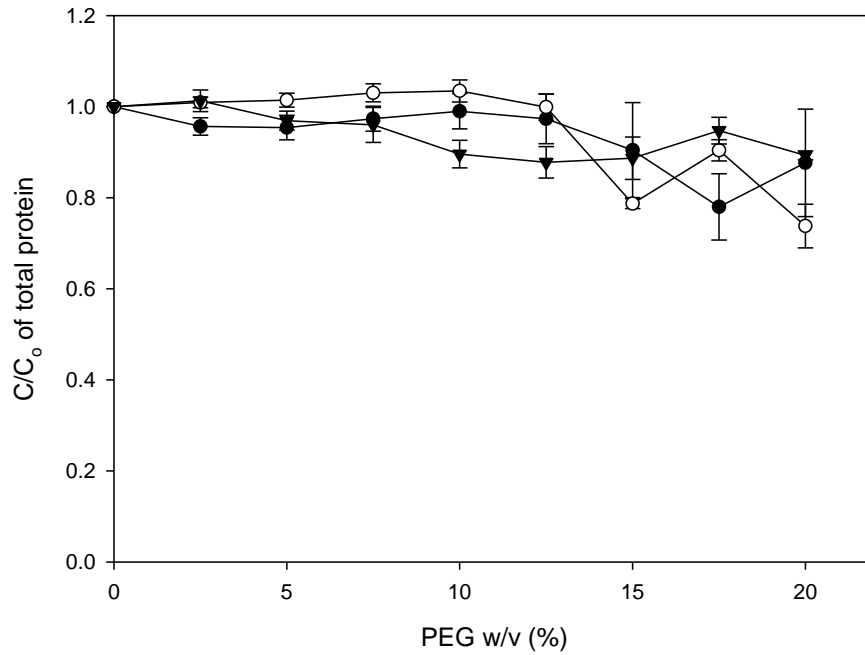
Figure 3.6: *Effect of PEG 4000 (○), 6000 (●) and 8000 (▼) on the solubility of total protein at 6 mL scale at pH 7.4. C_o for total protein was 4.6 g L^{-1}. The samples were mixed for a total of 60 minutes at turbulent mixing conditions. 2 mL samples were taken and centrifuged, and then the supernatant was analysed for total protein concentration as described in section 2.2. Error bars are shown for one standard deviation for triplicate experiment repeats*
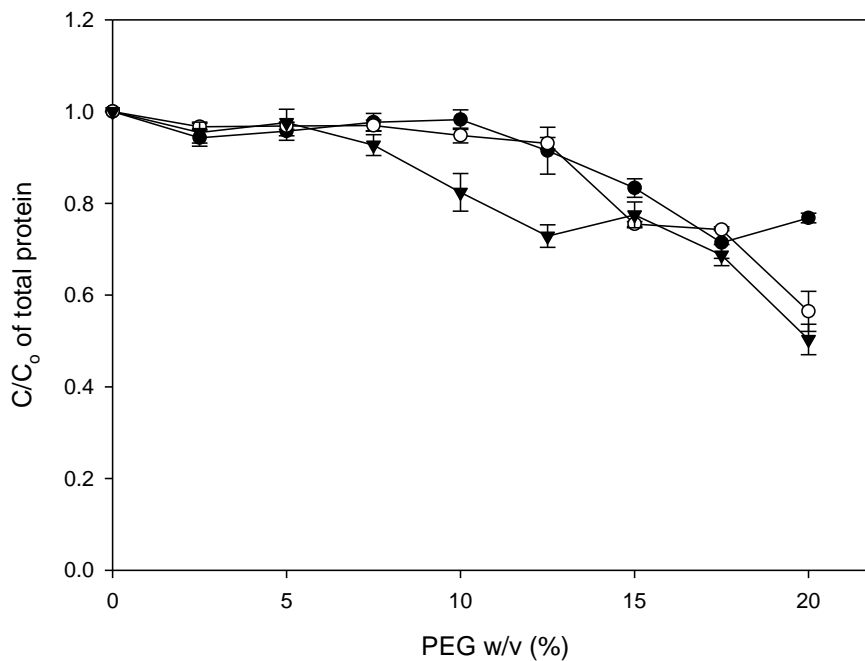
Figure 3.7: *Effect of PEG 10000 (●), 12000 (○) and 20000 (▼) on the solubility of total protein at 6 mL scale at pH 7.4. C_o for total protein was 4.6 g L^{-1}. Samples were mixed for a total of 60 minutes at turbulent mixing conditions. 2 mL samples were taken and centrifuged, and then the supernatant was analysed for total protein concentration as described in section 2.2. Error bars are shown for one standard deviation for triplicate experiment repeats*
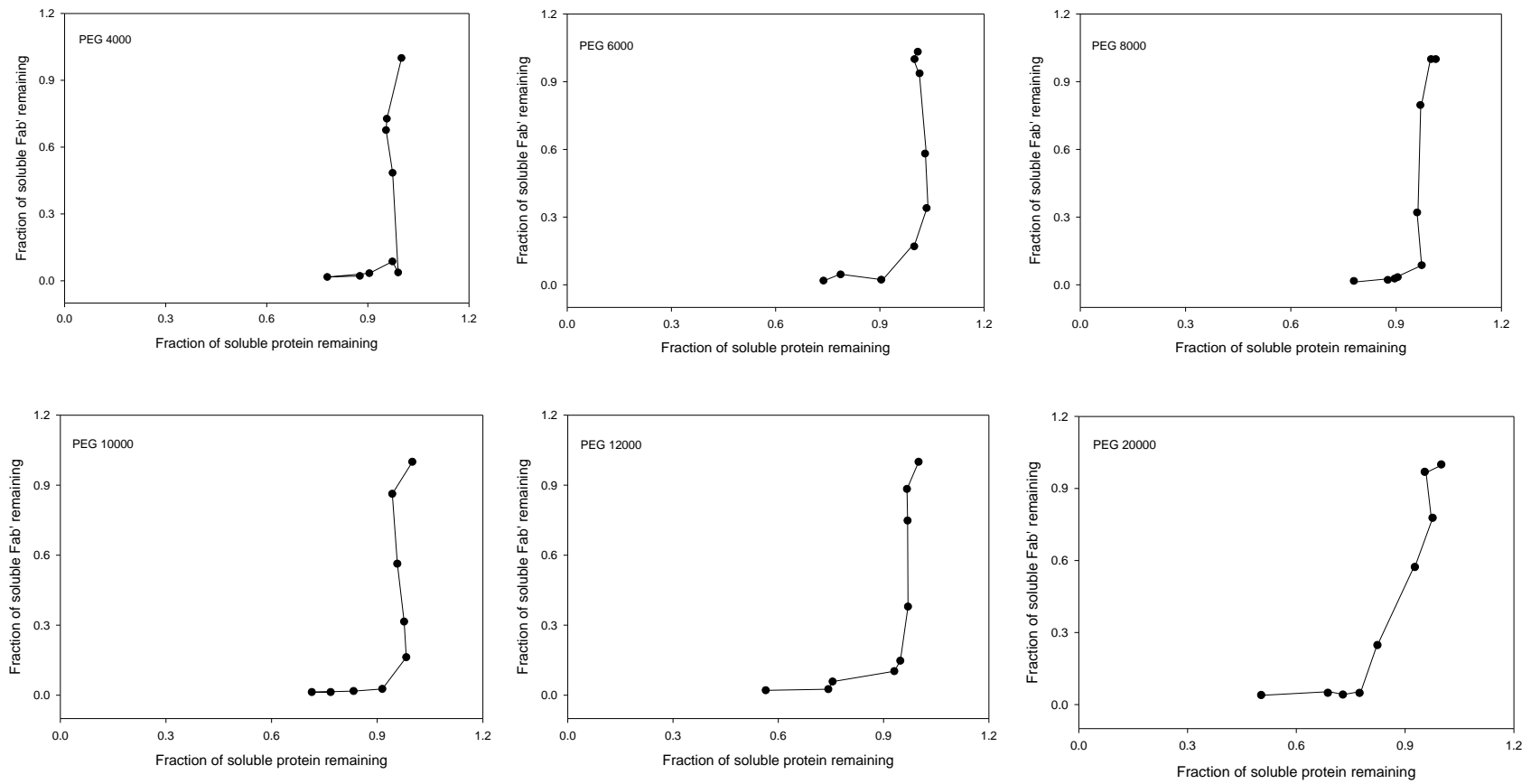
Figure 3.8: *Fab' and total protein fractionation diagrams derived from the solubility profiles shown in figures 3.4 to 3.7*

Figure 3.8 illustrates the total fractionation diagrams derived from the data of figures 3.4 to 3.7. The axes are the fraction of Fab' and total protein remaining soluble. The figure is obtained by dividing the adjusted solubility by the initial concentrations derived from the total protein Pierce BCA (Pierce, Rockford, USA) and Fab' Protein G HPLC (GE Healthcare, Uppsala, Sweden) assays. Figure 3.9 shows the combined fractionation diagrams of PEG 4000, 8000, 12000 and 20000 which illustrates an insignificant difference between PEG molecular weights in the range investigated for the precipitation of Fab' and total protein impurities. However, PEG 20000 precipitates more total protein than the shorter PEG polymers in the range investigated.
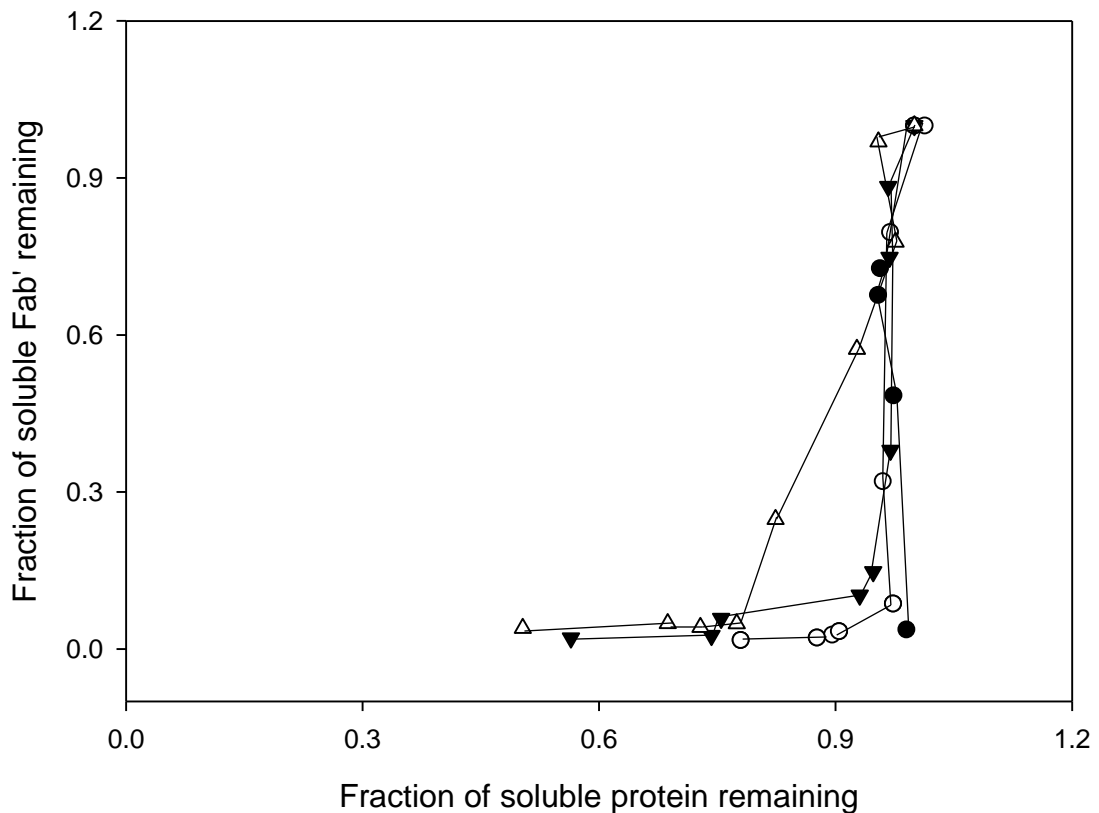
Figure 3.9: *Fab' and total protein fractionation diagrams derived from the Fab' and total protein solubility profiles using PEG 4000 (•), PEG 8000 (○), PEG 12000 (▼) and PEG 20000 (△) shown in figure 3.8*

Theoretically, the gradient of the straight line will give the purification factor, which could be calculated for 100% theoretical yield. Subsequently, a strategy could be developed to improve the purification factor by using a double cut fractionation approach as described by Richardson et *al.,* (1990). In essence, PEG is added to

precipitate the less soluble impurities, after which the concentration of PEG is increased to precipitate the Fab'. The fractionation efficiency could be affected by changes in temperature, pH and buffer.

3.3.3 Development and Automation of a Precipitation Platform on a Liquid Handling Robot

Rapid volume reduction and product concentration have become major issues in early downstream processing steps. To date, conventional processes performed in early development and optimisation experiments have reached their limits in terms of economics and processing speed (Bensch *et al.,* 2007). Furthermore, it does not always lead to the most robust processes since the parameter space cannot be fully explored. Microscale bioprocessing techniques offer a change in bioprocess development timelines, accelerating process development by enabling parallel experimentation and automation while requiring microscale quantities of material (Galaev 2005, Titchener-Hooker *et al.*, 2008). Critical bioprocess information can be obtained earlier in development providing better opportunity to understand process parameters. These microscale systems should be developed to mimic key engineering characteristics for scale up (Biddlecombe and Pleasance 1999). Microscale techniques enable a platform for next generation bioprocess development that decreases cycle times while increasing process understanding (Titchener-Hooker *et al.,* 2008).

Microscale bioprocess methods defined in this thesis refers to the significant scale down of a bioprocess unit operation or some feature of that operation, often with the goal being to directly model a critical parameter of the operation (e.g. shear during centrifugation described in section 5.4.1). This approach can be invaluable at the process definition stage of drug development when pilot scale trials are unfeasible or material is scarce i.e. for high value products. Large volumes of process data can be provided from low resource usage during route scouting experiments enabling strong drug candidates to be spotted earlier. Rapid and accurate process development also holds the key in weeding out weaker candidates and saving company resources.

High throughput microscale screening experiments can be used to explore the design space and thereby predict subsequent laboratory scale development. A

small number of focused optimisation experiments are required at the laboratory scale, where scale up effects to pilot and manufacturing scales are well understood (figure 3.10). Detailed information regarding the design space can be rapidly acquired from microscale experiments, and since only small amounts of material are required, these experiments can be done very early on in process development (Rege *et al.,* 2005).
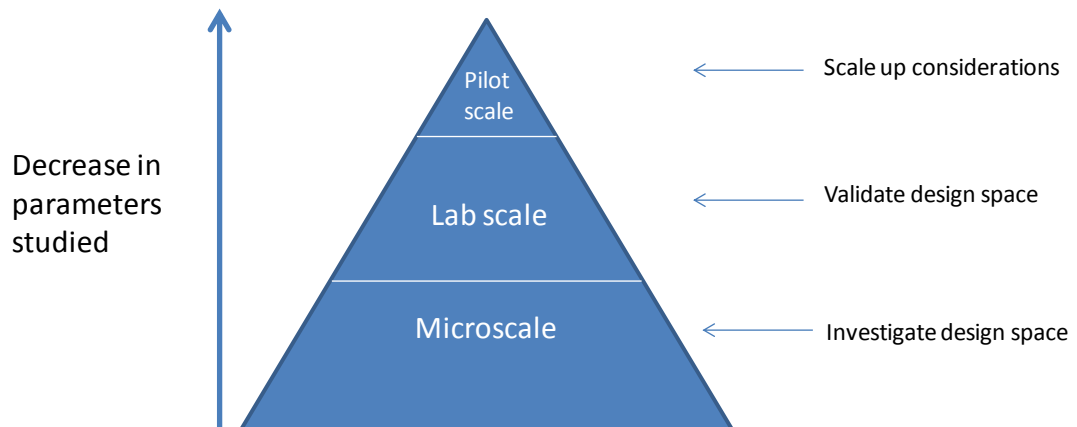
Figure 3.10: *Value of microscale experiments in process development. High throughput microscale experiments are used to map a design space and to achieve high robustness, which reduces further experimentation at larger scale and cost*

Current research on microwell unit operations has mostly focused on fermentation with little to show for downstream unit operations (Kostov *et al.,* 2000, Duetz *et al.*, 2001, Jackson *et al.,* 2006, Micheletti and Lye 2006). The use of robotic liquid handling and DoE has been successfully employed for a number of biological systems ranging from fermentation processes to assay development (Lutz, *et al.,* 1996). One particular case involved the screening for operating conditions of an *E.coli* fermentation process (Islam *et al.,* 2007). The use of a DoE approach enabled the complex fermentation system consisting of 10 key variables to be fully investigated. Of these 10 variables from initial screening, it was found that only six of these variables were significant. A second round of optimisation to improve the resolution around the expected optimum was performed, which reduced the number of key variables to 3. One of which was the plate shaking speeds pre and post induction. Further analysis then highlighted the importance of oxygen transfer in the fermentation at the microwell scale and allowed for appropriate considerations when scaling up to process scale (Islam *et al.*, 2007). The advantage of running this DoE

at microscale meant that for a process like fermentation where each experiment takes a significant amount of time, the ability to carry out 30 experiments with unique conditions was possible relatively quickly.

In a similar way, a microscale system was developed for the high throughput screening of precipitation conditions using a statistical Design of Experiments study in 96 deepwell plates. 96 deepwell plates are small plates consisting of identical wells capable of holding microlitre volumes and are available in various geometries. Their origins are in analytical and high throughput screening applications and are now finding their way into process design (Duetz *et al.*, 2001).

Precipitation in 96 deepwell plates can be fully automated improving reliability, and are suited to the automated batch experimentation in microlitre quantities (20-2000 μL). Although it can be performed manually with a pipette it is difficult to control consistency. An automated process enables the method to be easily deployed among a wide range of users.

There were a number of considerations considered when developing the high throughput screening system:

- Total reaction volume of 1 mL
- The buffer provides the pH environment for the proteins in solution. Buffer pH can change with temperature, the magnitude of the change being dependent on the buffer itself and thus experiments were performed at room temperature to normalise any effects of temperature.
- Accommodate PEG concentration in range of 0% to 20% w/v from 50% w/v stock solutions
- Appropriate method of mixing when all reagents are added
- Consideration for liquid handling of small volumes and in some cases handling highly viscous solutions
- Use of the automatic liquid handling to aid in the analysis of experiments namely, the total protein assay and preparation of solutions for HPLC analysis.

Nunc 96 deepwell plates (Nunc GmbH & Co., KG, Denmark) with a total working volume of 1.3 mL were used (figure 3.11). These plates were chosen to minimise

material consumption. The U-bottom design helps with forming compact sediment when centrifuged and for ease of removing supernatant without disturbing the precipitated pellet.
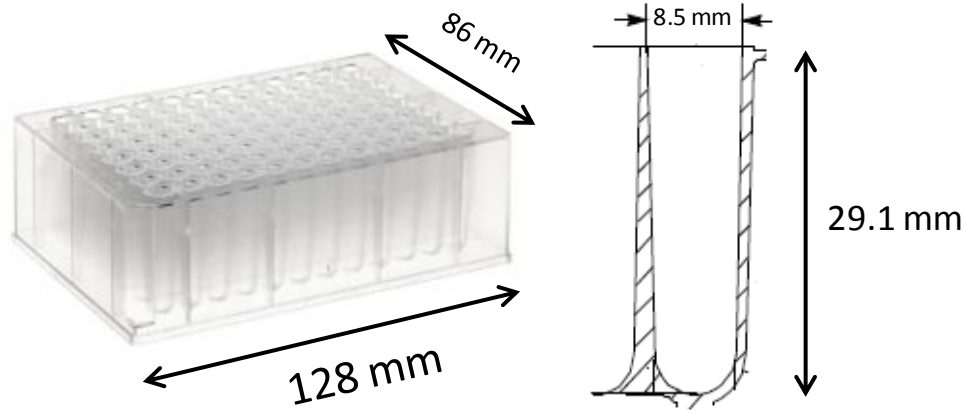
Figure 3.11: *Nunc 1.3 mL 96 deepwell plates (Nunc GmbH & Co., KG, Denmark) used in microscale experiments*

Mixing in the form of shaking plates was investigated. Micheletti *et al.,* (2006) investigated the current understanding of mixing and mass transfer phenomena in shaken bioreactors to show how these can be used to define initial conditions for reliable scale up of microscale cultures. They monitored liquid hydrodynamics using a camera and a critical frequency (*N*crit) to identify liquid height and surface area change. The equation for critical frequency is shown in equation 3.1, which gives a minimum frequency to disrupt liquid surface tension.

$$N_{\text{crit}} = \sqrt{\frac{\sigma d_w}{4\pi V_L \rho d_s}}.$$

(3.1)

Equation 3.1: *Critical frequency where σ is the liquid surface tension (N m^{-1}), d_w is the shaken microwell diameter (m), V_L is the liquid volume (m^3), ρ is the liquid density (kg m^{-3}), d_s is the shaken diameter (m) (Micheletti et al., 2006)*

Critical frequency was calculated to be 233 rpm for a Thermo Scientific orbital plate shaker (Thermo Scientific, LA, USA), with an d_s of 0.003 m and assuming liquid surface tension and density of water of 0.08 N m^{-1} and 1000 kg m^{-3} respectively.

However, mixing by shaking proved difficult even at maximum shaking speed (1000 rpm) with concentrations of PEG greater than 10% w/v due to its viscosity. For many bioprocess applications, such as stability assays, shaken systems are not appropriate and mixing should be performed in static microplates (Aucamp *et al.*, 2005). Rapid and efficient mixing can be provided from the liquid addition by the pipette tip of a liquid handling robot followed by repeated reaspirations and dispenses (jet mixing). However, this method does not suit the high throughput nature of the tests (Nealon *et al.*, 2006). Therefore, due to size of the wells and for future process scale up considerations, magnetic coin stirrers were used as the method of agitation (figure 3.12). However, the control of the rate of agitation of these stirrers was difficult as a PC-611 magnetic stirrer plate (Corning, New York, USA) was used, which did not have mixing speed outputs. The rate of agitation was therefore not quantifiable and further scale up to 50 mL stirred tank reactors (STR) and 5 L STR pilot scale would prove difficult at this stage.

Small PTFE magnetic coin stirrers (model VP 772FN) capable of fitting in each of the 96 wells were sourced from V&P Scientific (V&P Scientific, San Diego, USA) (figure 3.12). The PTFE magnetic discs were 5 mm in diameter and 2.27 mm thick.
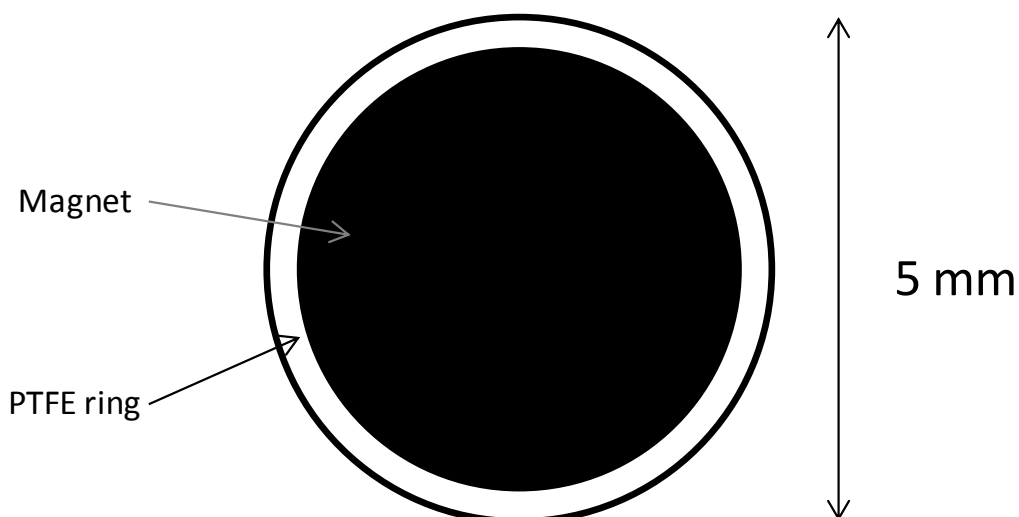
Figure 3.12: *Diagram represents magnetic coin stirrers (model VP 772FN) used for microscale experiments The stirrers were sourced from V&P Scientific (V&P Scientific, San Diego, USA)*

All microscale precipitation experiments were automated and performed by a four tip, Multiprobe II EX (Packard Instrument Co., Meriden, USA) liquid handling robot

(LHR). The Multiprobe II EX workstation (Packard Instrument Co., Meriden, USA) (figure 3.13 A) was equipped with a four channel liquid handling arm for transferring liquids between labware and pipetting through the micro tips. 1 mL disposable conductive BioRobotix tips (VWR International Ltd., Leighton, UK) were used for liquid handling. The Multiprobe II EX (Packard Instrument Co., Meriden, USA) was configured for picking up the micro tips and setting the micro tips back into their racks only when buffer was used. Tips were discarded when used for the transfer of PEG and homogenate feed. Four micro tips were picked up at a time in each automated experiment.

A typical deck layout for the experiments in this chapter is shown in figure 3.13 B, and the layout was modified for a specific application or higher throughput. In the setup shown, the deck is configured with three carriers for holding microtiter plates and deepwell plates. In addition, additional carriers were used for holding reagent troughs and micro tips.
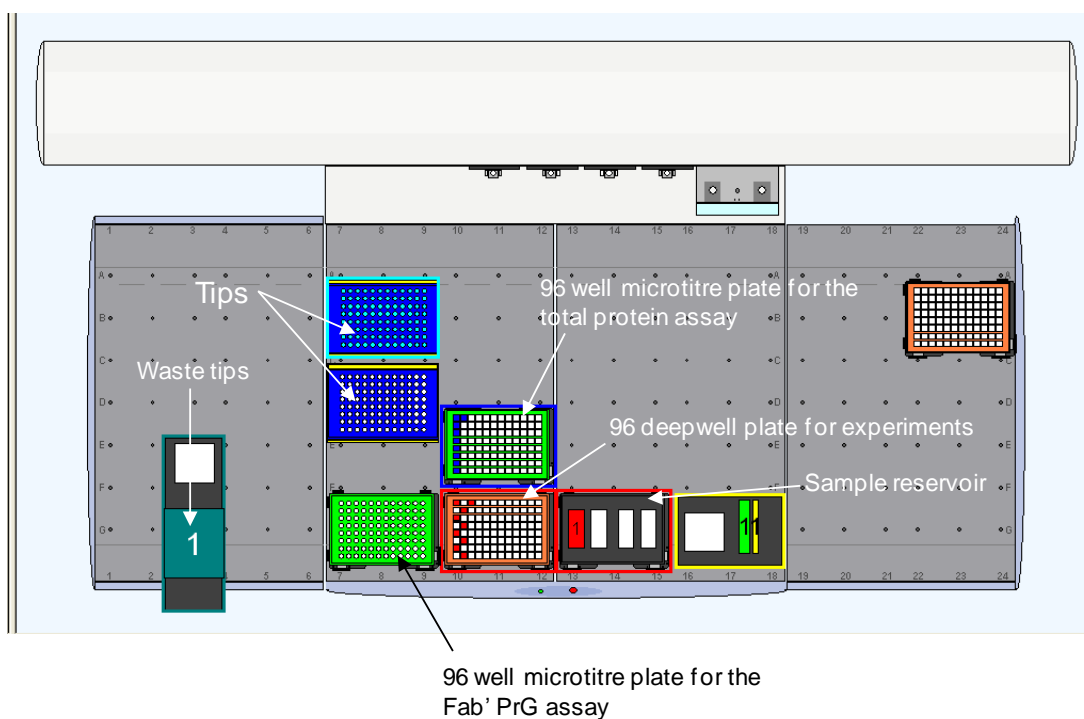
Figure 3.13: *Multiprobe II EX (Packard Instrument Co., Meriden, USA) liquid handling robot (LHR) used for microscale experiments. (A) photograph of instrument and (B) is an example deck layout for experiments*

The WINPREP application software controls the Multiprobe. BioRobotix (VWR International Ltd., Leighton, UK) disposable tips with a size of $d_{internal} = 0.8$ mm were used at injection flowrates of 7 µL s^{-1} (turbulent). Well additions were made at the

liquid surface, with liquid tracking to minimise droplet formation. The jet nozzle position was 1 mm below the liquid surface for which the liquid handling robot's tracking function allowed the tip to follow the liquid surface as it rises or descends. The microconducive tips used were disposable. Experiments were performed with disposable tips due to corrosion concerns associated with the precipitant. The performance files in the form of .csv data files were used by the software for governing pipetting precision and accuracy, which had previously been optimised to within a 5% CV limit for low viscosity liquids (Nealon *et al.,* 2006).

The 6 mL design was scaled down to 1 mL and therefore, a volume of 330 μL of *E.coli* Fab' homogenate in each reaction was used. The remaining 670 μL of the reaction volume was split between a combination of PEG and 100 mM Tris HCl pH 7.4.

The V&P Scientific (model VP 772FN) PTFE magnetic coin stirrers (V&P Scientific, San Diego, USA) were too strong leading to interference between the magnets in adjacent wells. A compromise of using alternate wells was reached, limiting throughput to 48 individual experiments on one plate (figure 3.14). A heavy duty stirrer, PC-611 (Corning, New York, USA) was used to stir the coin magnets within the wells (set to dial number 7). Mixing was similar to a tumbling effect and lasted 60 minutes and a sealing film was used on each plate to prevent contamination.
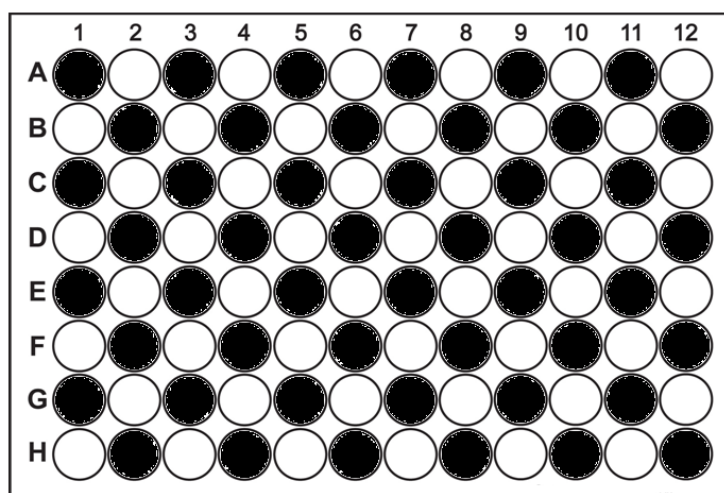
Figure 3.14: *Top view representation of the wells used in a 1.3 mL 96 deepwell plate (Nunc GmbH & Co., KG, Denmark) for the microscale experiments. Shaded wells indicated wells used due to the strength of the magnets limiting throughput to 48 individual experiments on one plate*

A number of performance files were set up to deal with the different viscosities of PEG molecular weights. The Multiprobe II EX (Packard Instrument Co., Meriden, USA) liquid handling robot had by default an operation setting specifically for products of similar density and viscosity to water. This proved problematic with pipetting PEG accurately due to the PEG having a much higher viscosity than water (section 3.3.2). A change in a number of settings was required in order to ensure correct volumes were dispensed. This required changing liquid tracking settings, speed of aspiration and dispensing (7 μL s^{-1} for buffers and 1 μL s^{-1} for PEG), using the slowest speed of retraction of the tips from the solution and the use of 0.8 mm wider bore pipette tips. A number of tests were performed to ensure that no drop was left in the tips following a reagent transfer. Particularly with lower volume transfers, the presence of 1 drop in the pipette tip can yield a significant error.

Following mixing, to separate the precipitated material from the solution, a deepwell 0.45 µm filter plate (Millipore, Hertfordshire, UK) was initially trialled as an appropriate method for solid-liquid separation. This operation was desirable, as it would enable the resuspension of the pellet on the filter. Performing analysis of the samples with this method would allow a full total protein mass balance on the system to be performed relatively quickly by running the BCA total protein assay simultaneously on the deck. However, this proved problematic particularly with PEG of molecular weights ≥ 8000. Operating under vacuum helped to pass precipitated material through the filter plate, however for highly viscous solutions of high concentrations of PEG ≥ 8000 and ≥ 15% w/v, the material would not filter and crystallised. Centrifugation of the plates for solid-liquid separation was used in all experiments and is more typical of a downstream purification process (Farid 2006). It was found that centrifugation at 4000 rpm using a Eppendorf 5810R centrifuge (Eppendorf UK Ltd., Cambridge, UK) for 25 minutes separated the precipitated material to leave a pellet at the bottom of the microwell. A performance file was created to carefully remove the supernatant without disturbing the pellet and transfer samples to the appropriate 96 well microtiter plate for Fab' and total protein analysis.

3.3.4 Comparative Study to Verify the High Throughput System

Previous data in section 3.3.1 suggested that most Fab' precipitation takes place between 30 minutes and 60 minutes of mixing dependant on the PEG molecular weight used, and therefore for consistency 60 minutes of mixing time was used throughout. Table 3.3 list the experiments and the corresponding volumes of components performed at this stage of the study for comparison with 6 mL scale.

Final PEG concentration (% w/v)	Volume of PEG (µL)	Volume of 100 mM Tris HCl pH 7.4 (µL)	Volume of homogenate (µL)
0.0	0	670	330
2.5	50	620	330
5.0	100	570	330
7.5	150	520	330
10.0	200	470	330
12.5	250	420	330
15.0	300	370	330
17.5	350	320	330
20.0	400	270	330

Table 3.3: *Table lists the volumes of homogenate pH 7.4, PEG 4000, 6000, 8000, 10000, 12000 and 20000 (from a stock concentration of 50% w/v pH 7.4) and 100 mM Tris HCl pH 7.4 that were used in this experiment. C_o for Fab' and total protein was 0.7 g L^{-1} and 4.6 g L^{-1} respectively. This experiment was performed in 1.3 mL 96 deepwell plates (Nunc GmbH & Co., KG, Denmark) at 1 mL scale per well using a Multiprobe II EX (Packard Instrument Co., Meriden, USA) for liquid handling. Samples were mixed for a total of 60 minutes using VP 772FN coin magnets (V&P Scientific, San Diego, USA) at turbulent mixing conditions on a PC-611 (Corning, New York, USA) stirrer. The plate was centrifuged and then the supernatant was analysed for Fab' and total protein concentration as described in sections 2.1 and 2.2 respectively. The experiments were repeated in triplicate for robustness*

Experiments from table 3.3 were performed using a range of different molecular weights of PEG, corresponding to the same molecular weight as in the 6 mL

studies; these were PEG 4000, 6000, 8000, 10000, 12000 and 20000 made at stock concentrations of 50% w/v in 100 mM Tris HCl pH 7.4.

The reagents were added using the Multiprobe II EX (Packard Instrument Co., Meriden, USA) LHR and the experiment completed as per the designed protocol as follows (defined in .csv performance files):

- 100 mM Tris HCl pH 7.4 was added to appropriate wells of a 96 deepwell plate

- PEG of appropriate molecular weight (stock 50% w/v pH 7.4) was taken from its carrier and added to its corresponding well on the 96 deepwell plate giving a total volume of 670 µL combined with 100 mM Tris HCl pH 7.4

- Magnetic coin stirrers were added, and the plate was sealed with a sealing film, and the PEG/buffer mixture was mixed for 2 minutes on a PC-611 stirrer (Corning, New York, USA) to ensure homogeneity

- The 96 deepwell plate was returned to the Multiprobe II EX (Packard Instrument Co., Meriden, USA) LHR and 330 µL of Fab' homogenate was added to the wells used

- The 96 deepwell plate was resealed with a sealing film

- The 96 deepwell plate was then placed on a PC-611 stirrer (Corning, New York, USA) and mixed for 60 minutes

- The 96 deepwell plate was centrifuged at 4000 rpm for 25 minutes using an Eppendorf 5810R centrifuge (Eppendorf UK Ltd., Cambridge, UK)

- The supernatant was then carefully removed without disturbing the precipitated pellet and transferred to an appropriate 96 microtiter plate for Fab' and total protein concentration analysis as detailed in sections 2.1 and 2.2 respectively.

Figure 3.15 shows fractionation diagrams of soluble Fab' and total protein remaining in solution at 6 mL (A) and 1 mL (B) total volume. It was observed that PEG 12000 was the best PEG molecular weight for precipitating Fab' whilst precipitating the least amount of total protein. This provides the basis of precipitation as a means of

primary purification using PEG. For example, PEG 12000 15% w/v precipitates Fab' whilst leaving significant protein impurities in solution (0.05% and 93% of Fab' and total protein remaining in solution respectively at 1 mL scale).

PEG 20000 was the most effective in precipitating total protein, yielding the highest insoluble protein concentration relative to the other PEG molecular weights. This is in agreement with Polson *et al.,* (1964), Atha and Ingram (1981) and Knevelman *et al.,* (2010). The total protein concentrations in solution at PEG 20000 20% w/v at both scales are comparable with 50% and 51% remaining soluble at the 6 mL and 1 mL scale respectively.

At the 6 mL scale, the Fab' concentration remaining soluble decreases rapidly and reaches its minimum solubility at 15% w/v (PEG 4000 to 20000). On average 0.04% of Fab' remains soluble at this point. However, at the 1 mL microwell scale the same level is not encountered, on average 0.08% of Fab' remains soluble, which drops on average to 0.03% at PEG 20% w/v (PEG 4000 to 20000).

The difference in these conditions in part could be due to the change in equipment design between the two scales. Both the height to diameter ratio of the mixing vessel and the magnetic stirrer mixing system cannot be emulated at the 1 mL scale. Due to the nature and geometry of the 96 deepwell plates, the design of the microwell scale is fixed. An appropriately designed system at a 6 mL scale may prove more useful in confirming the results of the high throughput system.

The combination of high agitation at an unknown speed and the magnets location at the bottom of the well may contribute to break up of some aggregates during precipitation, caused in part by unwanted abrasion effects (Nealon *et al.,* 2006, Titchener-Hooker *et al.,* 2008). The break up of aggregates at 1 mL scale may have resulted in the higher concentration of total protein and Fab' concentration observed in the solutions. In response to this issue, an alternative mixing strategy was used and is described in section 4.3.1. The two systems precipitation performances were comparable. However, there were differences in the fractionation profiles of PEG 4000 and 12000 at 6 mL and 1 mL, which could in part be attributable to experimental design change and mixing variation. The 1 mL scale platform was used for future experiments due to the ability to screen many experimental conditions whilst reducing the amount of material consumed.
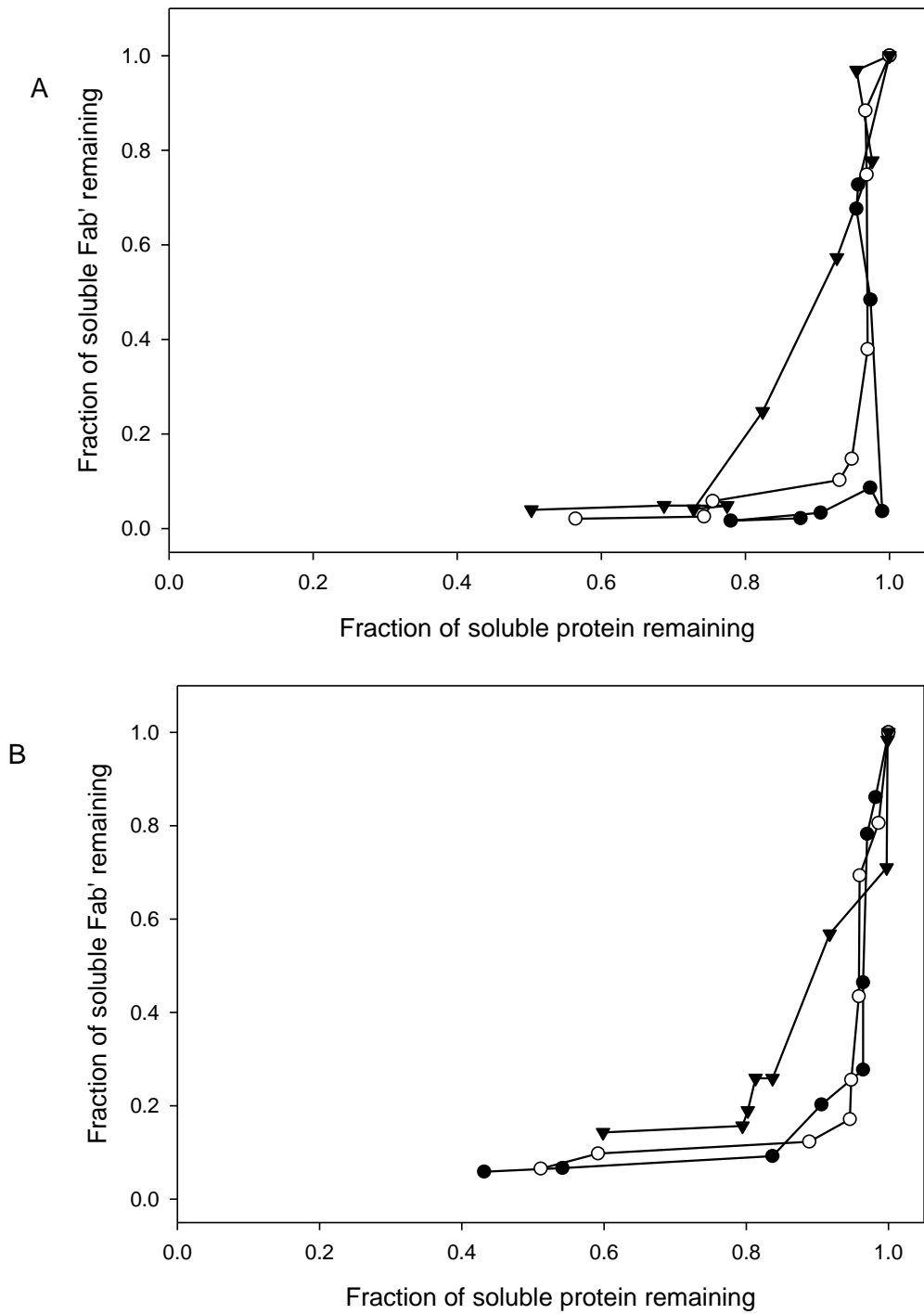
Figure 3.15: *Comparative Fab' and total protein fractionation diagrams at 6 mL (A) and 1 mL microscale (B) for PEG 4000 (●), 12000 (○) and 20000 (▼) respectively. Data for 6000, 8000 and 10000 PEG are not shown for simplicity and for the minimal differences between them (see figure 3.8 for comparison between different PEG molecular weights)*

STAGE 2

3.4 Results and Discussion

3.4.1 Evaluation of Variables for Fab' Precipitation using PEG

The experimental approach based on DoE has been used extensively in research (Lundstedt *et al.,* 1998). The purpose is to systematically analyse how the response of a system changes when parameters of that system are changed. DoE accommodates the variation of experimental conditions in a planned fashion and can give detailed information about how different experimental parameters influence the system response.

PEG as a precipitating agent has been well documented for larger proteins (Atha and Ingram 1981, Melander and Horváth 1988). The first stage of the DoE for Fab' precipitation was to screen parameters, which will affect the system. The key parameters investigated were PEG molecular weight, PEG concentration (% w/v), pH and homogenate dilution factor, these variables contribute to the factors studied in the initial development study. The variables of interest were:

- PEG molecular weight

- PEG concentration (% w/v)

- pH of mixture

- Dilution factor of homogenate

Other factors such as temperature which affects the rate of particle collisions and growth, and also determines the strength of the hydrophobic bond between proteins (Gibb's free energy) (Parker and Dalgleish 1977) were not investigated. All experiments were performed at room temperature as it was difficult to control temperature over a range with the current setup, and by operating at room temperature there would be reduced scalability issues.

The pKa of Tris HCl, the buffer of use in this system is 8.1, and has a buffering range varying from pH 7 to 9. The upper limit of pH to be investigated was set to pH 9. Previous work has shown pH induced precipitation at low pH and therefore the lower limit for this factor was set at 5 (Balasundarum *et al.,* 2011). Tris HCl pH 5 had

no issues with buffering capacity at 100 mM despite the pKa of 8.1. Although pH 5 is not low, it was chosen to have the process as generic as possible and avoid acid precipitation at lower pH values. The centre point in this case was pH 7.4 and a constant molarity of 100 mM was used in all cases. The pH of the buffers, precipitants and homogenate was pH adjusted to the appropriate pH using hydrochloric acid (37% HCl solution) and sodium hydroxide (5 M NaOH) where necessary to maintain consistency of pH. The specifications for maintaining pH in the system was ± 0.2 pH units.

The inlet concentration or dilution factor of homogenate was the third factor investigated. There is a trade-off between the dilution of product before downstream processing and the cost involved in dealing with larger volumes (Balasundarum et al., 2011). Conversely, the performance of precipitation at lower inlet concentrations may prove worthwhile and was investigated. The upper limit was chosen to be clarified homogenate with no dilution (dilution factor of 1). A lower limit of inlet concentration was chosen to be a 5x dilution. While this may be unreasonable in a process setting, it is important in DoE screening studies not to confine the design space as valuable data may be lost. A centre point of dilution factor of 1.67 was chosen based on an estimate of 0.9 g L^{-1} of Fab' in the starting homogenate and the required dilution to bring this down to 0.6 g L^{-1} was a 1.67x dilution (approximately the average Fab' concentration between 1 and 5 homogenate dilution factor). The lower limit was set at a Fab' concentration of 0.2 g L^{-1} (5x dilution).

Yield is defined by the concentration of Fab' precipitated as a percentage of the initial Fab' added in the homogenate (equation 3.2). The initial Fab' in the homogenate is taken to be the maximum calculated for all the experiments to allow for the potential PEGing in effect.

$$Yield = \frac{total\ concentration\ of\ Fab' - concentration\ of\ Fab'\ in\ supernatant}{total\ concentration\ of\ Fab'} \times 100 \qquad \textbf{(3.2)}$$

Equation 3.2: *Yield defined by the concentration of Fab' precipitated*

For a primary purification step, the first priority is to maintain a high yield, followed by a suitable purification factor. Maximising yield at this point is necessary to maintain the cost effectiveness of the step and to ensure that the losses incurred

further downstream are minimal. A second parameter of interest in a purification process is the purification factor.

The purification factor is a ratio of the purity of the product following the precipitation reaction to that of the initial purity of the feedstream (equation 3.3). The purification factor is defined as the concentration of Fab' divided by the concentration of total protein in the sample. Therefore initial purification factor is set at the concentration of Fab' in the feed divided by the total protein concentration in the feed.

$$Purification\ factor = \frac{concentration\ of\ Fab'\ out}{concentration\ of\ total\ protein\ out} \div \frac{concentration\ of\ Fab'\ in}{concentration\ of\ total\ protein\ in} \quad \textbf{(3.3)}$$

Equation 3.3: *Purification factor as a ratio of the purity of the product to that of the initial purity of the feedstream*

The yield should be kept to a maximum value with a high purification factor for an effective operation. However, as both Fab' and protein impurities are precipitated, albeit at different rates, there will be a trade-off between the two. The criteria chosen for acceptable Fab' yield was ≥ 90% with a purification ≥ 1.4.
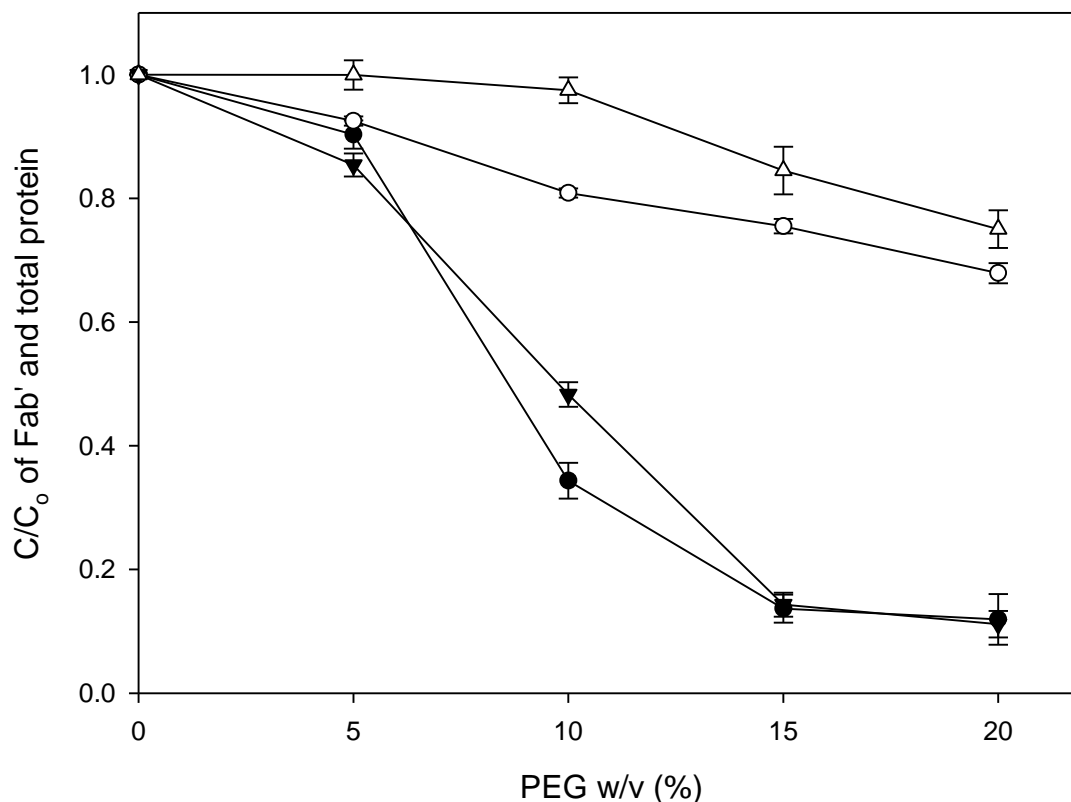
Figure 3.16: *Effect of PEG 20000 on the solubility of Fab' at pH 5 (●) and pH 9 (▼) and total protein at pH 5 (○) and pH 9 (Δ) at a homogenate dilution factor of 1. C_o for Fab' and total protein was 0.9 g L^{-1} and 4.8 g L^{-1} respectively. This experiment was performed in 1.3 mL 96 deepwell plates (Nunc GmbH & Co., KG, Denmark) at 1 mL scale per well using a Multiprobe II EX (Packard Instrument Co., Meriden, USA) for liquid handling. Samples were mixed for a total of 60 minutes using VP 772FN coin magnets (V&P Scientific, San Diego, USA) at turbulent mixing conditions on a PC-611 stirrer (Corning, New York, USA). The plate was centrifuged and then the supernatant was analysed for Fab' and total protein concentration as described in sections 2.1 and 2.2 respectively. Error bars are shown for one standard deviation for triplicate experiment repeats*

Figure 3.16 shows the solubility profiles of Fab' and total protein for changes in pH using PEG 20000 with a homogenate dilution factor of 1. The data is presented in a dimensionless form with the initial concentration taken to be the initial measured concentration, which was 0.9 g L^{-1} and 4.8 g L^{-1} for Fab' and total protein respectively. The solubility profiles of Fab' and total protein with PEG 20000 at pH 5 was steeper than at pH 9. This suggests that low pH accelerates precipitation of both Fab' and total protein, the effect of which in part is more pronounced at lower

PEG concentrations. The greatest variation was observed at 10% w/v of PEG, where at pH 5, 35% and 80% of Fab' and total protein remained soluble, and at pH 9, 50% and 98% Fab' and total protein remained soluble. At higher concentrations of PEG ≥ 15% w/v pH had minimal impact on precipitation suggesting that the PEG concentration was sufficiently high to become the driving force of the process. The same trend was observed with PEG 4000 (figure 3.17). Lee and Lee (1981) suggested that the system always provides a driving force to a more thermodynamically favourable state and that the magnitude of this driving force was found to increase with increasing concentration of the polymer.
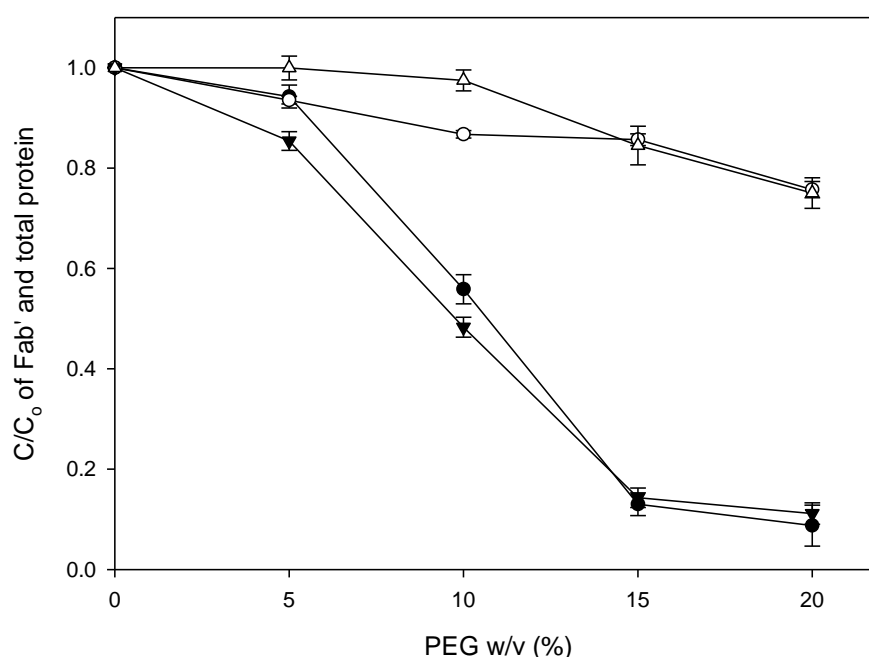
Figure 3.17: *Effect of PEG 4000 on the solubility of Fab' (●) and total protein (○) at pH 9 and the effect of PEG 20000 on the solubility of Fab' (▼) and total protein (Δ) at pH 9. Homogenate dilution factor of 1 was used in both cases. C_o for Fab' and total protein was 0.9 g L^{-1} and 4.8 g L^{-1} respectively. This experiment was performed in 1.3 mL 96 deepwell plates (Nunc GmbH & Co., KG, Denmark) at 1 mL scale per well using a Multiprobe II EX (Packard Instrument Co., Meriden, USA) for liquid handling. Samples were mixed for a total of 60 minutes using VP 772FN coin magnets (V&P Scientific, San Diego, USA) at turbulent mixing conditions on a PC-611 stirrer (Corning, New York, USA). The plate was centrifuged and then the supernatant was analysed for Fab' and total protein concentration as described in sections 2.1 and 2.2 respectively. Error bars are shown for one standard deviation for triplicate experiment repeats*

Figure 3.17 shows the solubility profiles of Fab' and total protein at pH 9 with PEG 4000 and 20000 with a homogenate dilution factor of 1. It was observed that Fab' concentration was lower at higher PEG molecular weights between 5% to 15% w/v, indicating that the use of a high molecular weight PEG at these interim concentrations would give a greater yield than the lower molecular weight PEG. The percentage remaining soluble Fab' at 10% PEG was 58% and 41% for PEG 4000 and 20000 respectively.

The total protein solubility profile with PEG 20000 was relatively constant to PEG 10% w/v, which decreases further by 20% at PEG 20000 20% w/v. The decrease in total protein solubility with PEG 4000 was more gradual over this range with a 10% reduction in total protein at PEG 4000 20% w/v.

Operation between PEG 15% w/v to 20% w/v offers no significant difference in Fab' solubility profiles between PEG 4000 and 20000. In terms of operating space this is a robust region where the use of PEG concentration is flexible in the range investigated for Fab' precipitation. However, total protein drops on average for both PEG molecular weights by 12% in this range, which may be of particular significance in the choice of operating parameters at scale. Further experimentation in this range would be useful in developing a robust design space for both Fab' and total protein precipitation.
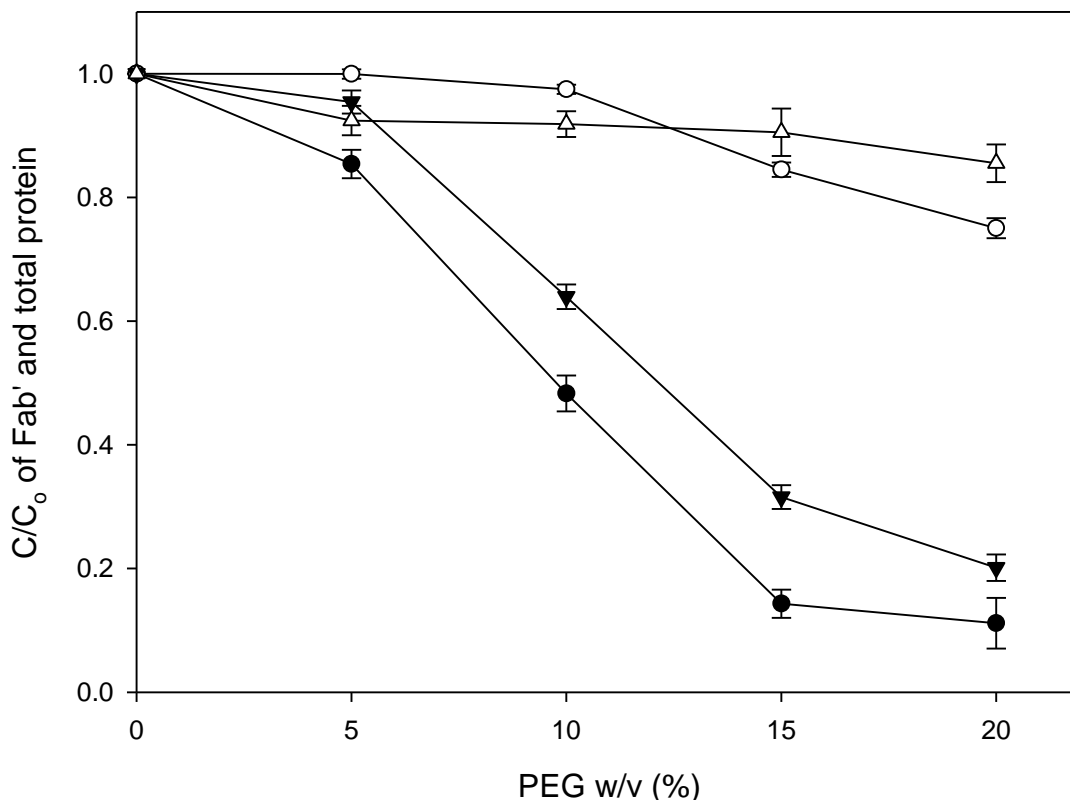
Figure 3.18: *Effect of feed dilution factor (DF) on solubility of Fab' at DF 1 (●), DF 5 (▼), total protein solubility at DF 1 (○) and DF 5 (△) with PEG 20000 at pH 9. C_o for Fab' and total protein was 0.9 g L^{-1} and 4.8 g L^{-1} respectively. This experiment was performed in 1.3 mL 96 deepwell plates (Nunc GmbH & Co., KG, Denmark) at 1 mL scale per well using a Multiprobe II EX (Packard Instrument Co., Meriden, USA) for liquid handling. Samples were mixed for a total of 60 minutes using VP 772FN coin magnets (V&P Scientific, San Diego, USA) at turbulent mixing conditions on a PC-611 stirrer (Corning, New York, USA). The plate was centrifuged and then the supernatant was analysed for Fab' and total protein concentration as described in sections 2.1 and 2.2 respectively. Error bars are shown for one standard deviation for triplicate experiment repeats*

Figure 3.18 outlines the effect of dilution on Fab' and total protein solubility with PEG 20000 over 0% to 20% w/v at pH 9. There was a significant difference in the solubility profiles of Fab' when the initial homogenate was diluted 5x compared to undiluted homogenate. On average there was a 17% decrease in Fab' precipitation when the homogenate was diluted 5x over a PEG 5% to 20% w/v range. However, total protein concentration remains stable across the PEG concentration range relative to undiluted homogenate. At 20% w/v there was a 10% increase in total

protein solubility when homogenate was diluted 5x, which equates to a 1.7x increase in purification factor. However, Fab' yield at PEG 20% w/v and 5x homogenate dilution was 80% relative to 90% at 20% w/v and 1x homogenate dilution. This would suggest that dilution factor was a strong factor in the determination of optimal conditions, particularly at PEG 20% w/v concentration. Therefore, a high yield was obtained with no dilution of feed material, whereas the purification factor increased with dilution of the feed material, and thus a trade-off was required between the two for optimum process conditions. Whilst traditional experimental designs are useful in spotting overall trends, information regarding possible interaction between factors is lost by only analysing one parameter at a time. The DoE approach of analysis allows further insight into the weighting of each of these parameters on performance, and provides an indication into interaction effects between parameters.

3.4.2 Full Factorial DoE for the Study of Fab' Precipitation Using PEG

The full factorial and central composite face centred DoE designs that are described in this thesis to optimise precipitation operations were designed and analysed using MODDE 9.1 statistical software (Umetrics, Malmö, Sweden). A statistical DoE software package can evaluate multiple variables and response factors simultaneously. In addition, statistical analysis can allow specifications to be placed on data, requiring a result to be made between a minimum and maximum value for the output responses. The resulting design space is useful for understanding process limits and how design parameters affect process behaviour in order to decide how to operate at full scale. This capability is the practical realisation of Quality by Design. In a full factorial design, investigating the four variables described in section 3.4.1 over 2 levels with 2 centre points would require (2^4 + 2) 18 experiments. However, it is known that Fab' precipitation with PEG is highly non linear over the range previously examined (figures 3.4 to 3.7) and it was decided to carry out this design with a greater number of levels. The numbers of levels were set at increments of 5% PEG w/v over the effective range of PEG 0% to 20% w/v to provide a better understanding of how changes to PEG concentration would affect the precipitation of Fab' and protein impurities. Therefore, the four factor full two level factorial design was completed with a range of PEG concentrations ranging from 0% to 20% w/v.

For each of the conditions outlined in table 3.4 the yield and purification factor was calculated as described in section 3.4.1. As a key requirement for a primary purification process, minimum yield of Fab' of 90% was chosen for this primary process step.

Experiment number	pH	PEG molecular weight	Homogenate dilution factor	Final PEG concentration (% w/v)
1	5.0	4000	1.00	5
2	9.0	4000	1.00	5
3	5.0	20000	1.00	5
4	9.0	20000	1.00	5
5	5.0	4000	5.00	5
6	9.0	4000	5.00	5
7	5.0	20000	5.00	5
8	9.0	20000	5.00	5
9	5.0	4000	1.00	20
10	9.0	4000	1.00	20
11	5.0	20000	1.00	20
12	9.0	20000	1.00	20
13	5.0	4000	5.00	20
14	9.0	4000	5.00	20
15	5.0	20000	5.00	20
16	9.0	20000	5.00	20
17	7.4	12000	1.67	15
18	7.4	12000	1.67	15

Table 3.4: *Table listing the full two level factorial DoE experiments for the initial screening study. Homogenate (at the appropriate pH), PEG (from a stock concentration of 50% w/v at the appropriate pH) and 100 mM Tris HCl at the appropriate pH were prepared for this experiment. C_o for Fab' and total protein was 0.9 g L^{-1} and 4.8 g L^{-1} respectively. This experiment was performed in 1.3 mL 96 deepwell plates (Nunc GmbH & Co., KG, Denmark) at 1 mL scale per well using a Multiprobe II EX (Packard Instrument Co., Meriden, USA) for liquid handling. Samples were mixed for a total of 60 minutes using VP 772FN coin magnets (V&P Scientific, San Diego, USA) at turbulent mixing conditions on a PC-611 stirrer (Corning, New York, USA). The plate was centrifuged and then the supernatant was analysed for Fab' and total protein concentration as described in sections 2.1 and 2.2 respectively. Experiments were repeated in triplicate for robustness*

One hundred and fifty experiments were run in triplicate and split over three microtiter plates with yield and purification factor as key responses. The precipitated pellets dissolved readily in 1 mL of 100 mM Tris HCl pH 7.4.
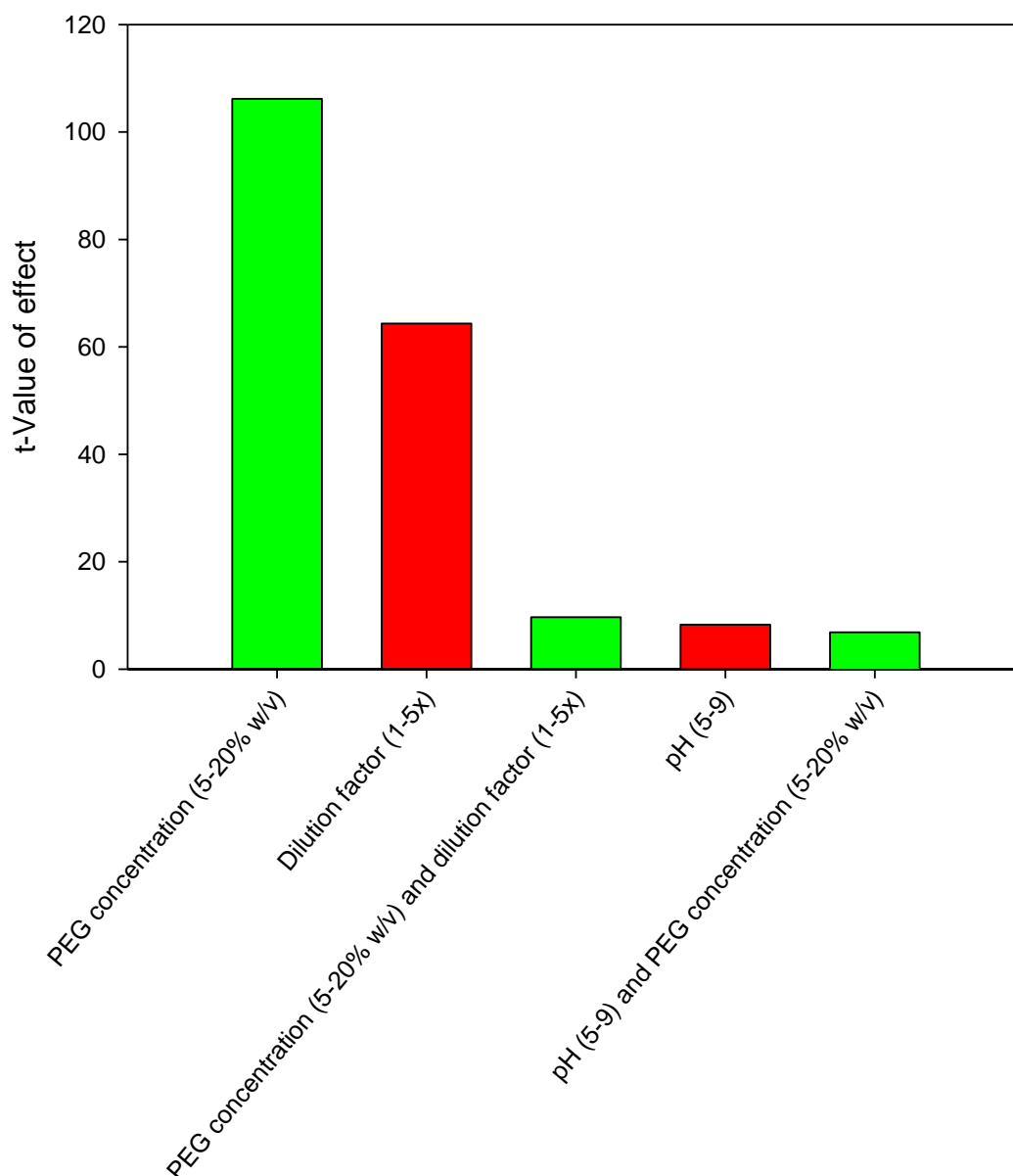
Figure 3.19: *Bar chart ranking the significant process parameters from high to low in terms of effect on Fab' yield. Green and red bars have a positive and negative effect on yield respectively. Effects are significant in the range investigated, which are above the t-Value limit of 2.18 and p < 0.05 confidence level. Effects below these limits are not shown*

There are a number of parameters, which are significant in relation to yield. Figure 3.19 shows the t-Values for each of the parameters that have either a positive or negative effect on yield, which are above the t-Value limit of 2.18 and $p < 0.05$ confidence level.

Figure 3.19 shows that PEG concentration was the most important factor in the determination of yield for the range investigated. This is in agreement by experiments performed by Knevelman *et al.,* (2010). PEG concentration had a positive effect in the range of variables investigated for improving Fab' yield.

Dilution factor was the second most important factor calculated based on the t-test analysis. This factor had a negative effect, signifying that the greater the dilution factor the lower the yield obtained. It was possible that when the feed material was diluted, although large amounts of PEG were present, the PEG had difficulty excluding water from the protein domain and causing precipitation of the protein. Water is more likely to be drawn from the water based buffer instead, and may require longer than 60 minutes mixing time for precipitation to effect. At no homogenate dilution, there was a higher concentration of Fab' and other proteins in the sample where the PEG could work to remove relatively less water from around the proteins inducing precipitation. The third ranked parameter was a combination of PEG concentration and dilution of feed, which had a positive effect on yield. This was expected as PEG concentration had a larger positive effect individually than the negative effect imposed by dilution factor. The two factors effects on their own had positive and negative effects on yield respectively.

High pH had a negative effect on yield. It was observed that a lower pH in the range of 5 to 9 can induce precipitation of Fab' and increase yield. This is in agreement with previous analysis (figure 3.16) and as in agreement with previous research, which suggested that pH induced precipitation can take place at low pH values (Knevelman *et al.,* 2010). This is interesting from the point of view that theory suggests that precipitation increases by operating at a pH in or around the pI value of the protein (Virkar *et al.*, 1982). Fab' pI was determined to be around pH 6.5.

The final effect was an interaction effect between pH and PEG concentration. PEG molecular weight was not a significant factor in determination of yield (figures 3.8-3.9). This is an interesting observation in that it is expected that a longer PEG

polymer size would be able to induce a greater level of hydration and induce more precipitation (Atha and Ingram 1981). It may be the case where this positive effect of increased hydration potential is negated by the fact that a smaller polymer size may be more mobile and can be accommodated more easily in the protein domain, allowing greater access to draw water and induce precipitation. Mahadevan and Hall (1990) have suggested that stearic constraints where polymers are excluded from the space separating two protein molecules are significant. The distribution of the polymer causes a "pressure imbalance" that pushes the proteins against each other. The positive chemical potentials of the proteins on addition of PEG indicate that the predominant interactions between PEG and proteins in aqueous medium are repulsive in nature and that this repulsion becomes stronger with an increase in PEG size (Mahadevan and Hall 1990).
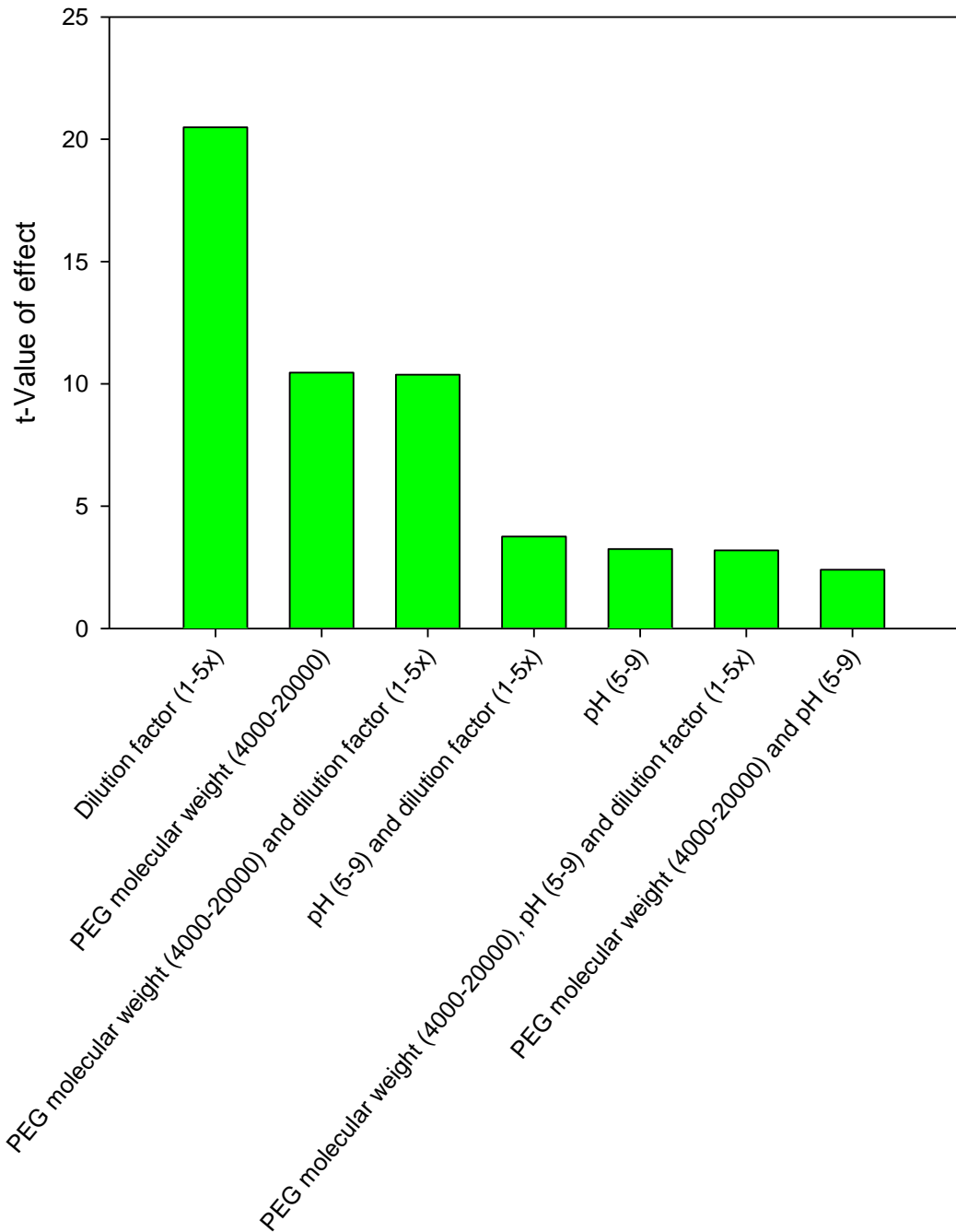
Figure 3.20: *Bar chart ranking the significant process parameters from high to low in terms of effect on purification factor. Green bars have a positive effect on purification factor. Effects are significant in the range investigated, which is above the t-Value limit of 2.23 and p < 0.05 confidence level. Effects below this limit are not shown*

Figure 3.20 illustrates that dilution factor had the strongest effect on purification factor in the range investigated. In this case, this factor had a positive effect on the purification factor, and therefore a higher value of dilution factor would result in a higher purification factor. A trade-off between high and no dilution of feed material was required as an increase in the dilution of feed reduces yield (figure 3.19). The use of undiluted feed material was used in future studies, prioritising yield as the precipitation step is proposed as a primary purification step.

It was suggested that PEG molecular weight was a significant factor for purification factor but it was not a significant factor for yield. There are process implications for using high PEG molecular weights and concentrations due to its viscosity (Lee and Lee 1981 and section 3.3.2), although increasing PEG molecular weight increases purification factor. Interestingly as per the volume excluded theory as the size of the polymer is increased the amount of volume left for protein molecules is reduced. However, it is possible that Fab' is sufficiently small to penetrate the interior spaces of the polymer coil whereas the larger protein impurities are not, which may explain the negligible effect of PEG molecular weight on yield and not purification factor. Therefore, a compromise of working with the highest possible PEG molecular weight, which does not hinder the process is required as yield is the most important response for a primary purification step. For example operating with PEG 12000 can be acceptable at scale, while still more viscous than PEG 4000, it is manageable.

Other positive effects include pH and a number of interaction effects between the parameters already deemed significant on their own. It is noted that PEG concentration was not deemed to have any effect on the purification factor in range between PEG 10% to 20% w/v. This is in part due to the ratio of precipitated Fab' and total protein remains relatively constant at all concentrations, hence no improvement in purification factor.

A summary of the factors affecting Fab' yield and purification factor is shown in table 3.5.

Favourable yield	Favourable purification factor
High PEG concentration (% w/v)	High PEG molecular weight
Low dilution factor	High dilution factor
Low pH	High pH
Interaction Effects	**Interaction Effects**
PEG concentration (% w/v) and dilution factor	PEG molecular weight and dilution factor
pH and PEG concentration (% w/v)	pH and dilution factor
	PEG molecular weight, pH and dilution factor
	PEG molecular weight and pH

Table 3.5: *Summary of factors that had a positive effect on Fab' yield and purification factor in the range investigated*

Q^2 is the goodness of prediction, which estimates the predictive power of the model. Q^2 has the upper limit of 1, and the lower limit is minus infinity. The model had a Q^2 value of -0.11, which indicates that this model had poor predicitive power. The ANOVA parameters, calculated by MODDE 9.1 (Umetrics, Malmö, Sweden), indicated that the curvature in the model was significant (the p-value was 0.003). The two level full factorial design can show interactions between the factors, but cannot model curvature. A model with quadratic terms, can adequately model curvature, and therefore a response surface design in the form of a CCF DoE was performed as the next step to find an optimum range of conditions to deliver a high Fab yield and purification factor in the range investigated (section 3.5.1).

STAGE 3

3.5 Results and Discussion

3.5.1 Central Composite Face Centred DoE for Finding an Optimum

The purpose of the full factorial study was to screen conditions for the precipitation of Fab' and to attempt to achieve some selectivity. Precipitation can be desirable for an initial capture step in order to reduce the burden of subsequent downstream steps. In the first study, conditions were identified, summarised in table 3.5, for the precipitation of Fab' from partially clarified cell culture fluid. In this second study, a response surface methodology design in the form of a central composite face centred (CCF) DoE was performed building on the factorial design for finding a range of optimal experimental conditions for high Fab' yield and purification factor since the ANOVA showed that curvature was significant. In this design, the experiments are centred on the face of the cube, which implies that all factors have three levels, instead of two levels in the factorial design (figure 3.21). The flexibility of three levels per factor allows support for a quadratic model for response surface modelling. Quadratic models are flexible and can mimic many different types of response function (Lundstedt *et al.,* 1998).
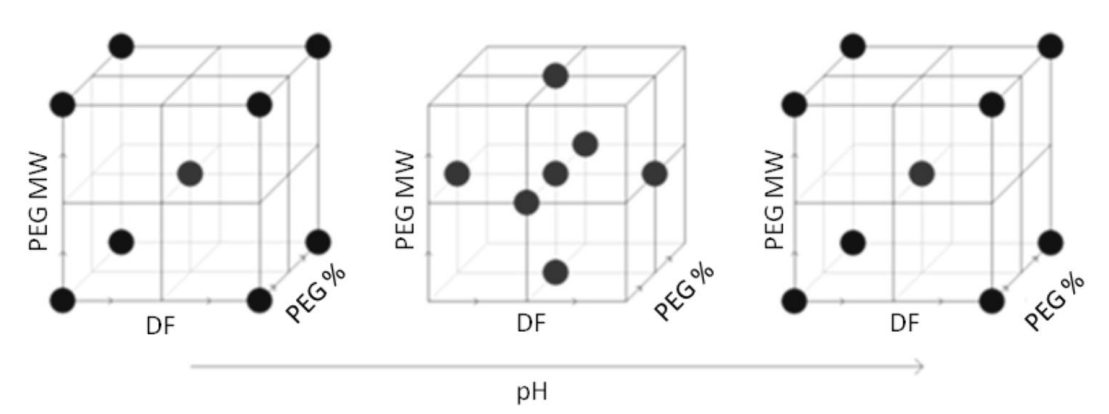
Figure 3.21: *CCF design for finding a range of optimal experimental conditions to deliver a high Fab' yield and purification factor in the range investigated. In this design no further constraints were placed on parameter input ranges (pH 5 to 9; dilution factor 1 to 5; PEG molecular weight 4000 to 20000) except PEG concentration which was limited to 10% to 20% w/v as it was found that less than PEG 10% w/v resulted in unfavourable Fab' yield < 90%*

In this design no further constraints were placed on parameter input ranges (pH 5 to 9; dilution factor 1 to 5; PEG molecular weight 4000 to 20000) except PEG concentration which was limited to 10% to 20% w/v as it was found that less than PEG 10% w/v resulted in unfavourable Fab' yield of less than 90%. The experimental design is shown in table 3.6.

Experiment number	PEG molecular weight	Dilution factor	Final PEG concentration (% w/v)	pH
1	4000	1.00	10	5.0
2	20000	1.00	10	5.0
3	4000	5.00	10	5.0
4	20000	5.00	10	5.0
5	4000	1.00	20	5.0
6	20000	1.00	20	5.0
7	4000	5.00	20	5.0
8	20000	5.00	20	5.0
9	4000	1.00	10	9.0
10	20000	1.00	10	9.0
11	4000	5.00	10	9.0
12	20000	5.00	10	9.0
13	4000	1.00	20	9.0
14	20000	1.00	20	9.0
15	4000	5.00	20	9.0
16	20000	5.00	20	9.0
17	4000	1.67	15	7.4
18	20000	1.67	15	7.4
19	12000	1.67	15	7.4
20	12000	5.00	15	7.4
21	12000	1.67	10	7.4
22	12000	1.67	20	7.4
23	12000	1.67	15	5.0
24	12000	1.67	15	9.0
25	12000	1.67	15	7.4

Table 3.6: *Table listing the CCF DoE experiments. Homogenate (at the appropriate pH), PEG (from a stock concentration of 50% w/v at the appropriate pH) and 100 mM Tris HCl at the appropriate pH were prepared for this experiment. C_O for Fab' and total protein was 0.9 g L^{-1} and 4.8 g L^{-1} respectively. This experiment was performed in 1.3 mL 96 deepwell plates (Nunc GmbH & Co., KG, Denmark) at 1 mL scale per well using a Multiprobe II EX (Packard Instrument Co., Meriden, USA) for liquid handling. Samples were mixed for a total of 60 minutes using VP 772FN magnets (V&P Scientific, San Diego, USA) at turbulent mixing conditions on a PC-611 stirrer (Corning, New York, USA). The plates were centrifuged and then the supernatant was analysed for Fab' and total protein concentration as described in sections 2.1 and 2.2 respectively. Experiments were repeated in triplicate for robustness*
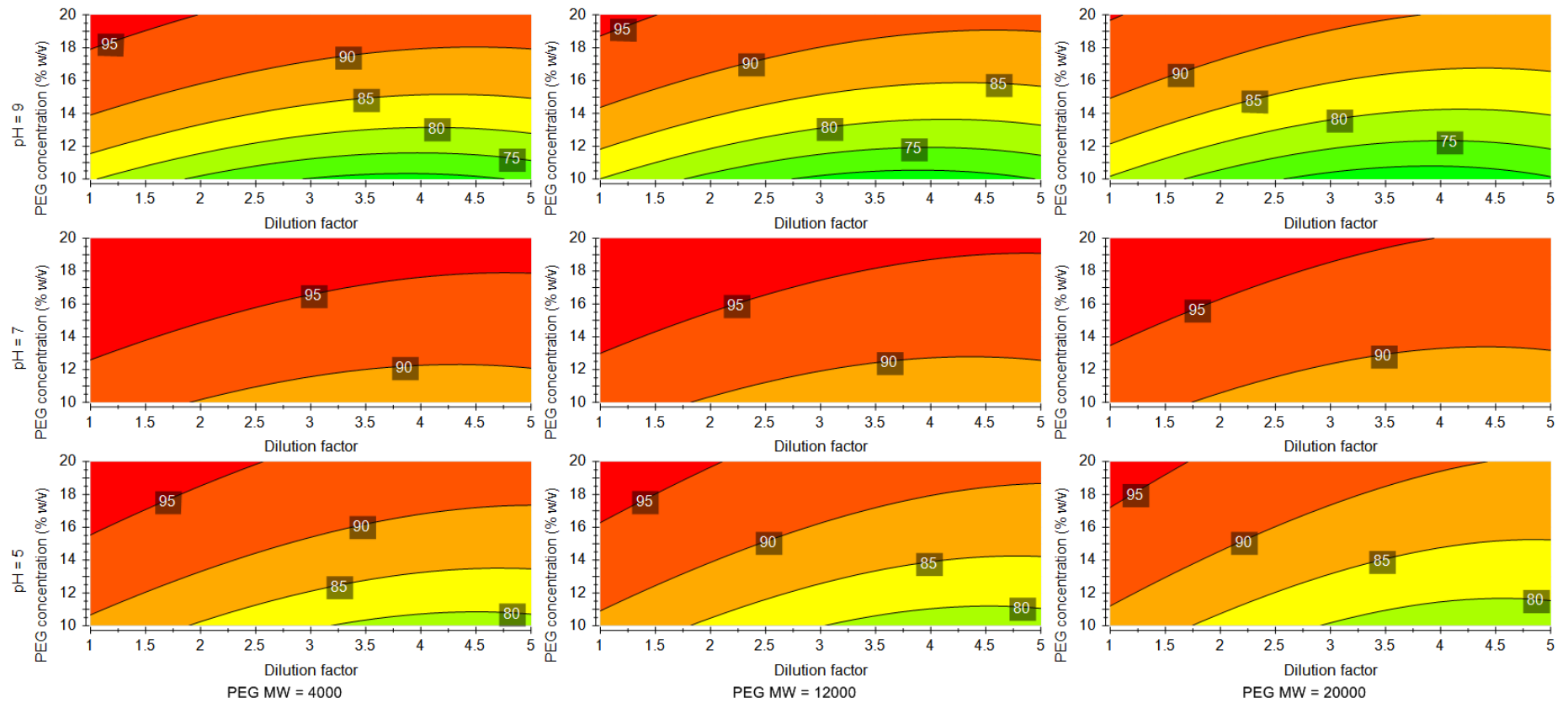
Figure 3.22: *4D contour plots showing the yield of Fab' as a function of PEG concentration (% w/v) and dilution factor at varying pH and PEG molecular weights. The response surfaces for yield were fit with a quadratic model. All data fitting was performed using the software package MODDE 9.1 (Umetrics, Malmö, Sweden)*
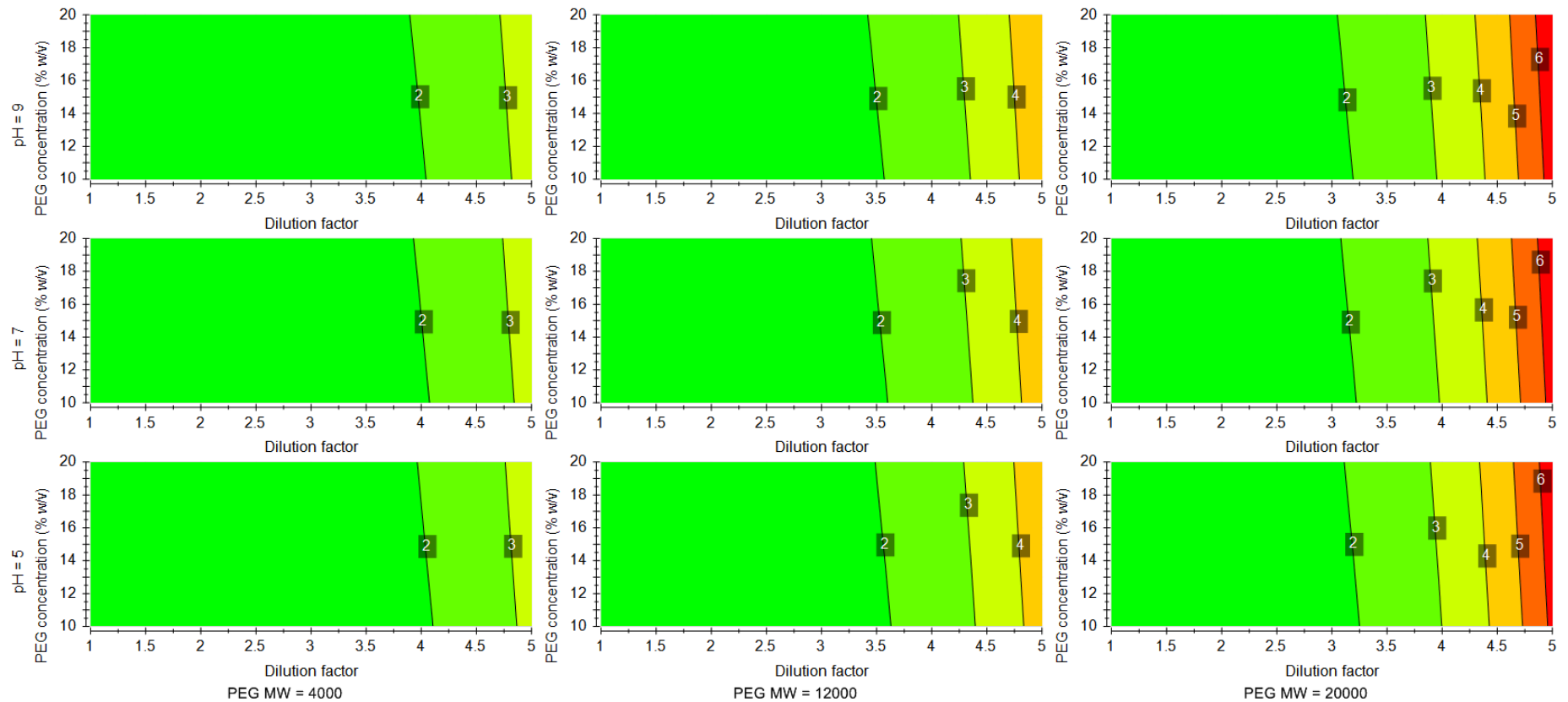
Figure 3.23: *4D contour plots showing the purification factor of Fab' as a function of PEG concentration (% w/v) and dilution factor at varying pH and PEG molecular weights. The response surfaces for purification factor were fit with a quadratic model. All data fitting was performed using the software package MODDE 9.1 (Umetrics, Malmö, Sweden)*

Figures 3.22 and 3.23 show the response surface plots all of the variables investigated in the CCF DoE for yield and purification factor respectively. These plots were created using MODDE 9.1 (Umetrics, Malmö, Sweden). The response surface plot of yield (figure 3.22) suggested that operating at a condition to give maximum yield would require a high PEG w/v percentage, and under these conditions, PEG molecular weight was not a significant factor. This suggested that chemical interactions involving attractive or repulsive forces between different PEG molecular weights and Fab' are relatively unimportant in the precipitation mechanism. However, an increase in purification factor was observed with increasing PEG molecular weight. For example, the purification factor doubled at PEG 20000 15% w/v, pH 5 and dilution factor of 5, compared to PEG 4000 at identical conditons.

To achieve a Fab' yield > 90%, PEG concentration should be ≥ 10% w/v whilst operating at a dilution factor of 1. Generally, an increase in dilution factor decreased yield. For example, by increasing the dilution factor from 1x to 5x using PEG 4000 10% w/v at pH 5 the Fab' yield dropped from ~90% to ~80%. It was suggested that as the feed was diluted the effect of PEG on Fab' became negligible as per the excluded volume theory. As per this theory, it was expected that as the concentration was increased the amount of volume excluded per molecule was reduced resulting in precipitation. This was in agreement with work performed by Knevelman *et al.,* (2010) who observed similar effects using IgG. However, an ~5 fold increase in purification factor was observed with increasing dilution factor from 1 to 5 at PEG 20000 20% w/v at pH 9, which is interesting as water is a key impurity. A 5x dilution is undesirable, as this will result in a greater volume of material to process at large scale where space and size of tankers can be limited.

Figure 3.22 indicates that a lower pH increases Fab' yield in the range investigated, whereas there was an minimal effect of pH observed with respect to purification factor from pH 5 to 9 (figure 3.23). Figure 3.22 suggests that an increase in yield was more pronounced at pH values below the Fab' pI of 6.5, peaking at pH 5 and PEG 20% w/v (Coleman and Mahler 2003). Lee and Lee (1981) suggested that the concentration of polymer required to precipitate a protein component is a function of the net charge on the molecule as determined by the pH of the medium in which the molecule is suspended and there is some evidence to support this in figure 3.22.

ANOVA analysis suggested that the model had no lack of fit as the p-value was > 0.05 (p-value was 0.22), with an Q^2 value of 0.90. Therefore, this model can be used to find a sweet spot in the experimental design space, in which the combination and interactions of the process inputs reliably deliver a product with the desired quality. Recommendations as described in ICH Q8 (R2) guideline was used to create a design space by combining the response surface plots of yield and purification factor shown in figure 3.24. The proposed design space is a region where the combination of ranges delivers a Fab' yield ≥ 90% with a maximum purification factor of 1.7.
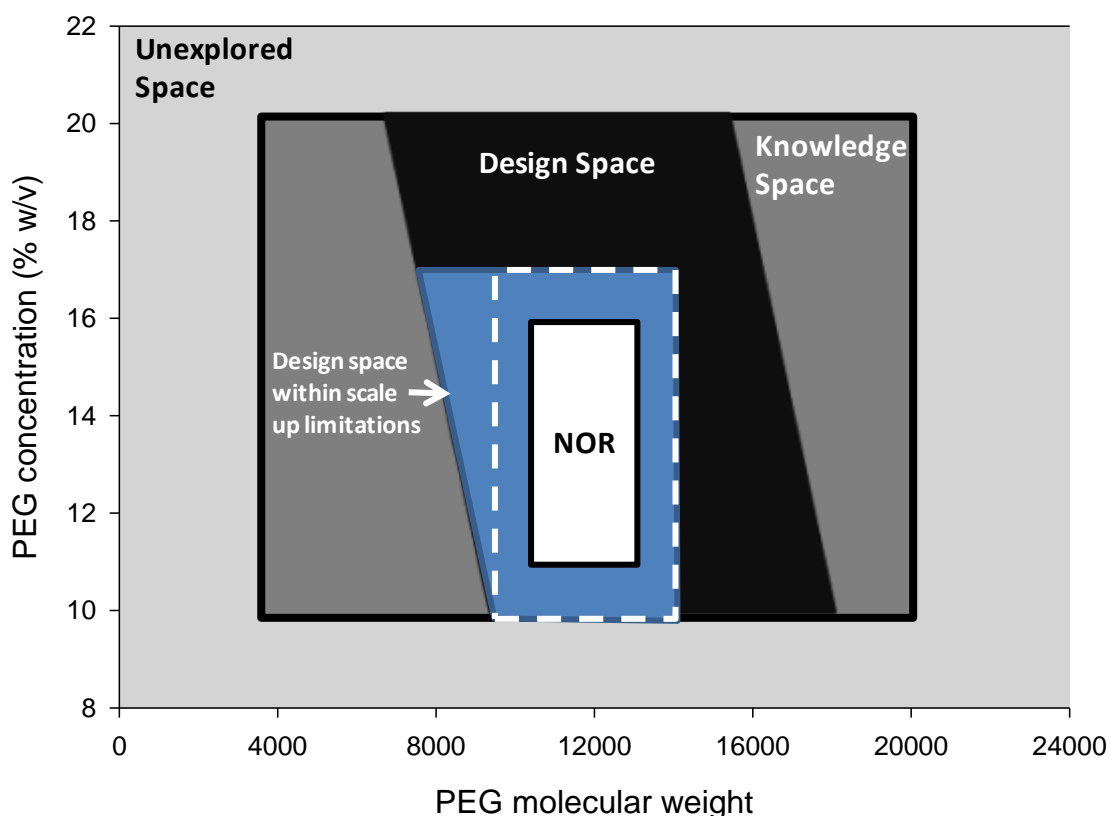
Figure 3.24: *Proposed Fab' precipitation design space comprised of the overlap region for yield (%) and purification factor created using MODDE 9.1 (Umetrics, Malmö, Sweden). Knowledge space refers to the region of process understanding based on the CCF DoE inputs. Inputs were PEG molecular weight, PEG concentration, pH 7.4 and undiluted homogenate. The design space is a region where the combination of ranges that delivers a Fab' yield ≥ 90% with a maximum purification factor of 1.7. The selected area within the design space was the proposed design space for scale up for operational simplicity. Outside of this region, viscosity of PEG may become an issue at process scale and therefore the Normal Operating Range (NOR) was set to ± PEG 1000 and ± 1% w/v within the dashed area of this design space*

Figure 3.24 is a graphical representation of the knowledge space (within the unexplored space), which refers to the region of process understanding defined by the input boundaries of the CCF DoE. The input boundaries were PEG 4000 to 20000, PEG concentration 10% to 20% w/v, pH 7.4 and no homogenate dilution (DF of 1). The design space is comprised of the overlap of Fab' yield (%) and purification

factor to give a robust region where Fab' yield was ≥ 90% with a maximum purification factor of 1.7 within the knowledge space. However, the highlighted area within the design space is the proposed design space for operational simplicity. This is due to the use of PEG as precipitant, since at high PEG molecular weights and concentrations, the high viscosity of PEG could cause difficulties in processing at large scale. Therefore, the normal operating range (NOR) or control space was defined in a way that can be "demonstrated to provide assurance of quality" (ICH Q8 (R2) 2009) by having the distance from the edge of the design space at ± PEG 1000 and ± 1% w/v. This is highlighted by the dashed area in figure 3.24 within the highlighted area of the design space. This allows for flexibility and robustness at manufacturing scale since "working within the design space is not considered as a change" (ICH Q8 (R2) 2009). Movement out of the design space is considered to be a change and would normally initiate a regulatory post-approval-change process. In essence, the knowledge of the factors affecting Fab' yield and purification factor can assist in the development of a process manufacturing design space which lies at the heart of a practical realisation of Quality by Design. A robustness test was performed within the NOR using PEG 12000 15% w/v pH 7.4, which delivered a Fab' yield and purification factor of 93% and 1.5 respectively. The model predicted a Fab' yield of 95% and purification factor of 1.4, which was in good agreement with the experimental data. This result was within the specification of the design space.

3.6 Summary

This chapter has described procedures for developing methods for precipitating Fab' directly from clarified homogenate using PEG, the approach is summarised in figure 3.25. Comparisons of the effects that multiple variables have on precipitation performance have been performed successfully in a high throughput format. A Fab' precipitation screening study in the form of a full factorial design was performed to investigate a large design space based on Quality by Design principles (ICH guideline Q8 (R2)). Parameters of investigation were PEG concentration (% w/v), PEG molecular weight (MW), pH and dilution of the homogenate. This was followed by a central composite face centred design to find an optimal range of experimental conditions to deliver a high Fab' yield and purification factor within the ranges investigated. A design space comprised of the responses percentage Fab' yield and purification factor was created to give a robust region where Fab' yield was ≥ 90% with a maximum purification factor of 1.7. A normal operating range (NOR) was

defined within this design space and a confirmatory run was completed with PEG 12000 15% w/v at pH 7.4 and undiluted homogenate, which resulted in a Fab' yield and purification factor of 93% and 1.5 respectively.
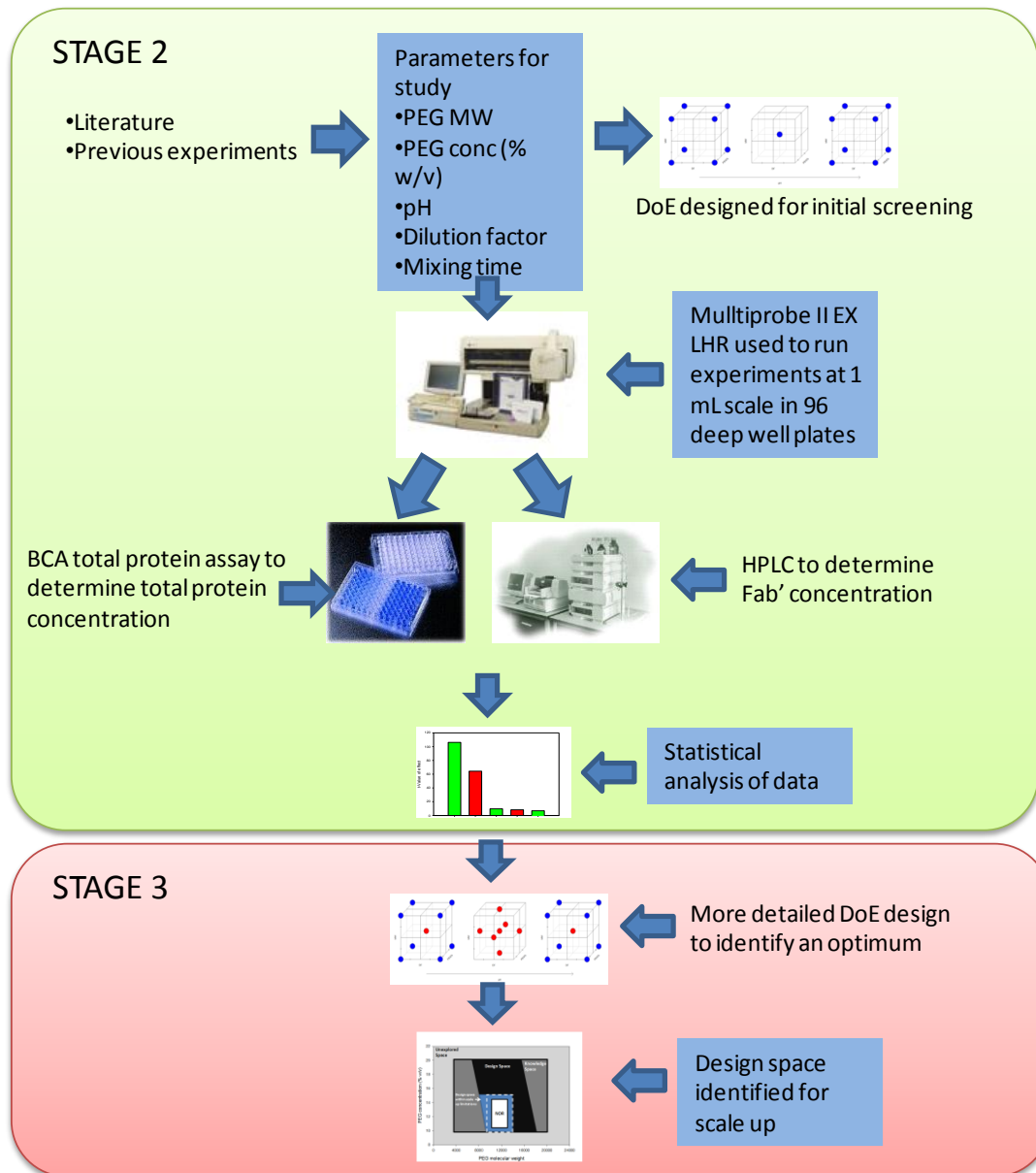
Figure 3.25: *Diagram to show use of microscale techniques described in this chapter for investigating Fab' precipitation using PEG. Microscale techniques were used for range finding (stage 2) and optimisation (stage 3)*

4. MICROSCALE MULTIMODAL PRECIPITATION TO ESTABLISH POLYETHYLENE GLYCOL AND SALT INTERACTION EFFECTS

4.1 Abstract

The setup, automation and operation of precipitation on a Tecan Freedom EVO 200 liquid handling robot (Tecan, Reading, UK) combined with using a microscale mixing device increased throughput and speed of liquid handling by 50% relative to the mixing conditions described in section 3.3.3.

A Fab' precipitation study in the form of a response surface methodology DoE (three level full factorial) was performed to investigate a large multimodal precipitation design space based on the Quality by Design principles stated in the ICH guideline Q8 (R2) to improve the performance of single mode precipitation described in chapter 3. Parameters of investigation were PEG concentration (% w/v), PEG molecular weight (MW), pH, dilution of the homogenate, ammonium sulphate concentration and sodium citrate concentration. Salt concentrations ≥ 0.8 M with ≥ 5% w/v PEG resulted in aqueous two phase formation which affected 40% of the design space. This was excluded from analysis as a two phase system was beyond the scope of this project.

A second round of response surface experimentation in the form a CCF DoE with reduced ranges to avoid two phase formation was performed combining optimum operating conditions from the PEG CCF design space (section 3.5.1) for multimodal operation. PEG 12000 in addition to three salts, ammonium sulphate, sodium citrate and sodium chloride chosen from their locations in the Hofmeister series (section 1.4.1) were used for multimodal precipitation. It was found that 90% Fab' yield with a purification factor of 1.9 was achievable with PEG 12000 15% w/v/0.30 M sodium citrate/0.15 M ammonium sulphate pH 7.4. This was an improvement of 26% relative to the use of 15% w/v PEG 12000 pH 7.4 in single mode. However an alternative precipitation strategy to precipitate ~20% of protein impurities whilst Fab' remained soluble in solution using PEG 12000 6.25% w/v/0.4 M sodium citrate pH 7.4 was favoured instead. The advantage of this system at process scale is the potential ease of processing due to removal of a solubilisation step and the significantly reduced viscosity of the precipitating agent relative to that of high concentrations of PEG.

4.2 Introduction

This chapter describes the evaluation of a microscale mixing device with a new LHR to improve throughput and scalability of the precipitation platform to investigate and potentially improve single mode Fab' precipitation (PEG precipitant was discussed in chapter 3) by adding complexity in the form of a multimodal operation. Multimodal operation was investigated by combining two different types of precipitant, PEG with a mixture of ammonium sulphate, sodium citrate and sodium chloride concentrations. Salts as precipitating agents were chosen due to being readily accepted by regulatory bodies and by their different precipitating mechanism to that of PEG. It has been suggested that PEG has little interaction with proteins and precipitation is caused by excluded volume effects (Middaugh *et al.,* 1979, Atha and Ingham 1981). Excluded volume refers to that part of the PEG molecule that cannot occupy space that is already occupied by another part of the same PEG molecule (Atha and Ingham 1981). PEG acts as an "inert solvent sponge" that prevents interaction of all proteins present with the solvent, effectively increasing their concentration until solubility is exceeded, and precipitation occurs (Lewis and Metcalf 1988). However, salts are known to interact with proteins (Harinarayan *et al.,* 2008), and have been ranked in the Hofmeister series by their ability to reduce protein solubility (figure 1.5). The addition of neutral salts results in their ions bonding with water molecules, which would otherwise be hydrating proteins. Proteins will be forced by reduced hydration to aggregate and precipitate in these conditions. This loss in the water monolayer surrounding the protein reduces the barrier to aggregation as high concentrations of salt ions are introduced in the system allowing aggregation from solute collisions, which is intensified by mixing.

Figure 4.1 highlights the structure of this chapter. At stage 1, an alternative mixing strategy with a new LHR (Tecan Freedom EVO 200 liquid handling robot (Tecan, Reading, UK)) was evaluated to improve throughput and scalability of the precipitation platform. At stage 2, a three level full factorial DoE was undertaken to investigate Fab' precipitation using PEG and salts with Fab' yield and purification factor as key responses. At stage 3, a second round of experimentation was conducted with more focused PEG and salt conditions to find a range of operating conditions to give a high Fab' yield and purification factor. This was then followed by robustness testing.

Stage 1

Evaluation of a microscale mixing device with a new LHR for better scalability to laboratory and pilot scale.

Stage 2

A response surface methodology design in the form of a 3 level full factorial DoE to model Fab' precipitation by varying PEG molecular weight (4000 to 12000), pH (5 to 9), PEG concentration w/v (0% to 15% w/v), ammonium sulphate, sodium citrate (0 to 1 M) and DF 1 with yield and purification factor as key responses. Black dots represent experimental conditions in the design space
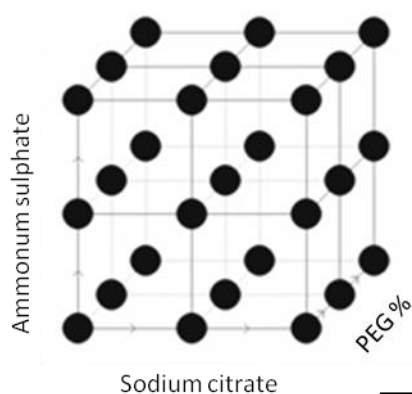
Design repeated (x9) for PEG 4000, 8000 and 12000 at pH 5, 7.4 and 9
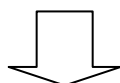
Stage 3

A second round of experimentation (CCF DoE) was conducted with more focused PEG conditions (PEG 12000, 0% to 20% w/v), salt conditions (0 to 0.6 M) at pH 7.4 and DF 1 with yield and purification factor as key responses This was followed by robustness testing. Black dots represent experimental conditions in the design space
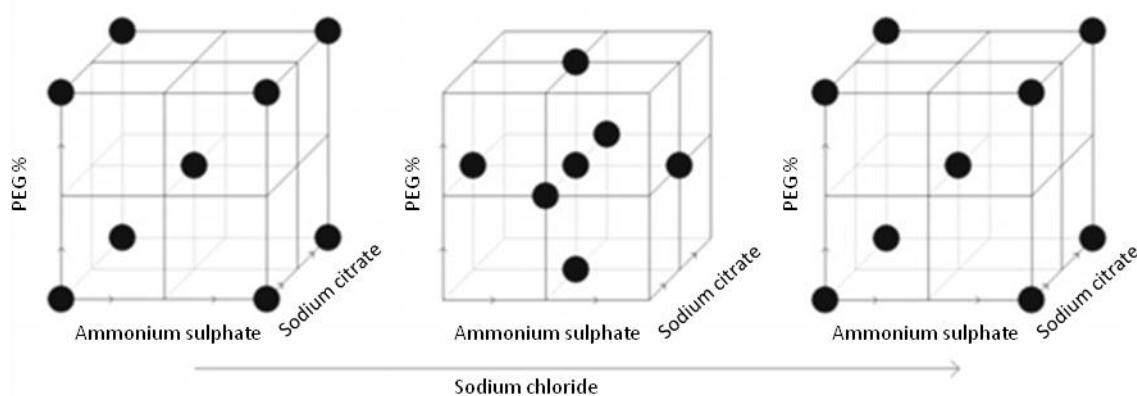
Figure 4.1: *Flowchart of the approach used in this chapter to explore conditions for the initial Fab' precipitation steps. Since the primary aim of such steps was to recover and purify the product, yield and purification factor was used as the key responses to judge performance*

STAGE 1

4.3 Results and Discussion

4.3.1 Validation of a Microscale Mixing Device

Previous experimental DoE and automation were performed using a Multiprobe II EX (Packard Instrument Co., Meriden, USA) liquid handling robot. The Multiprobe II EX workstation (figure 3.13 A) was equipped with a four channel liquid handling arm for transferring liquids between labware and pipetting through the micro tips. The Tecan (Tecan, Reading, UK) was more advantageous as it was equipped with an eight channel liquid handling arm (LiHa) instead of the Multiprobe II EX (Packard Instrument Co., Meriden, USA) four channel arm, which increased liquid handling transfer by 50%. Furthermore, it was quicker, had superior reliability and was more customisable than the Multiprobe II EX (Packard Instrument Co., Meriden, USA). This part of the chapter describes the setup, automation and operation of a Tecan Freedom EVO 200 liquid handling robot (Tecan, Reading, UK) controlled by the Freedom EVOware software for microscale experiments.

Accuracy of liquid handling on the Tecan (Tecan, Reading, UK) was controlled by water in the tubing and syringes to ensure pipetting accuracy. Liquid handling was defined by a set of conditions referred to as "liquid classes". The parameters of which includes pipette calibration settings, aspiration dispense speeds in $\mu L \ s^{-1}$ (range between 0.5 to 900 $\mu L \ s^{-1}$), airgap post aspiration (μL), height, depth and location of pipette positions (z, y and x positioning), delay and detection modes. The Freedom EVOware software had predefined liquid classes for different applications and it was critical for the accuracy and precision of pipetting that the liquid classes were optimised to ensure accurate and reproducible results compared to the Multiprobe II EX (Packard Instrument Co., Meriden, USA) liquid handling robot.

Custom liquid classes were developed for the pipetting of PEG to ensure accuracy. This involved decreasing the aspiration and dispense speeds from the standard 500 $\mu L \ s^{-1}$ to 1 $\mu L \ s^{-1}$ and the z-max (depth of dispense) to dispense 1 mm below the stirrer plate surface (figure 4.3). Liquid tracking, which allows the tip to follow the liquid surface as it rises or descends was used to minimise droplet formation from continuing aspiration and dispense cycles, and the air gap post aspiration was set to

10 μL. Water flushes were performed regularly to reduce cross contamination between liquid transfers.

A typical deck layout for the experiments described in this chapter is shown in figure 4.2 B; the layout was modified for a specific application or higher throughput. In the setup shown, the deck is configured with three carriers for holding microtiter plates and deepwell plates. In addition, the additional carriers are for holding reagent troughs.
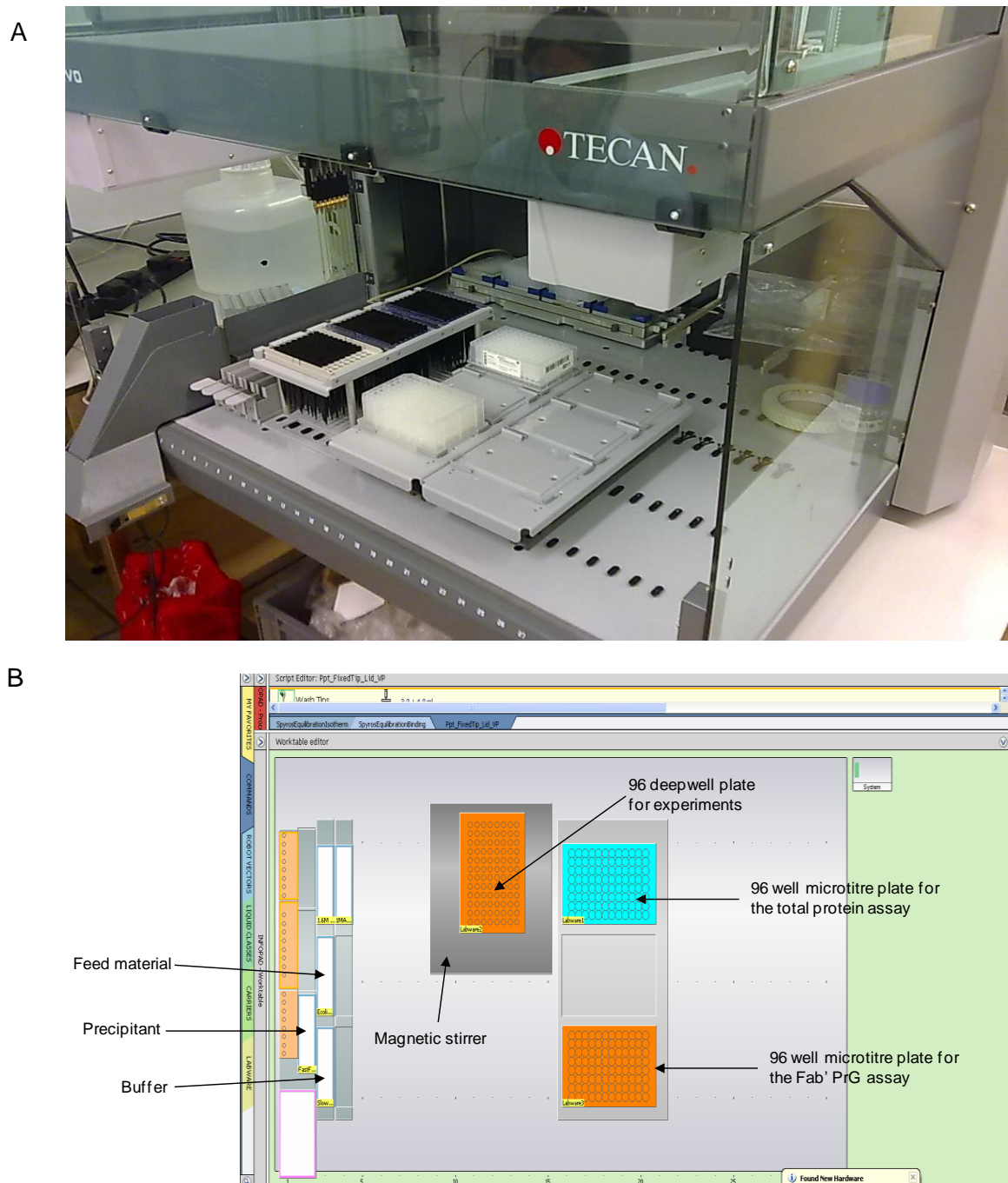
Figure 4.2: *Tecan Freedom EVO 200 liquid handling robot (LHR) (Tecan, Reading, UK) used for microscale experiments. (A) photograph of instrument and (B) is an example deck layout for experiments*

Mixing by the VP 772FN coin stirrers (V&P Scientific, San Diego, USA) at the bottom of microwells performed well under turbulent mixing speeds (section 3.3.3). However, it would be difficult to use the Power per unit volume as a scale up

parameter with this type of mixing due to the lack of control of speed and consistency of mixing. This parameter has been used successfully in scaling up bioreactors (Marques *et al.,* 2010). There has been work on different forms of mixing within microwells including jet mixing, magnetic impellers and shaken microplates (Nealon *et al.,* 2006, Titchener-Hooker *et al.,* 2008). Efficient mixing in the form of jet mixing can be provided from the liquid addition by the pipette tip of the Tecan (Tecan, Reading, UK) followed by repeated reaspirations and dispenses (Nealon *et al.*, 2006). However, this method does not suit the high throughput nature of this work. An alternative, robust and non variable mixing system was engineered and tested for better system scale up. The 5 mm PTFE magnetic coin stirrers (model VP 772FN) that were sourced from V&P Scientific (V&P Scientific, San Diego, USA) were mounted onto an acrylic plate to sit on top of the 1.3 mL 96 deepwell plate (Nunc GmbH & Co., KG, Denmark). This allowed use of all 96 deepwells and control over the speed of mixing. The speed of the mixing was controlled by a custom magnetic stirrer system connected to a tachometer, which was placed underneath the 96 deepwell plate (figure 4.2 B). The use of all 96 deepwells improved throughput by 50% allowing twice the number of experimental conditions to be investigated on one plate compared to experimental conditions described in section 3.3.3. The mixing efficiency was visually observed using red food dye mixed with PEG 12000 15% w/v pH 7.4.

For microscale data to be useful at large scale the design of the engineering environment within microwells needs to be understood and characterised. Rapid and efficient mixing is a key bioprocessing feature and underpins the quantification of precipitation reactions. There are a number of engineering principles to be considered for reactor design such as the impeller being located 1/3 of tank diameter off the bottom, impeller diameter 1/3 of tank diameter and liquid height = tank diameter. The impeller depth typically ranges from 1/3 to 1/6 off the vessel bottom. A very small clearance can cause radial flow with high shear, which may be beneficial for sweeping solids from the well bottom at the expense of bulk homogeneity (Boychyn *et al.,* 2000, 2004). In this case, the stirrers were located approximately 1/3 from the bottom of the microwell. If the stirrers were mounted nearer to the base of the microwell this would have allowed use of smaller working volumes. However, this could have generated excessive turbulence and undesirable effects on the sensitive material. However, mixing at 1/3 clearance resulted in satisfactory mixing efficiency.

Port for additions

20 mm

5 mm

29.1 mm

8.5 mm

Microwell

Magnetically driven rotating disc rotating on its horizontal axis

128 mm

86 mm
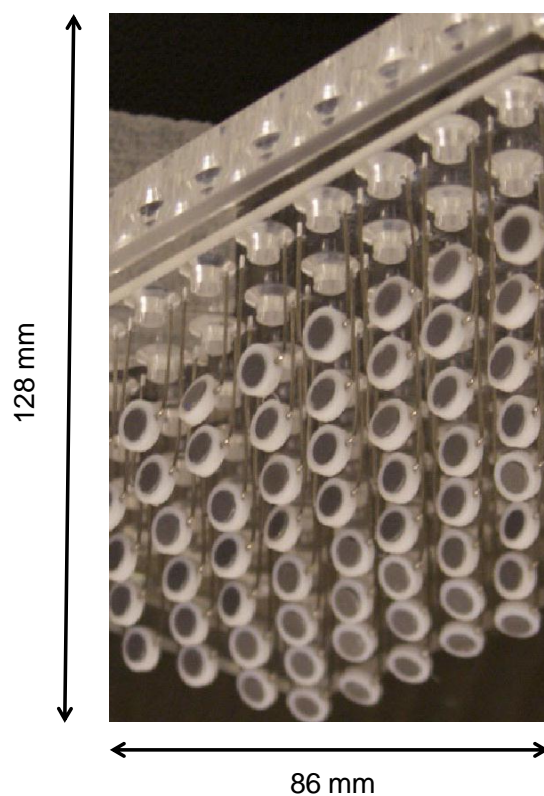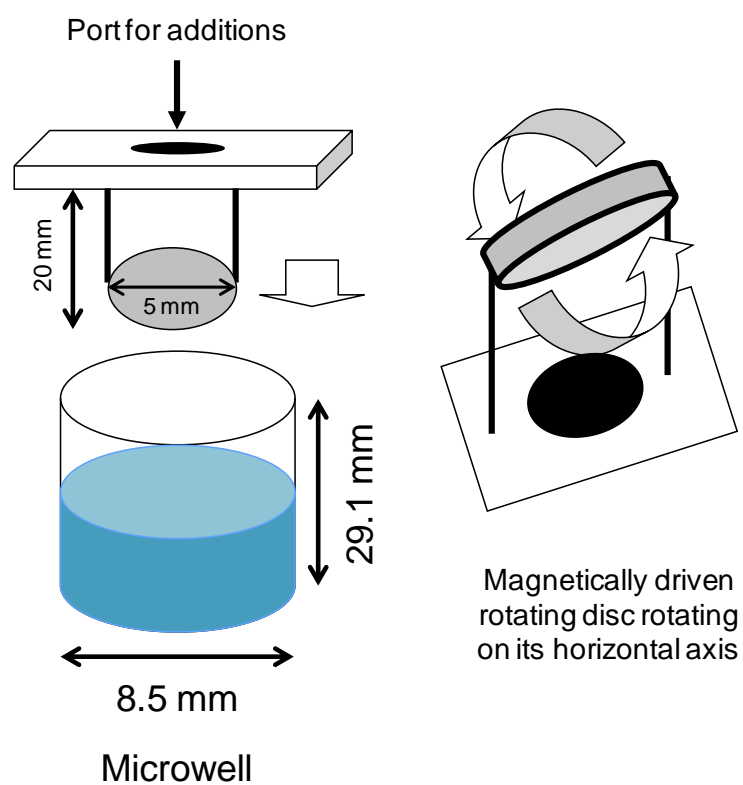
Figure 4.3: *Diagram to show the microscale mixing device used for mixing with 1.3 mL 96 deepwell plates (Nunc GmbH & Co., KG, Denmark). Stirrers (model VP 772FN) were sourced from V&P Scientific (V&P Scientific, San Diego, USA)*

A study to verify the reproducibility and robustness between the LHRs were performed at 1 mL scale on both the Multiprobe II EX (Packard Instrument Co., Meriden, USA) and Tecan (Tecan, Reading, UK) LHRs. Two experiments precipitating Fab' in single and multimodal modes were performed on both LHRs. In single mode PEG 12000 was used to precipitate Fab' and in multimodal mode PEG 12000 was combined with 0.4 M sodium citrate.

Stock solutions of PEG 12000 50% w/v in 100 mM Tris HCl pH 7.4 and 2.2 M sodium citrate pH 7.4 were made. The experiments were performed on a Tecan (Tecan, Reading, UK) and Multiprobe II EX (Packard Instrument Co., Meriden, USA) in 1.3 mL 96 deepwell plates (Nunc GmbH & Co., KG, Denmark). With the Tecan (Tecan, Reading, UK), the microscale mixing device (figure 4.3) was used for mixing. Mixing was controlled by a custom magnetic stirrer system connected to a tachometer placed underneath the 96 deepwell plate. Mixing speed was set to 1000 rpm, which was sufficient to enable turbulent conditions. With the Multiprobe II EX (Packard Instrument Co., Meriden, USA), the V&P Scientific magnetic stirrers, model VP 772FN were placed at the bottom of the microwells for mixing. Mixing was controlled by a Corning PC-611 stirrer plate (Corning, New York, USA) set to an appropriate speed (dial number 7) to enable turbulent conditions.

On both systems, 100 mM Tris HCl pH 7.4 and PEG (and sodium citrate in the second experiment) were added to appropriate wells of a 96 deepwell plate to give a volume of 670 μL, followed by the addition of 330 μL of homogenate feed to give a total volume of 1000 μL. On the Tecan (Tecan, Reading, UK) the port on the microscale mixing device allowed liquid additions whilst mixing, as the stirrer plate was integrated into the workstation. Once liquid transfer was complete, the samples were mixed for 60 minutes. Mixing in this way was not possible on the Multiprobe II EX (Packard Instrument Co., Meriden, USA) and on this system, all reagents were added (PEG and buffer (and sodium citrate in the second experiment)), mixed for 2 minutes prior to the addition of homogenate to ensure homogeneity of the precipitant) and then mixed for 60 minutes.

After 60 minutes of mixing on both systems, the 96 deepwell plates were centrifuged at 4000 rpm for 25 minutes using an Eppendorf 5810R centrifuge (Eppendorf UK Ltd., Cambridge, UK). The supernatant was then carefully removed by the LHRs without disturbing the precipitated pellet and transferred to an

appropriate 96 well microtiter plate for Fab' and total protein concentration analysis. Supernatant was analysed for Fab' and total protein concentration using a 1 mL Protein G column (GE Healthcare, Uppsala, Sweden) on a Agilent 1200 HPLC system (Agilent, Edinburgh, UK) and the Pierce BCA total protein assay (Pierce, Rockford, USA) as described in sections 2.1 and 2.2 respectively. The precipitated pellets readily dissolved in 1 mL of 100 mM Tris HCl pH 7.4. Tables 4.1 and 4.2 give the list of conditions and the corresponding volumes of components for single and multimodal precipitation on both LHRs.

Final PEG 12000 concentration (% w/v)	Volume of PEG (µL)	Volume of 100 mM Tris HCl pH 7.4 (µL)	Volume of homogenate (µL)
0.0	0	670	330
2.5	50	620	330
5.0	100	570	330
7.5	150	520	330
10.0	200	470	330
12.5	250	420	330
15.0	300	370	330
17.5	350	320	330
20.0	400	270	330

Table 4.1: *Table listing the composition of reaction mixtures for the comparative study between the LHRs at 1 mL scale per well in 1.3 mL deepwell plates for single mode precipitation. Table lists the volumes of homogenate pH 7.4, PEG 12000 (from a stock concentration of 50% w/v pH 7.4) and 100 mM Tris HCl pH 7.4 that were used in this experiment. C_o for Fab' and total protein was 0.9 g L^{-1} and 4.5 g L^{-1} respectively. This experiment was performed in 1.3 mL 96 deepwell plates (Nunc GmbH & Co., KG, Denmark) at 1 mL scale per well using a Multiprobe II EX (Packard Instrument Co., Meriden, USA) and a Tecan (Tecan, Reading, UK) for liquid handling. Samples that were prepared by the Multiprobe II EX (Packard Instrument Co., Meriden, USA) were mixed for a total of 60 minutes using VP 772FN coin magnets (V&P Scientific, San Diego, USA) at turbulent mixing conditions on a Corning PC-611 stirrer plate (Corning, New York, USA). Samples that were prepared by the Tecan (Tecan, Reading, UK) were mixed for a total of 60 minutes using the microscale mixing device at 1000 rpm. The plates were centrifuged and then the supernatant was analysed for Fab' and total protein concentration as described in sections 2.1 and 2.2 respectively. The experiments were repeated in triplicate for robustness*

Final PEG 12000 concentration (% w/v)	Volume of PEG (µL)	Volume of 100 mM Tris HCl pH 7.4 (mL)	Volume of sodium citrate (µL)	Volume of homogenate (µL)
0.0	0	490	180	330
2.5	50	440	180	330
5.0	100	390	180	330
7.5	150	340	180	330
10.0	200	290	180	330
12.5	250	240	180	330
15.0	300	190	180	330
17.5	350	140	180	330
20.0	400	90	180	330

Table 4.2: *Table listing the composition of reaction mixtures for the comparative study between the LHRs at 1 mL scale per well in 1.3 mL deepwell plates for multimodal precipitation. Table lists the volumes of homogenate pH 7.4, PEG 12000 (from a stock concentration of 50% w/v pH 7.4), sodium citrate to give 0.4 M concentration (from a stock concentration of 2.2 M pH 7.4) and 100 mM Tris HCl pH 7.4 that were used in this experiment. C_o for Fab' and total protein was 0.9 g L^{-1} and 4.5 g L^{-1} respectively. This experiment was performed in 1.3 mL 96 deepwell plates (Nunc GmbH & Co., KG, Denmark) at 1 mL scale per well using a Multiprobe II EX (Packard Instrument Co., Meriden, USA) and a Tecan (Tecan, Reading, UK) for liquid handling. Samples that were prepared by the Multiprobe II EX (Packard Instrument Co., Meriden, USA) were mixed for a total of 60 minutes using VP 772FN coin magnets (V&P Scientific, San Diego, USA) at turbulent mixing conditions on a Corning PC-611 stirrer plate (Corning, New York, USA). Samples prepared by the Tecan (Tecan, Reading, UK) were mixed for a total of 60 minutes using the microscale mixing device at 1000 rpm. The plates were centrifuged and then the supernatant was analysed for Fab' and total protein concentration as described in sections 2.1 and 2.2 respectively. The experiments were repeated in triplicate for robustness*
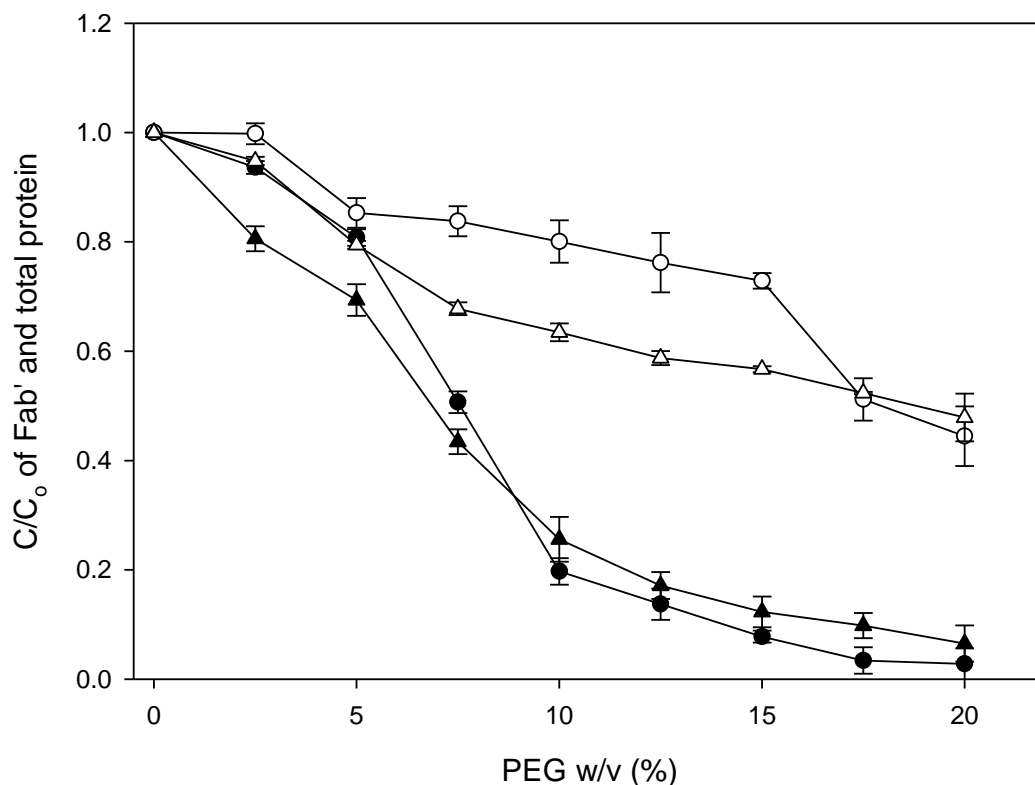
Figure 4.4: *Effect of PEG 12000 pH 7.4 on the solubility of Fab' (●) and total protein (○) at 1 mL scale per well in a 1.3 mL deepwell plate using a Multiprobe II EX (Packard Instrument Co., Meriden, USA) for liquid handling and the effect of PEG 12000 on the solubility of Fab' (▲) total protein (△) at 1 mL scale per well in a 1.3 mL deepwell plate using a Tecan (Tecan, Reading, UK) for liquid handling. Homogenate pH 7.4, PEG 12000 (from a stock concentration of 50% w/v pH 7.4) and 100 mM Tris HCl pH 7.4 were used in this experiment. C_o for Fab' and total protein was 0.9 g L^{-1} and 4.5 g L^{-1} respectively. This experiment was performed in 1.3 mL 96 deepwell plates (Nunc GmbH & Co., KG, Denmark) at 1 mL scale per well using a Multiprobe II EX (Packard Instrument Co., Meriden, USA) and a Tecan (Tecan, Reading, UK) for liquid handling. Samples that were prepared by the Multiprobe II EX (Packard Instrument Co., Meriden, USA) were mixed for a total of 60 minutes using VP 772FN coin magnets (V&P Scientific, San Diego, USA) at turbulent mixing conditions on a Corning PC-611 stirrer plate (Corning, New York, USA). Samples that were prepared by the Tecan (Tecan, Reading, UK) were mixed for a total of 60 minutes using the microscale mixing device at 1000 rpm. The plates were centrifuged and then the supernatant was analysed for Fab' and total protein concentration as described in sections 2.1 and 2.2 respectively. Error bars are shown for one standard deviation for triplicate experiment repeats*

Figure 4.5: *Effect of PEG 12000/0.4 M sodium citrate pH 7.4 on the solubility of Fab' at 1 mL scale per well in a 1.3 mL deepwell plate using the Tecan (Tecan, Reading, UK) for liquid handling with the microscale mixing device (▲) and Multiprobe II EX (Packard Instrument Co., Meriden, USA) (●) for liquid handling. C_o for Fab' was 0.9 g L^{-1}. This experiment was performed in 1.3 mL 96 deepwell plates (Nunc GmbH & Co., KG, Denmark) at 1 mL scale per well using a Multiprobe II EX (Packard Instrument Co., Meriden, USA) and a Tecan (Tecan, Reading, UK) for liquid handling. Homogenate pH 7.4, PEG 12000 (from a stock concentration of 50% w/v pH 7.4), sodium citrate to give 0.4 M concentration (from a stock concentration of 2.2 M pH 7.4) and 100 mM Tris HCl pH 7.4 were used in this experiment. Samples that were prepared by the Multiprobe II EX (Packard Instrument Co., Meriden, USA) were mixed for a total of 60 minutes using VP 772FN coin magnets (V&P Scientific, San Diego, USA) at turbulent mixing conditions. Samples that were prepared by the Tecan (Tecan, Reading, UK) were mixed for a total of 60 minutes using the microscale mixing device at 1000 rpm. The plates were centrifuged and then the supernatant was analysed for Fab' as described in section 2.1. Error bars are shown for one standard deviation for triplicate experiment repeats*

A comparative study was performed to evaluate the performance of the Tecan (Tecan, Reading, UK) to that of the Multiprobe II EX (Packard Instrument Co., Meriden, USA). Figure 4.4 shows the effect of PEG 12000 pH 7.4 on the solubility profiles of Fab' and total protein using both LHRs. There was a 9% and 12% difference on average between the Fab' and total protein solubility profiles for the Tecan (Tecan, Reading, UK) and Multiprobe II EX (Packard Instrument Co., Meriden, USA) LHRs respectively. Figure 4.5 shows the effect of PEG 12000/0.4 M sodium citrate pH 7.4 on the Fab' solubility profiles for both LHRs. There was a 5% difference on average between the Fab' solubility profiles for the Tecan (Tecan, Reading, UK) and Multiprobe II EX (Packard Instrument Co., Meriden, USA) LHRs respectively. Interestingly, in both figures the percentage difference between the two LHRs was significantly reduced with increasing PEG concentration (> 8.5% PEG w/v) suggesting that any difference in liquid handling was normalised by the higher concentrations of PEG in the system. This is in part caused by the PEG becoming the driving force of the process.

The two systems performance were comparable and the variation that was observed could be attributed in part to the experimental error in liquid transfer of the Multiprobe II EX (Packard Instrument Co., Meriden, USA) and the difference in mixing conditions. The disadvantage of using the Multiprobe II EX (Packard Instrument Co., Meriden, USA) for liquid handling, other than the four channel arm, was that the mixing conditions were difficult to control and thus difficult to use the Power per unit volume as a scale up parameter. This is a key scale up parameter, and has been used successfully in scaling up bioreactors for example (Marques *et al.,* 2010). The combination of high agitation at an unknown speed and the magnets location at the bottom of the microwells may have contributed to break up of some aggregates during nucleation caused in part by unwanted abrasion effects (Nealon *et al.,* 2006, Titchener-Hooker *et al.,* 2008). The consistency of pipetting was visually better with the Tecan (Tecan, Reading, UK). The Tecan (Tecan, Reading, UK) has an eight channel arm (LiHa), is more efficient, faster, reliable than the Multiprobe II EX (Packard Instrument Co., Meriden, USA) LHR and can integrate the microscale mixing device into the workstation (which was used for scale up studies described in section 5.3.2). The Tecan (Tecan, Reading, UK) can reportedly reproduce accurate pipetting within one microlitre (Wenger 2010) and was used for all future studies.

STAGE 2

4.4 Results and Discussion

Salts have two different and opposing effects on the solubility of proteins, firstly, electrostatic interactions at low salt concentrations, which increase the solubility of proteins (termed salting in), and secondly at higher salt concentrations hydrophobic effects result in salting out of proteins. Melander and Horváth (1977) proposed a "cavity theory" to describe the solubility of proteins in the presence of salts based on thermodynamics. This theory postulates that the surface tension of the water must be reduced to create a cavity that will accommodate the protein molecule in solution. Therefore, with the addition of high concentrations of salts, the solvent surface tension increases exposing the hydrophobic regions of the protein reducing protein solubility until precipitation occurs. The sequence of salts as described by Melandar and Horváth (1977) is a quantitative measure of the well known Hofmeister series (section 1.4.1) that describes the relative effectiveness of salting out properties of salts (Balasundaram *et al.,* 2011). The addition of neutral salts results in their ions bonding with water molecules, which would otherwise be hydrating proteins. Proteins will be forced by reduced hydration to aggregate and precipitate in these conditions. This loss in the water monolayer surrounding the protein reduces the barrier to aggregation as high concentrations of salt ions are introduced to the system allowing aggregation from solute collisions, which is intensified by mixing.

In chapter 3, experimental conditions within the NOR of the design space (figure 3.23) for the precipitation of Fab' from partially clarified cell culture fluid using PEG 12000 15% w/v (undiluted homogenate and pH 7.4), delivered a Fab' yield of 93% and a purification factor of 1.5. To improve the yield and purification factor, multimodal operation was investigated by combining PEG with a mixture of ammonium sulphate and sodium citrate concentrations. Salts were chosen due to being readily accepted by regulatory bodies and their different precipitating mechanism to that of single mode precipitation with PEG. Balasundaram *et al.,* (2011) reported positive precipitation profiles of Fab' using only ammonium sulphate and sodium citrate as precipitating agents at concentrations > 0.4 M. It was reported that the higher the salt concentration used, the greater mass of total protein was precipitated.

4.4.1 Full Three Level Factorial DoE for the Study of Fab' Precipitation Using PEG, Ammonium Sulphate and Sodium Citrate

In section 3.4.2, a two level full factorial DoE design was used to screen conditions for Fab' precipitation, which was followed by a CCF DoE (section 3.5.1) for optimisation using the Multiprobe II EX (Packard Instrument Co., Meriden, USA) for liquid handling. The full factorial DoE was completed first and then followed by a CCF DoE, reducing the number of potential experiments for the efficient mapping of the Fab' precipitation system using PEG. This approach was taken due to the limitations of the LHR by having a four channel arm and only being able to use half a 96 deepwell plate caused by the strength of the magnets. However, the Tecan (Tecan, Reading, UK) had an eight channel arm (LiHa) and the microscale mixing device allowed for use of all 96 deepwells improving throughput by at least 50% relative to conditions described in section 3.3.3. Therefore, multimodal operation was investigated by combining PEG with a mixture of ammonium sulphate concentrations and sodium citrate concentrations in a three level full factorial design to efficiently map out a large design space without completing a screening study first. This design allowed the mapping of possible curvature in the response function in one experiment, essentially the equivalent of combining the DoE described in sections 3.4.2 and 3.5.1 in one experiment. Examples of both two and three level factorial designs are shown in figure 4.6.

Two level full factorial design   Three level full factorial design
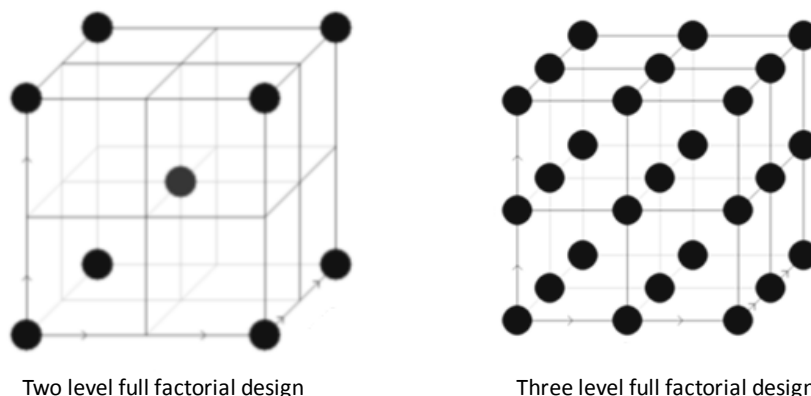
Figure 4.6: *Examples of two and three level full factorial designs. The black dots represent the experiments in the design space. A three level full factorial design is a response surface methodology design allowing for full mapping of the response surface (which includes curvature). A full factorial two level design requires other designs such as CCF design to be augmented for mapping curvature in the design space*

PEG 4000, 8000 and 12000 at stock concentrations of 50% w/v were made in 100 mM Tris HCl pH 5, 7.4 and 9. Stock solutions of each of the salts were made up to a maximum molarity of 2.2 M (pH 5, 7.4 and 9), limited by the difficulty in solubilising sodium citrate at higher concentrations. In addition, ammonium sulphate can made to 4 M; however, the maximum salt concentration that can be used without interfering with the Pierce BCA total protein assay is 1.5 M as per the manufacturer's instructions. Therefore, all salts were made to a stock concentration of 2.2 M, and thus the maximum salt concentration in the system was 1.4 M as per table 4.3. 1 mL total working volume was used in 1.3 mL 96 deepwell plates (Nunc GmbH & Co., KG, Denmark), of this 1 mL volume, Fab' homogenate was 330 μL in each microwell. The remaining 670 μL was split between a combination of PEG, salts and buffer for multimodal operation. The maximum molar stock solution of salt was 2.2 M, which resulted in a maximum of 1.4 M in the reaction mixture with PEG 0% w/v. This value dropped to 0.8 M with the addition of 15% PEG (Table 4.3). The Tecan (Tecan, Reading, UK) was preprogramed to carry out all liquid handling.

Maximum salt molarity combinations was determined at different PEG concentrations (0% to 20% w/v), ensuring that the maximum salt concentration was not exceeded in the DoE (table 4.3).

PEG (% w/v)	Volume of PEG (μL)	Maximum molar of salt [M]	Volume of salt (μL)	Volume of buffer (μL)	Volume of homogenate (μL)
0	0	1.4	635	35	330
5	100	1.2	545	25	330
10	200	1.0	455	15	330
15	300	0.8	365	5	330

Table 4.3: *Table listing the maximum molarity of salt possible at 1 mL scale using stock 2.2 M salt concentrations, PEG (stock 50% w/v concentration of PEG 4000, 8000 and 12000) and 100 mM Tris HCl solutions in the pH range of 5 to 9*

For each of the conditions outlined in table 4.4 the yield and purification factor was calculated as described in section 3.4.1. As a key requirement for a primary purification process, a minimum yield of Fab' of 90% was chosen as acceptable for this primary process step. The inputs of the DoE were:

- pH 5, 7.4 and 9

- PEG molecular weights of 4000, 8000 and 12000

- PEG concentration 5% to 15% w/v

- Ammonium sulphate concentration 0 to 1 M

- Sodium citrate concentration 0 to 1 M

However, due to the limitations of stock PEG and salt concentrations. The maximum concentration of salt at PEG 15% w/v was 0.8 M (table 4.3). Salt concentrations in experiment number 16-17, 24-26 and 31-34 (table 4.4) were modified to the maximum amount of salt concentration possible in the system. This resulted in the upper right hand corner of the experimental design space being inaccessible for experimentation as shown in figure 4.7.

Design repeated (x9) for PEG 4000, 8000 and 12000 at pH 5, 7.4 and 9

Ammonium sulphate concentration 0-1 M

Sodium citrate concentration 0-1 M

PEG concentration 5%-15% w/v
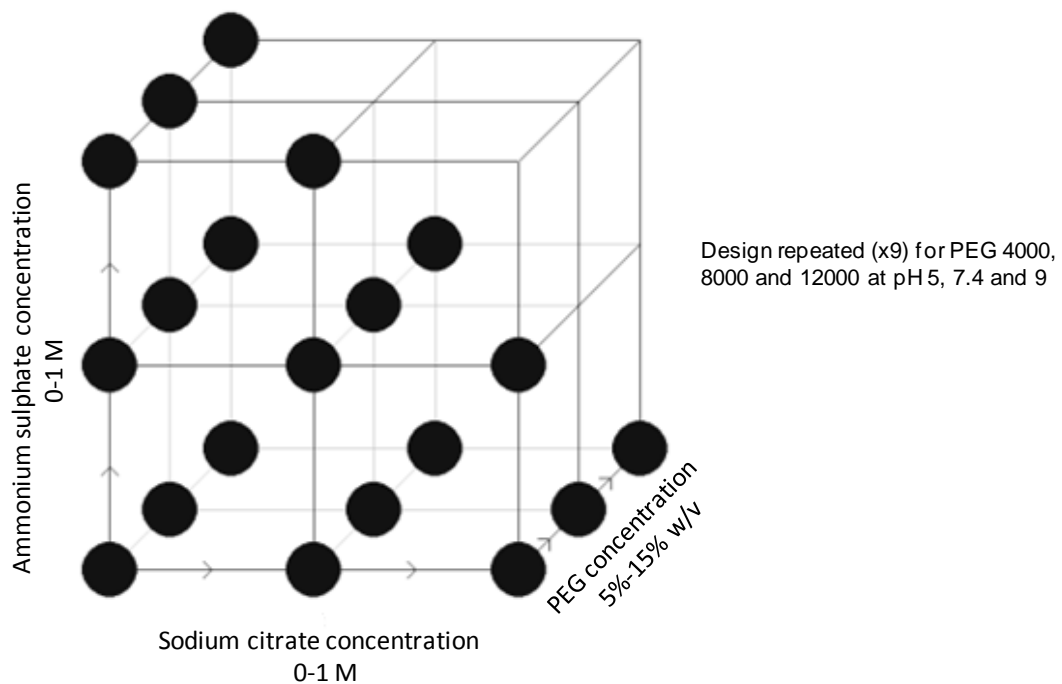
Figure 4.7: *Shows the irregular experimental design space where the upper right hand corner of the experimental design space was inaccessible for experimentation due to process limitations governed by stock salt and PEG concentrations used. For example the maximum concentration of salt possible in a microwell at PEG 15% w/v was 0.8 M (table 4.3). The black dots represent the experimental conditions in the design space. This experimental design was repeated for each PEG molecular weight (4000, 8000 and 12000) and pH (5, 7.4 and 9)*

The experimental plan in table 4.4 was performed at pH 5, 7.4 and 9 using PEG 4000, 8000 and 12000, and PEG concentrations 5% to 15% w/v. The experimental design was also completed at 0% w/v independently of the DoE shown in table 4.4 resulting in a total of 324 experimental conditions. A study with this many conditions would not have been feasible at laboratory scale, highlighting a benefit of operating at microscale.

Run	PEG (% w/v)	Ammonium sulphate [M]	Sodium citrate [M]	Run	PEG (% w/v)	Ammonium sulphate [M]	Sodium citrate [M]
1	0	0.00	0.00	19	10	0.40	0.00
2	0	0.40	0.00	20	10	0.00	0.40
3	0	0.00	0.40	21	10	0.40	0.40
4	0	0.40	0.40	22	10	0.00	1.00
5	0	0.00	1.00	23	10	1.00	0.00
6	0	1.00	0.00	24	10	0.50	0.50
7	0	0.75	0.75	25	10	0.27	0.67
8	0	0.40	1.00	26	10	0.67	0.27
9	0	1.00	0.40	27	15	0.00	0.00
10	5	0.00	0.00	28	15	0.40	0.00
11	5	0.40	0.00	29	15	0.00	0.40
12	5	0.00	0.40	30	15	0.40	0.40
13	5	0.40	0.40	31	15	0.00	0.80
14	5	0.00	1.00	32	15	0.80	0.00
15	5	1.00	0.00	33	15	0.21	0.53
16	5	0.20	1.00	34	15	0.53	0.21
17	5	1.00	0.20	35	10	0.50	0.50
18	10	0.00	0.00	36	10	0.50	0.50

Table 4.4: *Table listing the full three level factorial design for multimodal precipitation. The experiments in this table were performed for PEG 4000, 8000 and 12000 at pH 5, 7.4 and 9. The highlighted values (▨ ammonium sulphate and ▨ sodium citrate) were modified to allow for the maximum salt concentration in the system (table 4.3). Homogenate at the appropriate pH, PEG (from a stock concentration of 50% w/v at the appropriate pH), sodium citrate and ammonium sulphate (from a stock concentration of 2.2 M at the appropriate pH) and 100 mM Tris HCl at the appropriate pH were prepared for this experiment. C_o for Fab' and total protein was 0.9 g L^{-1} and 4.5 g L^{-1} respectively. This experiment was performed in 1.3 mL 96 deepwell plates (Nunc GmbH & Co., KG, Denmark) at 1 mL scale per well using a Tecan (Tecan, Reading, UK) for liquid handling. Samples that were prepared by the Tecan (Tecan, Reading, UK) were mixed for a total of 60 minutes using the microscale mixing device at 1000 rpm. The plates were centrifuged and then the supernatant was analysed for Fab' and total protein concentration as described in sections 2.1 and 2.2 respectively*

Interestingly, an aqueous two phase system was observed between PEG and salt at concentrations of salt ≥ 0.8 M and PEG concentrations ≥ 5% w/v after the centrifugation step, post precipitation at all PEG molecular weights investigated. The two phases may have been present before the addition of Fab' and the centrifugation step, although it was difficult to observe this in non transparent deepwell plates. This affected 40% of the irregular design space, which was excluded from analysis as the study of an aqueous two phase system was beyond the scope of this project (figure 4.8). In this case, the initial design was too large resulting in an irregular design space, which was further reduced by the formation of an aqueous two phase system in 40% of that design space. If this study was conducted at laboratory scale where the volumes required are much larger than at microscale (10-100 mL relative to 20-2000 μL), this study would have resulted in the waste of time and resources for minimal gain. In theory, there are two methods of handling irregular designs. The first is to shrink the factor ranges so that the design becomes regular and the second is the use of D-optimal design, which is adapted to spreading experiments in an irregular region (Lundstedt *et al.,* 1998).

Design repeated (x9) for PEG 4000, 8000 and 12000 at pH 5, 7.4 and 9
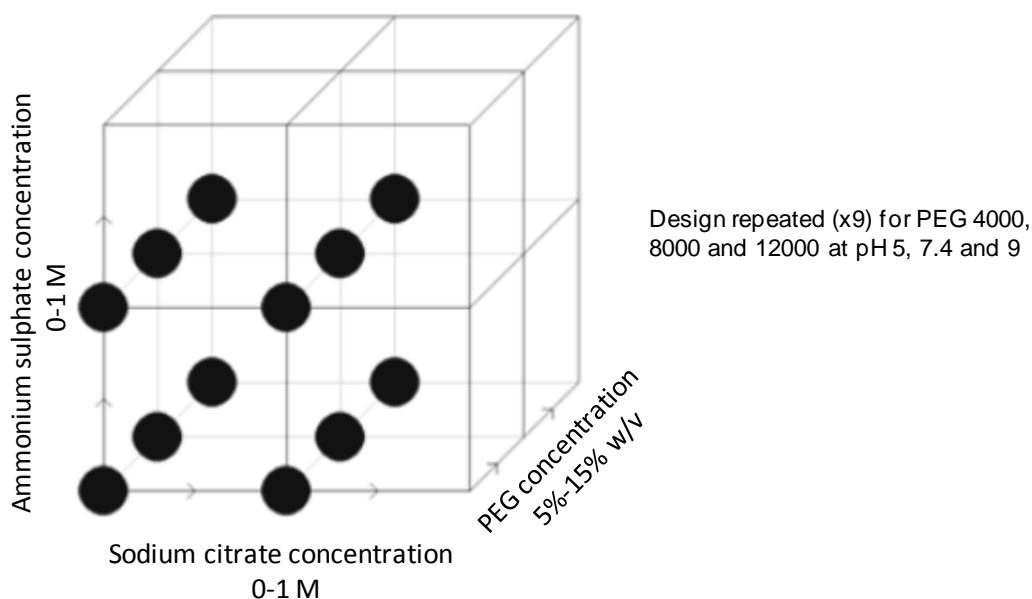
Figure 4.8: *The black dots represent the experimental conditions where two phase formation does not to occur in the irregular design space (figure 4.7). Two phase formation affected 40% of the irregular design space shown in figure 4.7. Two phase formation was observed at salt concentrations ≥ 0.8 M with PEG concentrations ≥ 5% w/v. This design was repeated for each PEG molecular weight (4000, 8000 and 12000) and pH (5, 7.4 and 9)*

Eiteman and Gainer (1991), Perumalsamy and Murugesan (2006) and Rosa *et al.,* (2007) reported two phase systems with PEG and sodium citrate at similar conditions. The aqueous two phase system of PEG and salt has been discussed in literature previously (Azevedo *et al.,* 2009 (b)). Aqueous two phase systems are formed spontaneously upon mixing two aqueous solutions of structurally different components, such as two polymers or a polymer and a salt, above a certain critical concentration (Azevedo *et al.,* 2009 (a)). An example is shown in figure 4.9 for PEG and salt (Azevedo *et al.,* 2009 (a)). The partitions of proteins in aqueous two phase systems form as a result of the phase separation of mixtures of PEG polymer and salt (Huddleston *et al.,* 1994, Huddleston *et al.,* 1996). PEG and salt are present in the top and bottom phase respectively, due to the increase in hydrophobicity of PEG molecules (Perumalsamy and Murugesan 2006). Marcos *et al.,* (1998) and Aguilar *et al.,* (2006) demonstrated purification of penicillin acylase from extracts of *E.coli* from PEG and sodium phosphate systems.
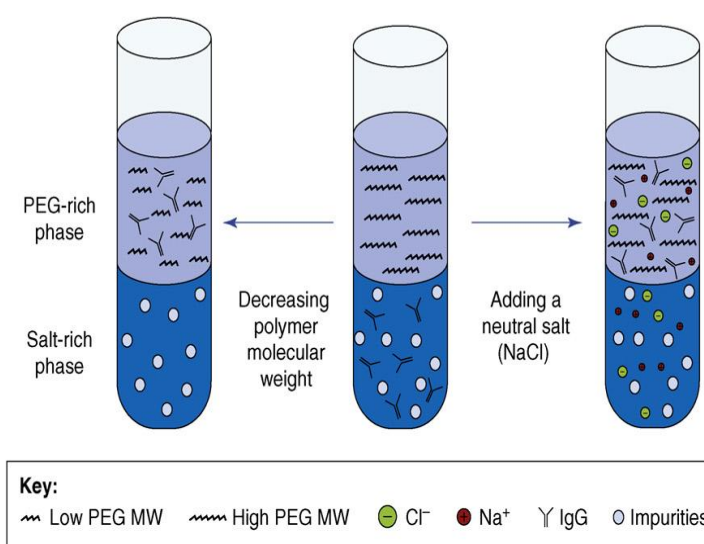
Figure 4.9: *Schematic diagram illustrating the behaviour of antibodies and impurities in a PEG–salt two phase system (Azevedo et al., 2009 (a))*

A PLS (partial least square) model was used to analyse the design matrix as this method can be useful for handling missing data in the response matrix (Lundstedt *et al.,* 1998). However, the resulting model had a poor fit due to 40% of the irregular design space being omitted for analysis, and that the omitted results were not randomly scattered throughout the design space. Therefore, a more focused DoE was performed, which reduced the design space to form a regular design, avoiding the two phase formation between salts and PEG, discussed in section 4.5.2.

However, it was possible to observe the effect of several combinations of ammonium sulphate and sodium citrate at different ratios on the solubility profile of Fab' through synergistic or antagonistic effects at zero PEG added (figure 4.10). The experimental conditions are listed in table 4.4 of which experiment run numbers 1 to 9 were performed at pH 5, 7.4 and 9. ANOVA analysis suggested that the model had no lack of fit as the p-value was $>$ 0.05 (p-value was 0.16), with an Q^2 value of 0.92.
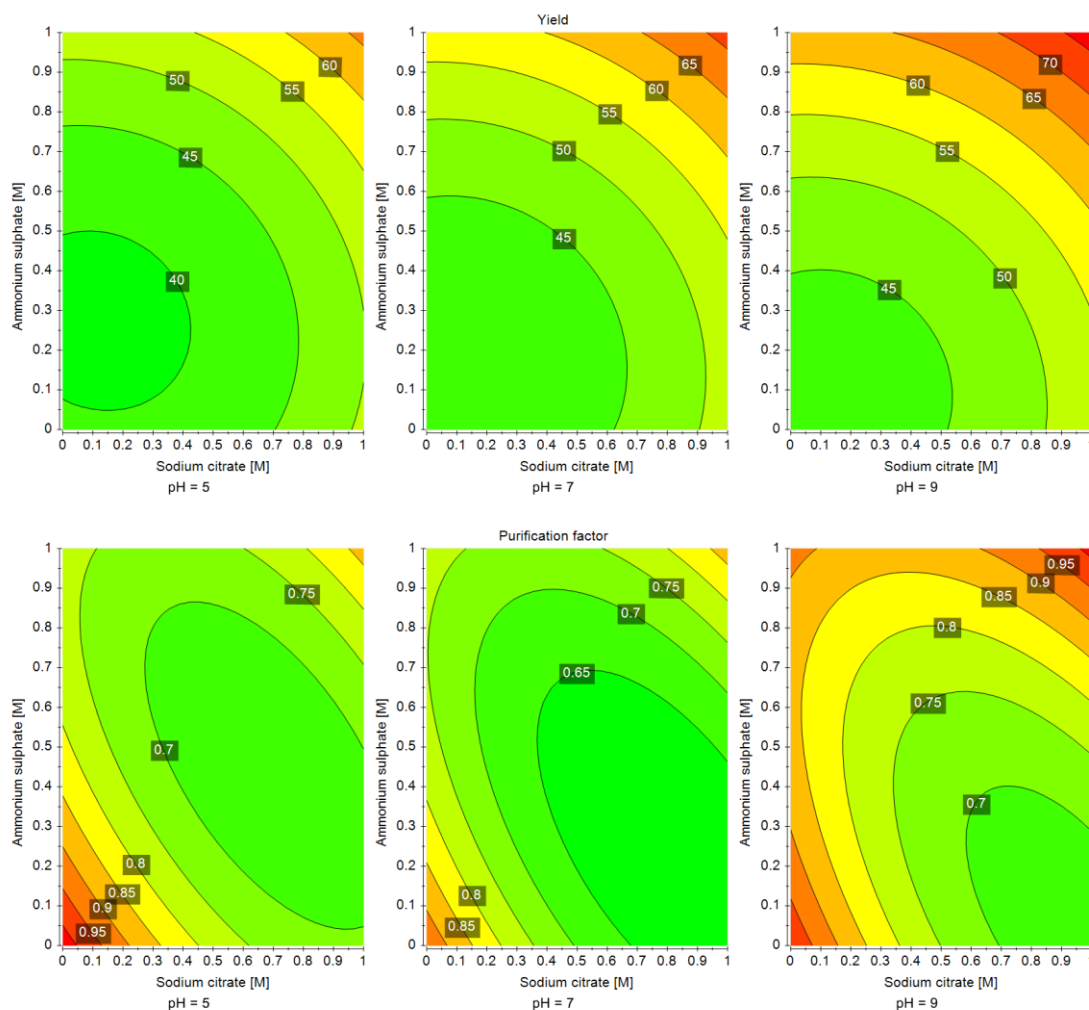
Figure 4.10: *4D contour plots showing the yield and purification factor of Fab' as a function of ammonium sulphate concentration [M] and sodium citrate concentration [M] at varying pH. Experiment numbers 1 to 9 were performed at pH 5, 7.4 and 9 as per table 4.4. The experiment setup is described in the table 4.4 legend. The response surfaces for yield and purification factor were fit with a quadratic model. All data fitting was performed using the software package MODDE 9.1 (Umetrics, Malmö, Sweden)*

Figure 4.10 shows contour plots for Fab' yield and purification factor at pH 5, 7.4 and 9. Figure 4.10 suggests that the precipitation of both Fab' and proteins somewhat increased with the decrease in pH (at 1 M ammonium sulphate Fab' yield increased from 52% at pH 9 to 56% at pH 5; purification factor decreased from 0.8 at pH 9 to 0.6 at pH 5). Similar results with sodium citrate were observed (at 1 M sodium citrate Fab' yield increased from 55% at pH 9 to 66% at pH 5; purification factor decreased from 0.8 at pH 9 to 0.6 at pH 5. The solubility of protein decreases with either decrease in pH or increase in salt concentration used, as reported previously (Foster *et al.,* 1976).

At ≤ 0.4 M concentrations of sodium citrate and ammonium sulphate Fab' precipitation was low < 40% on average in the pH range suggesting electrostatic interactions dominate at this concentration range. The introduction of low concentrations of salt may be thermodynamically favourable resulting in an increase in solubility of the protein (Arakawa and Timasheff 1982). The precipitating potential of ammonium sulphate and sodium citrate at > 0.6 M results in much higher Fab' precipitation which suggests hydrophobic interactions are overwhelming electrostatic effects at higher salt concentrations. This is in agreement with the solvophobic theory proposed by Melander and Horváth (1977) who suggested that at high salt concentrations solvent surface tension is increased exposing hydrophobic regions of proteins resulting in precipitation. Harinarayan *et al.,* (2008) suggested that the binding of citrate ions with Fab' at high citrate concentrations could potentially displace water molecules from the Fab' directly, helping to reduce solubility.

At 1.5 M combined concentration, the combination of salts resulted in 20% to 30% greater precipitation of Fab' compared to individual salts concentrations at 0.4 M. This indicates the synergistic effects of ammonium sulphate and sodium citrate on the precipitation of Fab'. This behaviour appears to be specific for Fab' and not for protein impurities as the purification factor increased ~1.5x at this salt concentration and in the pH range investigated suggesting some selectivity. It is known that for a salting out system the solubility of a protein increases with salt concentration until the salt concentration becomes sufficiently high to cause salting out (Dixon and Webb 1961). Sodium citrate in single mode did not precipitate Fab' efficiently (~55% at 1 M within the pH range investigated) indicating that hydrophobic effects by increasing sodium citrate concentration were not sufficient to precipitate Fab' to

obtain high yields. Combining ammonium sulphate and sodium citrate at 2 M, Fab yield increased to ~70% within the pH range investigated. The purification factor was low (maximum of ~1.1 PF), which increased with increasing pH in the range investigated. Therefore, in the range investigated, to maximise yield and purification factor, precipitation conditions using high concentrations of ammonium sulphate and sodium citrate (> 1 M) and pH 9 are recommended. It was hypothesised that the synergistic properties of sodium citrate and ammonium sulphate with the addition of PEG in multimodal mode may improve both the Fab' yield and purification factor.
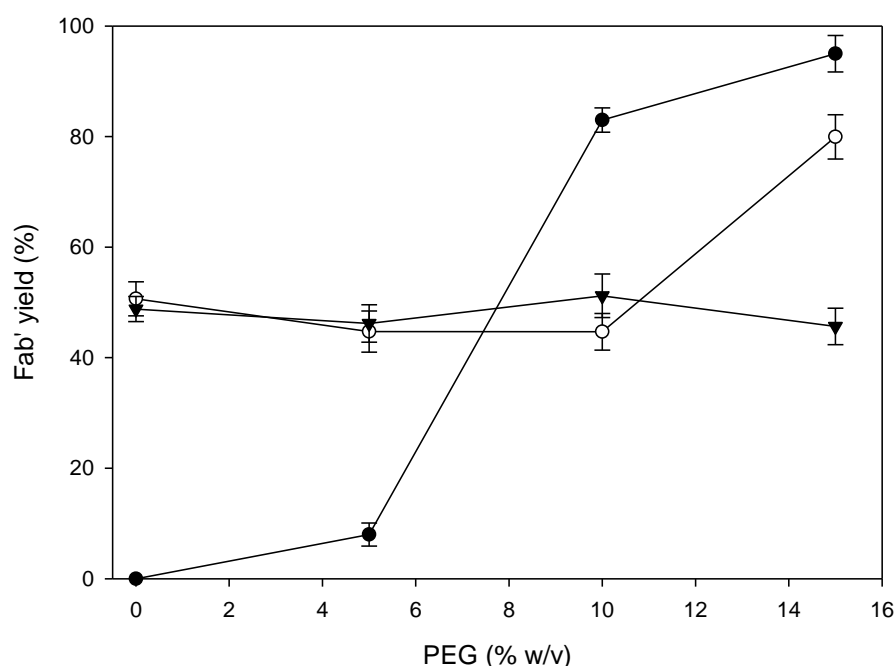
Figure 4.11: *The effect of PEG 12000 (●), PEG 12000/0.4 M ammonium sulphate (○) and PEG 12000/0.4 M sodium citrate (▼) at pH 7.4 on Fab' yield. C_o for Fab' was 0.9 g L^{-1}. Homogenate pH 7.4, PEG (from a stock concentration of 50% w/v pH 7.4), sodium citrate and ammonium sulphate (from a stock concentration of 2.2 M pH 7.4) and 100 mM Tris HCl pH 7.4 were used in this experiment. This experiment was performed in 1.3 mL 96 deepwell plates (Nunc GmbH & Co., KG, Denmark) at 1 mL scale per well using a Tecan (Tecan, Reading, UK) for liquid handling. Samples that were prepared by the Tecan (Tecan, Reading, UK) were mixed for a total of 60 minutes using the microscale mixing device at 1000 rpm. The plates were centrifuged and then the supernatant was analysed for Fab' as described in section 2.1. Error bars are shown for one standard deviation for triplicate experiment repeats*

Figure 4.12: *The effect of PEG 12000 (●), PEG 12000/0.4 M ammonium sulphate (○) and PEG 12000/0.4 M sodium citrate (▼) at pH 7.4 on Fab' purity. C_o for Fab' and total protein was 0.9 g L^{-1} and 4.5 g L^{-1} respectively. Homogenate pH 7.4, PEG (from a stock concentration of 50% w/v pH 7.4), sodium citrate and ammonium sulphate (from a stock concentration of 2.2 M pH 7.4) and 100 mM Tris HCl pH 7.4 were used in this experiment. This experiment was performed in 1.3 mL 96 deepwell plates (Nunc GmbH & Co., KG, Denmark) at 1 mL scale per well using a Tecan (Tecan, Reading, UK) for liquid handling. Samples that were prepared by the Tecan (Tecan, Reading, UK) were mixed for a total of 60 minutes using the microscale mixing device at 1000 rpm. The plates were centrifuged and then the supernatant was analysed for Fab' and total protein concentration as described in sections 2.1 and 2.2 respectively. Error bars are shown for one standard deviation for triplicate experiment repeats*

Figure 4.11 shows the resultant Fab' solubility profiles combining salt with PEG. The addition of ammonium sulphate and sodium citrate at a salt concentration of 0.4 M with PEG was investigated at microscale. PEG 12000 15% w/v pH 7.4 was required to obtain a yield of 95%, whereas 83% yield was achievable at 10% w/v. The percentage purity (calculated from the Pierce BCA total protein assay kit) did not increase beyond 20% indicating that substantial material was insolubilised due to non specific precipitation by PEG (figure 4.12).

At 5% PEG with no salt added Fab' percentage purity was 2%, which increased to 54% and 49% with ammonium sulphate and sodium citrate at 0.6 M respectively (figure 4.12). Fab' yield increased from 45% to 80% with PEG 10% and 15% w/v with 0.6 M ammonium sulphate respectively. This suggested that the concentration of ammonium sulphate was sufficiently low to induce a salting in effect of Fab'. At PEG 15% w/v Fab' yield increased, due to the PEG becoming the driving force of the process resulting in a more thermodynamically favourable state (Lee and Lee 1981) (figure 4.11). Interestingly, at this point purity dropped from to 37% from 57%, due to the increase in proteins precipitated simultaneously by the PEG. A two cut fractional precipitation process can be operated to selectively precipitate impurities according to their different solubilities. However, more investigation is required as ammonium sulphate does not appear to selectively solubilise Fab' as the percentage purity does not alter significantly between PEG 0% to 10% w/v (figure 4.12).

The addition of 0.4 M sodium citrate caused purity to increase from 16% to 55% with PEG 0% w/v and 15% w/v respectively (figure 4.12). There appeared to be no change in yield by increasing concentrations of PEG, which on average was 48% (figure 4.11). Harinarayan *et al.,* (2008) suggested that there was an electrostatic interaction associated with the trivalent citrate ions and Fab, which may in part explain the insignificant change in yield with increasing PEG concentration. This complicates the understanding of the behaviour of this protein in a complex mixture of salts containing citrate ions. Janson and Rydén (1998) discussed that larger proteins are less soluble than smaller proteins, and proteins with surfaces rich in hydrophobic amino acids are less soluble in water than those proteins whose surfaces are rich in hydrophilic amino acids. However, Fab' was observed to precipitate out readily with PEG in part due to its size (~54 kDa) and higher hydrophobic properties. However, these properties in multimodal conditions may be

shielded increasing the solubility of Fab', as a result of the added complexity of the multimodal precipitation mechanism. The differences in Fab' and total protein solubility profiles between different PEG molecular weights and different pH values were marginal.

STAGE 3

4.5 Results and Discussion

4.5.1 Evaluation of Variables for Fab' Precipitation using PEG, Ammonium Sulphate, Sodium Citrate and Sodium Chloride

The experimental approach based on DoE has been used extensively in research (Lundstedt *et al.,* 1998). The purpose is to systematically analyse how the response of a system changes when parameters of that system are changed. However some understanding of the limitations of the system prior to investigating large design spaces is important in preventing a waste of resources for minimal gain.

To prevent two phase formation between PEG and salts, the total salt concentration in the system was limited to 0.6 M. Further input ranges were limited to using PEG 12000, pH 7.4 and homogenate dilution factor of one, as it was found that the precipitation system was robust in a wide range of PEG molecular weights and pH. The dilution of the feed material is undesirable as it results in large processing volume at process scale. Thus, the investigations of multimodal precipitation conditions were studied without any dilution of the process stream. Sodium chloride, an extra salt, was additionally investigated, as incorporating an extra factor in the previous three level full factorial design (section 4.5.1) would have resulted in the number of experiments to become prohibitively large even at microscale. The number of experiments would have been 972 (1944 in duplicate).
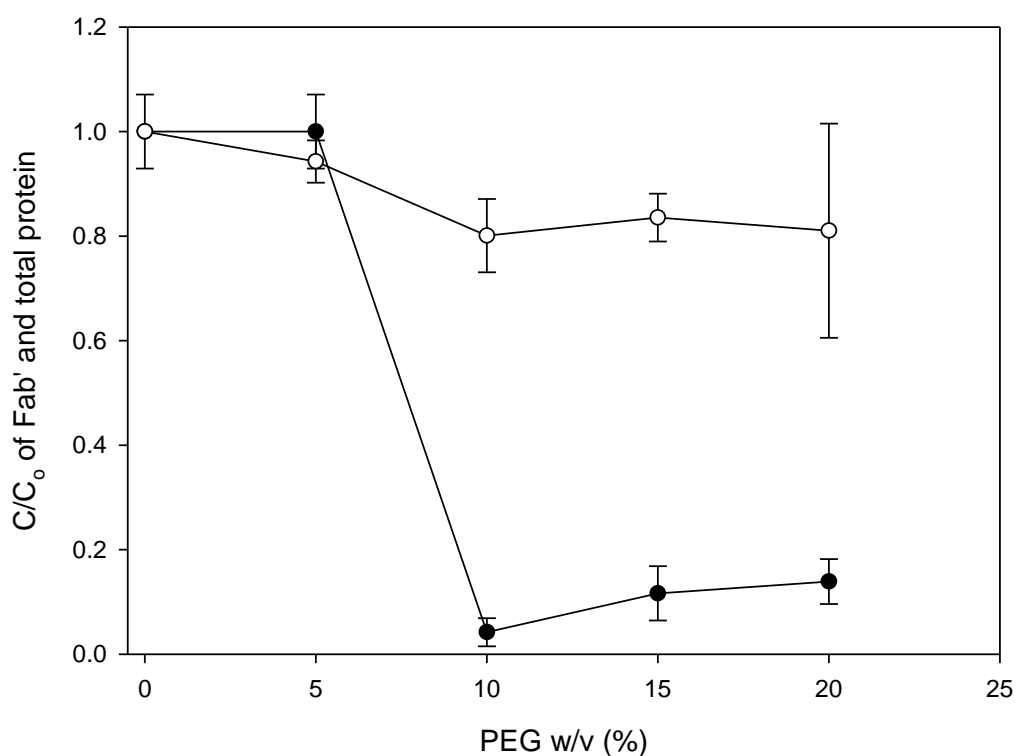
Figure 4.13: *The effect of PEG 12000/0.2 M ammonium sulphate/sodium citrate/sodium chloride pH 7.4 on the solubility of Fab' (●) and total protein (○). Homogenate pH 7.4, PEG (from a stock concentration of 50% w/v pH 7.4), sodium citrate and ammonium sulphate (from a stock concentration of 2.2 M pH 7.4) and 100 mM Tris HCl pH 7.4 were used in this experiment. C_o for Fab' and total protein was 0.9 g L^{-1} and 4.5 g L^{-1} respectively. This experiment was performed in 1.3 mL 96 deepwell plates (Nunc GmbH & Co., KG, Denmark) at 1 mL scale per well using a Tecan (Tecan, Reading, UK) for liquid handling. Samples prepared by the Tecan (Tecan, Reading, UK) were mixed for a total of 60 minutes using the microscale mixing device at 1000 rpm. The plates were centrifuged and then the supernatant was analysed for Fab' and total protein concentration as described in sections 2.1 and 2.2 respectively. Error bars are shown for one standard deviation for triplicate experiment repeats*

Figure 4.14: *The effect of PEG 12000/0.3 M ammonium sulphate/sodium citrate pH 7.4 on the solubility of Fab' (●) and total protein (○). Homogenate pH 7.4, PEG (from a stock concentration of 50% w/v pH 7.4), sodium citrate and ammonium sulphate (from a stock concentration of 2.2 M pH 7.4) and 100 mM Tris HCl pH 7.4 were used in this experiment. C_o for Fab' and total protein was 0.9 g L^{-1} and 4.5 g L^{-1} respectively. This experiment was performed in 1.3 mL 96 deepwell plates (Nunc GmbH & Co., KG, Denmark) at 1 mL scale per well using a Tecan (Tecan, Reading, UK) for liquid handling. Samples prepared by the Tecan (Tecan, Reading, UK) were mixed for a total of 60 minutes using the microscale mixing device at 1000 rpm. The plates were centrifuged and then the supernatant was analysed for Fab' and total protein concentration as described in sections 2.1 and 2.2 respectively. Error bars are shown for one standard deviation for triplicate experiment repeats*

Figures 4.13 and 4.14 show the solubility profiles for Fab' and total protein with PEG 12000/0.2 M ammonium sulphate/sodium citrate/sodium chloride pH 7.4 and PEG 12000/0.3 M ammonium sulphate/sodium citrate pH 7.4 respectively.

Increased solubility termed salting in at low concentrations of salt has been described earlier (Foster *et al.,* 1976). In figures 4.13 and 4.14, additional soluble Fab' was observed between PEG 0% to 5% w/v and low salt concentrations. In addition, in figure 4.14, the amount of Fab' that became soluble was high (10%) to be attributed to the salting in phenomenon alone (Balasundaram *et al.,* 2011). Balasundaram *et al.,* (2011) suggested that positively charged Fab' bound with negatively charged species such as micronised cell debris and chromosomal DNA in the homogenate via electrostatic interactions disassociate in the presence of low salt concentrations increasing Fab' concentration. As PEG concentration increases beyond 10% w/v the electrostatic forces brought about by low concentrations of salt are eventually overcome by the opposing hydrophobic effects of PEG as the system becomes more thermodynamically stable (Lee and Lee 1981).

In figure 4.13, the total protein content dropped by 20% from PEG 0% to 10% w/v, which then appeared to stabilise with increasing PEG concentrations, whilst the Fab' solubility increased by 7% from PEG 10% to 20% w/v. This suggests a combination of electrostatic and hydrophobic interactions between the salts and PEG. The Hofmeister series is a sequence of salts (anion) as described by Melander and Horváth (1977), which describes the relative effectiveness of salting out properties of salts in order of effectiveness in the increasing solvent surface tension to reduce the solubility of proteins (with citrate followed by sulphate followed by chloride). In this case, the behaviour of proteins in the presence of a mixture of salts with PEG is complex and hence the effectiveness of salts in multimodal precipitation with PEG cannot be predicted using Hofmeister series.
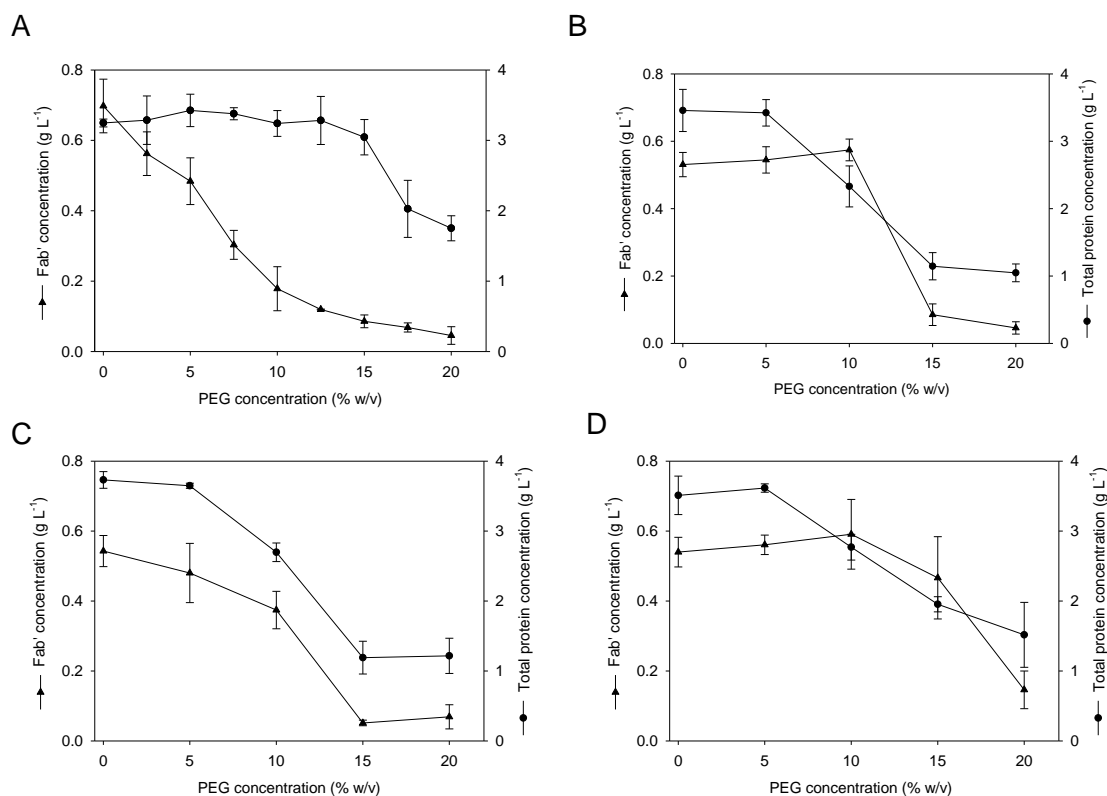
Figure 4.15: *The effect of single/multimodal conditions on the solubility of Fab' (▲) and total protein (●) at pH 7.4, (A) PEG 12000, (B) PEG 12000/0.6 M ammonium sulphate, (C) PEG 12000/0.6 M sodium citrate and (D) PEG 12000/0.6 M sodium chloride. Homogenate pH 7.4, PEG (from a stock concentration of 50% w/v pH 7.4), sodium citrate and ammonium sulphate (from a stock concentration of 2.2 M pH 7.4) and 100 mM Tris HCl pH 7.4 were used in this experiment. C_o for Fab' and total protein was 0.9 g L^{-1} and 4.5 g L^{-1} respectively. This experiment was performed in 1.3 mL 96 deepwell plates (Nunc GmbH & Co., KG, Denmark) at 1 mL scale per well using a Tecan (Tecan, Reading, UK) for liquid handling. Samples prepared by the Tecan (Tecan, Reading, UK) were mixed for a total of 60 minutes using the microscale mixing device at 1000 rpm. The plates were centrifuged and then the supernatant was analysed for Fab' and total protein concentration as described in sections 2.1 and 2.2 respectively. Error bars are shown for one standard deviation for triplicate experiment repeats*

Figure 4.15 shows the effect of multimodal conditions on the resultant solubility profiles of Fab' and total protein. As a comparison figure 4.10 (A) represents a Fab' and total protein solubility profile with PEG 12000 in single mode, (which has been discussed previously in section 3.3.2). An 18% increase in Fab' yield was observed from PEG 10% to 20% w/v. However, an increase of 39% of protein impurities were observed between PEG 15% to 20% w/v.

Figures 4.15 (B) and (D) show the solubility profiles of PEG 12000/0.6 M ammonium and PEG 12000/0.6 M sodium citrate. The phenomenon of increased solubility of salting in at low concentrations of salt is well known (Foster *et al.,* 1976). A salting in effect of Fab' over the PEG range 0% to 10% w/v was observed with ammonium sulphate and sodium chloride in part due to the electrostatic interactions, which appear to be specific to Fab'. Balasundaram *et al.,* (2011) suggested that positively charged Fab' bound with negatively charged species such as micronised cell debris and chromosomal DNA in the homogenate via electrostatic interactions disassociates in the presence of low salt concentrations increasing Fab' concentration. The total protein concentration dropped on average 32% and 46% between PEG range 5% to 10% w/v for ammonium sulphate and sodium chloride respectively. As the concentration of PEG was increased, the hydrophobic interactions overwhelmed the electrostatic interactions, exposing hydrophobic regions of proteins, resulting in increased precipitation. However, sodium chloride appears to have stronger electrostatic interactions than ammonium sulphate at PEG 15% w/v. Fab' solubility in the presence of sodium chloride decreased by 10% relative to 80% with ammonium sulphate. This is predicted by the Hofmeister series as described by Melander and Horváth (1977), who suggested that sulphate is more effective than chloride in increasing the solvent surface tension to reduce the solubility of proteins.

Figure 4.15 (C) shows the effect of sodium citrate on the resultant solubility profiles of Fab' and total protein. At PEG 15% w/v with 0.6 M sodium citrate, there was 8% Fab' remaining in the supernatant, which was the minimum solubility of Fab' for all the conditions studied. This is supported by the Hofmeister series, which suggests that citrate is more effective than sulphate and chloride for precipitating proteins (Melander and Horváth 1977). The advantage of this system is that less total protein is precipitated out between the PEG range 5% to 10% w/v relative to the multimodal system with ammonium sulphate (26% relative to 32%), increasing purification

factor. These results are consistent with that reported by Shih *et al.,* (1992) who found that the precipitation of lysozyme was improved with sulphate relative to chloride, consistent with the Hofmeister series.

4.5.2 Central Composite Face Centred DoE for the Study of Fab' and Protein Impurity Precipitation Using PEG, Ammonium Sulphate, Sodium Citrate and Sodium Chloride

Compared to the traditional one-factor-at-a-time method, DoE drastically reduces the number of runs required to determine the desirable settings. In terms of QbD, regulators want assurance that all unit operations meet specification. Then the objective is to define a processing window that provides a high level of confidence to meet specifications (for example ≥ 95% confidence). A design space, based on QbD principles, can be used to map out a region where the product can be reliably manufactured. This gives boundaries by buffering them with tolerance intervals allowing for the inevitable process drift from changing raw materials and other sources of natural variability.

A DoE was designed to study multimodal precipitation of Fab' and protein impurities, whilst reducing those variables that would not have a significant effect on the system based on previous experimental data described in sections 3.4.2, 3.5.1 and 4.5.1. A screening and optimisation DoE with PEG described in sections 3.4.2 and 3.5.1, found that the precipitation system was robust in a wide range of PEG molecular weights and pH conditions. Therefore, input ranges were reduced to using PEG 12000 and pH 7.4, although it was found and supported by Balasundaram *et al.,* (2011) that a decrease in Fab' solubility was observed by decreasing pH from 7 to 3.5. This may in part be caused by acid precipitation. Dilution factor of feed material of one was used throughout, as the dilution of the feed material was undesirable as it results in a large processing volume at process scale. Thus, the investigations of multimodal precipitation conditions were studied without any dilution of process stream. Whilst it was possible that the optimum conditions defined may change with the addition of salts, the reduction in the amount of experimental runs required justified the holding of these parameters constant. Multimodal operation involved the addition of three salts from varying positions in the Hofmeister series with PEG over a concentration range of 0% to 20% w/v. Salts, ammonium sulphate, sodium citrate and sodium chloride were

added in varying combinations to give a maximum concentration of 0.6 M to prevent two phase formation with PEG, and to maintain a regular design space.

A central composite face centred DoE was designed using MODDE 9.1 (Umetrics, Malmö, Sweden) as it was known that each of the salts have a significant effect on the precipitation of Fab' and protein impurities (Foster *et al.,* 1971, Foster *et al.,* 1976, Melander and Horváth 1977, Shih *et al.,* 1992, Balasundaram *et al.,* 2010 and figure 4.10). A screening study at this point would just show that these variables are significant over the range chosen. In this design the experiments are centred on the face of the cube, which implies that all factors have three levels, instead of two levels in the factorial design. The flexibility of three levels per factor allows support for a quadratic model for response surface modelling (figure 4.16).
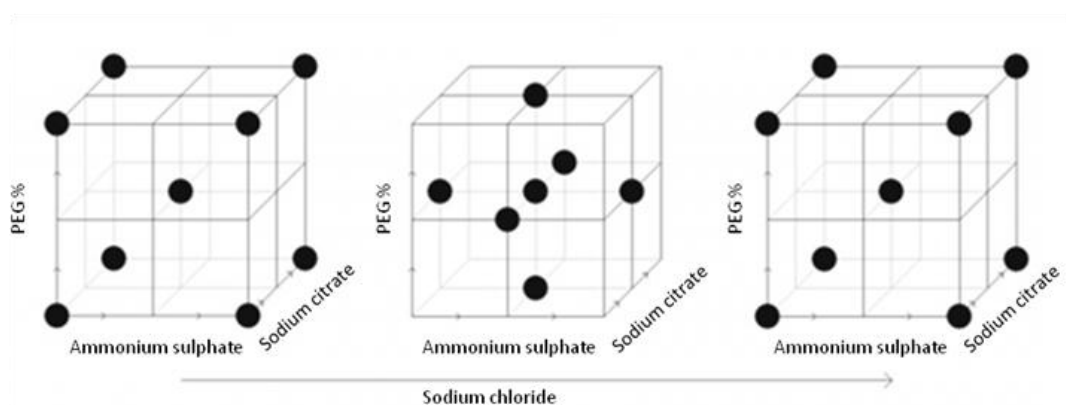
Figure 4.16: *CCF design for investigating Fab' and total protein precipitation using PEG and salts in multimodal mode. Black dots represent experiments in the design space. Ranges were PEG 12000 0% to 20% w/v, ammonium sulphate, sodium citrate and sodium chloride 0 to 0.6 M at pH 7.4, and a homogenate dilution factor of 1*

To prevent the formation of two phases with PEG and salts, the maximum concentration of salts at PEG ≥ 5% w/v was 0.6 M. Salt concentrations in table 4.4, experiment number 15-16 were modified to maintain a maximum of 0.6 M salt concentration in the system. Although experiment number 15 did not require the salt concentration to be altered, this was done to retain comparability with experiment 16. PEG concentrations ranging from 0% w/v to 20% w/v were investigated due to the non linearity of the precipitation system. The solubility of both total protein and Fab' varies considerably in this range and failure to account for this would result in

167

an inaccurate model for the system. The experimental design was repeated in duplicate for robustness.

The Tecan (Tecan, Reading, UK) was preprogramed to carry out all liquid handling. PEG 12000 was made at a stock concentration of 50% w/v in 100 mM Tris HCl pH 7.4. Stock solutions of each of the salts were made up to a maximum molarity of 2.2 M at pH 7.4. 1 mL total working volume was used in 1.3 mL 96 deepwell plates (Nunc GmbH & Co., KG, Denmark), of this 1 mL, depending on conditions needed, 670 μL or reaction volume was split between a combination of PEG, salts and buffer for multimodal operation and the remaining 330 μL was *E.coli* Fab' homogenate, which was added last. Following addition, the plate was mixed for 60 minutes with the microscale mixing device at 1000 rpm, followed by centrifugation at 4000 rpm for 25 minutes using a Eppendorf 5810R centrifuge (Eppendorf UK Ltd., Cambridge, UK). The supernatant was then carefully removed by the Tecan (Tecan, Reading, UK) and assayed for Fab' and total protein concentration as described in sections 2.1 and 2.2. The precipitated pellets dissolved readily with 1 mL 100 mM Tris HCl pH 7.4.

Experiment number	PEG concentration (% w/v)	Ammonium sulphate [M]	Sodium citrate [M]	Sodium chloride [M]
1	0	0.00	0.00	0.00
2	20	0.00	0.00	0.00
3	0	0.60	0.00	0.00
4	20	0.60	0.00	0.00
5	0	0.00	0.60	0.00
6	20	0.00	0.60	0.00
7	0	0.30	0.30	0.00
8	20	0.30	0.30	0.00
9	0	0.00	0.00	0.60
10	20	0.00	0.00	0.60
11	0	0.30	0.00	0.30
12	20	0.30	0.00	0.30
13	0	0.00	0.30	0.30
14	20	0.00	0.30	0.30
15	0	0.20	0.20	0.20
16	20	0.20	0.20	0.20
17	0	0.15	0.15	0.15
18	20	0.15	0.15	0.15
19	10	0.00	0.15	0.15
20	10	0.30	0.15	0.15
21	10	0.15	0.00	0.15
22	10	0.15	0.30	0.15
23	10	0.15	0.15	0.00
24	10	0.15	0.15	0.30
25	10	0.15	0.15	0.15
26	10	0.15	0.15	0.15

Table 4.5: *Table listing the statistically designed experiments (CCF DoE) for multimodal precipitation using ammonium sulphate, sodium citrate and sodium chloride and PEG 12000 at pH 7.4. The experiment numbers 15 and 16 were modified to the salt concentration of 0.6 M to prevent aqueous two phase formation with PEG. Homogenate pH 7.4, PEG (from a stock concentration of 50% w/v pH 7.4), sodium citrate and ammonium sulphate (from a stock concentration of 2.2 M pH 7.4) and 100 mM Tris HCl pH 7.4 were prepared for this experiment. C_o for Fab' and total protein was 0.9 g L^{-1} and 4.5 g L^{-1} respectively. This experiment was performed in 1.3 mL 96 deepwell plates (Nunc GmbH & Co., KG, Denmark) at 1 mL scale per well using a Tecan (Tecan, Reading, UK) for liquid handling. Samples prepared by the Tecan (Tecan, Reading, UK) were mixed for a total of 60 minutes using the microscale mixing device at 1000 rpm. The plates were centrifuged and then the supernatant was analysed for Fab' and total protein concentration as described in sections 2.1 and 2.2 respectively*

4.5.2.1 Ionic Strength of Salt

The ionic strength of a solution is a measure of the concentration of ions in that solution. The total ionic concentration of the salts will affect the solubility of Fab' and protein impurities.

The ionic strength, *I*, of a solution is a function of the concentration of all the ions present in solution (equation 4.1).

$$I = \tfrac{1}{2} \sum_{i=1}^{n} c_i z_i^2$$

(4.1)

Equation 4.1: *Ionic strength in moles, where c_i is the molarity of ion [M], z_i is the charge number of that ion, and the sum is taken of all salt ions in the solution (Balasundaram et al., 2011)*

The ionic strength was calculated for the three salts as per the CCF DoE inputs shown in table 4.6

Ammonium sulphate concentration [M]	Sodium citrate concentration [M]	Sodium chloride concentration [M]	Ammonium sulphate ions	Sodium citrate ions	Sodium chloride ions	Total ions
0.00	0.00	0.00	0.00	0.00	0.00	0.00
0.00	0.00	0.60	0.00	0.00	0.60	0.60
0.15	0.15	0.30	0.40	0.90	0.30	1.60
0.60	0.00	0.00	1.80	0.00	0.00	1.80
0.30	0.00	0.30	1.50	0.00	0.30	1.80
0.20	0.20	0.20	0.60	1.20	0.20	2.00
0.00	0.30	0.30	0.00	1.80	0.30	2.10
0.15	0.30	0.15	0.40	1.80	0.15	2.40
0.30	0.15	0.15	1.50	0.90	0.15	2.50
0.30	0.30	0.00	1.50	1.80	0.00	3.30
0.00	0.60	0.00	0.00	3.60	0.00	3.60

Table 4.6: *Ionic strength of ammonium sulphate, sodium citrate and sodium chloride calculated from the CCF DoE inputs*

The precipitation data was shown as a function of ionic strength of salts calculated using equation 4.1. Figure 4.17 shows the solubility profiles of Fab' and total protein using PEG 12000 at pH 7.4 between 0% and 15% w/v PEG concentration. The solubility profile of Fab' at PEG 0% w/v (figure 4.17 A) shows the solubility of Fab' in the supernatant dropping to 65% on average at 3.6 [M], and the total protein appears to be significantly affected by increasing ionic strength, with solubility dropping to 48% on average at 3.6 [M].

Figure 4.17 (B) shows the effect of increasing ionic strength of salt in PEG 5% w/v. The addition of PEG 5% w/v at zero salt causes the initial precipitation of Fab', resulting in 20% yield. It was observed that on average 70% of Fab' remained in solution at 3.6 [M], and there was on average 42% total protein remaining at 3.6 [M]. It was suggested that the addition of salt stabilises the precipitation of Fab', leading to a possible alternative flowthrough process (figure 4.26). Interestingly, at 1.6 [M] there was 70% Fab' and 43% total protein remaining in solution on average suggesting that there were synergistic effects of ammonium sulphate, sodium citrate and sodium chloride on the precipitation of Fab'. This behaviour appears to be specific for Fab' and not for protein impurities in the range investigated.

However, with increasing concentration of PEG at 10% and 15% (figures 4.17 C and D) the performance of multimodal operation was significantly altered. The maximum Fab' yield observed at PEG 10% and 15% w/v was 79% and 90% with 60% and 65% total protein being precipitated respectively. The addition of salts at low ionic strength appeared to resolubilise the proteins at PEG concentrations higher than 10% w/v. It was suggested that at lower ionic strength (0.5-1.6 [M]), which was the addition of ammonium sulphate and ammonium sulphate combined with sodium chloride with a maximum concentration of 0.6 M, the salt prevents the PEG from precipitating the Fab' and other proteins. However, as the ionic strength increased beyond 2 [M], which includes the presence of sodium citrate, a more traditional solubility curve was observed, where the Fab' and total protein are significantly precipitated. Increasing the ionic strength of the solution reduces the amount of water molecules available for any protein thus reducing the solubility indirectly, which is also reported by Melander and Horváth (1977) and Arakawa and Timasheff (1982). The addition of sodium citrate is the most significant salt when working with PEG in multimodal mode at higher concentrations of PEG to precipitant Fab' and other proteins. In the case of dual salt precipitations, this effect is augmented by the electrostatic interaction of citrate ion which has been shown to

have a binding site on Fab' that could potentially displace water molecules from the Fab' directly, helping to reduce the solubility further (Harinarayan *et al.,* 2008).

Further addition of ammonium sulphate or sodium citrate beyond these concentrations was limited by the solubility of the salts (since concentrated stock solutions were used for precipitation). Higher concentrations of ammonium sulphate or sodium citrate could only be achieved by adding the salt in solid form. Addition of salt in the solid form at process scale is undesirable due to the potential localised super saturation effects during the precipitation reaction (Balasundaram *et al.,* 2011).

Previous studies (Foster *et al.,* 1971) have described the importance of mixing in protein precipitation at large scale. A steep solubility curve similar to that obtained in figure 4.17 (C) is desirable at large scale since the over precipitation and micro mixing effect due to rate of addition of precipitant can be avoided. Therefore, in a large scale precipitation process where mixing has a significant impact, the conditions in figure 4.17 (C) at 10% w/v PEG 12000 and 2 [M] can be expected to be perform better than at PEG 0% w/v (figure 4.17 A), and that 90% of the product can be recovered using this approach. This is supported by findings by Balasundaram *et al.,* (2011) who reported 90% precipitation of Fab' at equivalent ionic strength in dual salt precipitation with ammonium sulphate and sodium citrate.
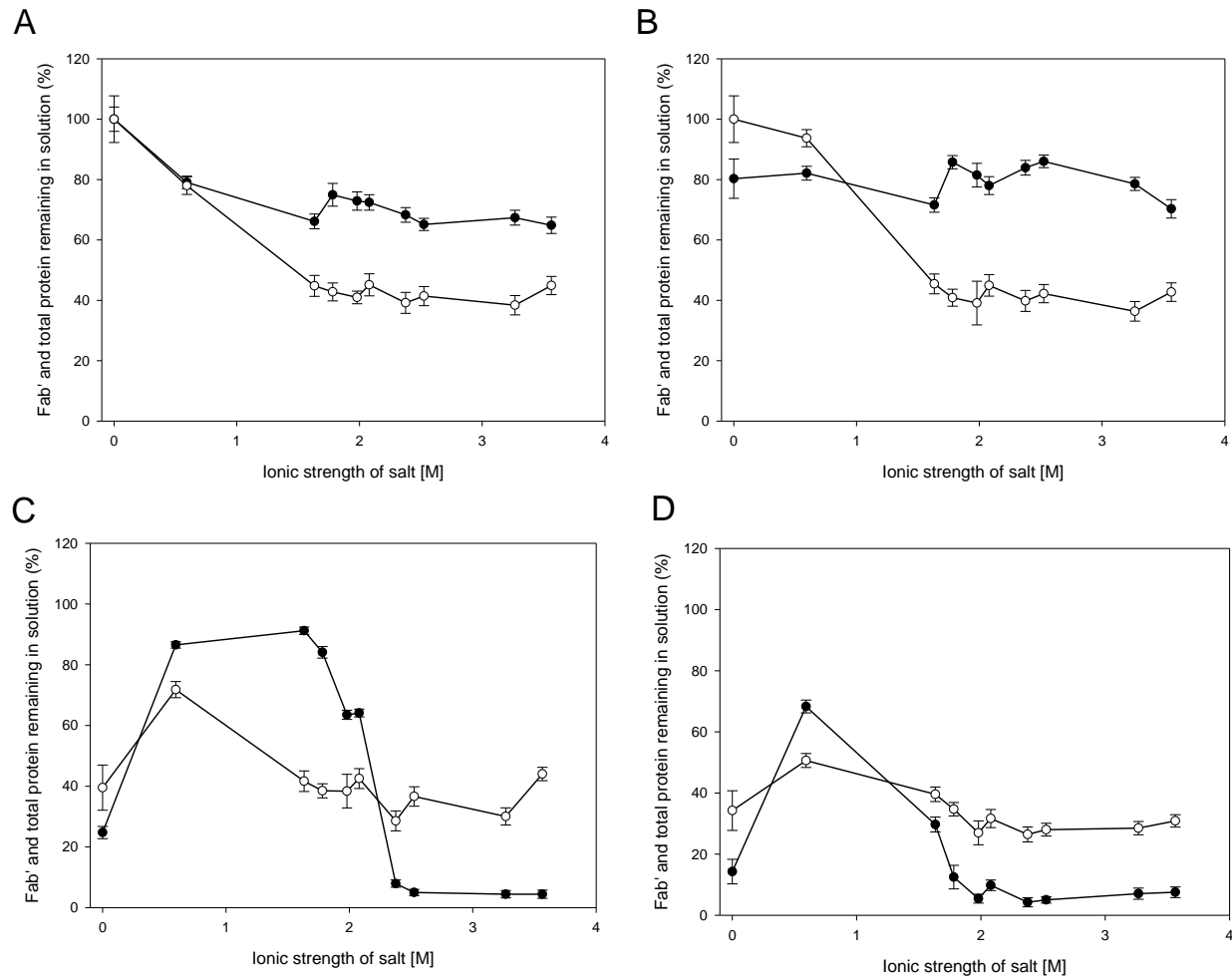
Figure 4.17: *The effect of increasing salt ionic strength on the solubility of Fab' (▲) and total protein (■) with PEG 12000 0% (A) 5% (B) 10% (C) and 15% (D) w/v at pH 7.4. Ionic strength of salt [M] was calculated for ammonium sulphate, sodium citrate and sodium chloride as listed in table 4.6. Average data is shown from duplicate experiment repeats*

Following the DoE, results were analysed to the two main responses of yield and purification factor as described in section 3.4.1. It was hypothesised that while maintaining the parameters previously examined in the Fab' precipitation study using PEG (chapter 3), all factors in the present study would be significant. This was a reasonable assumption based on previous experimental data.

In section 4.6.1, the initial screening with multimodal conditions suggested that the highest Fab' yields were obtainable in the PEG range between 15% to 20% w/v. However, it had been observed that electrostatic interactions at low salt concentrations resulted in protein impurities being precipitated in favour of Fab'. Therefore, there were two possible windows of operation, the first maximising Fab' yield by maximising conditions to favour hydrophobic interactions and the second by minimising Fab' loss by maximising conditions to favour electrostatic interactions. MODDE 9.1 (Umetrics, Malmö, Sweden) was used to evaluate multiple variables and response factors simultaneously and was useful for the understanding of the process limits and how design parameters affect process behaviour to decide, which type of precipitation system would be better to operate at full scale.
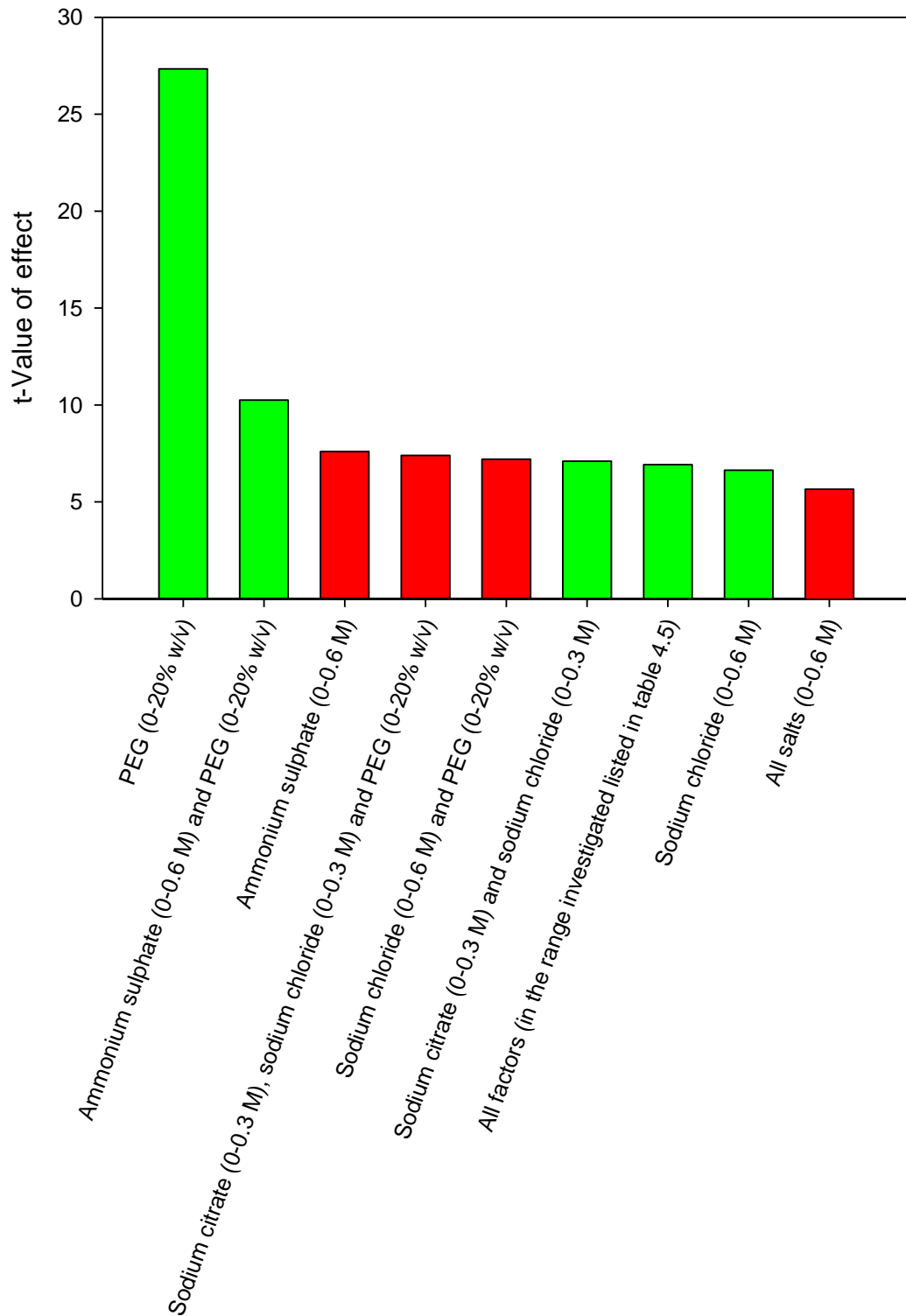
Figure 4.18: *Bar chart ranking the significant process parameters from high to low in terms of significance on Fab' yield. Green and red bars have a positive and negative effect on yield respectively. Effects are significant in the range investigated which are above the t-Value limit of 2.36 and $p < 0.05$ confidence level. Effects below these limits are not shown*

There were a number of parameters, which were significant to Fab' yield. Figure 4.18 shows the t-Values for each of the parameters that have either a positive or negative effect on Fab' yield, which are above the t-Value limit of 2.36 and $p < 0.05$ confidence level.

Figure 4.18 showed that PEG concentration was the most positive factor in the determination of yield in the range investigated, which may in part be due the increased exclusion volume effect, as concentration of PEG is increased. This agreed with experiments performed by Knevelman *et al.,* (2010). The combination of ammonium sulphate and PEG had a positive effect on yield in part due to the electrostatic interactions at low ammonium sulphate concentrations that are overcome by the opposing hydrophobic effects of PEG as the system becomes more thermodynamically stable (Lee and Lee 1981).

Ammonium sulphate on its own and a combination of salts and PEG had a negative influence on Fab' yield, which is supported by previous data described in this chapter. Singanoglu and Abdulnar (1965) have suggested that the free energy of cavity formation reflected in the surface tension of solvent has a key role in the stability of proteins. The addition of low concentrations of salts increase solvent surface tension increasing the stability of Fab', as the thermodynamic effect is favourable at low salt concentrations. Further positive effects were observed with the combination of sodium citrate and sodium chloride, which suggests that there are synergistic effects for the precipitation of Fab'. Sodium citrate in single mode did not precipitate Fab' efficiently (section 4.5.1) indicating that hydrophobic effects by increasing sodium citrate concentration are not sufficient to precipitate Fab' to obtain high yields. However, combining sodium citrate and sodium chloride makes this factor significant. Interestingly, all three salts in combination had a negative influence on yield.
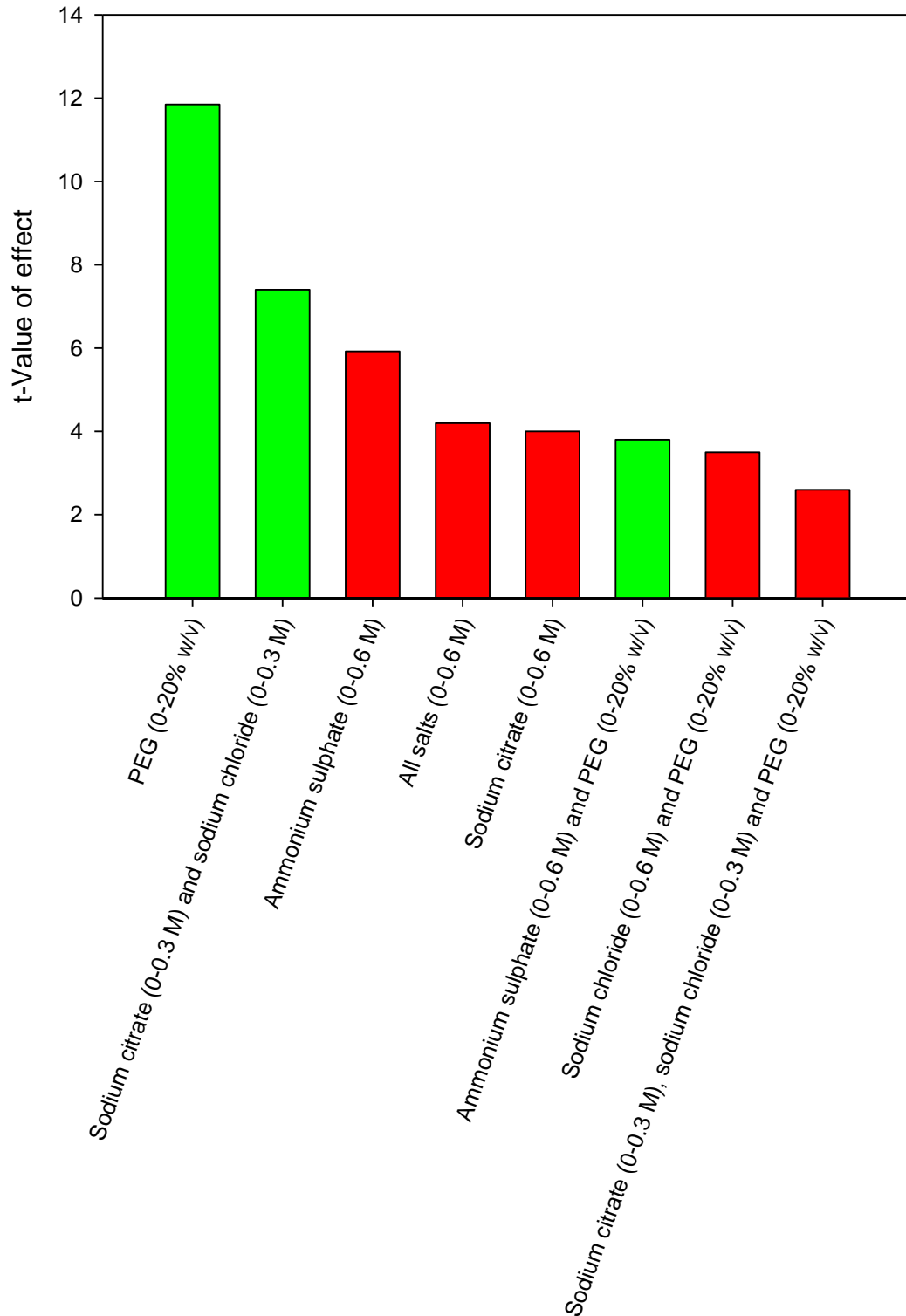
Figure 4.19: *Bar chart ranking the significant process parameters from high to low in terms of significance on purification factor. Green and red bars have a positive and negative effect on yield respectively. Effects are significant in the range investigated which are above the t-Value limit of 2.30 and p < 0.05 confidence level. Effects below these limits are not shown*

Figure 4.19 shows that PEG concentration (% w/v) had the strongest effect on purification factor in the range investigated. Sodium citrate with sodium chloride, ammonium sulphate with PEG had a positive effect on purification factor respectively. However, all combined salts have a negative influence on purification factor in the range investigated. It wassuggested that high concentrations of salts and high concentrations of salts with PEG, limit purification factor in part due to the reduced selectivity of precipitation by hydrophobic interactions.

A summary of the factors affecting Fab' yield and purification factor is shown in table 4.7.

Favourable yield	Favourable purification factor
PEG concentration (% w/v)	PEG concentration (% w/v)
Interaction Effects	**Interaction Effects**
Ammonium sulphate [M] and PEG concentration (% w/v)	Ammonium sulphate [M] and PEG concentration (% w/v)
Sodium citrate and sodium chloride [M]	Sodium citrate and sodium chloride [M]
All factors	
Sodium chloride [M]	

Table 4.7: *Summary of factors that had a positive effect on Fab' yield and purification factor in the range investigated*

Figures 4.20 and 4.21 show the response surface plots all of the variables investigated in the CCF DoE for Fab' yield and purification factor respectively. These plots were created using MODDE 9.1 (Umetrics, Malmö, Sweden). An increase in yield and purification factor was observed with increasing PEG and sodium citrate concentration. Interestingly, yield and purification factor increased with increasing ammonium sulphate concentration till approximately 0.15 M. Further increase in ammonium sulphate concentration reduced both yield and purification factor in the ranges investigated. Sodium chloride somewhat decreased both yield and purification factor when combined with ammonium sulphate and sodium citrate, which can be better observed in figures 4.22 and 4.23.

In terms of window of operation, this leads to a complex design task in which many variables must be considered simultaneously to select suitable values as to obtain a

desired level of performance. For example, one can operate at PEG 12000 15% w/v with 0.3 M sodium citrate and 0.15 M ammonium sulphate whilst giving a yield > 90% with a purification factor of approximately 1.9. However, to favour electrostatic interactions, low sodium citrate and PEG concentrations can be used to precipitate protein impurities in favour of Fab' (figures 4.24 and 4.25). This behaviour appears to be specific for Fab' and not for protein impurities. Arakawa and Timasheff (1982) suggested that the anion is responsible for the thermodynamic stability of proteins possibly by the binding of salts in the protein domain. The increased net charge of the protein due to binding of these ions results in the increase of electrostatic repulsive forces of the protein. These electrostatic forces prevent protein aggregation increasing the solubility of proteins in aqueous solutions of salts, which is in agreement with known salting in properties of salts (Arakawa and Timasheff 1985).

This data supports the Hofmeister series, which predicts that citrate followed by sulphate and chloride would require increasing concentrations of salt to precipitate proteins, in this case Fab'. It may be the case where this positive effect of increased hydration potential of Fab' allows PEG greater access to draw water and induce precipitation of protein impurities. Mahadevan and Hall (1990) have suggested that the distribution of the PEG polymer causes a "pressure imbalance" that pushes the proteins against each other. The positive chemical potentials of the proteins on addition of PEG indicate that the predominant interactions between PEG and proteins in aqueous medium are repulsive in nature and that this repulsion becomes stronger with an increase in PEG size and concentration. Furthermore, at higher concentrations of PEG ≥ 15% w/v, PEG concentration is sufficiently high to become the driving force of the process. Lee and Lee (1981) suggested that the system always provides a driving force to a more thermodynamically favourable state and that the magnitude of this driving force was found to increase with increasing concentration of the polymer.
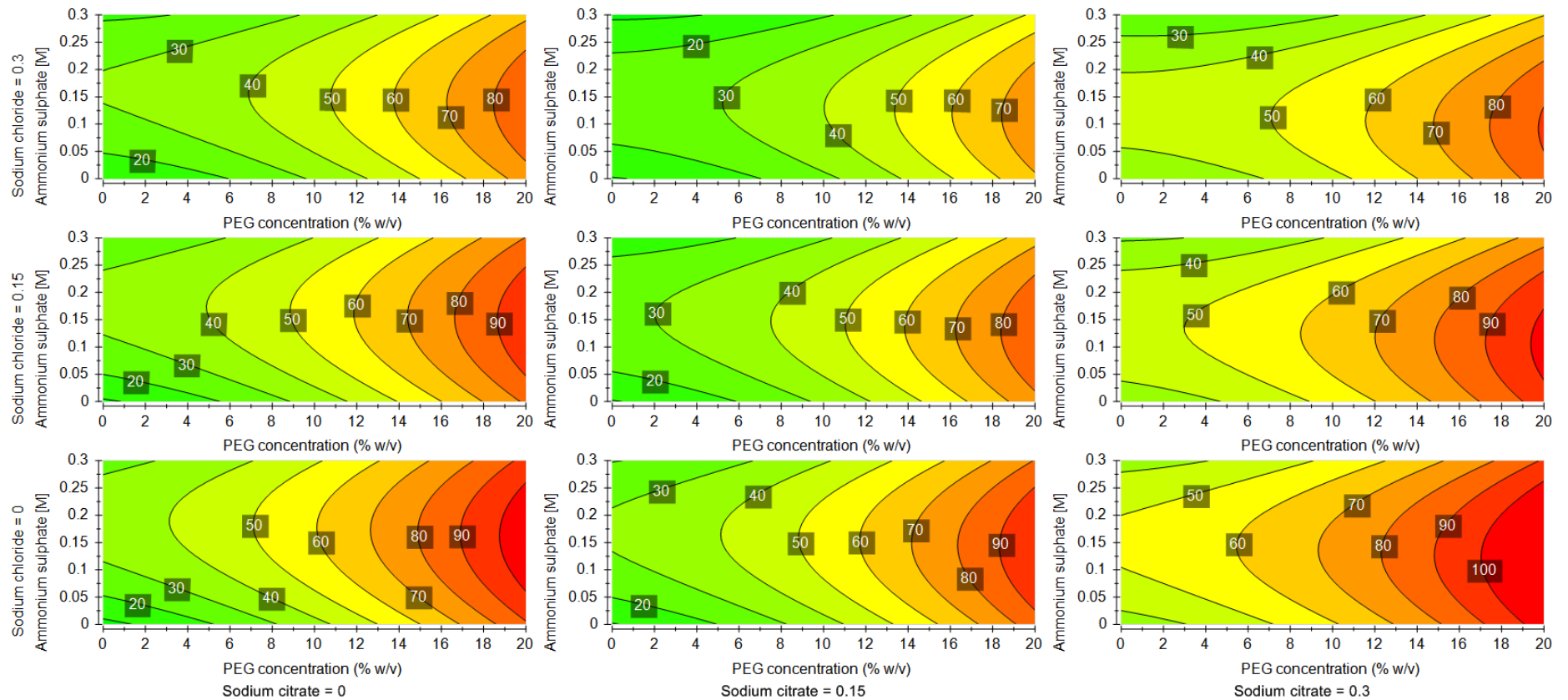
Figure 4.20: *4D contour plots showing the yield of Fab' as a function of ammonium sulphate concentration [M] and PEG 12000 concentration (% w/v) at varying sodium chloride concentrations [M] and sodium citrate concentrations [M] (at pH 7.4). The response surfaces for yield were fit with a quadratic model. All data fitting was performed using the software package MODDE 9.1 (Umetrics, Malmö, Sweden)*
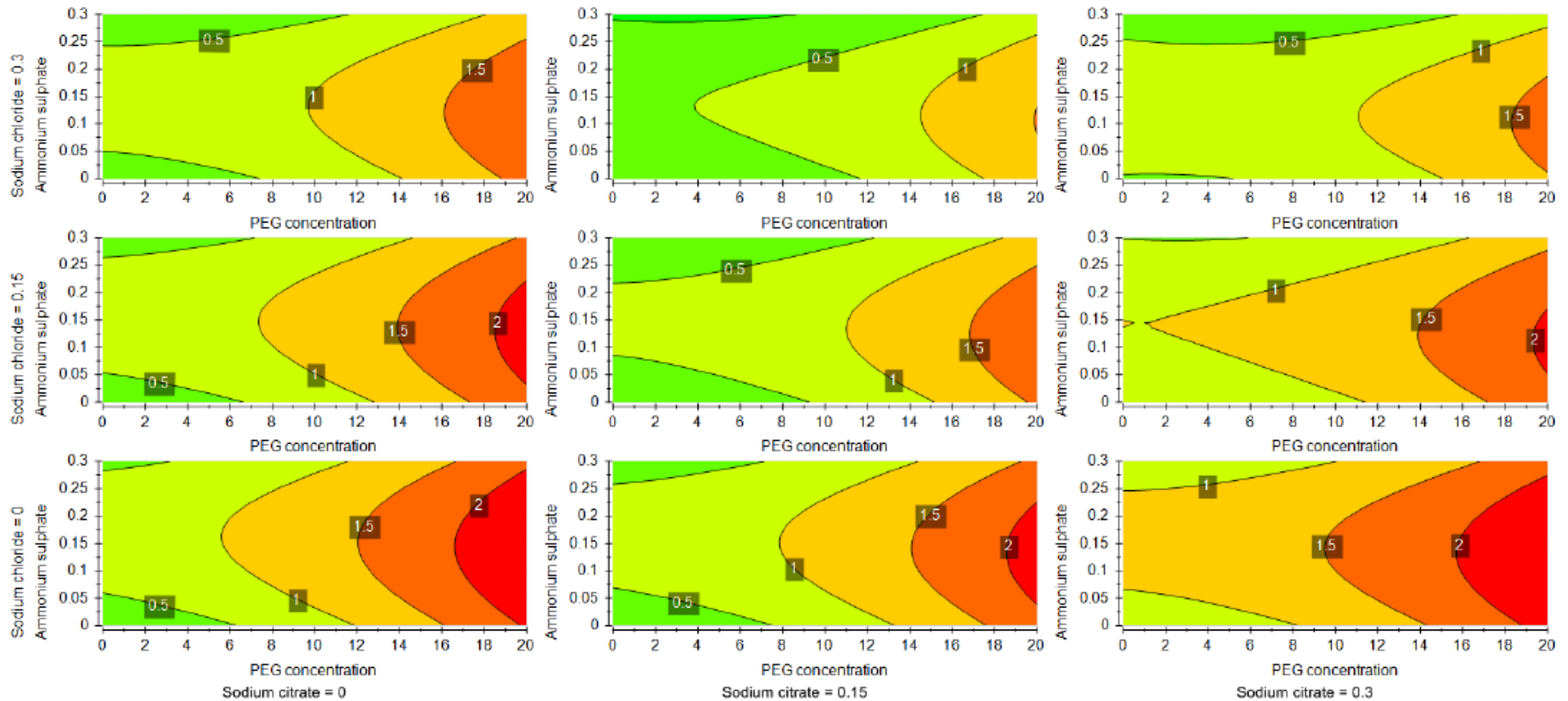
Figure 4.21: *4D contour plots showing the purification factor of Fab' as a function of ammonium sulphate concentration [M] and PEG 12000 concentration (% w/v) at varying sodium chloride concentrations [M] and sodium citrate concentrations [M] (at pH 7.4). The response surfaces for purification factor were fit with a quadratic model. All data fitting was performed using the software package MODDE 9.1 (Umetrics, Malmö, Sweden)*

ANOVA analysis suggested that the model had no lack of fit as the p-value was > 0.05 (p-value was 0.21), with an Q^2 value of 0.83. Therefore, this model can be used to find a sweet spot in the experimental design space, in which the combination and interactions of the process inputs reliably deliver a product with the desired quality. In terms of QbD, this sweet spot is the design space of the process (figures 4.22-4.24).

Figure 4.22 is a 4D plot created in MODDE 9.1 (Umetrics, Malmö, Sweden), to show the operational design space, created by superimposition of the yield and purification factor response contour plots (figures 4.20 and 4.21) to achieve a Fab' yield ≥ 70% with a maximum purification factor of 2.3 in the range of conditions investigated. The resulting window of operation increased with increasing sodium citrate and ammonium sulphate concentrations, (the reasons for which have been discussed in section 4.5.1). For example, these criteria are met with 0.3 M sodium citrate and 0.15 M ammonium sulphate with PEG ≥ 10% w/v. However, with increasing sodium chloride concentration in the system, the window of operation to achieve this becomes smaller. For example, to achieve this criteria, with 0.3 M sodium citrate, 0.15 M ammonium sulphate concentrations and 0.3 M sodium chloride, greater than PEG 15% w/v is required.

Figure 4.23 is a 4D plot, created by the superimposition of the yield and purification factor contour plots to achieve a Fab' yield ≥ 90% with a maximum purification factor of 2.3 in the range of conditions investigated (≥ 90% Fab' yield was selected as acceptable in section 3.4.1 for PEG). The addition of sodium chloride reduced this window of operation significantly, and as a result higher concentrations of PEG are required to achieve ≥ 90% Fab' yield. 90% Fab' yield with a purification factor of 1.9 was achievable using PEG 12000 15% w/v/0.30 M sodium citrate/0.15 M ammonium sulphate pH 7.4. The model predicted a Fab' yield of 93% and purification factor of 1.9, which was in good agreement with the experimental data. The resulting purification factor was an improvement of 26% relative to the use of 15% w/v PEG 12000 pH 7.4 in single mode.
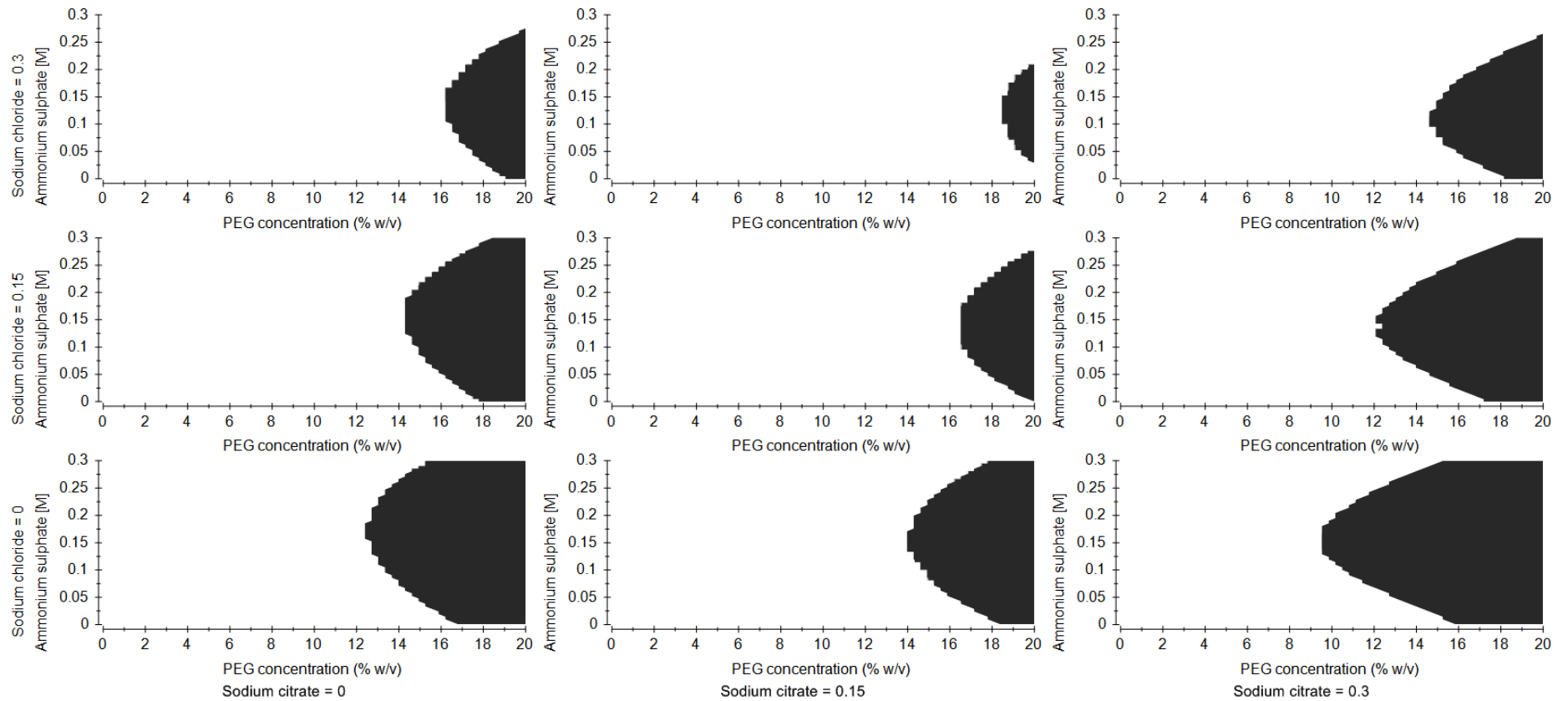
Figure 4.22: *Fab' precipitation design space comprised of the overlap region for yield (%) and purification factor created using MODDE 9.1 (Umetrics, Malmö, Sweden). Working within this design space delivers a Fab' yield ≥ 70% with a maximum purification factor of 2.3 in the range of variables investigated. Ammonium sulphate, sodium chloride and sodium citrate values are shown as molar concentrations*
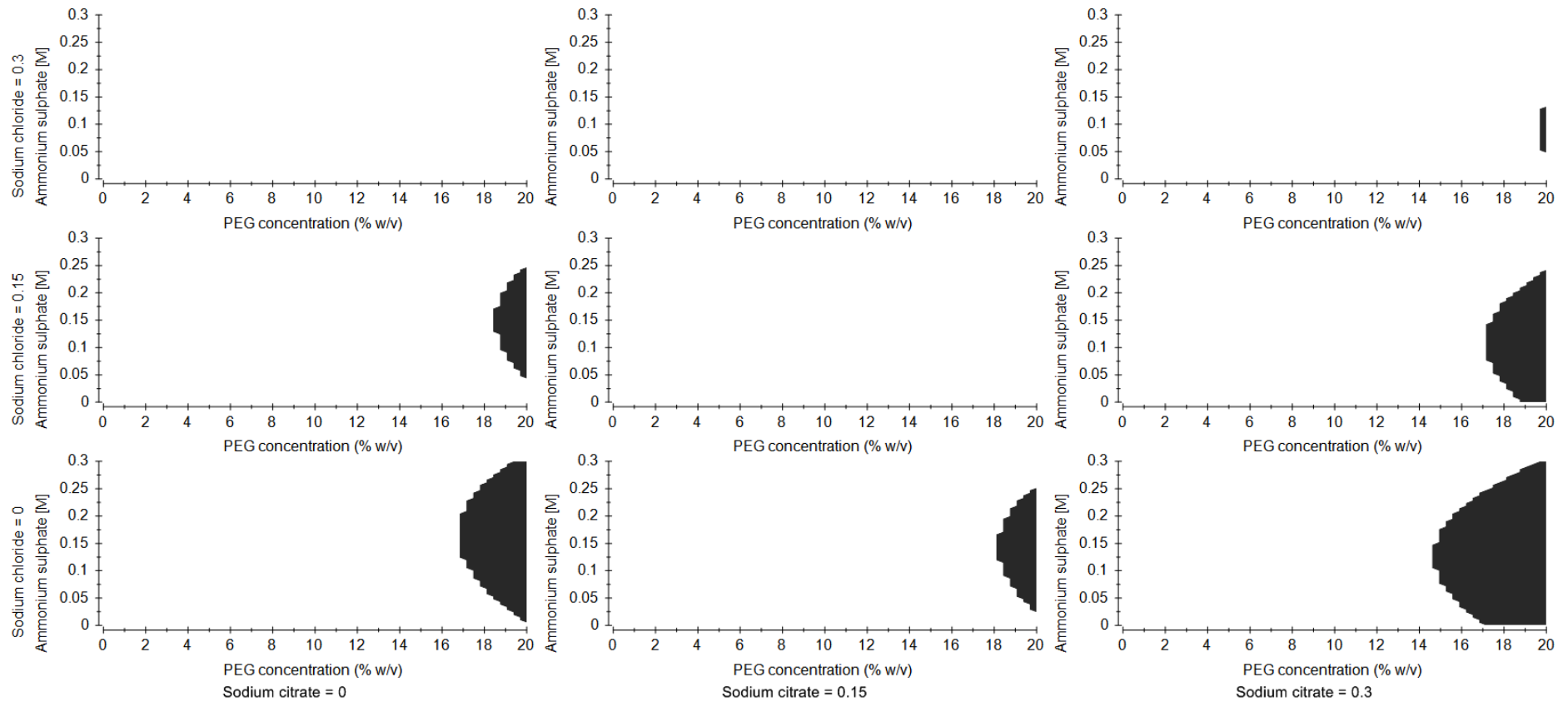
Figure 4.23: *Fab' precipitation design space comprised of the overlap region for yield (%) and purification factor created using MODDE 9.1 (Umetrics, Malmö, Sweden). Working within this design space delivers a Fab' yield ≥ 90% with a maximum purification factor of 2.3 in the range of variables investigated. Ammonium sulphate, sodium chloride and sodium citrate values are shown as molar concentrations*

Similar Fab' yield performance was observed with PEG as the precipitant (section 3.5.1). The addition of low concentrations of ammonium sulphate and sodium citrate increased purification factor by 26% relative to PEG, without significantly increasing the cost and viscosity of the precipitant. However, observations made during this study at low concentrations sodium citrate and PEG (ammonium sulphate and PEG have a similar effect albeit at high PEG concentrations) suggested that there are electrostatic interactions of citrate ions with Fab' resulting in precipitation of some protein impurities in favour of Fab'. This phenomenon appears to be specific to Fab' and the presence of PEG may increase the precipitation of protein impurities further. Harinarayan *et al.,* (2008) reported that there was an electrostatic interaction associated with the trivalent citrate ions and Fab at low citrate concentrations, which may in part explain the insignificant change in yield with increasing PEG concentration. For a primary process step it could be more beneficial to operate with this type of approach, where protein impurities are precipitated in favour of Fab', since there is no resolubilisation step and the viscosity of the precipitant is considerably lower. This will enable this primary process step to be integrated into an existing early downstream step with relative ease compared to a step where Fab' is precipitated, which requires high viscosity precipitant and a subsequent resolubilisation step.

Figure 4.24 is a graphical representation of the knowledge space (within the unexplored space), which refers to the region of process understanding defined by the input boundaries of the combination of the full factorial and CCF DoE's with sodium citrate and PEG 12000. The input boundaries were 0 to 1 M sodium citrate, PEG 12000, PEG concentration 0% to 20% w/v, pH 7.4 and homogenate dilution factor of 1. The design space, within this knowledge space, is comprised of the overlap of Fab' yield (%) and purification factor to give a robust region where purification factor was ≥ 0.8 and Fab' loss was ≤ 10%. The normal operating range (NOR) or control space was defined by a combination of PEG and sodium citrate concentration ranges at ± 0.5% w/v and ± 0.05 M respectively. This is highlighted by the dashed area in figure 4.24 within the design space to give a region of assurance of quality, flexibility and robustness at manufacturing scale.
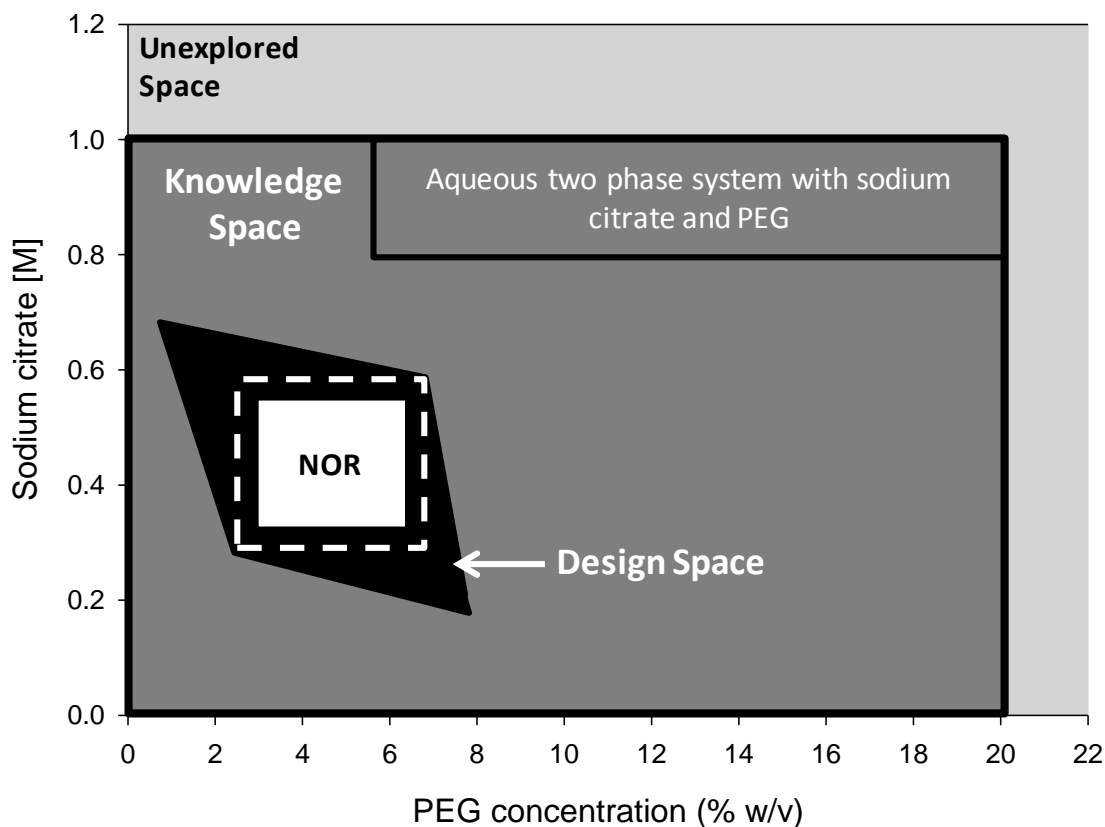
Figure 4.24: *Proposed protein impurity precipitation design space comprised of the overlap region for yield (%) and purification factor created using MODDE 9.1 (Umetrics, Malmö, Sweden). Knowledge space refers to the region of process understanding based on the full factorial and CCF DoE inputs. Inputs were PEG 12000, PEG concentration, sodium citrate concentration, pH 7.4 and homogenate dilution factor of 1. The design space is a region where the combination of ranges that delivers purification factor ≥ 0.8 and Fab' loss ≤ 10%. The Normal Operating Range (NOR) was set to as a minimum of ± PEG 0.5% w/v and ± 0.05 M sodium citrate concentration within the dashed area of the design space*

The robustness of the NOR within the design space was further investigated by combining sodium citrate at 0.4 M with a range of PEG 12000 concentrations (% w/v) at pH 7.4 and homogenate dilution factor of 1. Figure 4.25 shows the resultant Fab' and total protein solubility profiles using PEG 12000 pH 7.4 and PEG 12000/0.4 M sodium citrate pH 7.4 precipitants. At PEG 12000 6.25% w/v/0.4 M sodium citrate pH 7.4 the change in Fab' concentration was invariable. Fab' solubility remained close to 100%, and the concentration of total protein dropped by

~20%. Balasundarum *et al.,* (2011) suggested that millimolar quantities of sodium citrate may be sufficient in multimodal mode to precipitate protein impurities when combined with ammonium sulphate. However, present observations suggest higher concentrations of sodium citrate are required when combined with PEG 12000 in multimodal mode to achieve this. Sodium citrate on its own did not precipitate Fab' efficiently, indicating that the potential additive effect of salting out effects that can be achieved by increasing the concentration of sodium citrate alone is not sufficient to precipitate Fab'. Arakawa and Timasheff (1982) suggested that the anion is responsible for the thermodynamic stability of proteins possibly by the binding of salts in the protein domain. The increased net charge of the protein due to binding of these ions results in the increase of electrostatic repulsive forces of the protein. These electrostatic forces prevent protein aggregation, increasing the solubility of proteins in the aqueous solutions of salts, which is in agreement with known salting in properties of salts (Arakawa and Timasheff 1985). Working within the NOR as shown in figure 4.24, a flow through precipitation strategy with PEG 12000 6.25% w/v/0.4 M sodium citrate pH 7.4 (homogenate dilution factor of one) was used to precipitate ~20% of protein impurities early in the downstream process. The advantage at process scale is the potential ease of processing due to removal of a solubilisation step and the significantly reduced viscosity of the precipitating agent relative to that of PEG.
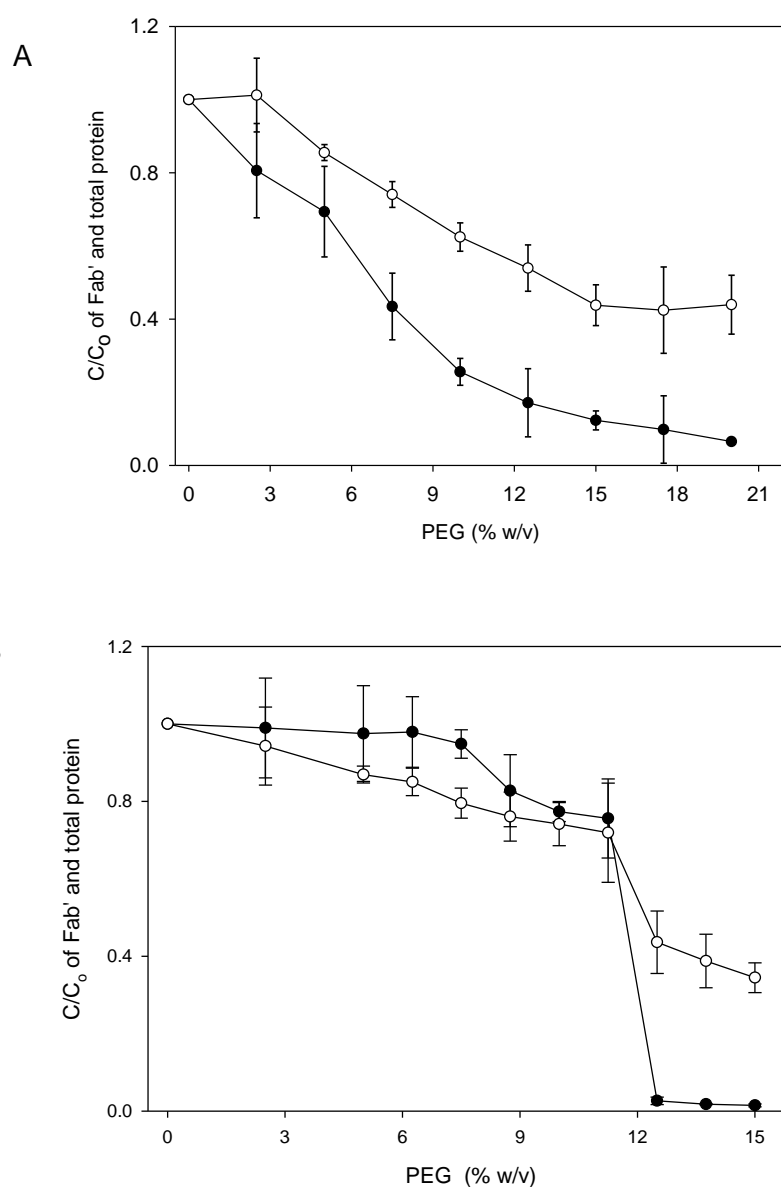
Figure 4.25: *Effect of single/multimodal conditions on the solubility of Fab' (●) and total protein (○), (A) PEG 12000 pH 7.4, (B) PEG 12000/0.4 M of sodium citrate pH 7.4. C_o was 0.9 g L^{-1} and 4.5 g L^{-1} for Fab' and total protein respectively. Homogenate pH 7.4, PEG (from a stock concentration of 50% w/v pH 7.4), sodium citrate (from a stock concentration of 2.2 M pH 7.4) and 100 mM Tris HCl pH 7.4 were used in this experiment. These experiments were performed in 1.3 mL 96 deepwell plates (Nunc GmbH & Co., KG, Denmark) at 1 mL scale per well using a Tecan (Tecan, Reading, UK) for liquid handling. Samples prepared by the Tecan (Tecan, Reading, UK) were mixed for a total of 60 minutes using the microscale mixing device at 1000 rpm. The plates were centrifuged and then the supernatant was analysed for Fab' and total protein concentration as described in sections 2.1 and 2.2 respectively. Error bars are shown for one standard deviation for triplicate experiment repeats*

An alternative strategy for precipitation is proposed for precipitating protein impurities early in the downstream process (figure 4.26). Multimodal precipitation is performed after homogenisation (500 bar for 1 pass) and primary clarification with PEG 12000 6.25% w/v/0.4 M sodium citrate pH 7.4 resulting in ~20% of protein impurities precipitating out, while Fab' remains soluble. The subsequent centrifugation step removes the precipitated impurities. The advantage at process scale is the potential ease of processing due to removal of a solubilisation step and the significantly reduced viscosity of the precipitating agent relative to that of high concentrations of PEG. Further concentrations of PEG could be added to precipitated Fab' if the process requires.
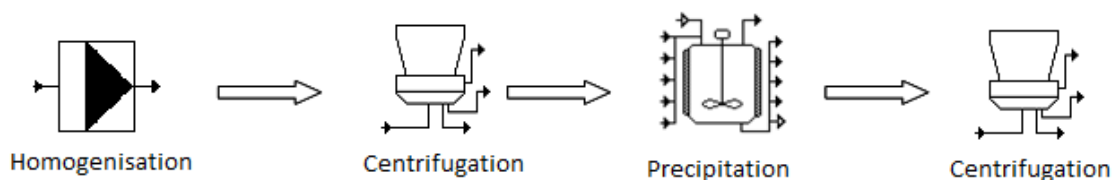
Figure 4.26: *Proposed precipitation strategy in early downstream processing. The combination of PEG 12000 6.25% w/v/0.4 M sodium citrate pH 7.4 could be used as a flow through step whereby protein impurities are selectively precipitated in favour of the Fab'*

4.6 Time and Cost Comparison between Automated Microscale and Laboratory Scale Studies

Microscale methodology increases throughput by approximately 8 fold relative to laboratory scale, dependent on whether or not replicates are performed. This value was calculated assuming that at laboratory scale a full factorial DoE was performed with four factors. Material consumption is therefore reduced by at least an order of magnitude, whilst labour is reduced by at least 50%. The Tecan (Tecan, Reading, UK) LHR can also be run continuously for 24 hours if required. A full 96 deepwell plate (1 mL in each microwell) would require 32 mL of sample and 64 mL of a mixture of buffer, PEG and salt (96 mL total volume). In contrast to run 96 experiments at 6 mL laboratory scale, the total volume required is increased six fold to 600 mL.

The predicted experimental schedules of microscale and 6 mL scale are shown in figure 4.27. The experimental time to complete a full factorial DoE at 6 mL laboratory scale was approximately 10 days based on an estimate to complete DoE studies. However, the time taken to complete triplicate DoE studies at 1 mL scale was approximately 5 days (3 fold the experiments), a saving of approximately 5 days, whilst giving an increase in confidence and robustness of the data by completing replicates. In addition to completing experiments in replicate, larger studies can be undertaken without significantly increasing time and cost. Therefore critical bioprocess information can be obtained earlier in development providing a better opportunity to understand more process parameters. However, it is noted that the bottleneck of completing experiments is shifted to the analysis of samples. However, the total protein assay used in this thesis was automated increasing throughput by ~50% relative to manual analysis.
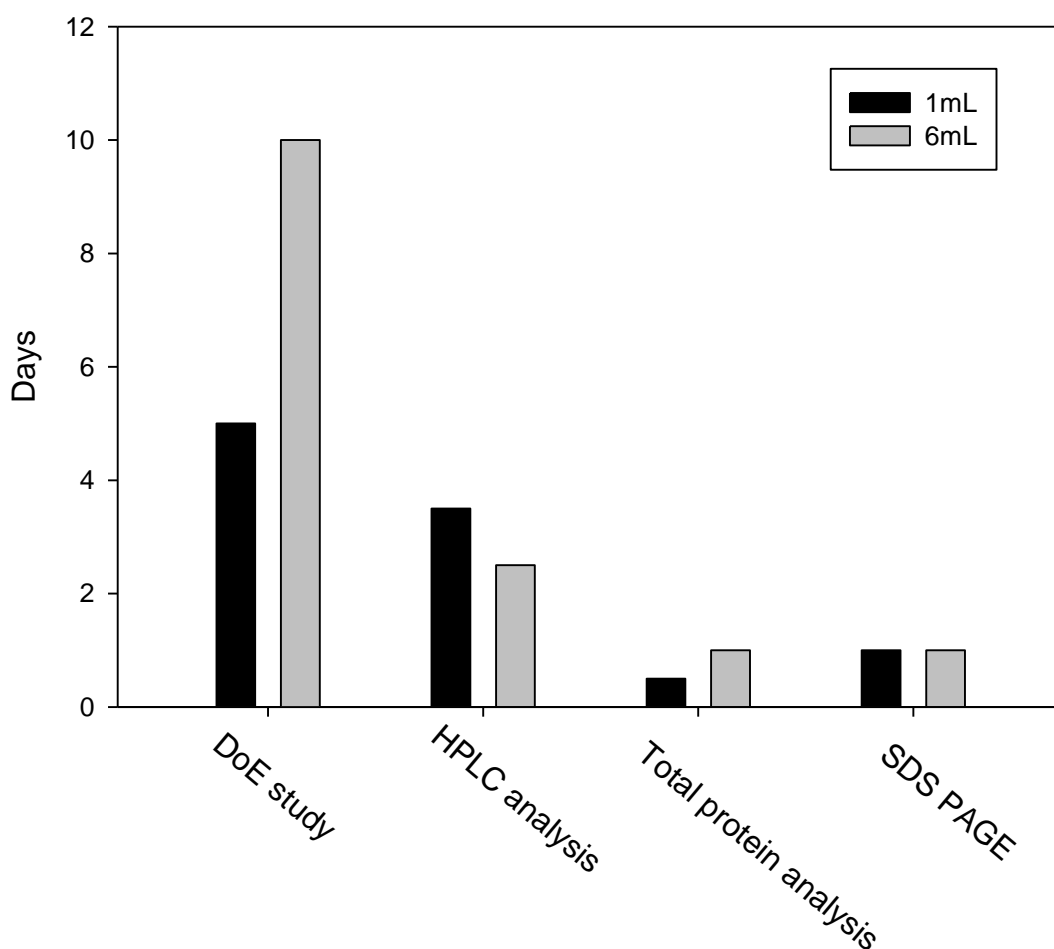
Figure 4.27: *Bar chart showing predicted schedules for automated microscale scale (■) and 6 mL laboratory scale (■) experiments*

Total consumables cost using the automated method was significantly cheaper than the total consumables cost using conventional laboratory scale method due to the use of microwells, which have significantly reduced the amount of consumables needed. The data presented was sufficient to justify the continued use of the newly designed high throughput system for DoE approach evaluation.

Kitchen and Wang (2002) developed a semi automated 96 well protein precipitation method for the determination of montelukast in human plasma using high performance liquid chromatography and fluorescence detection. Using this method, batch sample preparation of over 240 samples was easily accomplished in approximately 3.5 hours compared to approximately 6 to 8 hours with the manual method.

The miniaturisation and automation of this purification step significantly decreases the amount of sample required, successfully reducing the bottleneck, and allows the possibility to scale down other processes such as fermentation and cell disruption steps, enabling whole microscale bioprocess strategies (Wenger 2010).

4.7 Summary

The setup, automation and operation of precipitation on a Tecan Freedom EVO 200 liquid handling robot (Tecan, Reading, UK) combined with using a microscale mixing device increased throughput and speed of liquid handling by 50% relative to the mixing conditions described in section 3.3.3.

A Fab' precipitation study in the form of a response surface methodology DoE (three level full factorial) was performed to investigate a large multimodal precipitation design space based on the Quality by Design principles stated in the ICH guideline Q8 (R2) to improve the performance of single mode precipitation described in chapter 3. Parameters of investigation were PEG concentration (% w/v), PEG molecular weight (MW), pH, dilution of the homogenate, ammonium sulphate concentration and sodium citrate concentration. Salt concentrations ≥ 0.8 M with ≥ 5% w/v PEG resulted in aqueous two phase formation which affected 40% of the design space. This was excluded from analysis as a two phase system was beyond the scope of this project.

A second round of response surface experimentation in the form a CCF DoE with reduced ranges to avoid two phase formation was performed combining optimum operating conditions from the PEG CCF design space (section 3.5.1) for multimodal operation. PEG 12000 in addition to three salts, ammonium sulphate, sodium citrate and sodium chloride chosen from their locations in the Hofmeister series (section 1.4.1) were used for multimodal precipitation. It was found that 90% Fab' yield with a purification factor of 1.9 was achievable with PEG 12000 15% w/v/0.30 M sodium citrate/0.15 M ammonium sulphate pH 7.4. This was an improvement of 26% relative to the use of 15% w/v PEG 12000 pH 7.4 in single mode. However an alternative precipitation strategy to precipitate ~20% of protein impurities whilst Fab' remained soluble in solution using PEG 12000 6.25% w/v/0.4 M sodium citrate pH 7.4 was favoured instead. The advantage of this system at process scale is the potential ease of processing due to removal of a solubilisation step and the significantly reduced viscosity of the precipitating agent relative to that of high concentrations of PEG.

5. INTEGRATION OF PRECIPITATION INTO A DOWNSTREAM PROCESS

5.1 Abstract

A high throughput system utilising robotic handling was developed in microwells to investigate conditions to increase particle size. It was found that d_{50} particle size was 313 μm at low speed mixing conditions (800 rpm) with the addition of homogenate to PEG 12000 6.25% w/v/0.4 M sodium citrate pH 7.4 at 900 μL s^{-1} after 60 minutes of mixing.

A USD system was used to mimic the shear rates found in the feed zone of a disk stack centrifuge in the laboratory. Good agreement of clarification was achieved between laboratory scale and the pilot centrifuge. Laboratory scale efficiency was 93%, whereas the pilot scale separation efficiency was 87%.

A process run through was performed with homogenate pH 7.4 (control), multimodal (PEG 12000 6.25% w/v/0.4 M sodium citrate pH 7.4) and single mode (PEG 12000 15% w/v pH 7.4) feedstreams. The clarification of the three feedstreams was examined after a membrane filtration operation using an automated multiwell filtration technique prior to packed bed studies. Filtration experiments of three feedstreams were performed with Cuno Zeta Plus 30SP membrane filters (Cuno, Meridan, USA). This was followed by a diafiltration step to prepare material for the following cation exchange chromatography step. A 1 mL SP Sepharose Hi Trap pre packed bed column (GE Healthcare, Uppsala, Sweden) was used to capture Fab' from the three feedstreams. The final process purification factor of the three feedstreams were 2.5, 4.4 and 3.5 respectively. The use of multimodal precipitated impurities prior to a packed bed step had improved process performance by a purification factor of 1.9. Therefore, the investigation of whole process interactions with material prepared by precipitation demonstrated the importance of reducing impurities early in the process that can negatively interact with subsequent operations.

5.2   Introduction

Improvements in upstream processing have been shown to be effective in increasing the product titer in the bioreactor phase (Taipa *et al.,* 2001). However, the amount of impurities in the product stream must to be reduced prior to a chromatography step in order to realise the full benefits of this improvement. Precipitation through multimodal operation can remove contaminating proteins, improving the feedstream, prior to a costly chromatography step.

In this chapter, the multimodal precipitation of Fab' from homogenates was optimised by microscale mimics. The amount of shear in the system and the rate of addition of the feed to the precipitating agents are two important variables affecting the size and strength of the precipitates that are formed. These two factors were studied at microscale and verified at pilot scale. The process performance was evaluated through a process run through using particle size distribution of the precipitate, strength of the precipitate, amount of Fab' left in the supernatant, the ease of clarification of the precipitates through microscale centrifugation studies and by a final cation exchange chromatography step. The structure of this chapter is shown in figure 5.1.

Stage 1

A two level full factorial DoE was used to identify conditions for maximising size of particles

Stage 2

A USD system was used to mimic the pilot scale centrifuge in the laboratory by mimicking the amount of shear experienced by the precipitated material in the feed zone of the CSA-1 disk stack centrifuge (Westfalia Separator, AG, Germany)

Stage 3

Process run through integrating precipitation into a downstream purification process

Figure 5.1: *Flowchart of structure of chapter 5*

STAGE 1

5.3 Results and Discussion

5.3.1 Particle Size Characterisation

This part of the chapter describes the setup, automation and operation of particle size experiments performed on a Tecan Freedom EVO 200 liquid handling robot (Tecan, Reading, UK). A two level full factorial DoE was used to evaluate the parameters, which were believed to affect the particle size in the system for three feedstreams, namely homogenate pH 7.4 (control), PEG 12000 6.25% w/v/0.4 M sodium citrate pH 7.4 (multimodal) and PEG 12000 15% w/v pH 7.4 (single mode). The variables investigated were:

- Mixing speed (rpm)

- Mixing time (minutes)

- Flowrate of feed into the vessel (μL s^{-1})

A full factorial DoE, examining these three factors over two levels with one centre point would require $2^3+1= 9$ experiments with d_{50} particle size as the model output. The upper limit for mixing rpm was set to 2000 rpm (maximum speed of magnetic driven device) and the lower limit was set to 800 rpm, the minimum speed required for turbulent conditions. The Reynolds Number (equation 5.1) for turbulent mixing in literature is > 10 for non baffled, axial flow systems (Doran 1995).

$$Re = \frac{\mathrm{N}d_i{}^2\rho}{\mu}$$

(5.1)

Equation 5.1: *Reynolds Number, where N is the stirrer speed (rps), d_i is the impeller diameter (m), ρ is the density (kg m^{-3}), μ is the viscosity (Pa s) (Doran 1995)*

The Reynolds Number for mixing speeds at 800 rpm and 2000 rpm were calculated to be 111 and 278 respectively, which suggests that these speeds are turbulent mixing conditions.

$$Re = \frac{13.3 \text{ x } 0.005^2 \text{ x } 1000}{0.003} = 111 \text{ at 800 rpm mixing}$$

$$Re = \frac{33.3 \text{ x } 0.005^2 \text{ x } 1000}{0.003} = 278 \text{ at 2000 rpm mixing}$$

Mixing time has previously been investigated where it was found that at 60 minutes further precipitation was no longer observed (section 3.3.1). Therefore, the upper limit was set to 60 minutes with the lower limit set to 1 minute. While knowing this may be unreasonable in a process setting, it is important in DoE screening studies not to confine the design space as valuable data may be lost, and the design space can be refined with more detailed experiments once a suitable range has been identified. A centre point of 15.5 minutes was used.

The flowrate of addition of feed was set to either 900 μL s^{-1}, 12 μL s^{-1} and a centre point of 450 μL s^{-1} to give a wide operating range. The dispense speeds at low flowrates were used to avoid the Command Overflow, which occurs at slower addition rates. The Command Overflow results in a timeout from the pipetting command that does not answer after 5 to 6 minutes since the command is carried out for a long time. The reaction was quenched with 1 mL 100 mM Tris HCl pH 7.4 prior to particle size measurements using a Malvin particle size analyser (Malvern Instruments, Southborough, UK). The method for measurement is described in section 2.4. The experimental design is shown in table 5.1.

Experiment number	Mixing Speed (rpm)	Mixing time (min)	Flowrate of feed into vessel ($\mu L\ s^{-1}$)
1	2000	1	12
2	800	60	900
3	800	60	12
4	2000	1	900
5	2000	60	900
6	800	1	12
7	800	1	900
8	2000	60	12
9	1400	30	450

Table 5.1: *Table listing the full two level factorial DoE experiments with homogenate pH 7.4 (control), PEG 12000 6.25% w/v/0.4 M sodium citrate pH 7.4 (multimodal) and PEG 12000 15% w/v pH 7.4 (single mode) feedstreams for the study of particle size. Experiments were completed at 1 mL scale per well in 1.3 mL 96 deepwell plates (Nunc GmbH & Co., KG, Denmark) using a Tecan (Tecan, Reading, UK) for liquid handling. PEG (starting concentration 50% w/v pH 7.4), and sodium citrate (starting concentration 2.2 M pH 7.4) and 100 mM Tris HCl pH 7.4 were used in this experiment. Samples were quenched with 1 mL 100 mM Tris HCl pH 7.4 prior to particle size measurements using a Malvin particle size analyser (Malvern Instruments, Southborough, UK) as described in section 2.4. Measurements were made in triplicate with the d_{50} value used as the model output*
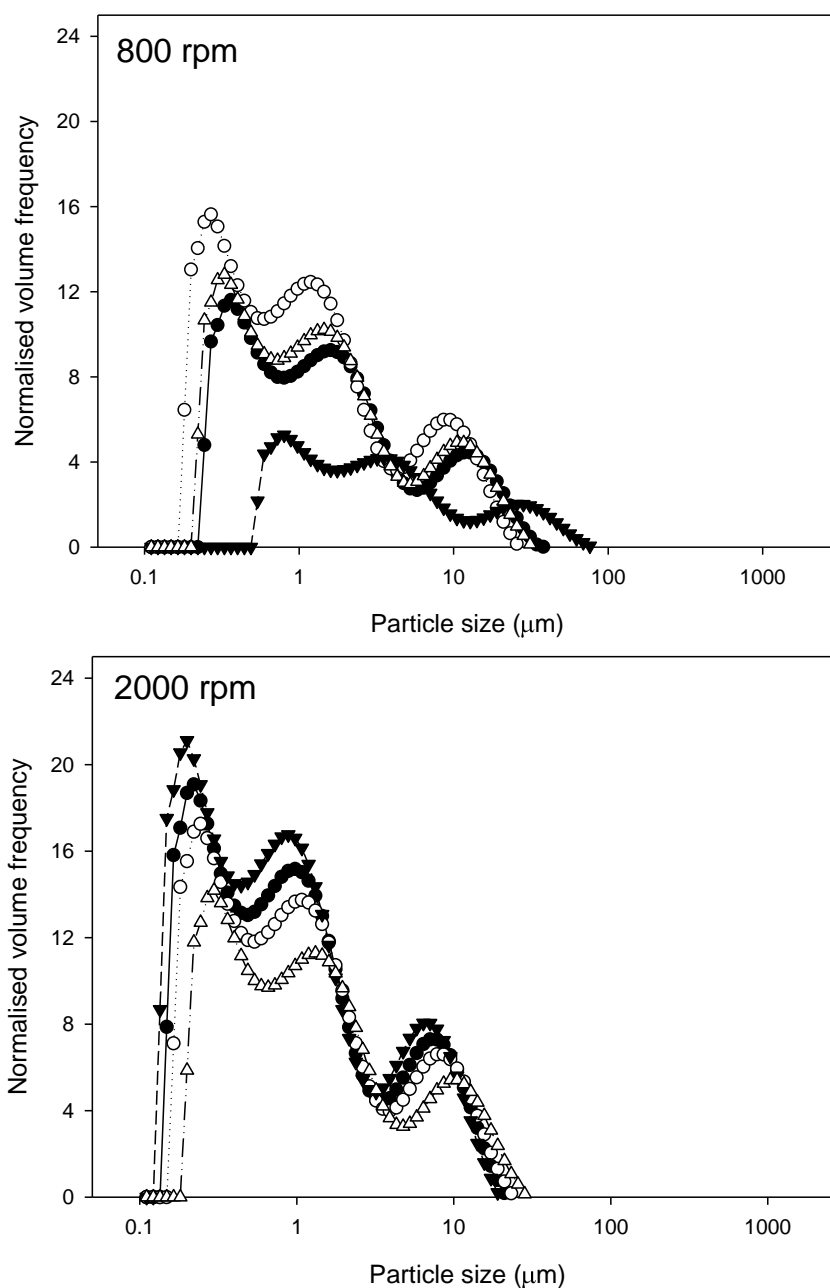
Figure 5.2: *Particle size distribution profiles of homogenate in 100 mM Tris HCl pH 7.4 at 1 minute mixing time and 12 μL s^{-1} feed addition rate ($\bullet$), 1 minute mixing time and 900 μL s^{-1} feed addition rate ($\circ$), 60 minutes mixing time and 12 μL s^{-1} feed addition rate ($\blacktriangledown$) and 60 minutes mixing time and 900 μL s^{-1} feed addition rate ($\triangle$) for 800 rpm and 2000 rpm mixing speeds respectively on a semi log plot. Measurements were made using a Malvin Mastersizer (Malvern Instruments, Southborough, UK) in triplicate as described in section 2.4. The standard deviation for measurements were ≤ 5%*

199
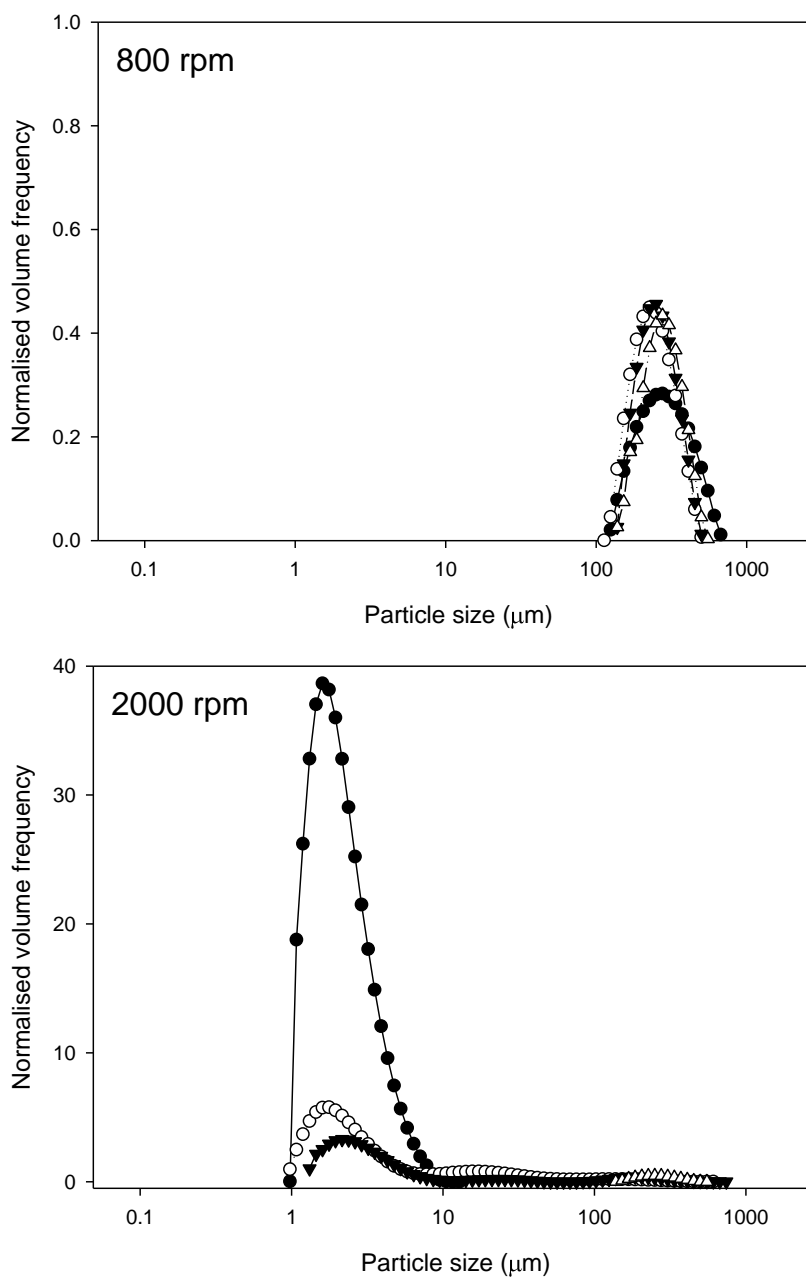
Figure 5.3: *Particle size distribution profiles of homogenate precipitated with PEG 12000 6.25% w/v/0.4 M sodium citrate pH 7.4 at 1 minute mixing time and 12 μL s^{-1} feed addition rate (●), 1 minute mixing time and 900 μL s^{-1} feed addition rate (○), 60 minutes mixing time and 12 μL s^{-1} feed addition rate (▼) and 60 minutes mixing time and 900 μL s^{-1} feed addition rate (△) for 800 rpm and 2000 rpm mixing speeds respectively on a semi log plot. Measurements were made using a Malvin Mastersizer (Malvern Instruments, Southborough, UK) in triplicate as described in section 2.4. The standard deviation for measurements were ≤ 5%*
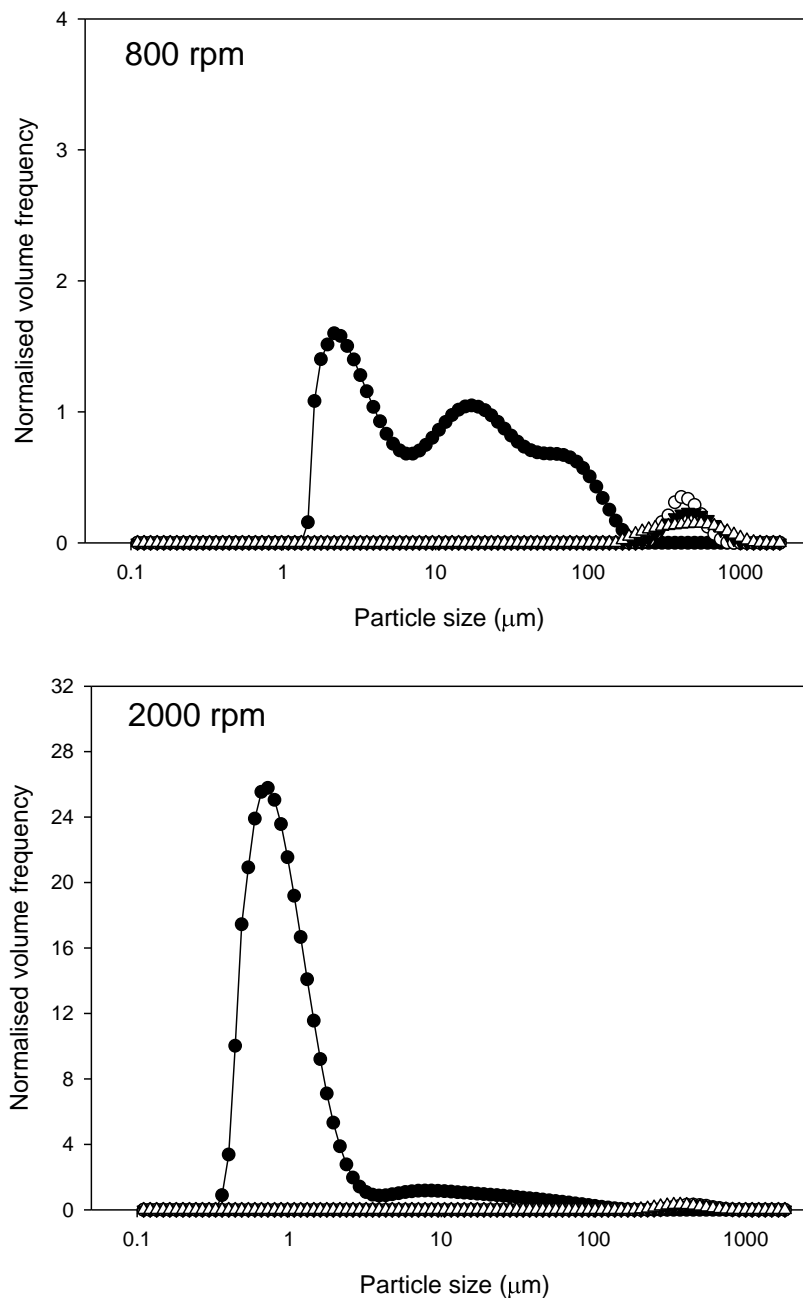
Figure 5.4: *Particle size distribution profiles of homogenate precipitated with PEG 12000 15% w/v pH 7.4 at 1 minute mixing time and 12 μL s^{-1} feed addition rate (●), 1 minute mixing time and 900 μL s^{-1} feed addition rate (○), 60 minutes mixing time and 12 μL s^{-1} feed addition rate (▼) and 60 minutes mixing time and 900 μL s^{-1} feed addition rate (△) for 800 rpm and 2000 rpm mixing speeds respectively on a semi log plot. Measurements were made using a Malvin Mastersizer (Malvern Instruments, Southborough, UK) in triplicate as described in section 2.4. The standard deviation for measurements were ≤ 5%*
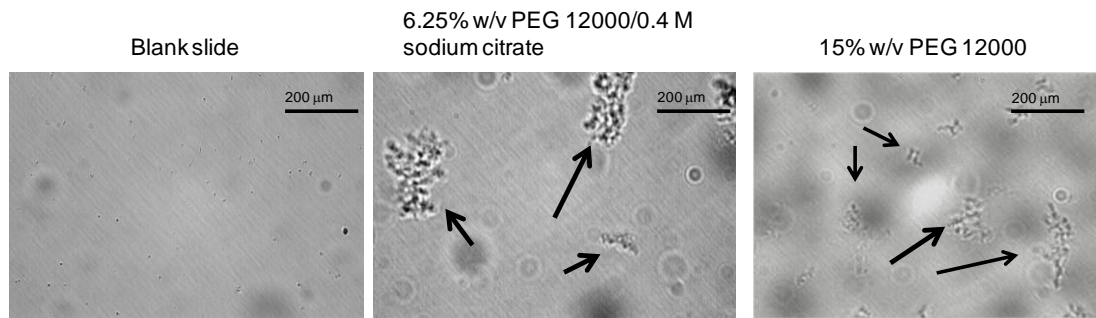
Figure 5.5: *Microscopic images of material that has been precipitated with PEG 12000 6.25% w/v/0.4 M sodium citrate pH 7.4 and PEG 12000 15% w/v pH 7.4 respectively. Images were taken with a Axioscope 2 plus microscope (Carl Zeiss Micro Imaging Inc., Thornword, USA) at 100x magnification of material that was mixed for 60 minutes at 800 rpm mixing speed with feed added at 900 $\mu L\ s^{-1}$. Arrows indicate examples of particulates of interest, which indicates a diverse size and morphology of particulates. Particulates appear to be agglomerated*

It is important to achieve sufficient mixing between the feed and the precipitant particularly during nucleation, or else, super saturation and under saturation regions will be present in the solution affecting subsequent separation. The mixing turbulence and time have a direct effect on particle size distribution, and it has been reported that precipitates that that are formed and aged under mild agitation conditions result in particle breakage (Byrne and Fitzpatrick 2002). Particles formed and aged under low shear conditions, though initially larger, are in fact weaker and fragment to a greater extent in turbulent flow. Sufficient strength of particles is necessary to withstand the fluid shear forces encountered through pumps and centrifuge feed zones, and therefore, they must meet the particle size and strength criteria for successful separation during subsequent steps such as centrifugation (Byrne and Fitzpatrick 2002).

The average d_{50} value for homogenised material mixed with 100 mM Tris HCl pH 7.4 for all conditions investigated was 15 μm and 12 μm at 800 and 2000 rpm mixing speeds respectively (figure 5.2). The particle size distribution profiles for the feed control were similar for each of the two mixing speeds.

Figure 5.3 shows the particle size distribution profiles for material precipitated with PEG 12000 6.25% w/v/0.4 M sodium citrate pH 7.4. The frequency of large particulates at 800 rpm mixing speed suggests that a reduction in the number of

small particles occured, which may be part of a mechanism involving the "mopping-up" of small particulates by the larger particulates. This is predicted by Smoluchowski's collision frequency theory, which states that the probability of collision between small and large particles is greater than the probability of collision between small particles, and so that large particles behave as nuclei around which small particles collect (Bell and Dunnill 1982). The d_{50} value was 313 μm at 800 rpm with the addition of feed at 900 μL s^{-1} after 60 minutes of mixing. However, at 2000 rpm the d_{50} particle size reduced to 197 μm, suggesting that high speed mixing results in partial break down of particles. Increased speed of mixing allows for an increase in collision frequency which can break down the larger particulates due to shear force effects. A similar trend was observed with the addition of PEG 12000 15% w/v pH 7.4 as precipitant (figure 5.4).

To understand the size and the morphology of the precipitated material, microscopic images were taken using a Axioscope 2 plus microscope at 100x magnification (Carl Zeiss Micro Imaging Inc., Thornword, USA) (figure 5.5). Material homogenised at 500 bar for 1 pass had a d_{50} particle size of 0.30 μm, which could not be observed at 100x magnification. An image of a blank slide was taken as a reference of background noise, and examples of the particulates of interest have been indicated in figure 5.5. Interestingly, the images show a diverse size and morphology of particulates. Particulates with multimodal precipitant appear to be agglomerated and almost globular. However, smaller agglomerated particulates were observed with PEG 12000 15% w/v pH 7.4, which were both irregular in shape and size.

MODDE 9.1 (Umetrics, Malmö, Sweden) was used to analyse the data from the particle size study. For the multimodal and PEG precipitated material it was found that d_{50} particle size increased at 800 rpm relative to 2000 rpm, when mixed for 60 minutes relative to 1 minute in the range investigated. It was found that the rate of addition of feed was not a significant factor to increase d_{50} particle size at 60 minutes mixing time. However, at one minute mixing time the faster addition rate (900 μL s^{-1} compared to 12 μL s^{-1}) may improve the distribution of the feed, resulting in more heterogeneous population of particle sizes, the effect of which is normalised after 60 minutes of mixing. Figure 5.6 shows a response surface plot for multimodal conditions fit as a two factor interaction model with mixing speed (rpm) and rate of addition (μL s^{-1}) at 60 minutes mixing time. The p-value for curvature was greater

than 0.05 (p-value was 0.30) by ANOVA analysis, which suggested that there was no conclusive evidence for curvature in the model. Although the Q^2 value of 0.33 was low, this interaction model was used to define the relationship between variables without proceeding with a response surface methodology DoE with these factors in the range investigated.

The data suggests that d_{50} particle size can be increased with a high rate of feed addition combined with a lower speed of mixing in the range investigated. For subsequent studies, mixing speed was maintained at 800 rpm for 60 minutes using a precipitant addition rate of 900 μL s^{-1}.
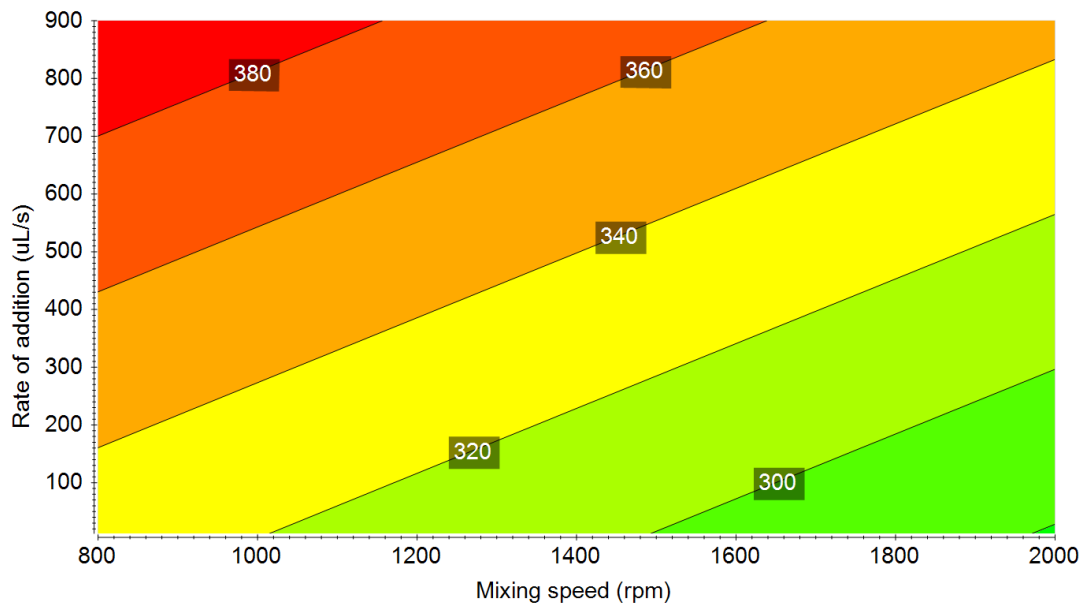
Figure 5.6: *Response surface plot of multimodal conditions at 60 minutes of mixing time (full factorial design, fit with a two factor interaction model). The contour lines indicate particle size in μm. The design of the experiments is outlined in table 5.1. All data fitting was performed using the software package MODDE 9.1 (Umetrics, Malmö, Sweden). This data suggests that d_{50} particle size can be increased with a high rate of feed addition combined with a lower speed of mixing (at 60 minutes mixing time) in the range investigated*

5.3.2 Scale Up of the Precipitation System to 50 mL Laboratory Scale and 5 L Pilot Scale

The ability to predict the performance of a large scale precipitation by microscale mimics is important for the rapid development of successful operations at large scale. Therefore, it was necessary to examine the translation of microscale/laboratory scale to pilot scale processes.

When scaling a precipitation process, the goal is to be able to mimic larger operating conditions and to provide the basis whereby the eventual larger scale process can be operated under identical feasible conditions. Several parameters should be kept constant, including tank geometry (height:diameter ratio), impeller type, diameter of the impeller relative to that of the tank, placement of the impeller and residence time (Boychyn *et al.,* 2000). Most stirred tanks are cylindrical with a height:diameter ratio greater than one ($H/d_v > 1$), and often have dished bottoms to prevent accumulation of solids in their corners (Boychyn *et al.,* 2000). This cylindrical shape can induce undesirable tangential flow or swirling of the liquid resulting in reduced power draw by the impeller and lower mixing efficiency, although such effects can be minimised by the introduction of wall baffles. By contrast, a non cylindrical profile ($H/d_v < 1$) can be beneficial for two reasons. First, the reduced height can improve top-to-bottom, axial-flow distribution; and second, the rectangular profile can minimise undesirable tangential flow, the corners acting like a baffle to break up the regular flow pattern and promote vertical flow (Botterill and Rawlings 2008).

Power unit per liquid volume, (equation 5.2) was used as the scale up parameter, calculated for the microscale system and kept constant at the different scales. This parameter has been used successfully in scaling up bioreactors (Marques *et al.,* 2010). A Power number of 6 was assumed for the high power/shear estimate.

$$\frac{P}{V} = \frac{P_0 \, \rho \, N^3 \, d_i^5}{(\pi/4)d_v^2 \, h}$$

Equation 5.2: *Power unit per liquid volume (W m^{-3}). Where P is the Power input (W), P$_0$ is the Power number, ρ is the liquid density (kg m^{-3}), N is the agitation rate (rps), d$_i$ is the impeller diameter (m), d$_V$ is the diameter of vessel (m), h is the reactor geometry height (m). P$_0$ = 6 for turbulent mixing in non baffled systems (Re > 10^3) (Rushton et al., 1950)*

Table 5.2 lists the dimensions of the precipitation reactors used in this study, shown visually in figure 5.7 for laboratory scale. The mean velocity gradient was calculated as per equation 1.3 assuming a dynamic viscosity of 0.003 Pa s (section 2.9). Minor differences such as the material type, bottom shape and impeller type exist between the three scales, however, scaling parameters such as impeller diameter:vessel diameter (d_i/d_v), mixing time, mixing Power per volume, mean velocity gradient and flowrate of feed into the vessel have been maintained constant. Stir tank geometries with $H/d_v < 1$ were used to improve axial-flow distribution and minimise tangential flow so that the corners of the vessel act like baffles to break up the regular flow pattern (Botterill and Rawlings 2008). At laboratory and pilot scale, the impellers were located approximately 1/3 off the vessel bottom to match the microscale mixing system. Lowering the impeller nearer to the base of the vessel can allow for use of smaller working volumes without exposing the impeller above the liquid surface. However, such exposure can generate excessive turbulence and undesirable effects on sensitive products.

At laboratory and pilot scale the flowrate of solutions into the vessel was 54 mL min^{-1} using a Watson Marlow 605 Di Peristaltic Pump (Watson Marlow Ltd., Falmouth, UK) to match the flowrate at microscale (900 μL s^{-1}). The flowrate was determined by calibration with water and direct measurement with the flow set to 54 mL min^{-1} to match the addition rate of 900 μL s^{-1} at microscale. In both cases the point of addition was located in the proximity to the impeller to mimic the same point at microscale. The experimental methodology at laboratory and pilot scale was completed to mimic that of the microscale process (described in section 4.3.1). Briefly, 100 mM Tris HCl pH 7.4 was added to the appropriate vessels, followed by the addition of PEG 12000 (stock 50% w/v at pH 7.4) and sodium citrate (stock 2.2

M at pH 7.4) as necessary. This mixture was then mixed for two minutes to ensure homogeneity of the precipitant (mixing speeds shown in table 5.2). This was followed by the addition of feed, and total mixing time was 60 minutes. At micro and laboratory scale both 42 and 670 W m^{-3} mixing Power per volume runs were performed. At pilot scale only the 42 W m^{-3} mixing Power per volume run was performed due to limited material availability.

Any differences in particle size may in part be caused by the differences in the time taken for the addition of feed to the precipitant between the three scales, although data in section 5.3.1 suggested that this effect might have become normalised after 60 minutes of mixing. However, the impact on resultant particle size will need to be further investigated, and further experiments are proposed in section 6.2.2 where the rate of precipitant addition at different scales is scaled up accordingly to maintain time of addition.

	Microscale		Laboratory scale		Pilot scale
Operating volume (mL)	1		50		5000
Maximum working volume (mL)	1.30		200		10000
Vessel height, H (mm)	29		110		300
Material type	PTFE		PTFE		Polyethylene
Bottom Shape	Round		Flat		Flat
Vessel diameter, d_v (mm)	8.50		63		270
Impeller diameter, d_i (mm)	5		40		162
d_i / d_v	0.58		0.63		0.54
Impeller type	5 mm VP 772FN PTFE coin magnets		6 blade Rushton turbine		12 blade Rushton turbine
Mixing speed (rpm)	800	2000	90	230	42
Mixing Power per volume (W m^{-3})	42 W m^{-3}	670 W m^{-3}	42 W m^{-3}	670 W m^{-3}	42 W m^{-3}
$\bar{G}$ (s^{-1})	120	473	115	472	122
Mixing time (min)	60		60		60
Flowrate of feed into vessel (mL min^{-1})	54		54		54
Volume of feed added (mL)	0.33		16.50		1650
Time taken for addition of feed (min)	0.01		0.30		28

Table 5.2: *Dimensions and characteristics of the precipitation vessels. Minor differences exist between the three scales, but scaling parameters such as d_i/d_v, mixing time, mixing Power per volume, mean velocity gradient and flowrate of feed into the vessel have been maintained constant. At laboratory and pilot scale the flowrate of feed into the vessel was 54 mL min^{-1} using a Watson Marlow 605 Di Peristaltic Pump (Watson Marlow Ltd., Falmouth, UK) to match the flowrate at microscale (900 μL s^{-1}). Any differences in particle size may in part be caused by the differences in the time taken for the addition of feed to the precipitant between the three scales, although data in section 5.3.1 suggests that this effect may become normalised at 60 minutes of mixing*
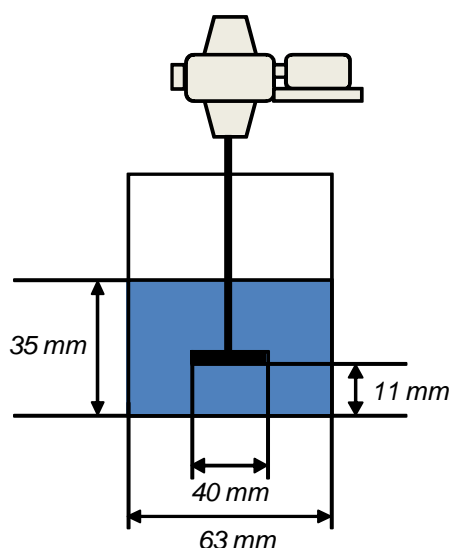
Figure 5.7: *Diagram to show the laboratory scale up. The stirred tank reactor was equipped with a 6 blade Rushton turbine impeller located approximately 1/3 off the vessel bottom. The flowrate of solutions into the vessel was 54 mL min^{-1} using a Watson Marlow 605 Di Peristaltic Pump (Watson Marlow Ltd., Falmouth, UK) to match the flowrate at microscale (900 μL s^{-1}). The point of addition was located in the proximity to the impeller to mimic the same point at microscale. The experimental methodology was completed to mimic that of the microscale process (described in section 4.3.1). Briefly, 100 mM Tris HCl pH 7.4 was added to the vessel, followed by the addition of PEG 12000 (stock concentration of 50% w/v pH 7.4) and sodium citrate (stock concentration of 2.2 M pH 7.4) as necessary. This mixture was then mixed for two minutes to ensure homogeneity of the precipitant. This was followed by the addition of feed, and total mixing time was 60 minutes. Mixing speeds are shown in table 5.2. At laboratory scale both 42 W m^{-3} and 670 W m^{-3} mixing Power per volume runs were completed*
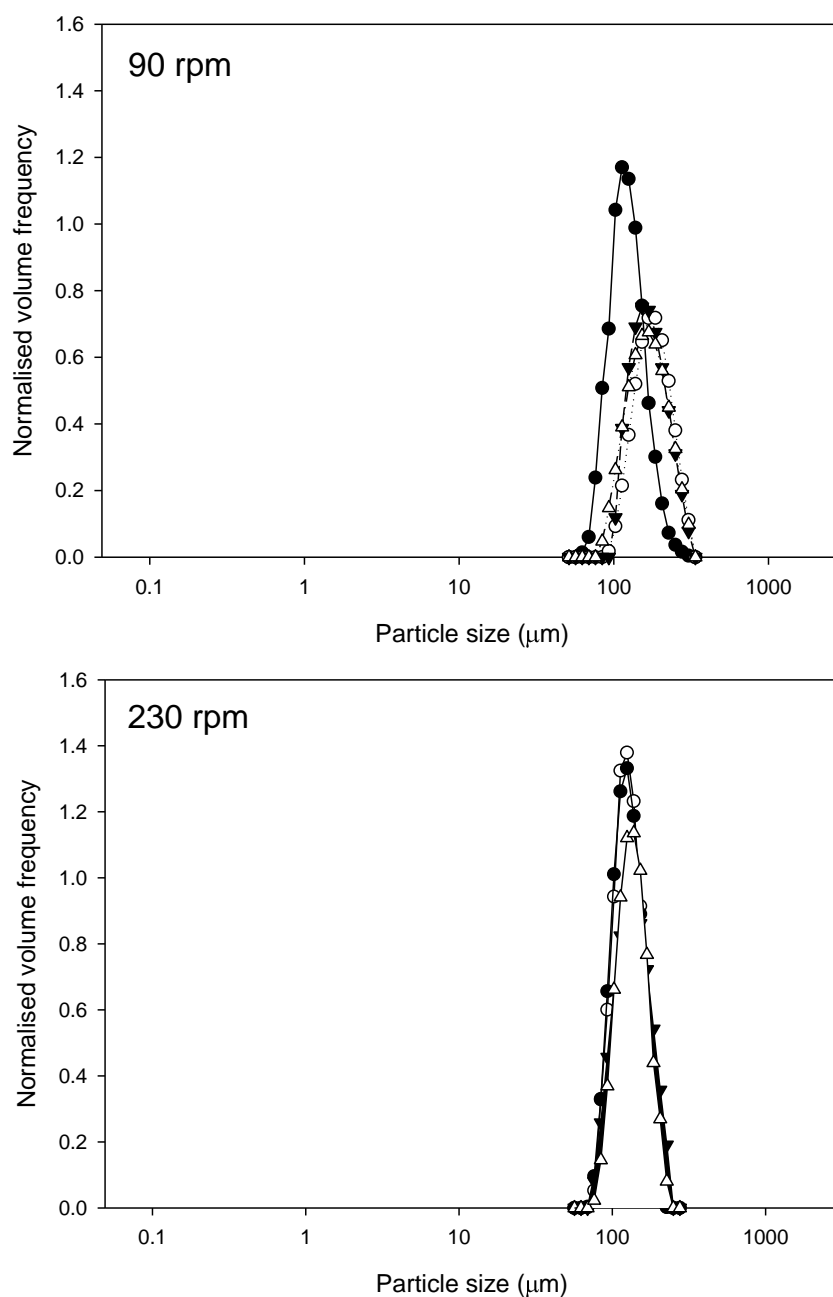
Figure 5.8: *Particle size distribution profiles of laboratory scale experiments of homogenate precipitated with PEG 12000 6.25% w/v/0.4 M sodium citrate at 1 minute mixing (●), 15 minutes mixing time (○), 20 minutes mixing time (▼) and 60 minutes mixing time (△) at 90 rpm and 230 rpm mixing speeds respectively on a semi log plot. Mixing was conducted with a 40 mm Rushton turbine. Measurements were made using a Malvin Mastersizer (Malvern Instruments, Southborough, UK) in triplicate as described in section 2.4. The standard deviation for measurements were ≤ 5%*

| Blank slide | 90 rpm | 230 rpm |
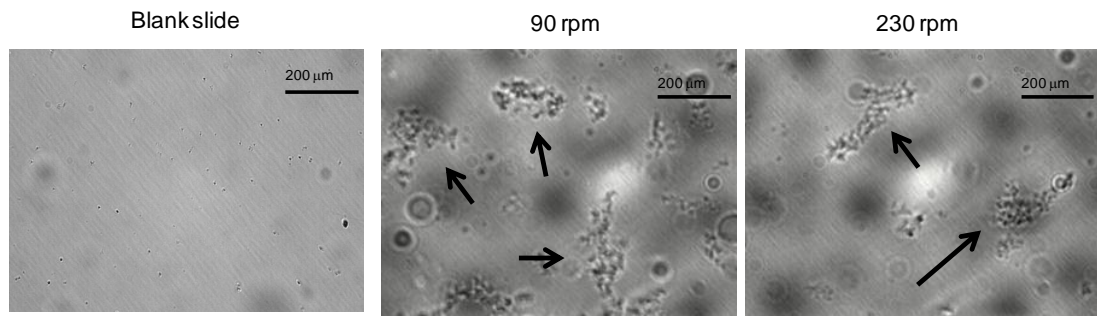
Figure 5.9: *Microscopic images of multimodal precipitated material at laboratory scale at 90 rpm and 230 rpm respectively. Images were taken using a Axioscope 2 plus microscope (Carl Zeiss Micro Imaging Inc., Thornword, USA) at 100x magnification of material that was mixed for 60 minutes with feed added at 54 mL min^{-1}. Arrows indicate examples of particulates of interest, which indicates a diverse size and morphology of particulates. Particulates appear to be agglomerated*

The size, strength and rheological characteristics of aggregates have all been linked to the precipitation reactor design and configuration. Vessel geometries, baffles, impellers and whether the operation is continuous or batch all contribute to the particulates characteristics. Larger and faster impellers have greater tip speeds and hence higher maximum energy dissipation at the tip to shear the aggregates. The particulates circulation time and the proportion of time spent near the impeller define precipitate strength and ageing (Shamlou *et al.*, 1996).

Bell and Dunnill (1982) demonstrated that continuous tubular reactors produced large, irregular, low density particles as compared with the stronger, smaller particles of the batch stirred tank. They attributed the differences to the magnitude and distribution of mean velocity gradients ($\bar{G}$), and residence times within the reactors. They observed that the batch aggregates had been exposed to high flow stress zones (impeller region) for longer periods than their continuous counterparts had. The larger continuous precipitates had a more open structure and a wider distribution of sizes. Particles had infrequently been exposed to impeller action in the continuous system (a lower residence time in a high velocity gradient zone). Their centrifugal recovery predictably resulted in reduced clarification (shear in the feed zone had broken these large, hollow particles into fine fragments found in the supernatant).

A good agreement was observed for the particle size distribution profiles for microscale and laboratory scale with multimodal precipitation conditions (figures 5.3 and 5.8 respectively). At laboratory scale, it was observed that the particle size was not as quickly formed relative to microscale. At one minute mixing time, the d_{50} value was 262 μm at microscale relative to 183 μm observed at laboratory scale at 42 W m^{-3} (90 rpm at laboratory scale). However, at 60 minutes of mixing, the d_{50} value for laboratory scale was 200 μm relative to 313 μm for microscale. This may in part be due to the difference in the rate of addition between the different scales. Interestingly, the particle size and formation was quicker and smaller at 670 W m^{-3} (230 rpm at laboratory scale; the d_{50} value after 60 minutes was 151 μm). This suggested that the speed of mixing provided turbulent conditions and sufficient energy to overcome the energy barrier for aggregation (Rushton *et al.,* 1950). However, it was noted that the d_{50} particle size at higher mixing speeds was smaller than that observed at slower mixing speeds (figure 5.8).

To understand the size and the morphology of the precipitated material, microscopic images were taken (figure 5.9). Microscopic images were taken using a Axioscope 2 plus microscope at 100x magnification (Carl Zeiss Micro Imaging Inc., Thornword, USA) after 60 minutes of mixing. Examples of the particulates of interest have been indicated in figure 5.9, which shows a diverse size and morphology of particulates with slightly smaller particles observed at 230 rpm. Particulates appear to be agglomerated and both irregular in shape and size. The increase in mixing speed has not reduced the size of the particles significantly. However, the pictures may not be truly representative of the precipitated particles as the pictures represent a small proportion of the material.

STAGE 2

5.4 Results and Discussion

5.4.1 Defining the Centrifugation Stage of the Precipitation Process

The size of the chromatography columns and buffers volumes used in processes are increasing (Ljunglöf *et al.,* 2007) and a precipitation step combined with a centrifugation step can be used to reduce the burden of subsequent chromatography steps. An ultra scale down (USD) method to measure the shear sensitivity of precipitated particles has been developed previously at University College London (Berrill *et al.,* 2008). The concept is to mimic the disk stack centrifuge at laboratory scale, by exposing the feed to shear rates that are similar to that experienced by the feed in the feed zone of the pilot scale centrifuge. This is performed by exposing the feed to different shear conditions and measuring ease of clarification.

The characteristics of the precipitated material are required to be strong and dense to prevent break up whilst in the feed zone of a disc stack centrifuge. In a disc stack centrifuge there are relatively high levels of shear, and the more resistant the particles are to shear the higher the speed the centrifuge can be operated at. This allows higher feed flow rates to be used without affecting yield and purification factor. To best mimic the pilot scale centrifuge, feed materials were exposed to shear levels similar to those found in the feed zone of the pilot centrifuge prior to laboratory centrifugation.

Sigma theory, is a concept used to describe the solid-liquid separation performance of a centrifuge. The theory and method of mimicking entry shear has been thoroughly described in the literature (Boychyn *et al.,* 2000, Reynolds *et al.,* 2003, Boychyn *et al.,* 2004). The sigma area, also called equivalent settling area, is defined as the surface area of a gravity settling tank with equivalent settling performance. Each type of centrifuge design has a unique correlation for calculating a sigma value. Equations 5.3 and 5.4 show the formulas for calculating the sigma value for laboratory and disc stack centrifuges respectively.

$$\Sigma_{lab} = \frac{V_{lab}\omega^2}{2g \ln\left(\dfrac{2R_2}{R_2 + R_1}\right)}$$

(5.3)

Equation 5.3: *Where Σ_{lab} is the equivalent settling area of the laboratory centrifuge (Eppendorf 5810R centrifuge) (m^2), V_{lab} is the volume of processed material, ω is $2\pi N$ (rad s^{-1}), N is the rotational speed (rps), g is the acceleration due to gravity (m s^{-2}), R_1 is the inner radius (m) (the distance between the centre of rotation and the top of the liquid), and R_2 is the outer radius (m) (the distance between the centre of rotation and the bottom of the tube) (Maybury et al., 1998)*

$$\Sigma = \frac{2\pi n_d \omega^2 (r_2^3 - r_1^3)}{3g \tan \theta}$$

(5.4)

Equation 5.4: *Where Σ is the equivalent settling area of the disc stack centrifuge (m^2), n_d is the number of active discs, r_1 and r_2 are the inner and outer disc radius (m), and θ is the half disc angle (degrees) (Boychyn et al., 2004)*

5.4.2 Microscale Precipitation and Centrifugation

The first stage in the precipitation of Fab' from partially clarified homogenates was optimised through the use of microscale mimics for two types of precipitating conditions namely PEG 12000 6.25% w/v/0.4 M sodium citrate pH 7.4 (multimodal) and PEG 12000 15% w/v pH 7.4 (single mode; partially clarified homogenised material was used as a control). The second stage, evaluated if low volume experiments could provide process relevant data similar to that obtained from a pilot scale study. Table 5.3 highlights the experimental procedures used.

Experimental procedure	Laboratory scale	Pilot scale
Homogenisation of feed material	APV Gaulin Lab60 homogeniser (APV International, West Sussex, UK)	APV Gaulin Lab60 homogeniser (APV International, West Sussex, UK)
Centrifugation	CARR P6 Powerfuge centrifuge (Pneumatic Scale Corporation, FL, USA)	CARR P6 Powerfuge centrifuge (Pneumatic Scale Corporation, FL, USA)
Precipitation	1. 100 mM Tris HCl pH 7.4 (control) 2. PEG 12000 6.25% w/v/0.4 M sodium citrate 3. PEG 12000 15% w/v	1. 100 mM Tris HCl pH 7.4 (control) 2. PEG 12000 6.25% w/v/0.4 M sodium citrate 3. PEG 12000 15% w/v
Shear	Low shear (6000 rpm) High shear (18000 rpm)	N/A
Centrifugation	Eppendorf 5810R centrifuge (Eppendorf UK Ltd., Cambridge, UK)	CSA-1 disc stack centrifuge (Westfalia Separator, AG, Germany)

Table 5.3: *Experimental procedure to mimic pilot scale centrifuge by exposing feed material to different levels of shear at laboratory scale*

Precipitation at laboratory scale was performed on a Tecan Freedom EVO 200 liquid handling workstation (Tecan, Reading, UK) controlled by the Freedom EVOware software with mixing at 800 rpm for 60 minutes and 900 μL s^{-1} feed addition rate. Thirty microwells were used for each of the three precipitation experiments to produce sufficient volume of material for the rotating disc shear device. The construction of this device has been described previously (Hutchinson *et al.,* 2006, Biddlecombe *et al.,* 2009). The working volume for the rotating disc shear device was 20 mL. The rotating disc shear device consisted of a 50 mm diameter stainless steel chamber and height of 10 mm mounted onto a stainless steel shaft. The rotating disc had a diameter of 40 mm and a depth of 1 mm. The shaft of the element was connected to a high speed DC motor powered from the mains via a transformer. The transformer provided a range of speeds from 0 to 20000 rpm measured using an optical probe. The top and bottom of the stainless

steel chamber were equipped with entrance and exit holes with luer fittings to allow the attachment of syringe fillers. The device was filled from the bottom allowing trapped air to escape through the top. Once the chamber was full, inlets and outlets were sealed prior to operation of the device. The assembly was mounted on a heavy metal base to reduce vibration during experiments (Hutchinson *et al.,* 2006).

The precipitated material was used to produce a well spun, low shear (6000 rpm) exposed material, and high shear (18000 rpm) exposed material samples. Shear exposure was performed for 20 s in the high speed rotating disc device (figure 5.10). This was to allow reproducible operation and to avoid excessive break up of particles at longer times shear exposure times. This has been shown to be sufficient time to ensure all the sample has been exposed to the highest shear region at the tip of the disc for all rotational speeds of the centrifuges to be used (Neal *et al.,* 2003, Boychyn *et al.,* 2004).
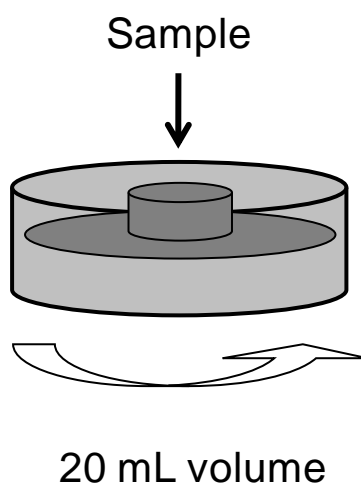
Figure 5.10: *Diagram representing the high speed rotating disc shear device. 20 mL samples of all three precipitating conditions (table 5.3) were sheared for 20 seconds at either low shear (6000 rpm) or high shear (18000 rpm)*

Low and high shear conditions of 6000 and 18000 rpm were used prior to centrifugation to mimic the impact of the shear regions in the inlet of the disc stack centrifuge (Neal *et al.,* 2003). The remaining suspension was kept as a no shear control condition. 1.5 mL samples were taken and placed in 2 mL Eppendorf tubes (Eppendorf UK Ltd., Cambridge, UK) from the three types of precipitated material at no shear (control), low and high shear. The tubes were spun in a Eppendorf 5810R

centrifuge, rotor T-60-11 (Eppendorf UK Ltd., Cambridge, UK; N = 1600-12600 rpm, Σ_{lab} = 0.009-0.617 m^2, t_{lab} = 12 min) at six different speeds for twelve minutes, detailed in table 5.4.

Centrifuge speed (rpm)	Time (min)	V/C.t.Σ (m s^{-1})
1600	12	2.7E-07
2800	12	9.0E-08
3200	12	6.9E-08
4400	12	3.6E-08
7800	12	1.2E-08
12600	12	4.4E-09

Table 5.4: *Centrifugal speeds in rpm and sigma values (equation 5.3) to mimic pilot scale clarification. Samples were spun for 12 minutes in an Eppendorf 5810R centrifuge, rotor T-60-11 (Eppendorf UK Ltd., Cambridge, UK; N = 1600-12600 rpm, Σ_{lab} = 0.009-0.617 m^2, t_{lab} = 12 min)*

A well spun sample was prepared for the purpose of a clarification reference sample N = 12600 rpm, t_{ref} = 30 minutes and the OD_{600} measured (OD_r) assuming 100% clarification. The optical density of the samples post centrifugation was measured at 600 nm (OD_{600}) using a Beckman DU 650 Spectrophotometer (Beckman Coulter Ltd., High Wycombe, UK) for both the sheared and the non sheared feed suspensions (OD_f) to generate data to calculate percentage clarification from equation 5.5. 100 mM Tris HCl pH 7.4 was used as a blank, and where necessary samples were diluted with 100 mM Tris HCl pH 7.4 in order to operate in the linear optical range of the spectrophotometer. The clarification level was determined using equation 5.5.

$$\%Clarification = \frac{OD_f - OD_s}{OD_f - ODr} x100 \qquad \textbf{(5.5)}$$

Equation 5.5: *Percentage clarification post centrifugation, where OD_f, OD_s and OD_r are the optical density of the feed, the sample supernatant and the supernatant of the reference sample respectively (Boychyn et al., 2000)*

5.4.3 Pilot Scale Precipitation and Centrifugation

When scaling a precipitation process, the goal is to be able to mimic larger operating conditions and to provide the basis whereby the eventual larger scale process can be operated under identical feasible conditions. Total volume was 5 L at pilot scale for each of the three conditions (three different precipitants as in table 5.3). This was performed in a 10 L vessel filled with 3.4 L of precipitant. The feed suspension of 1.6 L was fed continuously into vessel with the nozzle located in the proximity of a 162 mm Rushton impeller via a Watson Marlow 605 Di Peristaltic Pump (Watson Marlow Ltd., Falmouth, UK). Flowrate was maintained at 3.3 L hr^{-1} (54 mL min^{-1}) to replicate conditions at micro/laboratory scale. Impeller speed was set at 42 rpm to maintain the Power per unit volume of 42 W m^{-3} (equation 5.2 and table 5.2). The feed addition was monitored and controlled using a weighing balance. The total mixing time was 60 minutes (table 5.2).

The precipitated material was clarified using a CSA-1 disk stack centrifuge (Westfalia Separator, AG, Germany) at a flowrate of 100 L hr^{-1}. The optical density was measured at 600 nm (OD_{600}) with a Beckman DU 650 Spectrophotometer (Beckman Coulter Ltd., High Wycombe, UK) with 5 mL samples taken every minute. Temperature was maintained at approximately 7°C using a glycerol feed. The resulting solids were discharged immediately upon the bowl reaching capacity.

The strength and density of particles have been shown to be directly related and both are critical variables in centrifugal separation (Tambo and Hozumi 1979). The starting feed material at pilot scale prior to CSA-1 operation had a d_{50} particle size of 301 μm, which was in good agreement with microscale data, which had a d_{50} particle size of 313 μm at the same conditions. Particulates in the pilot feed were observed visually as shown in figure 5.11, which suggests that particulates had irregular morphology. At high shear, the particulates appeared to be smaller relative to the low sheared material suggesting that the material was sensitive to shear.
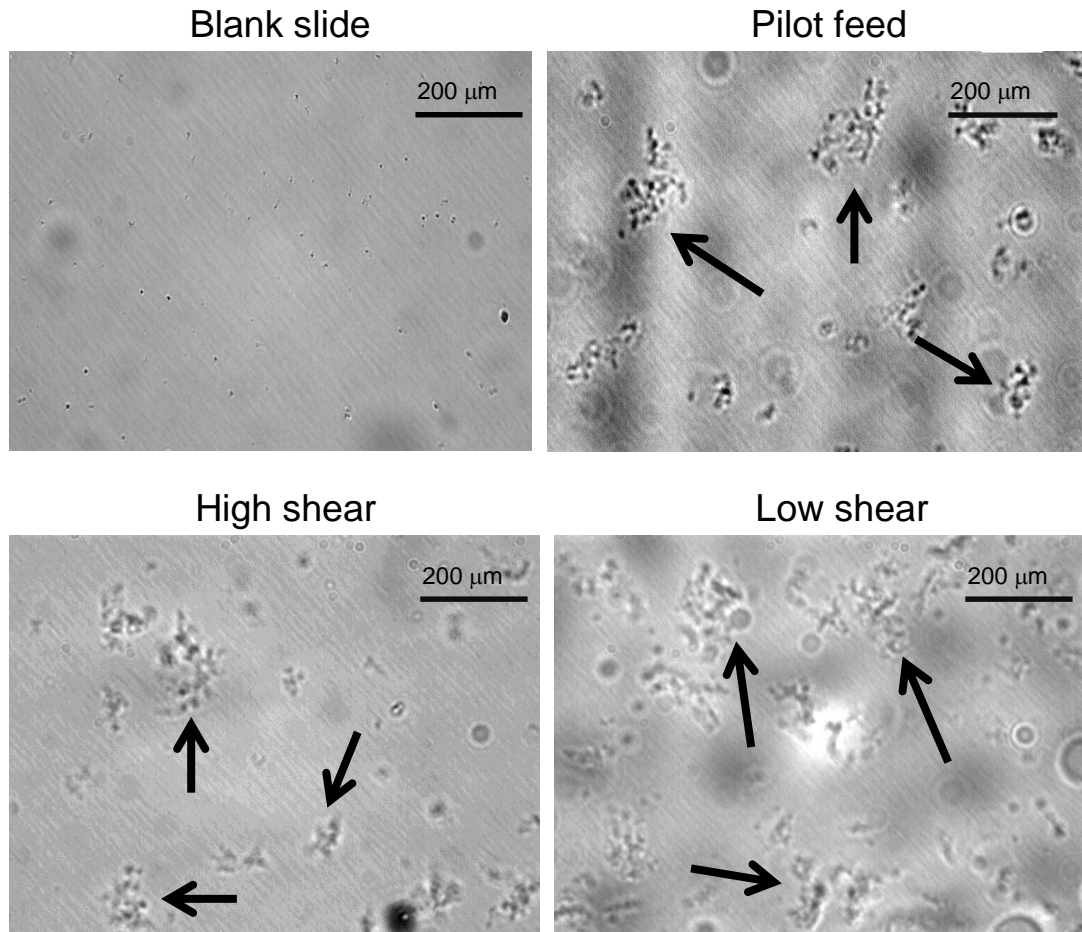
Figure 5.11: *Microscopic images of the feed at pilot scale and laboratory scale (high and low shear) for PEG 12000 6.25% w/v/0.4 M sodium citrate pH 7.4 precipitated material. Images were taken using a Axioscope 2 plus microscope (Carl Zeiss Micro Imaging Inc., Thornword, USA) at 100x magnification of multimodal material at pilot scale and laboratory scale exposed to 6000 rpm (low shear) and 18000 rpm (high shear). Arrows show examples of the particulates of interest, which indicate irregular shape and size of particulates in all conditions. Particulates appear to be smaller after being exposed to high shear suggesting particle break up, suggesting that the material was sensitive to shear*

Figure 5.12 suggests that the feed material was not shear sensitive with little effect on clarification without any precipitant added. This was confirmed with visual observation using microscopic images showing that there was an insignificant difference between different shear rates. The percentage clarification was low ≤ 80% throughout the V/C.t.$\sum$ (m s^{-1}) investigated. However, data in figures 5.13 and 5.14, which represents clarification of material precipitated with PEG 12000 15% w/v pH 7.4 and PEG 12000 6.25% w/v/0.4 M sodium citrate pH 7.4 respectively

suggests that the particle size decreases with increasing shear. It was possible that the breakage of particles during high shear resulted in sub visible particles, which may have consequences on the efficiency of the clarification of the material.

The centrifugation speed (equivalent flow rate to equivalent settling area ratio) was changed to the different spin down velocities shown in table 5.4 to adjust the equivalent settling area while maintaining the 12 minute centrifugation time. There was a significant difference in the percentage clarification between PEG single mode and multimodal precipitated material before and after material was exposed to high shear (figures 5.13 and 5.14). It was observed that low shear does not have a significant effect on clarification at higher speeds, where clarification of 99% was possible in some cases. This was in part due to the removal of smaller particles at higher centrifugation speeds. It was not possible to run the pilot centrifuge at these conditions as the lowest flowrate with the highest speed resulted in the data points shown in figure 5.14. Similar trends were observed by Tustian *et al.,* (2007) and Tait *et al.,* (2009).
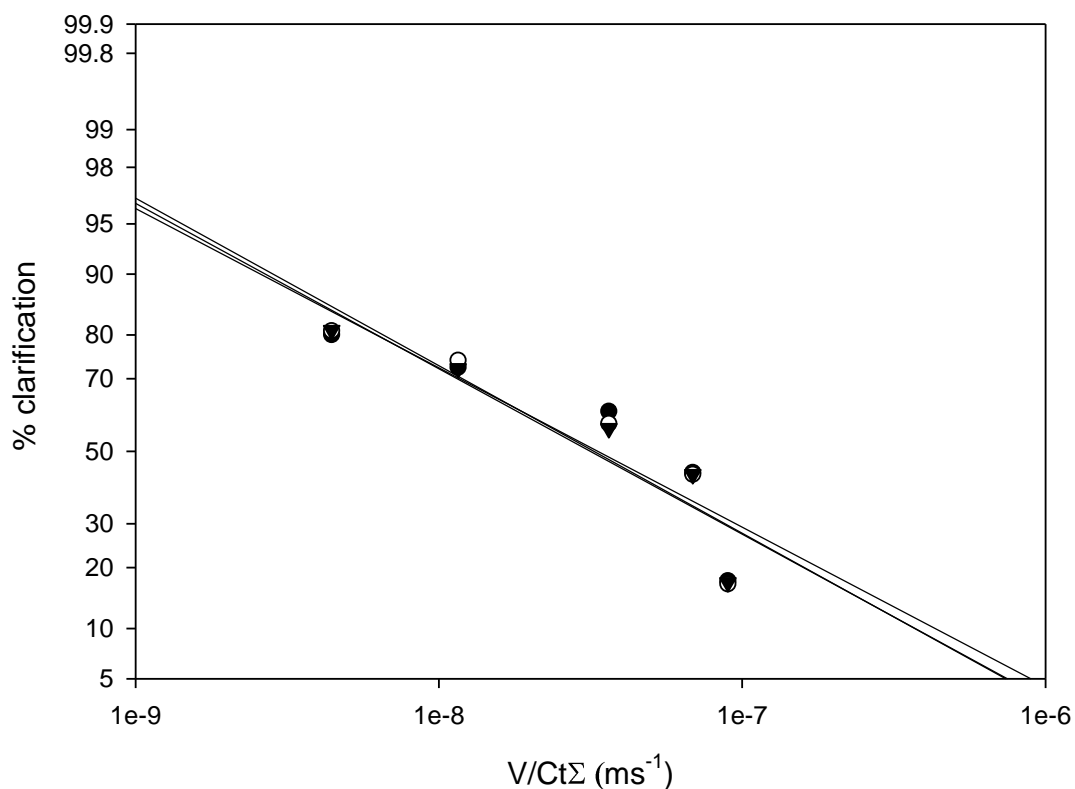
Figure 5.12: *The probability-log relationship of percentage clarification and equivalent flowrate for centrifuge separation area for homogenised feed material without added precipitant at pH 7.4. This material was exposed to no shear (●), 6000 rpm low shear for 20 s (○) and 18000 rpm high shear for 20 s (▼). Feed material was homogenised at 500 bar for 1 pass using an APV Manton-Gaulin Lab60 homogeniser (APV International, West Sussex, UK). The x-axis is the ratio of the equivalent flowrate to equivalent settling area. Data points were plotted on probability logarithmic axes. Solid line represents linear fit of data extended to axes*
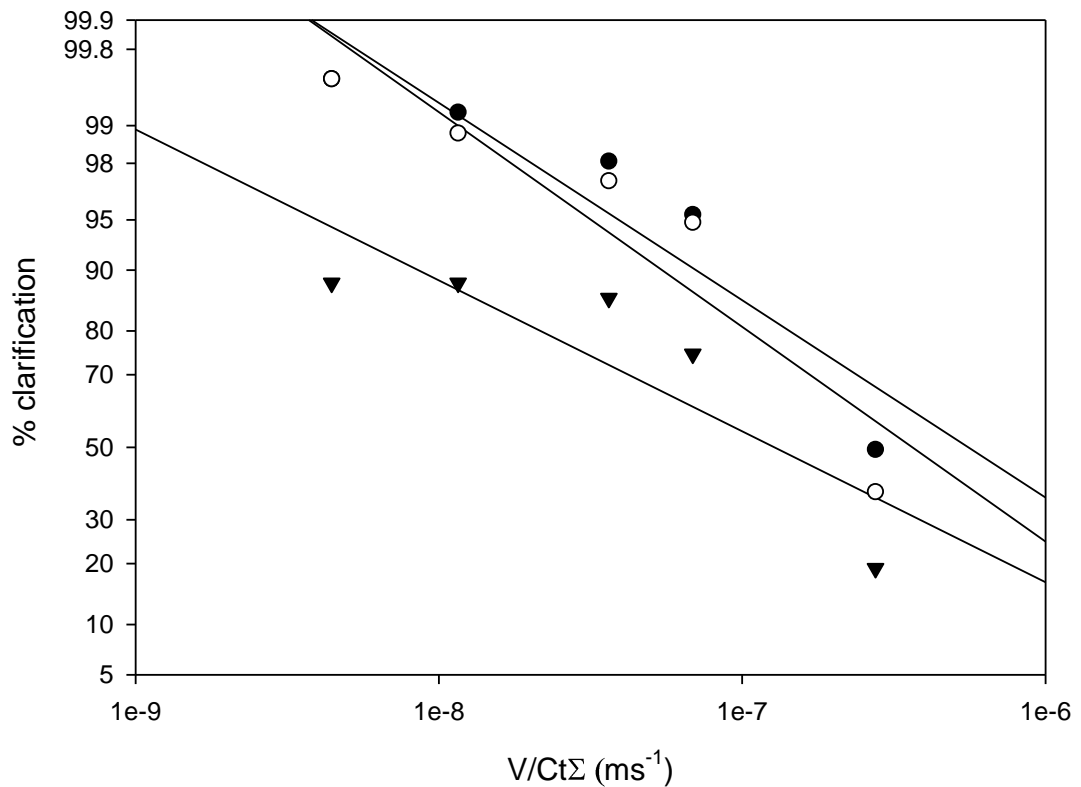
Figure 5.13: *The probability-log relationship of percentage clarification and equivalent flowrate for centrifuge separation area for homogenised feed material precipitated with PEG 12000 15% w/v pH 7.4. This material was exposed to no shear (●), 6000 rpm low shear for 20 s (○) and 18000 rpm high shear for 20 s (▼). The x-axis is the ratio of the equivalent flowrate to equivalent settling area. Feed material was homogenised at 500 bar for 1 pass using an APV Manton-Gaulin Lab60 homogeniser (APV International, West Sussex, UK). Data points were plotted on probability logarithmic axes. Solid line represents linear fit of data extended to axes*
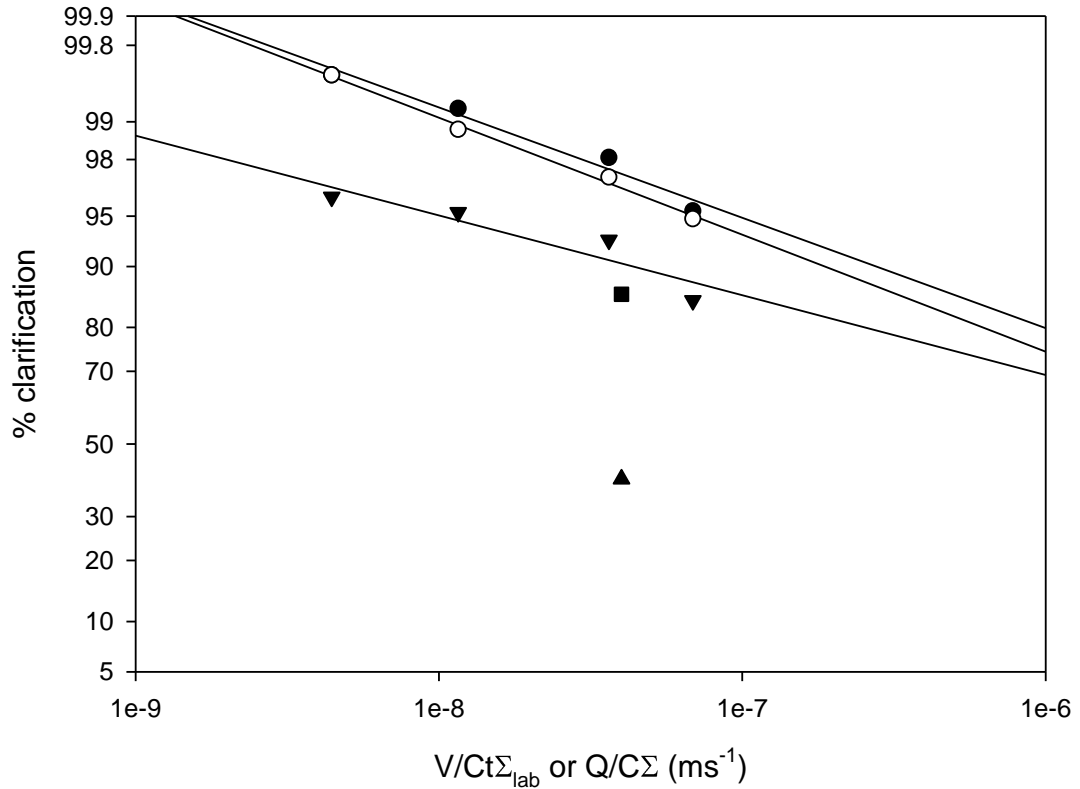
Figure 5.14: *The probability-log relationship of percentage clarification and equivalent flowrate for centrifuge separation area for homogenised feed material precipitated with PEG 12000 6.25% w/v/0.4 M sodium citrate pH 7.4 exposed to no shear (●), 6000 rpm low shear for 20 s (○), 18000 rpm high shear for 20 s (▼), pilot scale run 2 (feed homogenised for 500 bar for 1 pass) (■) and pilot scale run 1 (feed homogenised at 500 bar for 5 passes) (▲). Feed material was homogenised using an APV Manton-Gaulin Lab60 homogeniser (APV International, West Sussex, UK). The x-axis is the ratio of the equivalent flowrate to equivalent settling area. Data points were plotted on probability logarithmic axes. Solid line represents linear fit of data extended to axes*

A previous run at pilot scale with homogenisation conditions of 500 bar for 5 passes was investigated in which the clarification at pilot scale was not in agreement with the scale down prepared precipitates. Percentage clarification of 40% was observed for the pilot scale. The recoveries obtained for both laboratory and pilot scale were significantly different (80% and 54% respectively), which suggested possible differences in the settling properties of the precipitates in part caused by the excessive homogenisation step of 500 bar for 5 passes.

It has been shown in research that it is possible to over predict the clarification of solids at laboratory scale caused by the reaggregation of material at the laboratory scale (Berrill *et al.,* 2008). At laboratory scale, as the solids concentration increases, the settling rate of particles decreases due to interparticle forces. It is possible that the particles form a large floc that sweeps up the fine particles in the supernatant. This leads to an over prediction in the laboratory scale to that observed at the pilot scale. Hindered settling can occur when the solids concentration is high, which for this type of material, could be above 2% w/v. As the solids concentration increases, the settling rate of particles decreases due to the increase in interparticle forces. Particles settling slowest will be hindered by those underneath them. This is particularly noticeable in the confined space of a laboratory centrifuge. At very high solids what is known as "blanket" sedimentation can occur. This is when particles all settle at the same rate and form a large floc that sweeps up the fine particles in the liquid. This leads to an overprediction at laboratory scale to that of the pilot scale centrifuge (Berrill *et al.,* 2008).

In part, the much lower clarification observed at the pilot centrifuge was the result of break up of aggregates in the feed zone of the centrifuge, which was caused by the high flow stresses as the material enters the pilot centrifuge. The use of a peristaltic pump excluded the possibility of precipitate damage due to pumping, as Bell *et al.,* (1983) demonstrated that this type of pump had no disruptive effect on precipitates. However, at laboratory scale the length of time between shearing material and clarification may be enough to allow reaggregation, which consequently increases clarification performance in the laboratory scale compared to the pilot scale at an equivalent separation condition.

It was decided to homogenise *E.coli* cells at 500 bar for one pass to improve the percentage clarification at pilot scale. Homogenisation conditions were investigated in chapter 2. Figure 5.14 illustrates a significant improvement in percentage clarification compared to material homogenised through 5 passes (87% clarification compared to 40% clarification). It was suggested that the reduction of the level of sub visible particles had allowed a greater number of smaller debris to aggregate increasing strength and improving separation. A good agreement of clarification was achieved between the scale down and pilot centrifuge. The pilot scale separation efficiency improved from 40% to 87% with a recovery of 72%. The same conditions at laboratory scale with material exposed to high shear, 93% separation efficiency

was achieved. Since all the variables were kept constant and the significant difference in particle size distribution between the two levels of homogenisation for frozen *E.coli* cells, the gain in clarification was attributed in part to the reduction of micronisation of cell debris.

The benefits of better clarification will positively impact subsequent process steps. In this case, precipitated material has been used for selective product capture from a microbial homogenate and the selection of solid–liquid separations fit for purpose is critical. Post centrifugation cartridge or guard filters have been used to protect more expensive unit operations such as ultrafiltration and chromatography, by removing fine solids, which may foul them (Bracewell *et al.,* 2008). As the filter collects solids, an increasing pressure is required to maintain flow until it is not possible to maintain flow at which point the filter is changed. When preceding solid–liquid separation steps are performing well a guard filter is rarely heavily challenged and adds minimal capital and running costs, but can protect extremely valuable processes in many instances (Bracewell *et al.,* 2008). Step change improvement in clarification between low and high shear samples at the various clarification conditions studied was observed. For example, from figure 5.13 it can be observed that approximately 20% improvement in clarification can be expected at a V/C.t.$\sum$ of 6.8×10^{-8} m s^{-1}, and therefore the subsequent filter size could be reduced by 20% for similar performance. Further investigation with filters is described in section 5.5.2. In this case, microscale down methods that have been established for the study of operations such as centrifugation, which predict full scale operation is feasible (Boychyn *et al.,* 2004, Hutchinson *et al.,* 2006). However, it is necessary to predict the effect of this performance on the whole process before committing to large scale operations.

STAGE 3

5.5 Results and Discussion

5.5.1 Process Run Through Integrating Precipitation into a Down Stream Process

Cation exchange chromatography is a key step in generic purification processes (Farid 2006). In this section, a 1 mL SP Sepharose Hi Trap packed bed column (GE Healthcare, Uppsala, Sweden) was used to capture Fab' from the three feedstock solutions described in this chapter. Figure 5.15 highlights the process run through using three different feedstreams, namely partially clarified homogenate pH 7.4 (control), PEG 12000 6.25% w/v/0.4 M sodium citrate pH 7.4 (multimodal), and PEG 12000 15% w/v pH 7.4 (single mode).
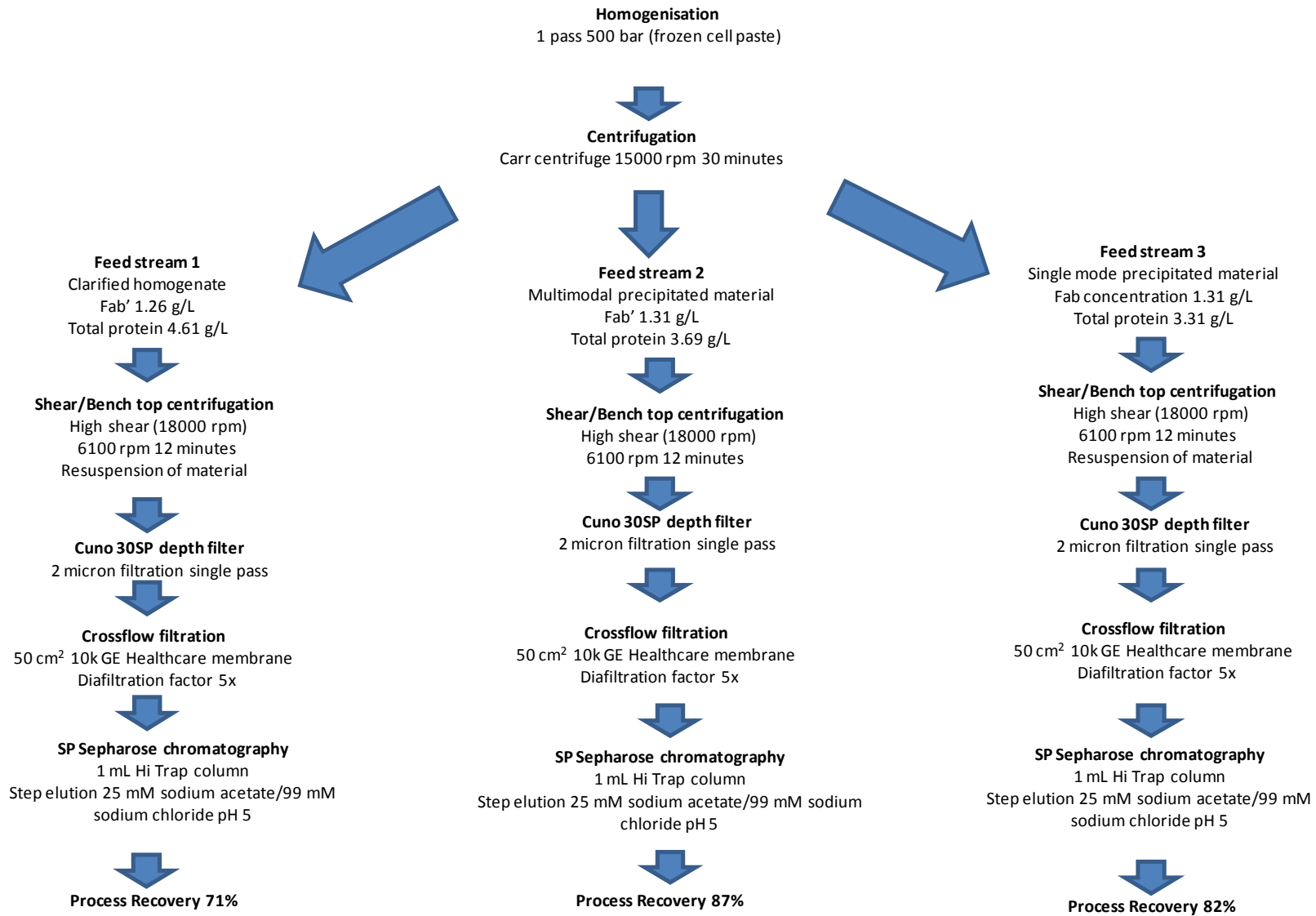
Figure 5.15: *Process run through based on three feedstreams described in section 5.5.1*

5.5.2 Automated Depth Filter Investigation Using an Eight Well Custom Filter Block Design

The clarification of the three feedstreams were examined during membrane filtration operation using an automated multiwell filtration technique prior to packed bed studies. The normal flow filtration method used has been established by Kong *et al.,* (2010). The build up of materials on or within the membrane pores would eventually lead to flux decline over time and the selection of membrane materials can affect the quality and recovery of the product (Kong *et al.,* 2010).

Filtration experiments of the three feedstreams were performed at room temperature using Cuno Zeta Plus 05SP and 30SP membrane filters (Cuno, Meriden, USA). 05SP and 30SP filters operate between 1-5 μm and 0.5-2 μm respectively. The filters were cut in-house to enable proper fitting into the custom membrane housings. The upper part of the housings was filled with 2 mL of feed material and all eight membrane housings were inserted into the custom filter block for triplicate runs (figure 5.16). The filtration area was 0.28 cm^2 with an operating pressure constant at 30 kPa throughout the filtration. A Tecan Freedom 200 EVO liquid handling system (Tecan, Reading, UK) was used to automate the filtration using a VacS two position vacuum manifold and the liquid handling (LiHa) arm of the Tecan (Tecan, Reading, UK). The Freedom EVOware software (Tecan, Reading, UK) was used independently to aspirate/dispense the feed material in parallel. Beneath each filter were individual tubes for filtrate collection.
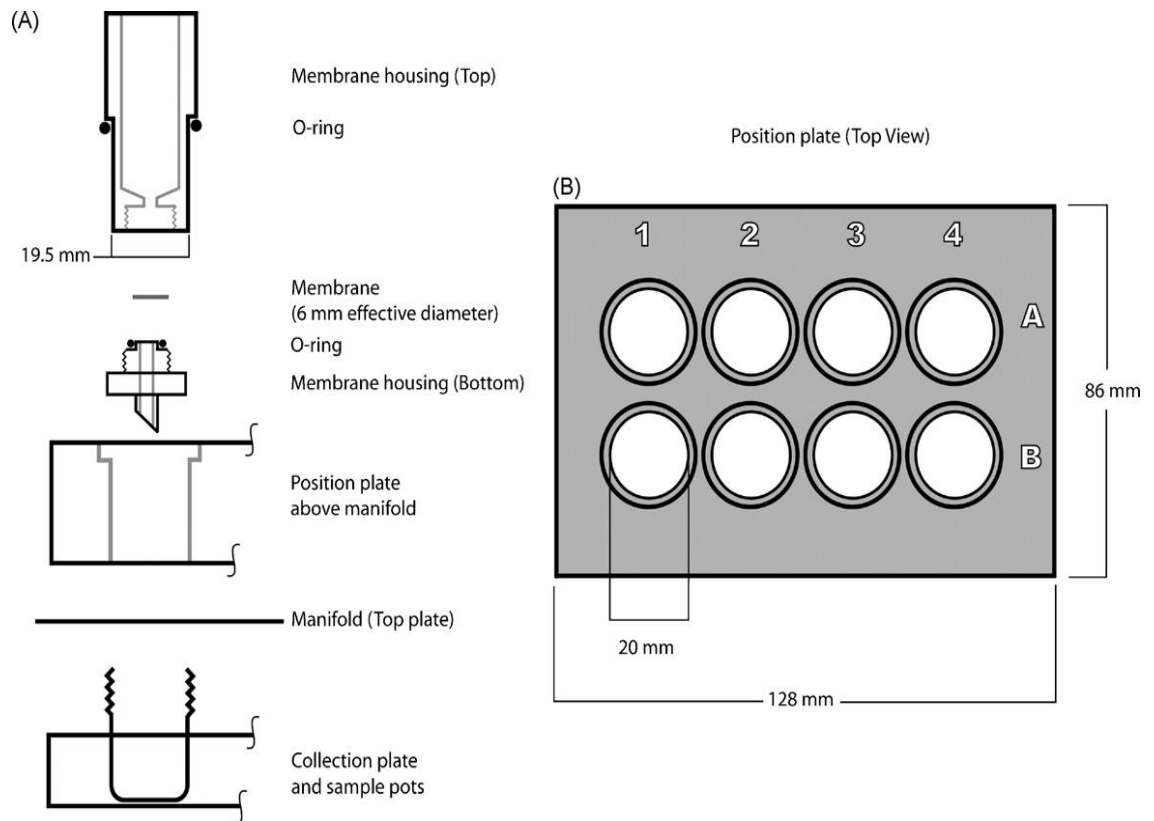
Figure 5.16: *Eight well custom filter block design for parallel microscale filtration. (A) cross-section of single filter membrane housing with sample pot on a collection plate. (B) top view of the position plate (diagram from Kong et al., 2010)*

The liquid handling arm was programmed to detect the retentate level on the top side of the membrane at specific time intervals throughout each experiment, which was logged for time and retentate volume. The amount of feed material removed from the top side of the membrane was assumed equal to the filtrate volume. The volumes detected by the LiHa arm and actual volumes (measured manually) had a correlation of more than 0.99. The variation for 18 repeated measurements was determined to be less than 5%. Data recording was terminated when 100% flux reduction rates were achieved.
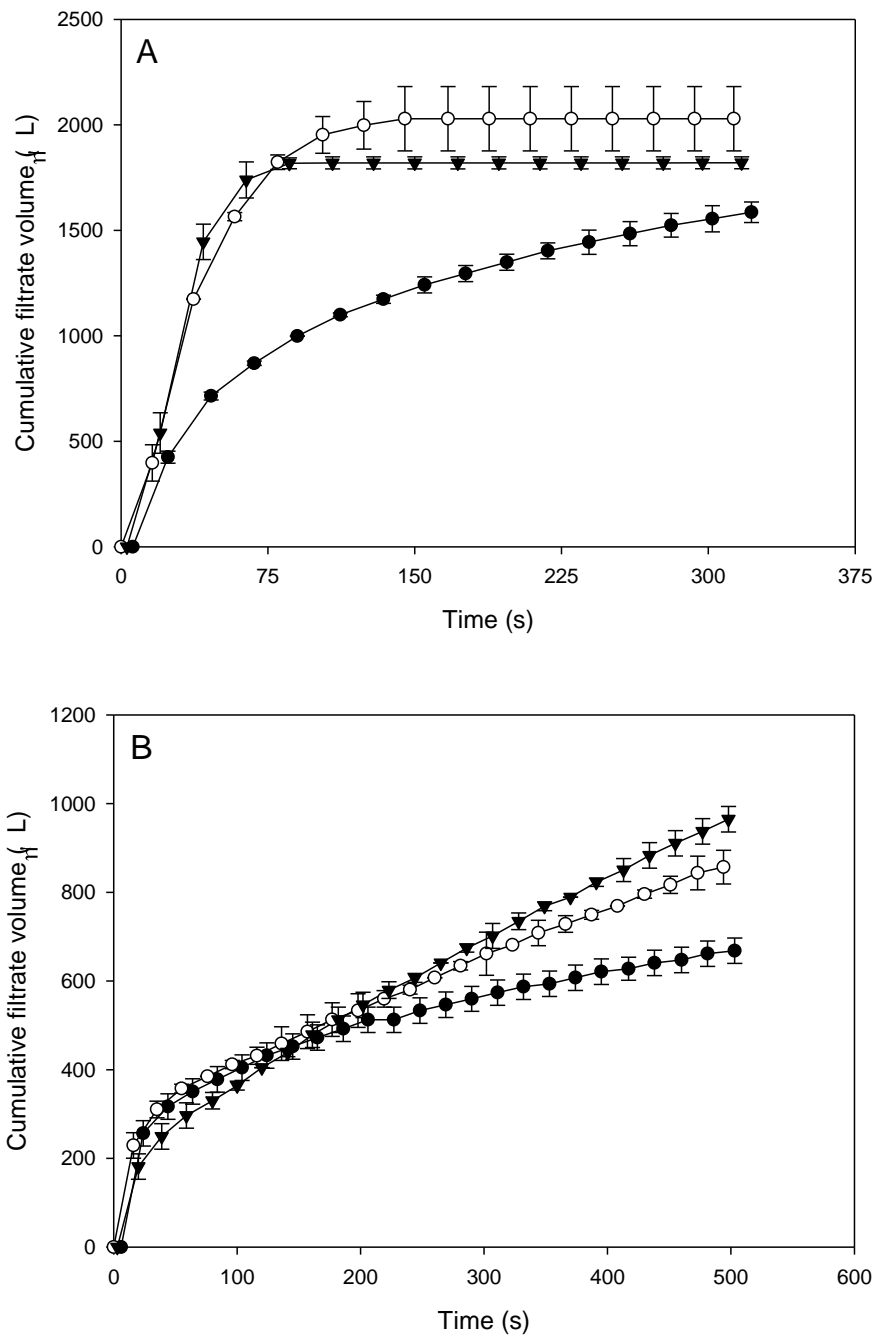
Figure 5.17: *Filtration of PEG 12000 15% w/v pH 7.4 (●), PEG 12000 6.25% w/v /0.4 M sodium citrate pH 7.4 (○) and clarified homogenate pH 7.4 (▼) through Cuno Zeta Plus 05SP (A) and Cuno Zeta Plus 30SP (B) depth filters at 30 kPa pressurey. Feed concentrations were 1.3 g L^{-1}, (4.6 g L^{-1}), 1.3 g L^{-1}, (3.7 g L^{-1}), 1.8 g L^{-1} and (3.3 g L^{-1}) of Fab' and (total protein) for clarified homogenate, PEG 12000 6.25% w/v/0.4 M sodium citrate pH 7.4 and PEG 12000 15% w/v pH 7.4 feedstreams respectively. Error bars are shown for one standard deviation for triplicate experiment repeats*

Figure 5.17 shows the cumulative filtrate volumes over time for the Cuno Zeta Plus 05SP and Cuno Zeta Plus 30SP filters respectively (Cuno, Meriden, USA). These membranes were selected due to their common availability and low adsorption properties. It is apparent from the data collected that the pore size has a significant impact on the volumes that can be filtered and on the filtration flux rates. The flow of material was quicker using the larger pore 05SP filter. The transmission of the Fab' and total protein was investigated at the end of each run after the filtration process. The collected filtrate samples were quantified using Protein G HPLC (GE Healthcare, Uppsala, Sweden) and the Pierce BCA assay for total protein (Pierce, Rockford, USA) as per sections 2.1 and 2.2 respectively. The experimental data shown in table 5.5 showed an increase in clarification when using the 30SP filter. The purification factor after filtration with 05SP membranes was 1.3 for the homogenate, multimodal and single mode feedstreams respectively. In the case of 30SP membranes, the purification factor was 1.4, 1.4 and 1.3 after filtration for the three feedstreams respectively. In future experiments, the 30SP filter was used as a depth filter due to its increase in performance over the 05SP filter.

Filter	Feedstreams	Initial Fab' conc ($g\ L^{-1}$)	Initial total protein conc ($g\ L^{-1}$)	Total protein conc post filtration ($g\ L^{-1}$)	Recovery (%)	Purification factor
05SP	Homogenate	1.26	4.61	3.69	98	1.30
	Multimodal	1.31	3.68	2.74	97	1.32
	Single mode	1.27	3.31	2.61	99	1.26
30SP	Homogenate	1.26	4.61	3.41	100	1.37
	Multimodal	1.31	3.68	2.62	99	1.39
	Single mode	1.27	3.21	2.51	98	1.33

Table 5.5: *Purification factor after filtration through Cuno Zeta Plus 05SP and Zeta Plus 30SP depth filters (Cuno, Meriden, USA) at microscale*

The V_{max} has been used to successfully describe filtration processes in the biopharmaceutical industry (Zydney and Ho 2002). This model describes the relationship for filter capacity limitations and flowrate of material through the filter (Kong *et al.,* 2010). These parameters can be used to estimate filter sizing (equation 5.6).

$$V_{max} = \frac{1}{gradient}$$

$$J_i = = \frac{1}{y\ intercept}$$

$$\text{Area} = \frac{Vb}{tb}\ x\ \left(\frac{tb}{Vmax} + \frac{1}{Ji}\right) \qquad\qquad \textbf{(5.6)}$$

Equation 5.6: *V_{max} where V is the total filtrate volume collected over time t, J_i is the initial volumetric filtrate flow rate (L m^{-2} h), and V_{max} is the maximum fluid volume that can be filtered before the membrane is completely fouled (L m^{-2}), Vb is the filtration volume (L), tb is the filtration batch time (h) (Zydney and Ho 2002)*
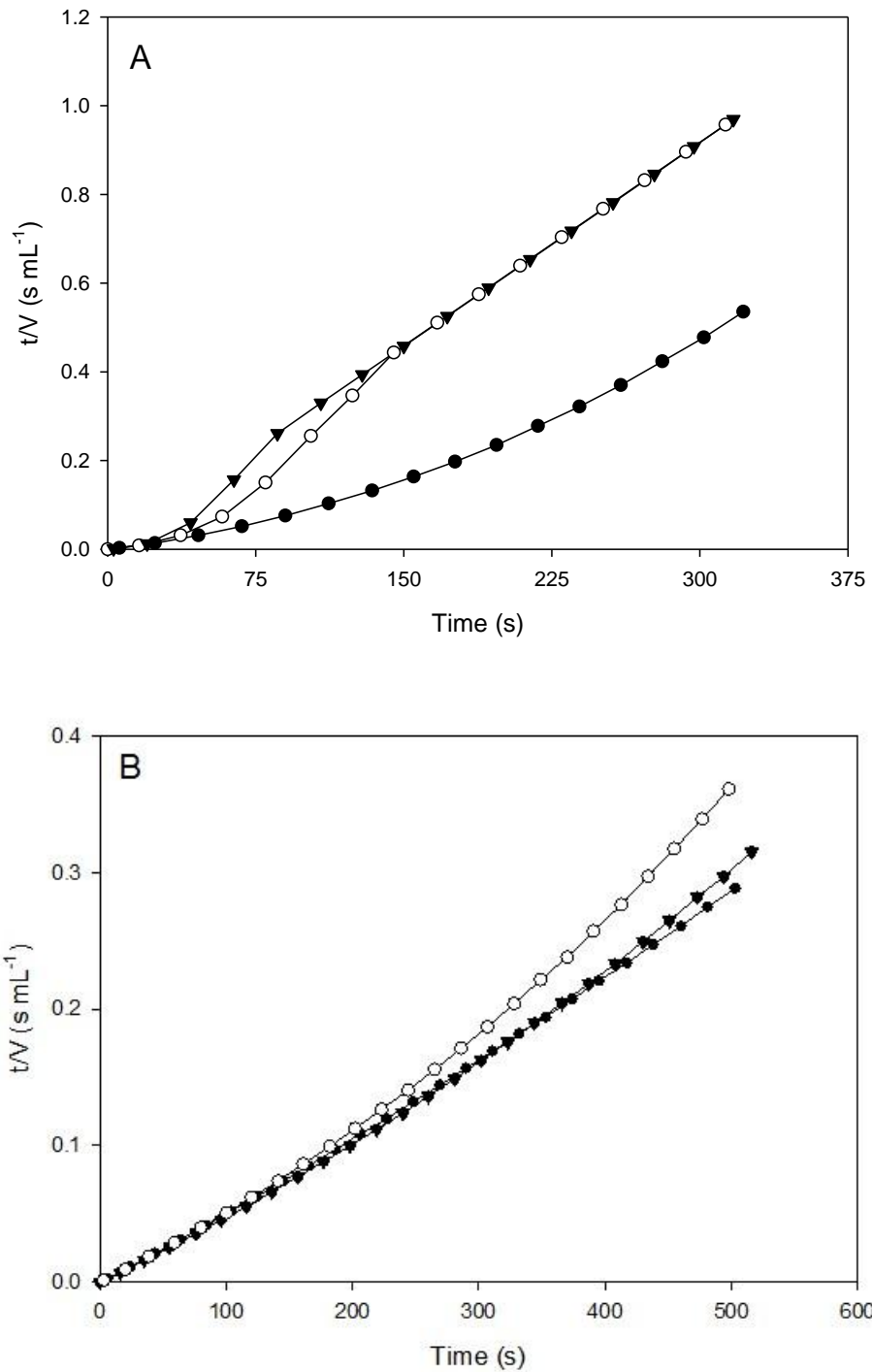
Figure 5.18: *V_{max} for clarified homogenate pH 7.4 (control) (○), PEG 12000 6.25% w/v/0.4 M sodium citrate pH 7.4 (multimodal) (▼) and PEG 12000 15% w/v pH 7.4 (single mode) (●) feedstreams for cumulative filtrate volume using a Cuno Zeta Plus 05SP filter (A) and Cuno Zeta Plus 30SP filter (B). V_{max} for the multimodal feedstream was calculated to be 200 and 400 L m^{-2} for 05SP and 30SP filters respectively*

V_{max} for the multimodal feedstream was calculated to be 200 and 400 L m^{-2} for 05SP and 30SP filters respectively (figure 5.19). A 205 cm^2 30SP filter would be sufficient to filter 1000 mL of material in 30 minutes.

To complete a process run through, 100 mL of the three feedstreams were prepared to generate sufficient material for depth filter clarification and subsequent steps. Feedstream 1 was clarified homogenate used as a standard, feedstream 2 was the multimodal feedstream where the Fab' is not precipitated, and feedstream 3 was material precipitated by PEG 12000 15% w/v pH 7.4 (single mode). The feed material was spun at 6100 rpm for 12 minutes in a Eppendorf 5810R centrifuge (Eppendorf UK Ltd., Cambridge, UK), which was equivalent flow rate to settling area ratio to the disc stack centrifuge. The spun down material in feedstreams 1 and 3 were resuspended using 100 mM Tris HCl pH 7.4 to 150 mL. Material was later diafiltered using the ÄKTA Crossflow (GE Healthcare, Uppsala, Sweden).

A BioCap 30 Filter (30SP) with 25 cm^2 area was used for the purpose of the run through. Table 5.6 highlights the clarification of the three feedstreams at 100 mL. Purification factor post filtration was 1.2, 1.4 and 1.2 for homogenate, multimodal and single mode feedstreams respectively.

Filter	Feedstreams	Initial Fab' conc ($g\ L^{-1}$)	Initial total protein conc ($g\ L^{-1}$)	Total protein conc post filtration ($g\ L^{-1}$)	Recovery (%)	Purification factor
30SP	Homogenate	1.26	4.61	3.66	97	1.21
	Multimodal	1.31	3.39	2.35	98	1.35
	Single mode	1.27	3.22	2.52	96	1.23

Table 5.6: *Purification factor after filtration of 100 mL of each feedstream through a Cuno BioCap 30 Filter (30SP, 25 cm^2 filter area) (Cuno, Meriden, USA)*

The experimental results showed that the clarification obtained in the multiwell filtration design and the conventional unstirred normal flow membrane systems were comparable. The microscale method allows for multiple filter and filter types to be investigated rapidly using small sample quantities. It was found that membrane pore size influence flux and transmission rates. This is in agreement with previous findings (Kong *et al.,* 2010).

5.5.3 Tangential Flow Ultrafiltration/Diafiltration Step Prior to Packed Bed Studies

It has been reported that monomer could be separated from dimers of the antibody Alemtuzumab using ultrafiltration in a stirred cell experiment (Wan *et al.,* 2004). Alemtuzumab had a molecular weight of ~155 and p*I* of 8.5-9.0. The experimental set up consisted of a stirred cell ultrafiltration module which had a working volume of 6.0 mL under constant volume diafiltration.

The aim of this study was to prepare the three feedstreams for packed bed studies and to reduce the level of total protein by retaining the Fab' in the retentate. A 50 cm^2 PES membrane (GE Healthcare, Uppsala, Sweden) was used to buffer exchange the feedstreams with 25 mM sodium acetate/25 mM sodium chloride pH 5 using an ÄKTA Crossflow system (GE Healthcare, Uppsala, Sweden), which had a tangential flow mechanism in contrast to the stirred cell apparatus evaluated by Wan *et al.,* (2004). The use of ultrafiltration/diafiltration to reduce total protein levels has the potential to improve the performance of subsequent packed bed steps.

The three feedstreams were diafiltered using a ÄKTA Crossflow (GE Healthcare, Uppsala, Sweden) with a 50 cm^2 PES membrane (GE Healthcare, Uppsala, Sweden) (table 5.7). Tangential flow was kept constant at 30 mL min^{-1}, with a constant TMP of 1 bar.

5.5.3.1 Preproduct Step

An ultrafiltration method was created using the method wizard. The method was split into three separate methods, namely preproduct, product and postproduct methods, to better control the runs. The method wizard exaggerated the preproduct cleaning step, and to reduce the time taken for the ÄKTA Crossflow (GE Healthcare, Uppsala, Sweden) to complete the preproduct method, the commands

'Fill_Reservoir_To_Max_Volume', 'Stop_Trans_Pump', and 'Empty_Reservoir_Completely' were deleted from the sub block 'Prepare_SystemAndReservoir' under the main block PREPRODUCT_STEP_CIP. The same commands were deleted from the main block PREPRODUCT_STEP_WATER_FLUSH.

The preproduct method was used to clean all the inlet and outlet lines of the ÄKTA Crossflow (GE Healthcare, Uppsala, Sweden) with 0.1 M sodium hydroxide followed by a rinse with the appropriate buffer (table 5.7). The membrane was cleaned and conditioned with 2 M sodium chloride, 0.1 M sodium hydroxide followed by deionised water prior completing a normalised water permeability (NWP) test. The NWP is the rate of clean water flux through the membrane under conditions of standard pressure and temperature, and is used for measuring the effect of cleaning of membranes. This test was performed in both pre and postproduct steps. Following the NWP test, the membrane was conditioned with 25 mM sodium acetate/25 mM sodium chloride pH 5 diafiltration buffer.

ÄKTA Crossflow inlet/outlet lines	Buffer
Inlet line 1	100 mL of sample
Inlet line 2	25 mM sodium acetate/25 mM sodium chloride pH 5
Inlet line 5	Deionised water
Inlet line 6	2 M sodium chloride
Inlet lines 7	0.1 M sodium hydroxide
Retentate outlet line 1	Flush collected post UF/DF
Retentate outlet line 2	Waste
Retentate outlet line 3	Product collected post UF/DF
Permeate outlet lines 1 to 3	Waste

Table 5.7: *ÄTKA Crossflow (GE Healthcare, Uppsala, Sweden) setup. All inlet and outlet lines were cleaned with 0.1 M sodium hydroxide followed by a rinse with the appropriate buffer. Inlet line 2 was also used for the conditioning of the membrane with diafiltration buffer prior to diafiltration. Inlet lines 3, 4 and 8 were not used. The permeate was not collected.*

5.5.3.2 Product Step

The buffer exchange replacing the sample buffer with 25 mM sodium acetate/25 mM sodium chloride pH 5 was performed over five diavolumes to reduce the conductivity of the feedstreams to 4.5 mS cm^{-1} ± 0.1. The ÄKTA Crossflow (GE Healthcare, Uppsala, Sweden) automatically determined when steady state had been reached. The diafiltration step was performed prior to the concentration step, which was omitted to overcome the precipitation issues occurring at pH 5 when the concentration of the feed material increased when using the conventional approach of concentration followed by diafiltration. Recovery of the product with a 10 mL flush was collected in all experimental runs after the flush had been recirculated for 30 minutes.

It was observed that the membrane retained significant amount of material (figure 5.19). The decrease in absorbance levels at the permeate side can be explained by rapid fouling of membrane when product was freshly exposed to the membrane. The gel layer that was building up across the membrane surface may have affected the passage of material through the membrane surface (Wan *et al.,* 2004).
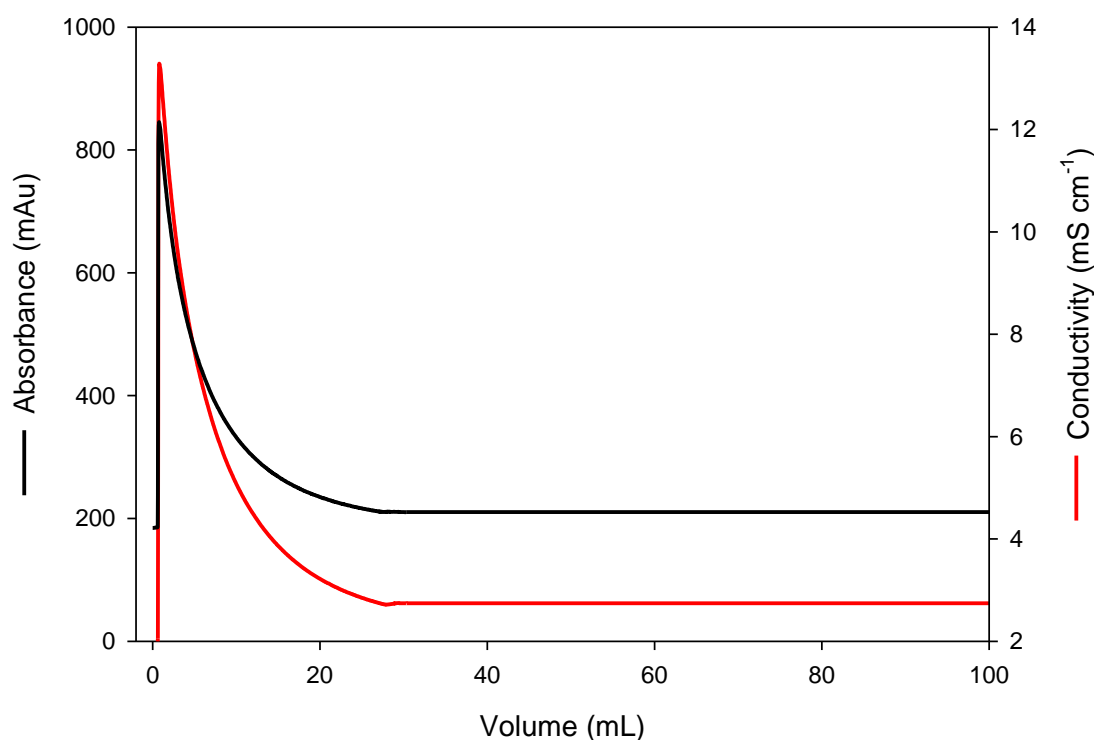
Figure 5.19: *Typical absorbance (-) and conductivity (-) profiles for the diafiltration of the feedstreams collected from the permeate side of the 50 cm² PES membrane (GE Healthcare, Uppsala, Sweden) (clarified homogenate shown in this case). Tangential flow was kept constant at 30 mL min⁻¹, with a constant TMP of 1 bar. Conductivity of all three feedstreams reached 4.5 mS cm⁻¹ ± 0.1 after 5 diavolumes*

5.5.3.3 Postproduct Step

The method was not reduced to avoid comprising the cleaning process of the membranes tested. 2 M NaCl and 0.1 M NaOH were used for CIP of the membrane. However, the PREPRODUCT_STEP_BUFFER_COND block from the preproduct method was inserted at the end of the postproduct method to reduce time taken to condition the membrane for subsequent runs. Table 5.8 highlights the Fab' concentration and recovery post UF/DF. The NWP clean postproduct runs for homogenate, multimodal and single mode feedstreams were calculated by the Unicorn software (GE Healthcare, Uppsala, Sweden) to be 90%, 89% and 87% of the original preproduct run value respectively, suggesting some irreversible fouling of the membrane. The membrane could have had a better NWP by using a harsher cleaning reagent such as 1 M NaOH after 2 M NaCl.

Feedstreams	Initial Fab' concentration ($g\ L^{-1}$)	Fab' concentration post UF/DF ($g\ L^{-1}$)	Recovery (%)	NWP (%)
Homogenate	1.22	1.06	87	90
Multimodal	1.28	1.24	97	89
Single mode	1.22	1.13	93	87

Table 5.8: *Fab' concentration and recovery post UF/DF using the ÄKTA Crossflow (GE Healthcare, Uppsala, Sweden) at TMP 1 bar, constant retentate flowrate of 30 mL min⁻¹*

5.5.4 Further Purification of Fab' Using Packed Bed Chromatography

5.5.4.1 Dynamic Binding Capacity, Gradient Elution and Step Elution Studies

The conventional affinity chromatography matrix consists of porous particle beads (Brochier *et al.,* 2008). The pores within the particles are blocked, and thus the liquid inside them is stagnant (Thömmes and Etzel 2007). Subsequently the molecules to be separated are transported between the blocked pores and back to the mobile phase via diffusion (Thömmes and Etzel 2007). Diffusion is a slow process, and in the case of large molecules with low diffusion coefficients, diffusion is the rate determining step of the overall separation time (Brochier *et al.,* 2008). Incidentally, separation resolution is dependent on residence time of the sample within the stationary phase, and therefore the velocity of mobile phase through the column (Brochier *et al.,* 2008).

Proteins have an either net positive or negative charge depending on their surrounding environment (i.e. buffer composition), and ion exchange chromatography is a key method at separating proteins based on differences in net charge. Ion exchange chromatography exploits differences in the net charge of proteins. The SP Sepharose (GE Healthcare, Uppsala, Sweden) resin is a strong cation exchange resin, which is negatively charged (SO_3^-) over a wide range of pH values. The buffer conditions used for SP Sepharose (GE Healthcare, Uppsala, Sweden) chromatography, results in the proteins having a net positive charge, therefore, the protein binds, whilst impurities flow through the column. The bound

protein is eluted when buffer conditions are altered with increasing salt concentration.

In this section, a 1 mL SP Sepharose Hi Trap pre packed bed column (GE Healthcare, Uppsala, Sweden) on a ÄKTA FPLC (GE Healthcare, Uppsala, Sweden) was used to capture Fab' from the three feedstock solutions. The column was operated at 1 mL min^{-1} and washed with ten column volumes of equilibration buffer (table 5.9). The feed material was then passed through a 0.22 μm filter prior to loading. A gradient elution of 25 mM to 200 mM sodium chloride pH 5 over 15 column volumes (CV) was used to elute bound material from the column. 1 mL (1 CV) fractions were taken of the load, and elution volume. The strip and post load wash (PLW) were collected in separate containers. The column was cleaned with 5 mL of strip buffer, followed by 2 mL clean with 0.1 M sodium hydroxide. The buffers used are listed in table 5.9. A height equivalent of a theoretical plate (HETP) test was performed at a flowrate of 1 mL min^{-1} using 0.02 CV of 0.5 M sodium hydroxide injected via a 0.5 mL superloop. The theoretical number of plates were 1849 with an asymmetry of 1.01 calculated by the Unicorn software (GE Healthcare, Uppsala, Sweden).

Step	Buffer	Volume (CV)
Equilibration	25 mM sodium acetate/25 mM sodium chloride pH 5	10
Load	1.06 g L^{-1}, 1.24 g L^{-1} and 1.13 g L^{-1} of homogenate, multimodal and single mode feedstreams respectively	25
Post Load Wash	25 mM sodium acetate/25 mM sodium chloride pH 5	5
Elution	A: 25 mM sodium acetate/25 mM sodium chloride pH 5 B: 25 mM sodium acetate/200 mM sodium chloride pH 5	0% B to 100% B over 15 CV
Strip	25 mM sodium acetate/2.0 M sodium chloride pH 5	5
Clean	0.1 M sodium hydroxide	2
Storage	20% ethanol	5

Table 5.9: *SP Sepharose (GE Healthcare, Uppsala, Sweden) DBC and gradient elution conditions*

Dynamic binding capacities (DBC) were estimated by passing the homogenate, multimodal and single mode feedstreams at a concentration of 1.1 g L^{-1}, 1.2 g L^{-1} and 1.1 g L^{-1} respectively through the column and measuring the volume at which 100% breakthrough occurred, using analysis by Protein G HPLC (GE Healthcare, Uppsala, Sweden) as described in section 2.1. These data are represented diagrammatically in figure 5.20.

$$DBC = \frac{P \times C}{V}$$

Equation 5.7: *The dynamic binding capacity (DBC) of Fab' using SP Sepharose (GE Healthcare, Uppsala, Sweden) (g L^{-1}) was calculated based on the volume of product loaded (P), the product concentration (C) and the column volume (V) (Wenger 2010)*
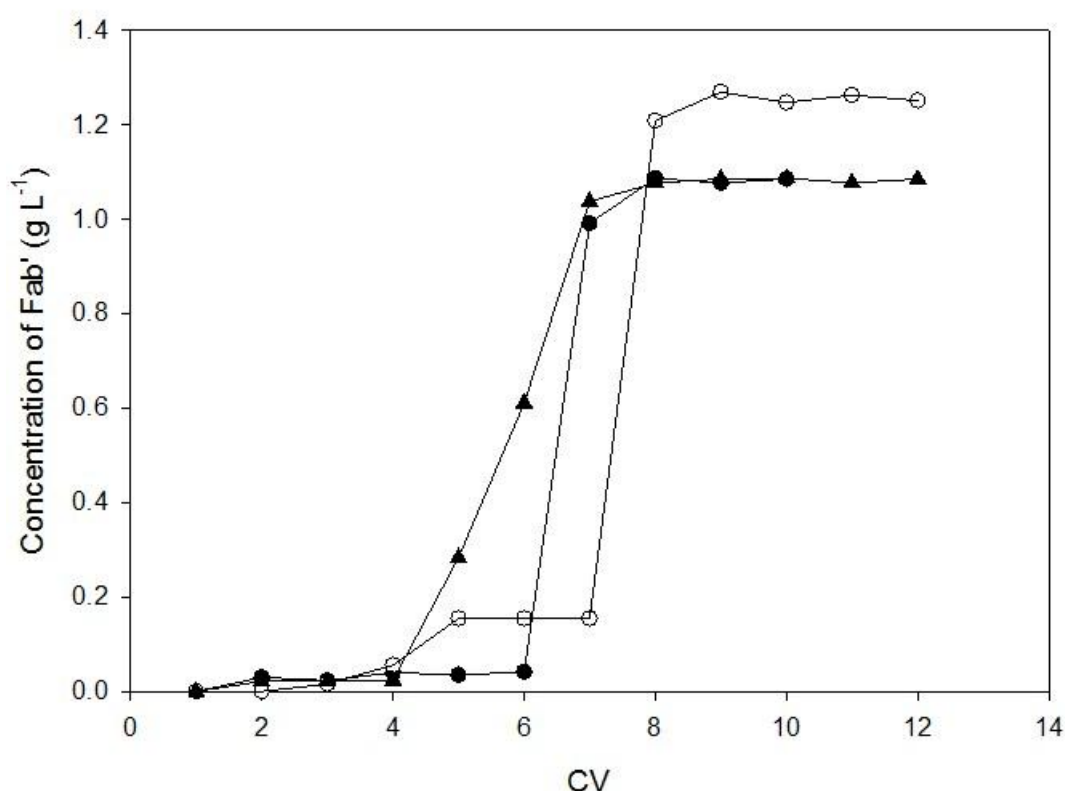
Figure 5.20: *Breakthrough curves of Fab' in clarified E.coli homogenate (control) (●), multimodal (PEG 12000 6.25% w/v/0.4 M sodium citrate) (○) and single mode (PEG 12000 15% w/v) (▲) feedstreams using SP Sepharose (GE Healthcare, Uppsala, Sweden) at 1 mL min^{-1}. DBC at 100% breakthrough was calculated to be 8.4 g L^{-1}, 11.1 g L^{-1} and 9.0 g L^{-1} respectively for these feedstreams. All runs were performed in a column volume of 1 mL and constant feed conductivity of 4.5 mS $cm^{-1} \pm 0.1$*

Figure 5.20 presents breakthrough curves obtained at linear velocities of 1 mL min^{-1} for the three feedstreams, and table 5.10 compares the dynamic binding capacities measured at 5% and 80% of 5% breakthrough for operational purposes. Binding

capacity data is used industrially during process development to assess adsorbent performance (Staby *et al.,* 2004). The breakthrough curves are very steep for the homogenate and multimodal feedstreams, indicating that virtually no Fab' was being adsorbed. In this case, the highest binding capacity observed was for the homogenate feedstream at 6.4 g L^{-1} as it had the sharpest breakthrough curve being able to utilise the capacity of the column. There was a minor decrease in the binding with the addition of multimodal precipitant of 6.2 g L^{-1}, which was reduced further to 5.7 g L^{-1} for the feed material with single mode precipitant. It is possible that in part the concentration of PEG 12000 has an effect on binding capacity possibly due to competition between several species for adsorbent binding sites. This may be countered by reducing the operating flowrate to increase Fab' binding capacity. In addition, Fab' is a small protein (~54 kDa) and will have a reduced number of binding sites relative to a full IgG protein, which in part explains the low binding capacity with this resin.

It was observed that breakthrough curve was shallower for the feedstock with the single mode precipitant. This could be explained in part due to the slight compression of the bed observed in these experiments. Colby *et al.,* (1996) suggested that the compression of the bed has no effect on the performance of the system, although it could result in variations in breakthrough curves. The compression of the bed reduces void volume resulting in premature breakthrough and curve development.

Feedstreams	5% Breakthrough (g L^{-1})	Adjusted 80% of 5% Breakthrough (g L^{-1})
Homogenate	6.36	5.09
Multimodal	6.20	4.96
Single mode	5.65	4.52

Table 5.10: *Binding capacity (g L^{-1}) at various product breakthrough levels for clarified feedstock's at 1 mL min^{-1} flowrate. All runs were performed with a 1 mL SP Sepharose Hi Trap column (GE Healthcare, Uppsala, Sweden) and constant feed conductivity of 4.5 mS cm^{-1} ± 0.1*
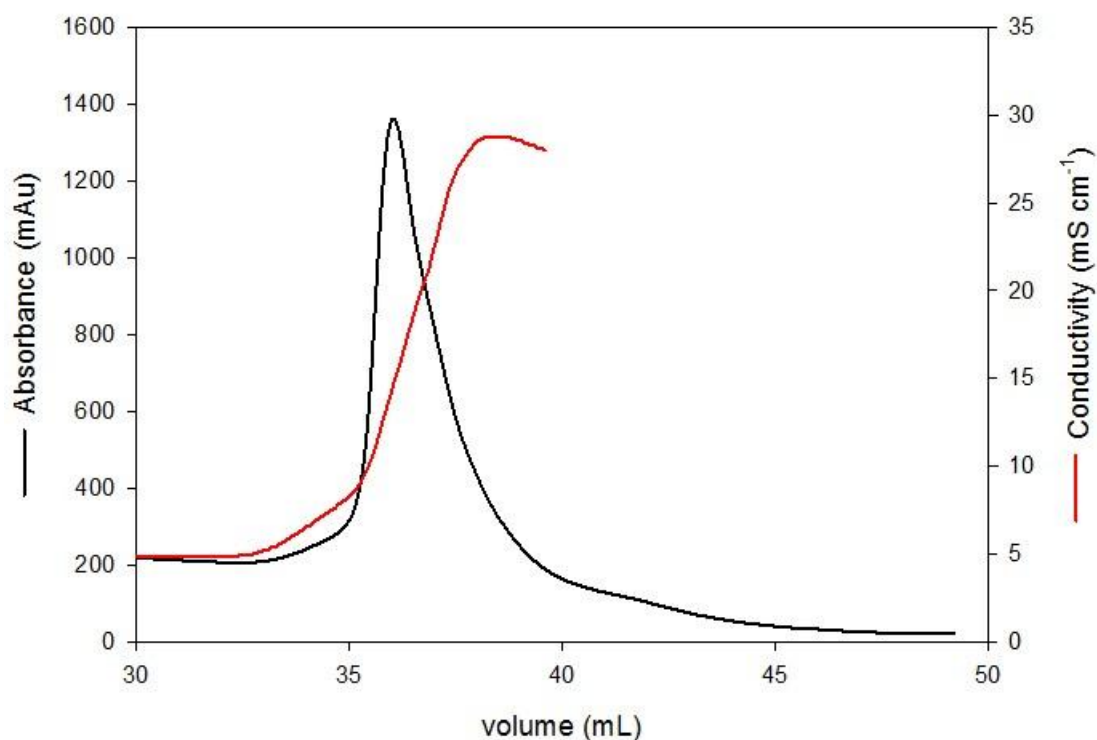
Figure 5.21: *Typical gradient elution peak of Fab' (-) (clarified homogenate shown in this case) with SP Sepharose (GE Healthcare, Uppsala, Sweden) at 1 mL min^{-1}. All runs were performed in a column volume of 1 mL and constant feed conductivity of 4.5 mS cm^{-1} ± 0.1. Gradient elution conditions were 25 mM sodium acetate/25 mM sodium chloride pH 5 to 25 mM sodium acetate/200 mM sodium chloride pH 5 over 15 CV (-)*

A gradient elution of 25 mM to 200 mM sodium chloride over 15 CV was used to elute bound material from the column. One mL fractions (1 CV) were taken of the elution volume programmed to start collecting at 100 mAu OD$_{280}$ and to stop collecting at 100 mAu OD$_{280}$ from the downslope of the peak. The strip and post load wash were collected in separate containers. The gradient elution chromatogram (figure 5.21) was typical of the elution profiles observed with all three feedstreams. Figure 5.21 shows the elution profile for clarified homogenate.

It was observed that the loading of all three feedstreams at 1 mL min^{-1} had an effect on the pressure drop, causing the system pressure limit of 0.1 MPa to be reached after one CV. The system pressure limit was increased to the column pressure limit

of 0.3 MPa to overcome the system alarm. It is possible that the increase in the pressure drop is related to the accumulation of impurities at the top of the column. The conductivity at the midpoint at the downslope occurred in fraction 8, which was measured at 11.5 mS cm^{-1} at 23°C. This was then used to calculate a sodium chloride concentration of 99 mM. Subsequently, buffers with the calculated salt concentrations were prepared for the step elution runs (table 5.10).

The three feed stocks at a concentration of 1.1 g L^{-1}, 1.2 g L^{-1} and 1.1 g L^{-1} for homogenate, multimodal and single mode feedstreams were used to run a step elution with 25 mM sodium acetate/99 mM sodium chloride pH 5 over 10 CV. Therefore, 4.8 mL, 4.0 mL and 4.4 mL of each feedstock was loaded via a 10 mL superloop using an ÄKTA FPLC (GE Healthcare, Uppsala, Sweden), which was the calculated volume for 80% of 5% breakthrough. This equated to 5.1 mg, 5.0 mg and 5.0 mg being loaded onto the column per millilitre of matrix respectively for the three feedstreams.

Feedstreams	Step	Volume collected (mL)	Conc (mg mL^{-1})	Mass (mg)	Total % mass	% Recovery elution	Final PF
Homogenate	Load	4.80	1.06	5.09	91.4	83.7	2.5
	FT	4.80	0.06	0.24			
	Wash	5.00	0.03	0.15			
	Elution	10.00	0.43	4.26			
Multimodal	Load	4.00	1.24	4.96	90.9	77.8	4.4
	FT	4.00	0.10	0.40			
	Wash	5.00	0.05	0.25			
	Elution	10.00	0.39	3.86			
Single mode	Load	4.39	1.13	4.96	90.7	83.5	3.5
	FT	4.39	0.07	0.31			
	Wash	5.00	0.01	0.05			
	Elution	10.00	0.41	4.14			

Table 5.11: *Experimental outputs for Fab' from the three feed stocks after the step elutions using a 1 mL Hi trap SP Sepharose column (GE Healthcare, Uppsala, Sweden). Feedstreams were loaded at 80% of 5% breakthrough (table 5.9) and the step elution buffer used was 25 mM sodium acetate/99 mM sodium chloride pH 5*

It was found that the percentage recovery of elution was 84%, 78% and 84% for homogenate, multimodal and single mode feedstreams respectively. Total mass accounted for was on average 90% for each of the runs. The final process purification factor for homogenate, multimodal and single mode feed stocks were 2.5, 4.4 and 3.5 respectively (table 5.11). The use of multimodal precipitated impurities prior to a packed bed step had improved process performance by a PF of 1.9. Therefore, this investigation of whole process interactions with material prepared by precipitation demonstrated the importance of reducing impurities early in the process that can negatively interact with subsequent operations. The results show how modest purification factor in the initial precipitation steps are amplified by interactions with subsequent operations leading to radically differing performance. This underlines the importance of whole bioprocess studies and scale down methods as a means of achieving this. The impact of which has the further potential to improve the longevity of chromatography resins and reducing overall downstream purification cost.

5.6 Summary

A high throughput system utilising robotic handling was developed in microwells to investigate conditions to increase particle size. It was found that d_{50} particle size was 313 μm at low speed mixing conditions (800 rpm) with the addition of homogenate to PEG 12000 6.25% w/v/0.4 M sodium citrate pH 7.4 at 900 μL s^{-1} after 60 minutes of mixing.

A USD system was used to mimic the shear rates found in the feed zone of a disk stack centrifuge in the laboratory. Good agreement of clarification was achieved between laboratory scale and the pilot centrifuge. Laboratory scale efficiency was 93%, whereas the pilot scale separation efficiency was 87%.

A process run through was performed with homogenate pH 7.4 (control), multimodal (PEG 12000 6.25% w/v/0.4 M sodium citrate pH 7.4) and single mode (PEG 12000 15% w/v pH 7.4) feedstreams. The clarification of the precipitated material was examined during a membrane filtration operation using an automated multiwell filtration technique prior to packed bed studies. Filtration experiments of three feedstreams were performed with Cuno Zeta Plus 30SP membrane filters (Cuno, Meridan, USA). This was followed by a diafiltration step to prepare material for the following cation exchange chromatography step. A 1 mL SP Sepharose Hi Trap pre

packed bed column (GE Healthcare, Uppsala, Sweden) was used to capture Fab' from the three feedstock solutions. The final process purification factor for the three feedstreams were 2.5, 4.4 and 3.5 respectively. The use of multimodal precipitated impurities prior to a packed bed step had improved process performance by PF 1.9.

6. CONCLUSIONS AND FUTURE DIRECTIONS

6.1 Conclusions

The efficient purification of recombinant proteins for therapeutic applications from cell culture fluid has become a major bottleneck for the industry due to the increasingly high titers found in upstream feeds (Taipa *et al.,* 2001). These process limitations are currently dominated by chromatography, which can account for more than 70% of downstream processing costs due to resin expenditure, throughput and complexity of scale up (Hahn *et al.,* 2003). Conventional downstream processes such as chromatography and filtration will soon reach their limits in terms of economics, processing speed and scale, including labour and overhead costs (Bensch *et al.,* 2007). Non chromatographic separation techniques such as precipitation can be used to remove impurities in cell culture fluid prior to a costly chromatography step. The removal of impurities prior to chromatography can be cost effective by improving binding capacity, reducing bed volume and buffer consumption, and potential for increasing the number of cycles the chromatography resin can be efficiently used for.

Conventionally, the study of precipitation conditions will seek to design a step to either precipitate the target protein, leaving process related impurities in solution, or to precipitate the impurities and leave the target protein in solution. At laboratory scale, the screening of a large number of precipitation conditions to find a suitable window of operation may not be economically feasible due to the large amount of feedstream and resources required for each experiment (10-100 mL). To overcome this issue, developing techniques that can generate data with minimal resource expenditure by mimicking large scale processes can be invaluable in early bioprocess development.

The next generation of bioprocess development will integrate microscale bioprocessing techniques into bioprocess development to alleviate the challenges facing it. Microscale platforms offer a change in bioprocess development by accelerating process development due to the flexibility for parallel experimentation and automation while requiring microscale quantities (20-2000 μL) of material (Galaev 2005, Titchener-Hooker *et al.*, 2008). Critical bioprocess information can be obtained earlier in development providing a better opportunity to understand

process parameters and for improved understanding of the robustness of each processing step.

A key consideration in this approach is the compatibility of microscale platforms with laboratory automation, specifically the Tecan robotic platform (Tecan, Reading, UK) (figure 4.2) to enable large experimental design spaces to be studied. The key to understanding the whole of bioprocess is to enable a fundamental understanding of each unit operation, in this case precipitation, and their impact on subsequent unit operations. In this thesis, microscale techniques enabled the study of large, multiparameter design spaces, specifically facilitated by its high throughput and low volume features.

6.1.1 First Major Milestone of Project

1. **Development of a high throughput system utilising automated robotic handling in 96 microwells at 1 mL scale to enable rapid screening of large design spaces in a Quality by Design (QbD) approach to integrate microscale bioprocessing techniques into conventional bioprocess development.**

In this thesis, the use of a Quality by Design approach outlined in ICH guideline Q8 (R2) has been utilised. Throughout the thesis this approach was used to select process parameters and unit operations that impact critical quality attributes to create a robust scalable process. This approach utilised in industry when combined with the appropriate control strategy can allow for more flexible regulatory applications.

In chapter 2, the release of Fab' from *E.coli* cells is described. Cell disruption by continuous homogenisation was investigated using an APV Manton-Gaulin Lab40 (APV International, West Sussex, UK) high pressure homogeniser. An increase in micronisation of cell debris occurred with increasing number of homogenisation passes, making solid-liquid separation more difficult (figure 2.6). As a result, maximal product release while avoiding micronisation was chosen as the criteria to determine the number of cycles required for future homogenisation. One pass at 500 bar was found to be sufficient to release the maximum amount of Fab' while minimising micronisation of cell debris (d_{50} 0.30 μm at 500 bar for 1 pass).

In chapter 3, a high throughput precipitation process utilising automated robotic handling was developed using 1.3 mL 96 deepwell plates (Nunc GmbH & Co., KG, Denmark), at 1 mL scale per well, to enable the rapid screening of a large number of variables in parallel using a Quality by Design approach based on ICH guidance Q8 (R2). 5 mm PTFE magnetic coin stirrers placed at the bottom of the deepwells were used for mixing. The strength of the magnets and their interference with each other limited throughput to 48 individual experiments on one plate.

The effect of PEG on the precipitation of Fab' was investigated in a screening study to identify key variables and their ranges for further study and scale up. This was studied using a full factorial two level Design of Experiments (DoE) approach to investigate yield and purification factor of Fab' by varying PEG molecular weight, PEG concentration (% w/v), homogenate concentration and pH. In the range investigated, PEG concentration had the most influence on yield and purification factor, whilst pH was found to have minimal influence on yield and purification factor in the range investigated. A high homogenate dilution factor between 3 and 5 negatively impacted yield and increased processing volumes whilst increasing the purification factor. Therefore, a trade-off between yield and purification factor was required, prioritising yield as the precipitation step is proposed as a primary purification step. An optimisation study, in the form of a central composite face centred (CCF) DoE was then performed. The goal was to adjust the key variables so that a favourable response profile with regard to Fab' yield and purification factor was obtained. In this design no further constraints were placed on parameter input ranges (pH 5 to 9; dilution factor 1 to 5; PEG molecular weight 4000 to 20000) except PEG concentration which was limited to 10% to 20% w/v as it was found that less than 10% w/v PEG resulted in unfavourable Fab' yield ≤ 50%.

Figure 6.1 is a graphical representation of the knowledge space (within the unexplored space), which refers to the region of process understanding defined by the input boundaries of the CCF DoE. The input boundaries were PEG 4000 to 20000, PEG concentration 10% to 20% w/v, pH 7.4 and homogenate dilution factor of 1. The design space is comprised of the overlap of Fab' yield (%) and purification factor to give a robust region where Fab' yield was ≥90% with a maximum purification factor of 1.7 within the knowledge space. However, the highlighted area within the design space is the proposed design space for operational simplicity. This is due to the use of PEG as precipitant, since at high molecular weights and

concentrations, the high viscosity of PEG could cause difficulties in processing at large scale. Therefore the normal operating range (NOR) or control space was defined in a way that can be "demonstrated to provide assurance of quality" (ICH Q8 (R2) 2009) by having the distance from the edge of the design space at ± PEG 1000 and ± 1% w/v. This is highlighted by the dashed area in figure 6.1 within the highlighted area of the design space; allowing for flexibility and robustness at manufacturing scale since "working within the design space is not considered as a change" (ICH Q8 (R2) 2009). Movement out of the design space is considered to be a change and would normally initiate a regulatory post-approval-change process. In essence, the knowledge of the factors affecting Fab' yield and purity can assist in the development of a process manufacturing design space which lies at the heart of a practical realisation of Quality by Design.
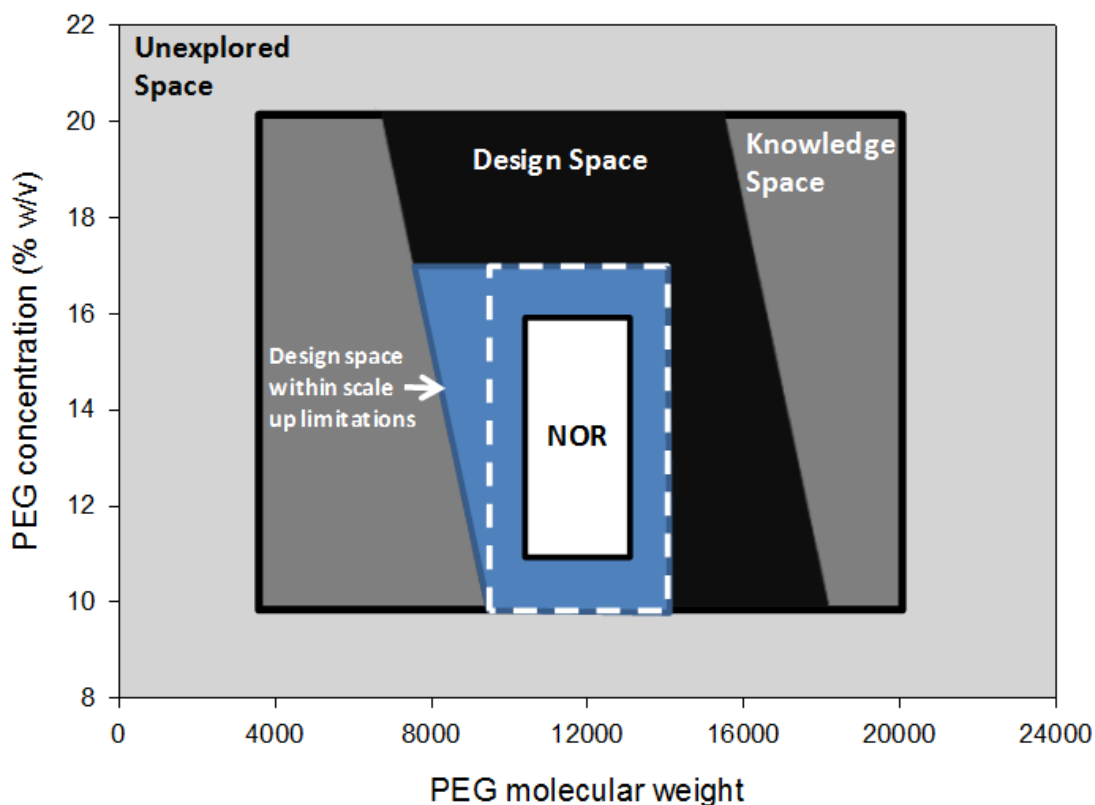
Figure 6.1: *Proposed Fab' precipitation design space comprised of the overlap region for yield (%) and purification factor created using MODDE 9.1 (Umetrics, Malmö, Sweden). Knowledge space refers to the region of process understanding based on the CCF DoE inputs. Inputs were PEG molecular weight, PEG concentration, pH 7.4 and undiluted homogenate. The design space is a region where the combination of ranges that delivers a Fab' yield ≥ 90% with a maximum purification factor of 1.7. The selected area within the design space was the proposed design space for scale up for operational simplicity. Outside of this region, viscosity of PEG may become an issue at process scale and therefore the Normal Operating Range (NOR) was set to ± PEG 1000 and ± 1% w/v within the dashed area of this design space*

6.1.2 Second Major Milestone of Project

> **2. Developing a novel multimodal precipitation process combining polyethylene glycol (PEG) with ammonium sulphate, sodium citrate and sodium chloride for the precipitation of Fab' and or protein impurities from partially clarified homogenised *E.coli* feedstocks.**

In chapter 4, mixing conditions were optimised by use of a microscale mixing system incorporating 96 x 5 mm PTFE magnetic coin stirrers (V&P Scientific, San Diego, USA). The magnets were mounted onto an acrylic plate, which would sit on top of a 1.3 mL 96 deepwell plate (Nunc GmbH & Co., KG, Denmark), suspending the coin stirrers approximately 1/6 off the bottom of each well (figure 4.3). This allowed use of all 96 wells in the plate increasing productivity by 50% relative to the previous mixing method described in chapter 3, and enabled control over the speed of the mixing, which enabled Power dissipation per unit volume to be used as a scale up parameter.

The system was used to study a novel multimodal precipitation process combining PEG with ammonium sulphate, sodium citrate and sodium chloride for the precipitation of Fab' and or protein impurities from partially clarified *E.coli* feedstocks. Each of the salts, members of the Hofmeister series are known to have an effect of inducing precipitation when used individually at different levels (Balasundaram *et al.,* 2011). A three level full factorial DoE was designed using PEG molecular weight, PEG concentration (% w/v), pH, ammonium sulphate concentration and sodium citrate concentration. However, with salt concentrations greater than 0.8 M combined with PEG concentrations greater than 5% w/v, a two phase system was observed. This affected 40% of the design space, which was excluded from analysis as a two phase system was beyond the scope of this project (this was further discussed in section 4.5.1).

An optimisation DoE (CCF DoE) was then designed to study multimodal precipitation of Fab' and protein impurities, whilst reducing those variables that would not have a significant effect on the system based on previous experimental data. Input ranges were reduced to using PEG 12000, pH 7.4, and dilution factor of feed material of one/undiluted (the dilution of the feed material is undesirable as it results in large processing volumes at process scale), with ammonium sulphate, sodium citrate and sodium chloride concentrations over a PEG concentration range

between 0% to 20% w/v. The maximum total molar salt concentration in the system was limited to 0.6 M to prevent aqueous two phase formation between PEG and the salts. It was found that PEG concentration (% w/v) was the most important factor for Fab' yield in the range investigated. 90% Fab' yield with a purification factor of 1.9 was achievable using 15% w/v PEG 12000/0.30 M sodium citrate/0.15 M ammonium sulphate. This was an improvement of 26% relative to the use of 15% w/v PEG 12000 pH 7.4 in single mode.

Changes in Fab' and total protein solubility profiles were observed with varying salt concentrations, for example sodium citrate was found to have a Fab' stabilising effect. At ≤ 0.4 M concentrations of sodium citrate Fab' precipitation was low, < 5% at pH 7.4 suggesting that electrostatic interactions dominate at this concentration range. The introduction of low concentrations of salt may be thermodynamically favourable resulting in an increase in solubility of the protein (Arakawa and Timasheff 1982). It is thought that this in part due to the positive interaction between Fab', salt and PEG attributed in part to the binding of positively charged Fab' via electrostatic interactions with negatively charged species such as micronised cell debris and chromosomal DNA in the homogenate which disassociates in the presence of salt (Balasundaram *et al.,* (2011). It was observed that at low concentrations of PEG and sodium citrate, ~20% protein impurities were precipitated in preference to Fab', which presented an opportunity for removal of protein impurities via a precipitation step (figure 6.2).

Figure 6.2 is a graphical representation of the knowledge space, which refers to the region of process understanding defined by the input boundaries of the combination of the full factorial and CCF DoE with sodium citrate and PEG 12000. The input boundaries were 0 to 1 M sodium citrate, PEG 12000, PEG concentration 0% to 20% w/v, pH 7.4 and homogenate dilution factor of 1. The design space, within the knowledge space, is comprised of the overlap of Fab' yield (%) and purification factor to give a robust region where purification factor was > 0.8 and Fab' loss was ≤ 10%. The normal operating range (NOR) or control space was defined by a combination of PEG and sodium citrate concentration ranges as ± 0.5% w/v and ± 0.05 M respectively. This is highlighted by the dashed area in figure 6.2 within the design space to give a region of assurance of quality, flexibility and robustness at manufacturing scale.

Working within the NOR, a flow through precipitation strategy with PEG 12000 6.25% w/v/0.4 M sodium citrate pH 7.4 (homogenate dilution factor of one) was used to precipitate protein impurities early in the downstream process. The advantage at process scale is the potential ease of processing due to removal of a solubilisation step and the significantly reduced viscosity of the precipitating agent relative to that of PEG in the NOR shown in figure 6.1.
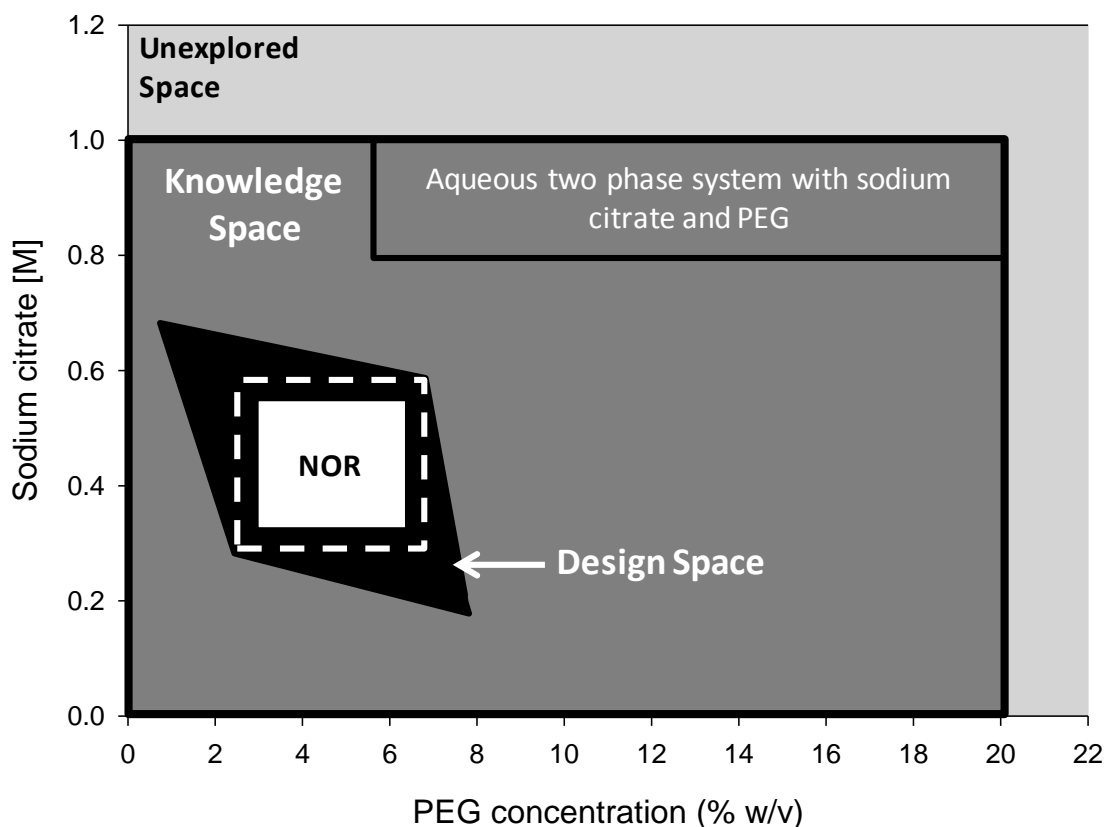
Figure 6.2: *Proposed protein impurity precipitation design space comprised of the overlap region for yield (%) and purification factor created using MODDE 9.1 (Umetrics, Malmö, Sweden). Knowledge space refers to the region of process understanding based on the full factorial and CCF DoE inputs. Inputs were PEG 12000, PEG concentration, sodium citrate concentration, pH 7.4 and homogenate dilution factor of 1. The design space is a region where the combination of ranges that delivers purification factor ≥ 0.8 and Fab' loss ≤ 10%. The Normal Operating Range (NOR) was set to as a minimum of ± PEG 0.5% w/v and ± 0.05 M sodium citrate concentration within the dashed area of the design space*

6.1.3 Third Major Milestone of Project

3. Scale up validation of the microscale approach to 50 mL laboratory scale and 5 L pilot scale for process interaction studies

6.1.3.1 Particle Size Characterisation

In chapter 5, the size and strength of the precipitates was evaluated by microscale mimics. For example, the amount of shear caused by mixing speed and the rate of addition of the precipitating agents are important variables affecting particle formation. These factors were investigated at microscale on a robotic platform and verified at pilot scale. This was followed by a process run through ending with a cation exchange chromatography step at laboratory scale.

The rate of addition of precipitant, speed of mixing and mixing time were investigated by using a full factorial DoE with an automated robotic platform with d_{50} particle size as the model output. At low mixing speed (800 rpm) and high rate of addition of precipitant (900 μL s^{-1}) after 60 minutes of mixing, a reduction in the number of small particles was observed. The d_{50} particle size at this condition was 313 μm for PEG 12000 6.25% w/v/0.4 M sodium citrate pH 7.4 relative to 0.30 μm for Fab' homogenates. Good agreement of d_{50} particle size was observed between laboratory and pilot scale.

6.1.3.2 Centrifugation

It was possible to incorporate a ultrascale down (USD) shear device in microscale studies with the aim of mimicking the impact of the high shear regions in the inlet of a CSA-1 disk stack centrifuge (Westfalia Separator, AG, Germany). To best mimic the pilot scale centrifuge, feed materials were exposed to shear rates similar to those found in the feed zone of the CSA-1 disk stack centrifuge prior to laboratory centrifugation. Good agreement of clarification was achieved between laboratory scale and the pilot centrifuge. The pilot scale separation efficiency was 87%. The same conditions at laboratory scale with material exposed to high shear, 93% separation efficiency was achieved.

6.1.3.3 Filtration

The clarification of the precipitated material was investigated during a membrane filtration operation using an automated multiwell filtration technique prior to packed bed studies. The normal flow filtration method used was established by Kong *et al.,* (2010). Filtration experiments of three feedstreams, namely Fab' homogenate, multimodal precipitated material (PEG 12000 6.25% w/v/0.4 M sodium citrate pH 7.4) and single mode precipitated material (PEG 12000 15% w/v pH 7.4) were performed with Cuno Zeta Plus 30SP membrane filters (Cuno, Meridan, USA). This was followed by a diafiltration step to prepare material for the cation exchange chromatography step.

6.1.3.4 Chromatography

1 mL SP Sepharose Hi Trap pre packed bed columns (GE Healthcare, Uppsala, Sweden) was used to capture Fab' from the three feedstock solutions. Final purification factor (PF) for control (homogenate), multimodal (PEG 12000 6.25% w/v/0.4 M sodium citrate) and single mode precipitated (PEG 12000 15% w/v) feed stocks were 2.5, 4.4 and 3.5 respectively. The use of multimodal precipitated impurities prior to a packed bed step had improved process performance by PF 1.9. Therefore, this investigation of whole process interactions with material prepared by precipitation demonstrated the importance of reducing impurities early in the process that can negatively interact with subsequent operations. The results show how modest purification factor in the initial precipitation steps are amplified by interactions with subsequent operations leading to radically differing performance. This underlines the importance of assessing the interaction of individual processing steps, and the implementation of appropriate scale down models as a means of achieving process parameter ranging understanding. The impact of which has the further potential to improve the longevity of chromatography resins and reducing overall downstream purification cost.

6.1.3.5 Final Remarks

In this thesis, techniques have been demonstrated for the precipitation of Fab' and protein impurities using microscale processing as an integral part of a high throughput and small scale mimic of large purification processes. This approach can be invaluable at the process definition stage of drug development when pilot scale

trials are unfeasible or material is scarce i.e. for high value products and limited feedstream availability.

6.2 Future Directions

Future challenges to the current purification of antibody based therapeutics will be provided by the scale of production for these types of products (Shukla *et al.,* 2007). One result of this is that in recent years, the successful increase in upstream titer, and challenging target molecules have resulted in the downstream process to become the limiting factor in the bioprocess industry (Farid 2006). After highlighting the outcome of the work performed in this thesis (Section 6.1) this section will present the necessary work in the short term and longer term in order to obtain a better understanding of the microscale precipitation systems developed in this work.

6.2.1 Future Short Term Directions in Homogenisation

Viscosity is an important property of the process stream and a significant factor in the optimisation of downstream processing unit operations such as homogenisation and centrifugation. The traditional mechanical method for cell disruption described in this thesis is very intense, resulting in the complete disruption of the cell. The subsequent release of chromosomal DNA increases the viscosity of the process stream significantly which will affect the efficiency of the subsequent solid-liquid separation step (indicated by Stoke's Law, equation 1.5). By reducing viscosity this can result in significant gains in the efficiency of downstream processing unit operations such as centrifugation and precipitation. This presents a greater challenge for the selective release of product from the periplasm (Balasundaram *et al.,* 2010). As a short term project for 6 to 9 months with one FTE, experiments can be conducted in relation to the above to reduce the viscosity of the process stream to improve subsequent processing steps. This has in part been investigated by Balasundaram *et al.,* (2009) who reported a reduction in the viscosity of homogenised material by reducing chromosomal DNA with nuclease to help improve further downstream processing. Furthermore, lipid removal can be investigated to further improve the feedstream.

An alternative 6 to 9 month project for the assessment of product release with one FTE could be the investigation of a combination of heat extraction and homogenisation, and by combining unit operations product release and purity can achieved in the same step (Balasundaram *et al.,* 2010). For example, prior to homogenisation, heat could be used to weaken cell walls, which could potentially

reduce the homogenisation discharge pressures required for product release. A broad range of temperatures can be studied so that a better understanding of the impact of cell disruption methods can be achieved. This is to enable the analysis of the different process trade-offs which may emerge. However, to investigate alternative process strategies, a large number of variables must be evaluated, which can involve large amounts of material. Therefore, employing microscale techniques that are representative of large scale processes may be more suitable for these studies.

6.2.2 Future Medium Term Directions in Precipitation

Further limitations stem from limited tankage for buffers and the inability to increase large scale chromatography column diameters to beyond 2 m without encountering significant issues with flow distribution and packing (Low *et al.*, 2007). It is possible that non chromatographic purification techniques such as precipitation will be further developed and improved over time resulting in a gradual evolution of the downstream purification platform over the next decade (Low *et al.,* 2007). Precipitation has been used in the plasma protein industry to purify proteins at large scale. The ability to reduce the impurity burden upstream of the purification process is the key in reducing the complexity of downstream processing steps. Lowering the levels of impurities can improve loading capacity and performance of costly chromatography columns. To achieve this, the development, validation and automation of high throughput microtiter scale platforms are important for enabling the investigation of the large operating experimental space for precipitation based processes. The development of a scale down automated precipitation process described in this thesis has allowed the use conventional DoE, such as factorial and central composite designs, for the investigation of a large range of operating parameters to support the definition of robust operating spaces for scale up manufacture.

As a medium term project for 2 to 4 years with one FTE, experiments are proposed to combine alternative polymers such as dextran with salts such as acetate and nitrate with zeta potential measurements to better understand precipitant interactions. Zeta potential describes the charge characteristics of particle surfaces, which can be used to determine the stability of proteins in solution, which will change with pH and salt content.

This microscale platform can be used to investigate alternative precipitation reagents such as acids and polyelectrolytes. A full factorial DoE to investigate these factors and interactions can produce over 1000 experiments. The use of sequential DoE can be employed to reduce experimental load, in which experiments are performed in a direction of improvement until the optimum is encircled. For example the simplex DoE method can accommodate a large number of variables with limited experimental runs, and does not require any assumptions with regards to the underlying model. Subsequent experiments are calculated by reflection towards improved conditions, for example to improve yield and purification factor. A simplex algorithm for the identification of Fab' precipitation operating conditions was partially investigated by Chhatre *et al.,* (2011) who reported 50% to 70% fewer points to the optimum compared to a conventional DoE approach. In essence, a simplex method can adjust the size of the design to further increase the rate of improvement (Box *et al.,* 1978).

Furthermore, the microscale platform which was developed and evaluated in Chapters 3 and 4 can be further assessed by applying it in the study of other industrially relevant feeds, such as mammalian cells and *Pichia pastoris*, which would cover a broad range of precipitation characteristics. The microscale mixing system described in chapter 4 for mixing in microwell plates could be used for mapping of these different feedstreams to mimic mixing at larger scale systems. Further development work for this application is needed, for example in this thesis the rate of addition of feed to the precipitant was kept constant throughout micro, laboratory and pilot scale, which resulted in increasing time of feed addition throughout these scales. This may have affected resultant particle size and strength, which will need to be further investigated. Experiments are proposed where the rate of precipitant addition at different scales is scaled up accordingly to maintain time of addition. However, achieving the full potential of microtiter bioprocessing techniques relies on validation methods, which can predict pilot and manufacturing scale performance without laboratory scale verification. The incorporation of a scale down shear device and laboratory centrifuge for the prediction of pilot scale performance in this thesis is an example of such a possibility.

There are challenges for the implementation of analytical techniques into high throughput process development (HTPD). A number of assays such as BCA total

protein assay and host cell protein ELISA can be automated on a robotic platform improving throughput and reducing labour. The time scale to carry out analytical techniques varies considerably with assays ranging from minutes, hours to days for incubation and conditioning of the samples prior to read out of the assay results. Assays require comparative measurements for quality control at defined time points involving blank, standard, and control samples for calibration (Fattinger 2010). Some of these issues can be reduced by improving the throughput of analytical methods. The arrangement of the samples in a linear array facilitates "parallel processing and conditioning" of the samples prior to readout of the assay results. The integration of the samples to be analysed in this way allows for integration of many process steps in the assay, such as allocation of the samples, sample preparation, incubation and conditioning and parallel readout of the analytical results (Fattinger 2010). It is important to the analytical strategy that well planned experiments with good experimental designs are performed to avoid overwhelming analytical groups.

In this thesis, microtiter experiments were performed with either four or eight channel arms dependant on the robotic platform. Tecan (Tecan, Reading, UK) have introduced 96 channel arms, which will be capable of utilising all 96 wells for parallel experiments in a single run. This is an increase in throughput by a factor of 12, reducing pipette delay times and will enable the implementation of high throughput assays such as the BCA total protein assay simultaneously with precipitation experiments for example. Incorporating these technologies with automated techniques can potentially reduce the bottleneck of high throughput development processes.

6.2.3 Future Medium Term Directions in Chromatography

Cation exchange chromatography at 1 mL laboratory scale was used post precipitation detailed in chapter 5. However, in terms of bioprocess development and the seamless integration of microscale bioprocessing techniques, the use of micro tip chromatography to investigate chromatography conditions is proposed as a medium term project for 2 to 4 years with one FTE. Chromatography is an integral part of the protein purification process and the capacity to use microscale chromatography can make an important contribution towards the development of robust and well characterised processes. Chromatography resins packed in micro

tips allows for robotic automation to mimic larger scale chromatography (Wenger 2010). Therefore using this approach multiple types of resins such as multimodal resins can be scouted for favourable binding conditions successfully. For example a multimodal resin such as Capto MMC (GE Healthcare, Uppsala, Sweden) can have a high salt tolerance and its elution conditions can be varied to remove product variants and aggregates, which may improve performance over traditional ion exchange resins such as SP Sepharose (GE Healthcare, Uppsala, Sweden) used in this thesis.

6.2.4 Future Long Term Directions in Bioprocess Development

Microscale techniques can shorten bioprocess development timelines by the early integration of these methods. These methods are used to acquire information to understand how best to implement control strategies that enable regulation of manufacturing operations, thus supporting validation package submissions when registering a process. The ability to understand how design parameters affect processes can provide information in how to operate at full scale. This capability is the practical basis on which Quality by Design is realised. In the long term microscale based research that seeks to mimic larger scale processes will be implemented throughout the whole of bioprocess development. For example, microscale data for fermentation process in terms of cell growth, product titer, and metabolite profiles have shown to be comparable to those obtained at pilot scale (Zhang *et al.,* 2007). The integration of microwell fermentation and cell culture operations will provide a resource for accelerated selection of cell hosts, expression systems, and conditions for growth with an additional consideration of processing implications. Adopting such an integrated approach to the whole of process development is becoming of greater importance as the recovery capacity of downstream processes are struggling to keep up with the rapid improvements in yield being achieved upstream (Tait *et al.,* 2009). Additionally, the same engineering principles have been shown previously for downstream processes such as centrifugation by Hutchinson *et al.,* (2006) and have been applied to chromatography (Wenger 2010).

A proposed integration of microtiter techniques based on a Quality by Design approach is shown in figure 6.3 using precipitation as an example. The results of microscale experiments are verified at laboratory scale with appropriate risk

management taken throughout the process stages (ICH guidelines Q8 (R2) and Q9). This is followed by scale up to pilot and manufacturing scales by providing a model for quality that can be implemented throughout product life cycle (ICH guideline Q10).
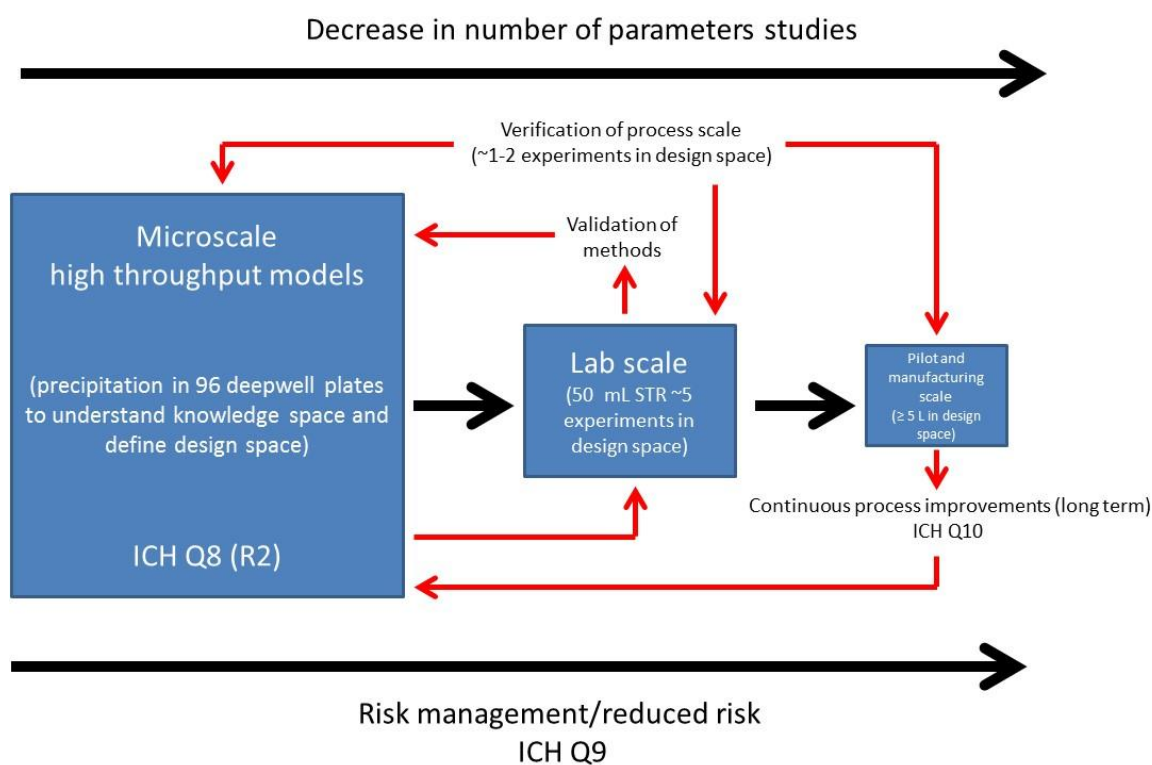
Figure 6.3: *Proposal for the integration and validation of microscale techniques into process development to facilitate QbD process development. Precipitation methodology as described in this thesis was used an example*

However, there are limitations to high throughput process development (HTPD) and some applications are difficult to scale. For example, HTPD systems as a scale down model for a chromatography step further downstream presents significant challenges, as there are many dynamic phenomena active in process columns that do not scale well from batch binding and single stage HTPD systems (Fattinger 2010). It has been suggested that by the next decade purification development HTPD will connect with multiple platform processing, such as multimodal protein conjugation (to toxins, or PEG) and chromatographic modelling, to accelerate process development.

A key focus of continued technology development efforts is to template as many parameters as possible for each unit operation. Improved understanding and refinement of the fundamentals microscale process development is an important area of future work (Shukla *et al.,* 2007). HTPD can be useful for emphasising concepts central to precipitation, chromatographic separations, experimental design and scale up (Kelly and Lester 2010). However, the complexity of biotech products and processes makes complete characterisation a challenge.

7. References

Aggarwal, S., (2009) What's fuelling the biotech engine. *Nat. Biotech.* 27; 987-993.

Aguilar, O., Albiter, V., Serrano-Carreón, L., Rito-Palomares, M., (2006) Direct comparison between ion-exchange chromatography and aqueous two-phase processes for the partial purification of penicillin acylase produced by *E.coli. J. Chrom. B.* 835; 77-83.

Ali, S., Perez-Pardo, M., Aucamp, J., Craig, A., Bracewell, D., **Baganz, F., (2012)** Characterisation and feasibility of a miniaturised stirred tank bioreactor to perform *E.coli* high cell density fedbatch fermentations. *Biotech. Prog.* 28; 66-75.

Anderssen, D., Reilly, D., (2004) Production technologies for monoclonal antibodies and their fragments. *Curr. Opin. Biotech.* 15; 456-462.

Atha, D., Ingham, K., (1981) Mechanism of precipitation of proteins by polyethylene glycol. *J. Biol. Chem.* 256; 12108-12117.

Arakawa, T., Timasheff, S., (1982) Preferential interactions of proteins with salts in concentrated solutions. *Biochem.* 21; 6545-6552.

Arakawa, T., Timasheff, S., (1985) The stabilisation of proteins by osmolytes. *J. Biophys.* 47; 411-414.

Aucamp, J., Cosme, A., Lye, G., Dalby, P., (2005) High-throughput measurement of protein stability in microtiter plates. *Biotech. Bioeng.* 89; 599-607.

Azevedo, A., Gabriela-Gomes, A., Rosa, P., Ferreira, I., Pisco, A., Aires-Barros, M., (2009) (a) Partitioning of human antibodies in polyethylene glycol–sodium citrate aqueous two-phase systems. *Sep. Pur. Tech.* 65; 14-21.

Azevedo, A., Rosa, P., Ferreira, I., Aires-Barros, M., (2009) (b) Chromatography-free recovery of biopharmaceuticals through aqueous two-phase processing. *Trend. Biotech.* 27; 240-247.

Balasundaram, B., Harrison, S., Bracewell, D., (2010) Advances in product release strategies and impact on bioprocess design. *Trend. Biotech.* 27; 477-485.

Balasundaram, B., Nesbeth, D., Ward, J., Keshavarz-Moore, E., Bracewell, D., (2009) Step change in the efficiency of centrifugation through cell engineering: co-expression of *Staphylococcal nuclease* to reduce the viscosity of the bioprocess feedstock. *Biotech. Bioeng.* 104; 134-142.

Balasundaram, B., Sachdeva, S., Bracewell, D., (2011) Dual salt precipitation for the recovery of a recombinant protein from *Escherichia coli*. *Biotech. Prog.* 27; 1306-1314.

Bell, D., Dunnill, P., (1982) Shear disruption of soya protein precipitate particles and the effect of ageing in a stirred tank. *Biotech. Bioeng.* 24; 1271-1285.

Bell, D., Hoare, M., Dunnill, P., (1983) The formation of protein precipitates and their centrifugal recovery. *Adv. Biochem. Eng. Biotech.* 26; 1-72.

Bensch, M., Selbach, B., Hubbuch, J., (2007) High throughput screening techniques in downstream processing: preparation, characterisation and optimisation of aqueous two-phase systems. *Chem. Eng. Sci.* 62; 2011-2021.

Berrill, A., Ho, S., Bracewell, D., (2008) Ultra scale-down to define and improve the relationship between flocculation and disc-stack centrifugation. *Biotech. Prog.* 24; 426-431.

Biddlecombe, J., Smith, G., Uddin, S., Mulot, S., Spencer, D., Gee, C., Fish, B., Bracewell, D., (2009) Factors influencing antibody stability at solid–liquid interfaces in a high shear environment. *Biotech. Prog.* 25; 1499-1507.

Biddlecombe, R., Pleasance, S., (1999) Automated protein precipitation by filtration in the 96-well format. *J. Chrom. B.* 734; 257-265.

Bonnerjea, J., Hoare, M., Dunnill, P., (1986) Protein-purification - the right step at the right time. *Biotech.* 4; 954-958.

Botterill, M., Rawlings, B., (2008) Applying good engineering practices to the design of single-use systems. *BioPro. Int.* 11; 18–25.

Boulding, N., Yim, S., Keshavarz-Moore, E., Shamlou, P., Berry, M., (2002) Ultra scale down to predict filtering centrifugation of secreted antibody fragments from fungal broth. *Biotech. Bioeng.* 79; 381-388.

Bowering, L., (2004) Microbial systems for the manufacture of therapeutic antibody fragments. *BioPro. Int.* 2; 40-47.

Box, G., Hunter, G., Hunter, S., (1978) Statistics for Experimenters. *John Wiley & Sons.* ISBN 0471718130; 281-313.

Boychyn, M., Doyle, W., Bulmer, M., More, J., Hoare, M., (2000) Laboratory scaledown of protein purification processes involving fractional precipitation and centrifugal recovery. *Biotech. Bioeng.* 69; 1-10.

Boychyn, M., Yim, S., Bulmer, M., More, J., Bracewell, D., Hoare, M., (2004) Performance prediction of industrial centrifuges using scale-down models. *Biopro. Biosyst. Eng.* 26; 385-391.

Bracewell, D., Boychyn, M., Baldascini, H., Storey, S., Bulmer, M., More, J., Hoare, M., (2008) Impact of clarification strategy on chromatographic separations: pre-processing of cell homogenates. *Biotech. Bioeng.* 100; 941-949.

Bramaud, C., Aimar, P., Daufin, G., (1997) Optimisation of a whey protein fractionation process based on the selective precipitation of α-lactalbumin. *Lait.* 77; 411-423.

Brochier, V., Schapman, A., Santambien, P., Britsch, L., (2008) Fast purification process optimisation using mixed-mode chromatography sorbents in pre-packed mini-columns. *J. Chrom. A.* 1177; 226-233.

Burgess, D., Duffy, E., Etzler, F., Hickey, A., (2004) Particle size analysis: AAPS workshop report, cosponsored by the Food and Drug Administration and the United States Pharmacopeia. *J. AAPS.* 6; 23-34.

Byrne, B., Fitzpatrick, P., (2002) Investigation of how agitation during precipitation and subsequent processing affects the particle size distribution and separation of α-lactalbumin enriched whey protein precipitates. *J. Biochem. Eng.* 10; 17-25.

Camp, T., Stein, P., (1943) Velocity gradients and internal work in fluid motion. *J. Bos. Soc. Civil. Eng.* 85; 219-237.

Chapman, A., (2002) PEGylated antibodies and antibody fragments for improved therapy: a review. *Adv. Drug. Del. Rev.* 54; 531-545.

Chapman, A., Antoniw, P., Spitali, M., West, S., Stephens, S., King, D., (1999) Therapeutic antibody fragments with prolonged in vivo half-lives. *Nat. Biotech.* 17; 780-783.

Chen, J., (1990) Novel affinity-based processes for protein purification. *J. Ferm. Bioeng.* 70; 199-209.

Cheng, Y., Lobo, R., Sandler, S., Lenhoff, A., (2005) Kinetics and equilibria of lysozyme precipitation and crystallisation in concentrated ammonium sulphate solutions. *Biotech. Bioeng.* 94; 177-188.

Chhatre, S., Konstantinidis, S., Ji, Y., Edwards-Parton, S., Zhou, Y., Titchener-Hooker, N., (2011) The simplex algorithm for the rapid identification of operating conditions during early bioprocess development: case studies in Fab' precipitation and multimodal chromatography. *Biotech. Bioeng.* 108; 2162-2170.

Chi, E., Krishnan, S., Randolph, T., Carpenter, J., (2003) Physical stability of proteins in aqueous solution: mechanism and driving forces in nonnative protein aggregation. *Pharm. Res.* 20; 1325-1336.

Colby, C., O'Neill, B., Vaughan, F., Middelberg, A., (1996) Simulation of compression effects during scale up of a commercial ion-exchange process. *Biotech. Prog.* 12; 662-681.

Coleman, L., Mahler, S., (2003) Purification of Fab' fragments from a monoclonal antibody papain digest by gradiflow electrophoresis. *Pro. Exp. Pur.* 32; 246-251.

Cui, Z., (2005) Protein separation using ultrafiltration — an example of multi-scale complex systems. *Chin. Part.* 3; 343-348.

Dainiak, M., Muronetz, V., Izumrudov, V., Galaev, I., Mattiasson, B., (2000) Production of Fab' fragments of monoclonal antibodies using polyelectrolyte complexes. *Anal. Biochem.* 227; 58-66.

Diels, A., Michiels, C., (2006) High pressure homogenisation as a non thermal technique for the inactivation of microorganisms. *Crit. Rev. Micro.* 32; 201-206.

Dixon, M., Webb, E., (1961) Enzyme fractionation by salting-out: a theoretical note. *Adv. Pro. Chem.* 16; 197-219.

Doran, P., (1995) Bioprocess Engineering Principles. *Academic Press.* ISBN 780122208553; 129-163.

Duetz, W., Beilen, J., Witholt, B., (2001) Using proteins in their natural environment: potential and limitations of microbial whole-cell hydroxylations in applied biocatalysis. *Curr. Opin. Biotech.* 12; 419-425.

Eiteman, M., Gainer, J., (1991) Predicting partition coefficients in polyethylene glycol-potassium phosphate aqueous two-phase systems. *J. Chrom. A.* 586; 341-346.

Englard, S., Seifter, S., (1990) Precipitation techniques. *Meth. Enzymol.* 182; 285-300.

Farid, S., (2006) Established bioprocesses for producing antibodies as a basis for future planning. *Adv. Bio. Eng. Biotech.* 101; 1-42.

Fattringer, C., (2010) High throughput techniques for small molecule drug discovery and early development: lessons learned. *HTPD conference, Kraków, Poland, Oct 4-7 2010.*

Ferreira-Torres, C., Micheletti, M., Lye, G., (2005) Microscale process evaluation of recombinant biocatalyst libraries: application to Baeyer–Villiger monooxygenase catalysed lactone synthesis. *Biopro. Biosys. Eng.* 28; 83-93.

Foster, P., Dunnill, P., Lilly, M., (1971) Salting out of enzymes with ammonium sulphate. *Biotech. Bioeng.* 13; 713-718.

Foster, P., Dunnill, P., Lilly, M., (1973) The precipitation of enzymes from cell extracts of *Saccharomyces cerevisiae* by PEG. *Biochem. Biophys. Acta.* 317; 505-516.

Foster, P., Dunnill, P., Lilly, M., (1976) The kinetics of protein salting out: precipitation of yeast enzymes by ammonium sulphate. *Biotech. Bioeng.* 18; 545-580.

Galaev, I., Dainiak, M., Plieva, F., Hatti-Kaul, R., Mattiasson, B., (2005) High throughput processing of particulate-containing samples using supermacroporous elastic monoliths in microtiter (multiwell) plate format. *J. Chrom. A.* 1065; 169-175.

Glatz, C., Hoare, M., Landa-Vertiz, J., (1986) The formation and growth of protein precipitates in a continuous stirred-tank reactor. *Biotech. Bioeng.* 32; 1196-1204.

Gonzalez-Tello, P., Camacho, F., Blazquez, G., (1994) Density and viscosity of concentrated aqueous solutions of polyethylene glycol. *J. Chem. Eng. Data.* 39; 611-614.

Haaland, P., (1989) Experimental Design in Biotechnology. *Taylor & Francis.* ISBN 9780824778811; 1-284.

Hahn, R., Schlegel, R., Jungbauer, A., (2003) Comparison of protein A affinity sorbents. *J. Chrom. B.* 790; 35-51.

Hames, B., Hooper, N., (2000) Instant Notes in Biochemistry 2nd Edition. *Bios Scientific Publishers.* ISBN 1859961428; 37-47.

Hansen, M., Lihme, A., Spitali, M., King, D., (1999) Capture of human Fab' fragments by expanded bed adsorption with a mixed mode adsorbent. *Biosep.* 8; 189-193.

Harden, V., Harris, J., (1952) The isoelectric point of bacterial cells. *J. Bacter.* 65; 198-202.

Harinarayan, C., Skidmore, K., Kao, Y., Zydney, A., Reis, R., (2008) Small molecule clearance in ultrafiltration/diafiltration in relation to protein interactions: study of citrate binding to a Fab'. *Biotech. Bioeng.* 102; 1718-1722.

Hicks, C., (1974) Fundamental Concepts of Design of Experiments. *Rhinehart and Winston.* ISBN 978-0195122732; 1-576.

Hillbrig, F., Freitag, R., (2003) Protein purification by affinity precipitation. *J. Chrom. A.* 790; 79-90.

Hood, E., Woodard, S., Horn, M., (2002) Monoclonal antibody manufacturing in transgenic plants — myths and realities. *Curr. Opin. Biotech.* 13; 630-635.

Horváth, C., Melander, W., Molnára, I., (1976) Solvophobic interactions in liquid chromatography with nonpolar stationary phases. *J. Chrom. A.* 125; 129-156.

Huddleston, J., Wang, R., Flanagan, J., O'Brien, S., Lyddiatt, A., (1994) Variation of protein partition coefficients with volume ratio in poly(ethylene glycol)-salt aqueous two-phase systems. *J. Chrom. A.* 668; 3-11.

Huddleston, J., Abelaira, J., Wang, R., Lyddiatt, A., (1996) Protein partition between the different phases comprising poly(ethylene glycol)-salt aqueous two-phase systems, hydrophobic interaction chromatography and precipitation: a generic description in terms of salting-out effects. *J. Chrom. B.* 680; 31-41.

Humphreys, D., Heywood, S., King, L., Bowering, L., Turner, J., Lane, S., (2004) Engineering of *Escherichia coli* to improve the purification of periplasmic Fab' fragments: changing the p*I* of the chromosomally encoded PhoS/PstS protein. *Pro. Exp. Pur.* 37; 109-118.

Hutchinson, N., Bingham, N., Murrell, N., Farid, S., Hoare, M., (2006) Shear stress analysis of mammalian cell suspensions for prediction of industrial centrifugation and its verification. *Biotech. Bioeng.* 95; 483-491.

ICH Harmonised Tripartite Guideline (2005) Quality risk management Q9. *Published by the European Medicines Agency;* 1-19.

ICH Harmonised Tripartite Guideline (2008) Pharmaceutical quality system Q10. *Published by the European Medicines Agency;* 1-17.

ICH Harmonised Tripartite Guideline (2009) Pharmaceutical development Q8 (R2). *Published by the European Medicines Agency;* 1-24.

ICH Harmonised Tripartite Guideline (2011) Development and manufacture of drug substances (chemical entities and biotechnological/biological entities) Q11. *Published by the European Medicines Agency;* 1-26.

Ingham, K., (1990) Precipitation of proteins with polyethylene glycol. *Meth. Enzymol.* 182; 301-306.

Islam, R., Tisi, D., Levy, M., Lye, G., (2007) Framework for the rapid optimisation of soluble protein expression in *Escherichia coli* combining microscale experiments and statistical experimental design. *Biotech. Prog.* 23; 785-793.

Jackson, N., Liddell, J., Lye, G., (2006) An automated microscale technique for quantitative and parallel analysis for microfiltration operation. *J. Mem. Sci.* 276; 31-41.

Janson, J., Rydén, L., (1998) Protein Purification 2nd Edition. *John Wiley & Sons.* ISBN 780471186267; 11-15.

Juckles, I., (1971) Fractionation of proteins and viruses with polyethylene glycol. *Biochim. Biophys. Acta.* 229; 535–546.

Jungbauer, A., (2005) Chromatographic media for bioseparation. *J. Chrom. A.* 1065; 3-12.

Kim, S., Bae, Y., (2003) Salt-induced protein precipitation in aqueous solution: single and binary protein systems. *Macro. Res.* 11; 53-61.

King, P., (1972) Separation of proteins by ammonium sulphate gradient solubilisation. *Biochem.* 11; 367-371.

Kitchen, C., Wang, A., Musson, D., Yang, A., Fisher, A., (2002) A semi-automated 96-well protein precipitation method for the determination of montelukast in human plasma using high performance liquid chromatography/fluorescence detection. *J. Pharm. Biomed. Anal.* 31; 647-654.

Kelly, B., Lester, P., (2010) Next decade of HTPD: evolution or revolution? *HTPD conference, Kraków, Poland, Oct 4-7 2010.*

Knevelman, C., Davies, J., Allen, L., Titchener-Hooker, N., (2010) High-throughput screening techniques for rapid PEG-based precipitation of IgG$_4$ mAb from clarified cell culture supernatant. *Biotech. Prog.* 26; 697-705.

Kong, S., Aucamp, J., Titchener-Hooker, N., (2010) Studies on membrane sterile filtration of plasmid DNA using an automated multiwell technique. *J. Mem. Sci.* 353; 144-150.

Kostov, Y., Harms, P., Randers-Eichhorn, L., Rao, G., (2000) Low-cost microbioreactor for high-throughput bioprocessing. *Biotech. Bioeng.* 72; 346-352.

Lee, J., Lee, L., (1981) Preferential solvent interactions between proteins and polyethylene glycols. *J. Bio. Chem.* 206; 625-631.

Lewis, G., Metcalf, T., (1988) Polyethylene glycol precipitation for recovery of pathogenic viruses, including hepatitis A virus and human rotavirus from oyster, water and sediment samples. *App. Environ. Micro.* 54; 1983-1988.

Ljunglöf, A., Lacki, K., Mueller, J., Harinarayan, C., Reis, R., Fahrner, R., Alistine, J., (2007) Ion exchange chromatography of antibody fragments. *Biotech. Bioeng.* 96; 515-524.

Low, D., O'Leary, R., Pujar, N., (2007) Future of antibody purification. *J. Chrom. B.* 848; 48-63.

Lundstedt, T., Seifert, E., Abramo, L., Thelin, B., Nyström, Å., Pettersen, J., Bergman, R., (1998) Experimental design and optimisation. *Chem. Intel. Lab. Sys.* 42; 3-40.

Lutz, M., Menius, J., Choi, T., Laskody, R., Domanico, P., Goetz, A., Saussy, D., (1996) Experimental design for high throughput screening. *Drug. Disc. To.* 1; 277-286.

Lye, G., Asenjo, A., Pyle, D., (1996) Reverse micellar spray column mass-transfer processes: extraction of lysozyme. *J. AlChe.* 42; 713-726.

Mahadevan, M., Hall, C., (1990) A statistical-mechanical model of protein precipitation by non ionic polymer. *J. AlChe.* 36; 1517-1528.

Marcos, J., Fonseca, L., Ramalho, M., Cabral, J., (1998) Variation of penicillin acylase partition coefficient with phase volume ratio in poly(ethylene glycol)–sodium citrate aqueous two phase systems. *J. Chrom. B.* 711; 295-299.

Marques, M., Cabral, J., Fernandes, P., (2010) Bioprocess scale-up: quest for parameters to be used as criterion to move from microreactors to lab-scale. *J. Chem. Tech. Biotech.* 85; 1184-1198.

Maybury, P., Mannweiler, K., Titchener-Hooker, N., Hoare, M., Dunnill, P., (1998) The performance of a scaled down industrial disc stack centrifuge with a reduced feed material requirement. *Biopro. Eng.* 18; 191-199.

Micheletti, M., Lye, G., (2006) Microscale process optimisation. *Curr. Opin. Biotech.* 17; 611-618.

Micheletti, M., Barrett, T., Doig, S., Baganz, F., Levy, M., Woodley, J., Lye, G (2006) Fluid mixing in shaken bioreactors: implications for scale up predictions from microlitre scale microbial and mammalian cell cultures. *Chem. Eng. Sci.* 61; 2939-2949.

Middaugh, C., Tisel, W., Haire, R., Rosenberg, A., (1979) Determination of the apparent thermodynamic activities of saturated protein solutions. *J. Bio. Chem.* 254; 367-370.

Middelberg, A., (1995) Process–scale disruption of microorganisms. *Biotech. Adv.* 13; 491–551.

Melander, W., Horváth, C., (1977) Salt effects on hydrophobic interactions in proteins. *Arch. Biochem. Biophys.* 183; 200-215.

Neal, G., Christie, J., Keshavarz-Moore, E., Shamlou, P., (2003) Ultra scale down approach for the prediction of full scale recovery of ovine polyclonal immunoglobulin's used in the manufacture of snake fragment. *Biotech. Bioeng.* 81; 149-157.

Nealon, A., O'Kennedy, R., Titchener-Hooker, N., Lye, G., (2006) Quantification and prediction of jet macro-mixing times in static microwell plates. *Chem. Eng. Sci.* 61; 4860-4870.

Nesbeth, D., Perez-Pardo, M., Ali, S., Ward, J., Keshavarz-Moore, E., (2012) Growth and productivity impacts of periplasmic nuclease expression in an *Escherichia coli* Fab' fragment production strain. *Biotech. Bioeng.* 109; 517-527.

Olsson, M., Johansson, E., Berntsson, M., Eriksson, L., Gottfries, J., Wold, S., (2006) Rational DoE protocols for 96-well plates. *Chem. Intel. Lab. Sys.* 83; 66-74.

Parker, T., Dalgleish, D., (1977) The use of light scattering and turbidity measurements to study the kinetics of extensively aggregated proteins: α_s-Casein. *Biopoly.* 16; 2533-2547.

Patapoff, T., Esue, O., (2009) Polysorbate 20 prevents the precipitation of a monoclonal antibody during shear. *Pharm. Dev. Tech.* 14; 659-664.

Perumalsamy, M., Murugesan, T., (2006) Prediction of liquid–liquid equilibria for PEG 2000–sodium citrate based aqueous two-phase systems. *Flu. Pha. Equil.* 244; 52-61.

Pollard, M., (2001) Process development automation: an evolutionary approach. *Org. Proc. Res. Dev.* 5; 273–282.

Polson, A., Potgieter, G., Largier, J., Mears, G., Joubert, F., (1964) The fractionation of protein mixtures by linear polymers of high molecular weight. *Biochim. Biophy. Acta.* 82; 463-475.

Przybycien, T., Bailey, J., (1989) Solubility-activity relationships in the inorganic salt-induced precipitation of α–chymotrypsin. *Enz. Micro. Tech.* 11; 264-276.

Przybycien, T., Pujar, N., Steele, L., (2004) Alternative bioseparation operations: life beyond packed-bed chromatography. *Curr. Opin. Biotech.* 15; 469-478.

Radola, B., (1973) Isoelectric focusing in layers of granulated gels: I. Thin-layer isoelectric focusing of proteins. *Biochim. Biophy. Acta.* 295; 412-428.

Rathore, S., Winkle, H., (2009) Quality by design for biopharmaceuticals. *Nat. Biotech.* 27; 26-34.

Rege K., Pepsin, M., Falcon, B., Steele, L., Heng, M., (2005) High-throughput process development for recombinant protein purification. *Biotech. Bioeng.* 93; 618-630.

Reichert, J., (2008) Monoclonal antibodies as innovative therapeutics. *Curr. Pharm. Biotech.* 9; 423-430.

Reynolds, T., Boychyn, M., Sanderson, T., Bulmer, M., More, J., Hoare, M., (2003) Scale-down of continuous filtration for rapid bioprocess design: recovery and dewatering of protein precipitate suspensions. *Biotech. Bioeng.* 83; 454-464.

Richardson, P., Hoare, M., Dunnill, P., (1990) A new biochemical engineering approach to the fractional precipitation of proteins. *Biotech. Bioeng.* 36; 354-366.

Rosa, P., Azevedo, A., Ferreira, I., Vries, J., Korporaal, R., Verhoef, H., Visser, T., Aires-Barros, M., (2007) Affinity partitioning of human antibodies in aqueous two-phase systems. *J. Chrom. A.* 1162; 103-111.

Rothstein, F., (1994) Differential precipitation of proteins. Science and technology. *Bio. Tech.* 18; 115-208.

Roush, D., Lu, Y., (2008) Advances in primary recovery: centrifugation and membrane technology. *Biotech. Prog.* 24; 488-495.

Rushton, J., Costich, E., Everett, H., (1950) Power characteristics of mixing impellers. *Chem. Eng. Prog.* 46; 395-404.

Scopes, R., (1987) Protein Purification Principles and Practice 2nd Edition. *Springer-Verlag.* ISBN 0-387-96555-6; 41-64.

Shamlou, P., Gierczycki, A., Titchener-Hooker, N., (1996) Breakage of flocs in liquid suspensions agitated by vibrating and rotating mixers. *J. Bio. Chem. Eng.* 62; 23-24.

Shih, Y., Prausnitz, J., Blanch, H., (1992) Some characteristics of protein precipitation by salts. *Biotech. Bioeng.* 40; 1155-1164.

Shukla, A., Hubbard, B., Tressel, T., Guhan, S., Low, D., (2007) Downstream processing of monoclonal antibodies-application of platform approaches. *J. Chrom. B.* 848; 28-39.

Siddiqi, S., Titchener-Hooker, N., Shamlou, P., (1996) Simulation of particle size distribution changes occurring during high-pressure disruption of bakers' yeast. *Biotech. Bioeng.* 50; 145–150.

Sinanoglu, O., Abdulnar, S., (1965) Effect of water and other solvents on the structure of biopolymers. *Fed. Proc.* 24; 12-23.

Staby, A., Sand, M., Hansen, R., Jacobsen, J., Andersen, L., Gerstenberg, M., Bruus, U., Jensen, I., (2004) Comparison of chromatographic ion-exchange resins: III strong cation-exchange resins. *J. Chrom. A.* 1034; 85-97.

Stavrinides, S., Shamlou, P., Hoare, M., (1993) Effects of engineering parameters on the precipitation, recovery and purification of proteins. *Pro. solid-liquid. Sus.* 69; 118-157.

Taipa, M., Kaul, R., Mattiasson, B., Cabral, J., (2001) Recovery of a monoclonal antibody from hybridoma culture supernatant by affinity precipitation with Eudragit S-100. *Biosep.* 9; 291-298**.**

Tait, A., Aucamp, J., Bugeon, A., Hoare, M., (2009) Ultra scale-down prediction using microwell technology of the industrial scale clarification characteristics by centrifugation of mammalian cell broths. *Biotech. Bioeng.* 104; 321-331.

Tambo, N., Hozumi, H., (1979) Physical characteristics of flocs—II strength of floc. *Wat. Res.* 13; 421-427.

Thömmes, J., Etzel, M., (2007) Alternatives to chromatographic separations. *Biotech. Prog.* 23; 42-45.

Thrash, S., Otto, J., Deits, T., (1991) Effect of divalent ions on protein precipitation with polyethylene glycol: mechanism of action and applications. *Pro. Exp. Purif.* 2; 83-89.

Titchener-Hooker, N., Dunnill, P., Hoare, M., (2008) Micro biochemical engineering to accelerate the design of industrial-scale downstream processes for biopharmaceutical proteins. *Biotech. Bioeng.* 100; 473-487.

Tustian, A., Salte, H., Willoughby, N., Hassan, I., Rose, M., Baganz, F., Hoare, M., Titchener-Hooker, N., (2007) Adapted ultra-scale-down approach for predicting the centrifugal separation behaviour of high cell density cultures. *Biotech. Prog.* 23; 1404-1410.

Virkar, P., Hoare, M., Chan, M., Dunnill, P., (1982) Kinetics of the acid precipitation of soya protein in a continuous-flow tubular reactor. *Biotech. Bioeng.* 24; 871-887.

Walsh, G., Headon, D., (1994) The industrial production of enzymes. *Biotech. Adv.* 12; 635-646.

Wan, Y., Vasan, S., Ghosh, R., Hale, G., Cui, Z., (2004) Separation of monoclonal antibody Alemtuzumab monomer and dimers using ultrafiltration. *Biotech. Bioeng.* 90; 422-432.

Weir, A., Nesbitt, A., Chapman, A., Popplewell, A., Antoniw, P., Lawson, A., (2002) Formatting antibody fragments to mediate specific therapeutic functions. *Biochem. Soc. Trans.* 30; 512–516.

Wenger, M., (2010) Micro-tip chromatography; a route to an integrated strategy for high throughput bioprocess development. *Thesis submitted in The Department of Biochemical Engineering UCL.*

Zhang, Y., Cremer, P., (2006) Interactions between macromolecules and ions: the Hofmeister series. *Curr. Opin. Chem. Bio.* 6; 658-663.

Zhang, Z., Perozziello, G., Boccazzi, P., Sinskey, A., Geschke, O., Jensen, K., (2007) Microbioreactors for bioprocess development. *J. Assoc. Lab. Autom.* 12; 143–151.

Zydney, A., Ho, C., (2002) Scale-up of microfiltration systems: fouling phenomena and V_{max} analysis. *Desal.* 146; 75-81.